OPTIMAL OPERATION OF SIMULATED MOVING BED AND VARICOL PROCESSES FOR BIO-SEPARATION

FALDY WONGSO

NATIONAL UNIVERSITY OF SINGAPORE

2003

OPTIMAL OPERATION OF SIMULATED MOVING BED AND VARICOL PROCESSES FOR BIO-SEPARATION

FALDY WONGSO

(B. Tech., University of Gadjah Mada, Indonesia)

A THESIS SUBMITTED

FOR THE DEGREE OF MASTER OF ENGINEERING

DEPARTMENT OF CHEMICAL & ENVIRONMENTAL ENGINEERING

NATIONAL UNIVERSITY OF SINGAPORE

2003

To my beloved parents

Acknowledgement

I would like to use this opportunity to salute my supervisor Prof. Ajay Kumar Ray for allocating his valuable time through incessant guidance, brilliant idea and outstanding patience during my 2 years of candidature in the National University of Singapore. It is right to express my deepest gratefulness for everything we have done together. I acknowledge the boundless thought and interest of Prof. Hidajat throughout my study and also for sourcing the interesting chiral compounds as the scope of this work.

I would also like to thank Prof. Andrezj Krasalawski (Lappeenranta University of Technology, Finland) for his sober assistance and advice prior and during the ESCAPE-13 symposium, Prof. Iftekhar Abubakar Karimi and Prof. Gade Pandu Rangaiah for the implied trust in my appointment as graduate tutor. My special thanks to Prof. Santosh Kumar Gupta for the NSGA jumping genes algorithm which is a superb tool in carrying out our work. It is a great honor to have Prof. Lakshminarayanan Samavedham's re-sourceful presence and input at my PG seminar. Thanks are also due to Prof. Marc Garland for the fruitful feedback on this thesis.

I want to express my gratitude to Mr Boey and Mr Mao Ning for the access to the workstation and Mr Toh for the Microsoft Visual Fortran software, Mr Chun See Chong for his assistance during my PG seminar, Mr Yeo Eng Hee and Mr Zhang Xinhuai from the SVU team for their excellent support in the execution of my simulation program. I always appreciate the National University of Singapore for the Research Scholarship which made this work possible.

I will not forget the sincerity of my senior, Dr Effendi Widjaja who has encouraged me to pursue my master degree in NUS. I'm thankful to Dr Zhang Ziyang for his cooperative assistance and comment in all my doubts. Million thanks to all my labmates and friends: Yu Weifang, Kanheya Mehrotra, Hari Prasad Janakiram Subramani, Chen Saoping, Kurup Anjushri Sreedhar, Eng Yongyong, Zhang Yan, Naveen Agrawal, Lee Yen Mei, and Paritam Kumar Dutta for the advices, jokes and time we spent together. I also thank my flatmate, Handoko for sharing his experience on Microsoft Visual Basic program. Foremost, my deepest gratitude goes to my beloved parents and all family members whose understanding, support and love have always inspired me this time round.

Table of Contents

SUMMARY

In recent years, there has been considerable interest in the synthesis and separation of enantiomer of organic compounds especially due to their importance in the biotechnology and pharmaceutical industry. There are two pedestal ways of producing pure enantiomer form of a compound, conventional chemical synthesis and asymmetric synthesis. Conventional synthesis, even though economically attractive, might result in chiral molecules. This method is favored for compounds where both enantiomers are of equal importance. Asymmetric synthesis, on the other hand, can selectively produce certain species. This method is highly preferred when one species of the optical isomer is toxic/harmful. However, it takes not only many years to develop asymmetric synthesis for any particular drug, but at times the process is expensive. Simulated moving bed (SMB) technology and its modification, Varicol process, has become an alternate technology for separation of such difficult or nearly impossible to separate mixtures with extremely low separation factor, which is difficult to be separated using conventional extraction, and the considerably low volatility gap makes it impractical to be purified using common distillation. In this technology, separation is achieved by differential migration rates of the two components, which is further enhanced by simulating countercurrent movement of the solid and the liquid phases. The general case of simulated countercurrent process is that successive switching of the feed and the product positions at timed interval simulates the movement of solid. By periodically changing the feed and the product locations sequentially along a fixed bed leads to high mass transfer driving forces. In traditional SMB process, a synchronous switch of all the inlet and outlet and streams are performed

while in the Varicol process a non-synchronous switch is employed to render more flexibility to the system. High product yield and purity can be achieved by selective adsorption in which compounds of a mixture are driven at different speeds through the chromatographic bed. However, like all methods, the chromatographic method suffers from certain drawbacks: requirement of expensive stationary phases, relatively higher volume of mobile phase consumption and high dilution of the separated products.

In this thesis, two separation problems are considered. The first is the separation of chiral drugs, SB-553261, and the second is the separation of chiral intermediates, 1,1'-bi-2-naphtol. Equilibrium dispersive model coupled with lumped kinetic approximation and non-linear equilibrium isotherm constitute the simulation model, which was verified with published experimental results for the above two systems. Single as well as multiple objective optimization studies were carried for many different meaningful optimization formulations. The optimization work was carried out using Non-Dominated Sorting Genetic Algorithm with jumping genes (NSGA II-JG). It employs the principles of genetics and the Darwinian principle of natural selection (i.e. survival of the fittest). A systematic optimization study is carried out involving the use of single objective as well as several objectives, which is often conflicting with each other. The use of non-dominated sorting genetic algorithm with jumping genes resulted in Pareto optimal solutions, which can easily be explained by the Triangle theory. Optimal operating conditions and optimal Pareto solutions clearly show that the concept of multiobjective optimization could be very useful in the design and operation of SMB and Varicol process for many important industrial applications. These optimal results help enhancing the performance of the existing design and serve as an important design tool for new developments.

Nomenclature

A	more retained component, column area (cm^2)
B	less retained component
C	liquid phase concentration (g/l)
CSP	chiral stationary phase
D	desorbent flow rate (ml/min)
D_L	apparent axial dispersion coefficient (cm_2/min)
E	extract flow rate (ml/min)
F	feed flow rate (ml/min)
H	height equivalent to theoretical plate (cm), Langmuir isotherm parameter
I	objective function index
J	theoretical number of cells
k	mass transfer coefficient (min^{-1})
K	adsorption constant, equilibrium constant
L_{col}	length of individual column (cm)
m	flow rate parameter
N	total number of column, switching index
P	zone I in SMB unit
Pr	productivity (g/h, g/day)
Pur	purity (%)
q	solid phase concentration (g/l)
Q	liquid flow rate (ml/min), zone II in SMB unit

R	raffinate flow rate (ml/min), zone III in SMB unit
Rec	recovery (%)
S	zone IV in SMB unit
SC	solvent consumption (m^3 desorbent/kg product)
SMB	simulated moving bed
t	time (min)
V_{col}	volume of individual column
Varicol	variable column system
Y	yield ($g/h/l_{solid}$ or $g/day/g_{solid}$)
z	axial coordinate (cm)

Greek Symbols

χ	column configuration
ΔP	pressure drop (psi)
ε	void fraction
δ	phase ratio
φ	zone index in SMB and varicol
σ	relative carrying capacity
ζ	pseudo solid phase velocity

Subscripts and Superscripts

col	column
D	desorbent

E	extract
F	feed
g	gas
i	component index
j	column index
k	cell index
R	raffinate
s	solid, switching

List of Figures

List of Tables

Chapter 1

Introduction

Synthesis and isolation of enantiomers of organic compounds has been gaining steady interest over the past few years owing to their advantages in the fine chemical and pharmaceutical industry. A number of synthesis techniques are available for the preparation of single enantiomer drugs. Among these methods, resolution by preparative chiral chromatography is receiving increasing attention nowadays. Chromatographic principle is believed to be one of the powerful tools in which components are separated by differential migration through a system of two phases: column packing which acts as stationary phase and liquid phase which acts as the mobile phase. Advantages such as high separating power, selectivity, versatility, low operating cost and mild operating conditions has led to the convenient utilization of chromatography in the field of enantioseparation. High product yield and purity can be achieved by selective adsorption in which compounds of a mixture are driven at different speeds through the chromatographic bed. However, like all methods, the chromatographic method suffers from certain drawbacks: large requirement of expensive stationary phases, relatively high volume of mobile phase consumption and high dilution of the separated products.

Recently the Simulated Moving Bed (SMB) chromatographic technology has been introduced for continuous separation of chemicals with extremely low separation factor, which is difficult to be separated using conventional extraction, and considerably low volatility gap makes it impractical to be purified using distillation. SMB chromatography has excellent prospects in the field of pharmaceutical and fine chemicals separation and its

development requires better understanding of the process dynamics. The concept of SMB is based on true moving bed process, in which a stream of solids flows countercurrent to an inert carrier fluid passing a stationary inlet, by periodically changing feed and product locations sequentially along a fixed bed leading to high mass transfer driving forces. Successive switching of the feed and product positions at timed interval simulates the countercurrent movement of solid. True countercurrent motion is thus replaced by a periodic motion, while overcoming the problems of solids handling and attrition inherent in moving bed operations, as well as avoiding flow channeling that might occur while scaling up to large column diameters.

Continuous chromatography based on simulated moving bed technology has been widely used in the separation and purification of chemicals, which are difficult to be separated using other methods. This has found ultimate interest in the area of biochemical, pharmaceutical and fine chemicals due to its ability to meet the market needs of high yield and high purity coupled with moderate processing conditions. This has become more popular in recent years due to the availability of chromatographic phases, while eliminating the drawbacks of batch chromatography, namely dilution of species and low adsorbent utilization leading to cleaner, smaller, safer and faster processes.

The design of a SMB unit depends on appropriate choice of operating conditions such as liquid and solid flow rates. Further investigation into the system reveals the complex interplay between variables, i.e. high feed rate increase the productivity at the expense of high eluent/desorbent rate and product purity making this system prone to optimization. The optimization problem for simulated countercurrent process is to find the optimum values of the key process parameters under certain specified constrains. In this work, the

efficiency of the SMB technology in carrying out enantio-separation of SB-553261 and 1,1'-bi-2-naphtol racemate at various operating configuration are examined.

Modeling and simulation of SMB process towards improvement in process performance have received great attention as this effort could yield significant savings for industry dealing with biotechnology, pharmaceutical and fine chemistry. There are two approaches of modeling SMB chromatographic process. The first is to model the true moving bed process to describe the dynamics neglecting cyclic switching. The second approach is to connect dynamic model of single chromatographic columns while considering the cyclic port switching. In this work, a model for prediction of cyclic steady state performance of SMB is developed based on the latter approach, direct simulation of port switching (SMB model). Two types of SMB model are considered here, namely, mixing cell model and continuous-flow model. The first model is known as equilibrium stage model, which is suitable under the usual conditions of high performance preparative chromatography. The latter model assumes axial dispersion flow for the liquid phase and linear driving force (LDF) approximation for intra-particle mass transfer rate. Both models take into account multi-component adsorption equilibrium.

A recent development in SMB technology is known as the Varicol process. The basic configuration of the Varicol process is similar to SMB, only the injection and collection lines are shifted at different times non-synchronously. Hence, there will be variations of zone length for a multicolumn systems and the system will return to its original position at the last periodic sub-interval. The zone lengths are continuously varying and the increase of one column is compensated for by the decrease of the adjacent one. Varicol process

results in variation of zone length over time thus allowing more flexibility and better process performance.

Purity and recovery of products, appropriate use of solvent consumption and adsorbent productivity characterize the SMB and Varicol performance. The design of such a unit depends on appropriate choice of operating conditions such as liquid and solid flow-rates, switching time, number and length of columns, etc. Further investigation into the system reveals the complex interplay between variables, i.e. high feed rate increase the productivity at the expense of high eluent rate and product purity making this system prone to optimization. When the effects of operating parameters such as switching time, internal flow rates, section length and number of columns per each section are studied in the sensitivity study, it was found that most of the parameters affect the process performance indicators (such as productivity, purity, eluent consumption, etc) in conflicting manner, which leads to the concept of Pareto set where infinite number of equally good and non-dominating solutions are obtained.

In this work, the multiobjective optimization was carried out using Non-dominated Sorting Genetic Algorithm (NSGA) with jumping genes for the design and operation of SMB and Varicol process. It employs the principles of genetics and the Darwinian principle of natural selection (i.e. survival of the fittest). It was found that use of jumping genes results in getting superior solutions (global optimal and spreading of solutions) in significantly less computational time over the conventional NSGA. This finding extends to the existing added value of genetic algorithm: the ability to handle several objective functions and to locate global optima even when multimodality persists.

In this study, verification of the mathematical model of the SMB system was done by fitting the model predicted results to the elution profiles of components in a single column experiments. The PDEs along with the initial and the boundary conditions, kinetic model equation and adsorption equilibrium were solved using the method of lines. In this method, the PDE is first discretized in space using the finite difference method to convert it into a set of several coupled ODE-IVPs. The numerical method of lines combines a numerical method for the initial value problem of ordinary differential equation and the numerical method for the boundary value problem. The resulting stiff ODEs of initial value kind was solved using DIVPAG, which is based on Gear's method, in the IMSL library. The agreement of simulated and experimental results obtained paved a way to further process improvement through simulation and optimization study. The process system was subsequently characterized by the sensitivity study. This study provides much useful rudimentary information such as the contradictive behavior of operating parameters on several performance parameters, feasible upper/lower bounds of decision variables, etc. Numerous optimization problems were formulated based on the economic consideration of the separation process. Many more formulation can be designed but only few examples are discussed in this thesis to illustrate the concept, techniques and interpretation of results. Finally, the optimum results were verified by locating them in the in the operating plane of binary separation based on the Triangle theory. Optimum points are well placed on the vertex of the triangle regime for pure separation. Optimal operating conditions and optimal Pareto solutions clearly show that the concept of multiobjective optimization could be very useful in the design and operation of SMB and Varicol process for many important industrial applications. These optimal results help in enhancing the

performance of the existing design and serve as an important design tool for new developments.

Chapter 2 Literature Review

2.1. Review on Stereochemistry

In recent years, there has been considerable interest in the synthesis and separation of enantiomers of organic compounds especially due to their importance in the biochemistry and pharmaceutical industries. Consequently, these growing trends have led to numerous terms and expressions in addition to those commonly used or recently recommended for the chemical and physical properties of chiral compound. Stereochemistry is basically about the shape and change of shape of molecules and basic understanding will be covered in this section.

2.1.1. An Overview on Chirality

The history of chirality began when French physicist, Jean-Baptiste Biot (1774-1862), studied the nature of plane-polarized light and found out that certain solutions of organic molecules rotated the plane of polarized light. Pasteur (1902) later studied the chemical, optical and crystallographic properties of tartrates preceded by some years of his studies of fermentations. He re-crystallized a concentrated solution of sodium ammonium tartrate and observed two distinct kinds of crystals. It was found that although a solution of the original salt was optically inactive, solutions of the individual piles were optically active and their specific rotations were equal in amount but opposite in sign.

Enantiomers are two chemically identical molecular species that differ from each other as non-superimposable mirror images. The most simple and vivid model for enantiomeric structures is our left and right hands. They demonstrate the sign of chirality

because they are each other's mirror image; no matter how much we twist and turn them, we can't superimpose the right hand image onto the left one. They are named according to rotation of the plane of polarized light (-l and –d enantiomer) and the 3-D arrangement of groups around the chiral center (-R and –S enantiomer). Enantiomers, in addition to diastereomers and *cis-trans*-isomers, are thus a special case of stereoisomers.

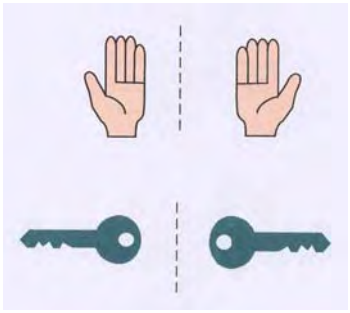

Figure 2.1 Non-superimposable mirror image structures

The chirality of enantiomeric molecules is caused by the presence of one or more chirality elements (chirality axis, chirality plane or chirality center, e.g. asymmetric carbon atom) in their structure. The chirality sense and optical activity of the enantiomers are determined by their absolute configuration, i.e. the spatial arrangement of the atoms in the molecule. In contrast to their conformation, the configuration of enantiomers cannot be changed without a change in the connectivity of constituent atoms. Many organic molecules exhibit chirality, for example, whenever four different groups are attached to a tetrahedral carbon atom.

Conventional chemical synthesis, in contrast to asymmetric synthesis, deals mostly with the transformations of achiral compounds. If these reactions result in the formation of a chirality element in the molecule, the reaction product appears to be an equivalent mixture of a pair of enantiomers, a racemate, which is optically inactive. Racemates are

also formed through racemisation of chiral compounds and they crystallize in the form of a racemic compound or, less frequently, as a conglomerate.

Direct enantiomeric resolutions are only feasible in chromatographic systems which contain an appropriate chiral selector. This chiral selector can be incorporated into the stationary phase (chiral stationary phase) or be permanently bonded to or coated onto the surface of the column packing material (chiral bonded and chiral coated stationary phases). In all these cases, it is appropriate to refer to the chromatographic column as enantioselective (chiral) column.

In the case of chiral stationary phases, the enantiomer that forms the more stable association with the chiral selector will be the more strongly retained species of the racemate. On the other hand, a chiral mobile phase reduces the retention time of the solute enantiomer which forms a stronger association with the chiral selector. The enantioselectivity of the chiral chromatographic system is then expressed as the ratio of the retention factors of the two enantiomers. Here, the limit for the enantioselectivity of the chiral chromatographic system is set by the enantioselectivity of the selector-solute association (in the mobile phase). However, in the majority of chiral mobile phase systems, the chiral selector as well as its association with the solute enantiomers is distributed between the mobile and stationary phases. The effective enantioselectivity of the chromatographic system will therefore be proportional to the ratio of the enantioselectivities of the association processes in the stationary and mobile phases. (Davankov et al., 1988).

2.1.2. Trends in Chiral Chemistry

Conventional chemical synthesis result in the formation of chirality element in the molecule and it ends up with substances which only differ in geometric orientation. The increased awareness of the differences in biological activity of the two enantiomers of chiral substances has raised the demand for optically pure product, particularly in the pharmaceutical industry.

Unfortunately, it is not unusual to find that one isomeric form of a chiral drug compound has a therapeutic effect on the human body, and is therefore, an effective medication while its enantiomer is inactive or even harmful. The S-isomer of Penicillamine is an effective drug for arthritis while the R-isomer is highly toxic. Thalidomide is a chiral drug that, in the early 1960s, was administered to pregnant woman as racemic mixture. It was realized that only one enantiomer is beneficial while the other one is believed to be responsible for major limb malformations in fetuses and other birth defects. Another example of chiral molecules with their distinct bioactivity is tabulated in Table 2.1. When one isomer of a chiral compound is 'good' and the other 'bad', there is obvious benefit in separating the two enantiomers to enhance its safety and tolerability.

Table 2.1 Chiral molecules and bioactivity

Category	Enantiomer Compound	Bioactivity
Drug	Amphetamine	d-isomer is a potent central nervous stimulant while the l-isomer has little, if any, effect
	Epinephrine	l-isomer is 10 times more active as vaso-constrictor than d-isomer
	Propanolol	Racemic compound is used as drug, only the (S)-(-)-isomer has the desired β-adrenergic blocking activity
	Propoxyphene	α-l-isomer is antitussive while α-d-isomer is analgesic

Table 2.1 Chiral molecules and bioactivity (Cont'd)

Category	Enantiomer Compound	Bioactivity
Vitamin	Ascoric Acid	(+)-isomer is a good antiscorbic while (-)-isomer has no such properties
Insecticide	Bermethrine	d-isomer is much more toxic than the l-isomer
Food	Asparagine	d-enantiomer tastes sweet while l-enantiomer tastes bitter
	Limonene	S-limonene smells like lemons while R-lemonene smells like oranges
	Carvone	S-(+)-carvone smells like caraway while R-(-)-carvone smell like spearmint

It was shown in early 1990's that significant benefits in terms of chiral stationary phase and eluent consumption could be achieved by performing the separation based on SMB technology (Rekoske, 2001). Consequently, separation of pharmaceutical compound began to be carried out using this technology, particularly after the recent development in chiral stationary phases (Pirkle et al., 1980; Shibata et al., 1986; Yashima and Okamoto, 1995) and non-linear chromatography theory (Guiochon et al., 1994). Further optimization work in CSP area (Schulte et al., 1997; Kartozia et al., 2002) as well as in the mobile phase (Guest, 1997) continues to improve separation performance. The combination of non-enantioselective synthesis of racemic mixtures and SMB chromatography might make drug development substantially faster and cheaper.

2.1.2.1. Trends in Pharmaceutical Industry

Pharmaceutical companies have proved to be very lucrative for fine chemical manufacturers as long as they are able to provide single enantiomers of chiral intermediates and active ingredient quickly and cost-effectively as a potent competitive advantage. They have been honing, acquiring, developing and expanding chiral

technologies to respond to the rising demand for chiral compounds, not only from drug companies but also from the agrochemical, food and beverage, and diagnostic and research industries.

According to market research firm Freedonia group, demand for chiral raw materials, intermediates and active ingredients will grow by 9.4% annually between 2000 and 2005. The total market will be US$15.1 billion with approximately 76% going to drug manufacturing. Technology Catalysts International has measured the impact of chiral compounds in terms of chiral drugs. Their analysis shows that of the US$ 410 billion in worldwide sales of formulated pharmaceutical products in 2001, about 36% was due to single-enantiomer drugs. The number extends the rising sales and market share of single-enantiomer drugs which were US$ 133 billion (34%) in 2000 and US$115 billion (32%) in 1999 and the trend is expected to continue.

Among the therapeutic areas observed in the study, Respiratory and Central Nervous System (CNS) are those that experience major growth in single-enantiomer drugs. Among CNS disorders, the biggest market is depression. The leading product, with sales in 2000 of almost US$ 2.6 billion, was Prozac (fluoxetine) by Eli Lilly. Other antidepressant, however, such as Paxil (paroxetine hydrochloride) from GlaxoSmithKline and Zoloft (sertraline) from Pfizer, are single-enantiomers.

One strategy to improve the bottom line of drug companies is to extend the profitable life of products by redeveloping single-enantiomer forms of drugs that had been approved as racemates. A recent example is the effort of Forest Laboratories to bring out a more potent version of its antidepression drugs, Celexa (citalopram), a racemate. The R isomer

is inactive, and they applied for approval of escitalopram, the S-enantiomer-only drug in early 2001 (Rouhi, 2002).

A number of synthetic strategies are available for the preparation of single enantiomer drugs (Crosby, 1992). In addition to diastereoisomeric crystallizations and enantio-selective synthesis (specific to one enantiomer), resolution by preparative chromatography is become increasingly interesting nowadays where numerous advantages have been explored (Nicoud et al., 1993). Among these, the possibility to obtain both species at once with high purity is beneficial to the compilation of required tests.

Another effort involves the use of chirality as a tool for drug life cycle management. There are two ways of doing it: the first, known as racemic switch, will be managing the life cycle of a drug by patenting the individual enantiomers of a racemate and switch drugs to prolong patent life. Sepracor is among the companies that is developing racemic switch of several drugs made by other company. The next table lists some compounds that Sepracor is working on (Stinson, 2000, 2001).

Table 2.2 Sepracor racemic switch project

Compound	Parent Drug	Manufacturer	Development Stage
Levalbuterol HCl (XOPENEX®)	VENTOLIN® PROVENTIL®	GlaxoSmithKline Schering	Launched and NDA filed for pediatric indication (for asthmatic bronchospasm)
Espopiclone (ESTORRA®)	IMOVANE® AMOBANE®	Aventis Pharma	Phase III Clinical Trials (treatment of insomnia)
(S)-oxybutynin	DITROPAN®	ALZA	Phase III Clinical Trials (for urinary constinence)
(S)-doxazosin	CARDURA®	Pfizer	Phase I Clinical Trials (for urinary tract/prostate gland)

The second effort will be mixing an old drug, soon to be off patent, with a new drug, not so soon to be off patent, that treats the same condition but under different mechanism.

One example is the collaboration between Merck and Schering over their two products: ZOCOR® and ezetimibe respectively. ZOCOR® is a statin and works by inhibiting the production of cholesterol in the liver while ezetimibe selectively inhibits the absorption of cholesterol in the intestines without interfering with the absorption of nutrients. Another combination is Merck's CLARITIN®, once daily leukotriene receptor antagonist for asthma, and Schering's SINGULAR®, non-sedating antihistamine (Stinson, 2000).

Another development from the drug discovery area, Synthon Chiragenics offers complex chiral compounds that have never before been readily available. Grouped by complexity into diamond, platinum, gold and silver collections, the compounds will enable drug discovery based on structure that were previously hard to target. Compounds in the diamond collection are the most complex, often with two or three chiral centers and they can be used in drug screening with minimum transformation. They include highly functionalized oxazolidinones, β-amino acids, morpholines, piperazines and pyrrolidinols.

The platinum collection is composed of functionally rich and structurally complex amino alcohols, β- and γ-amino acids, and oxazolidinones. They are suitable as cores or scaffolds for developing lead candidates. The gold and the silver collections include novel compounds with one chiral center. They can be used to generate core molecules for drug discovery or as chiral ligands.

Pharmaceutical industry potential problems are low productivity, hefty R&D spending and the flowering of genomics and combinatorial chemistry. Total number of new drugs approved by the Food & Drug Administration has been declining since 1996 and total drug development time has almost doubled from 8.1 years in the 1960s to 14.2 years in the 1990s. This might be due to the increasing complexity of the diseases that

pharmaceutical companies are now targeting. The time it takes for FDA to approve a new drug, after decreasing from about 30 months in the early 1990s to 11.7 months in 1998, has been rising again. The average was 16.4 months in 2001 and the drain on resources is exacerbated by patent expirations (Rouhi, 2002).

Clinical development represents around 40% of R&D spending and is considered the "make or break" point for a new drug. Despite latest technological advances in pharmaceutical R&D, nearly 80% of all clinical studies for new product fail to finish on time and 20% of those delayed for six months or longer (Kirkpatrick, 2002). There is a growing trend for pharmaceutical and biotech companies to outsource their clinical work to Contract Research Organization (CRO). Outsourcing enables companies to reduce overall cost, cover gaps in capacity and improve their skill base. It also allows them to focus their in house-efforts on other parts of R&D process. For small companies with limited internal resources, this allocation allows them to get the most out of their R&D investment.

2.1.2.2. Trends in Fine Chemical Industry

Recent survey notes that the trends in chiral technology are moving toward biocatalysis. That because it enables transformation in fewer steps, with fewer by-products and lower solvent use, than traditional chemical synthesis. Other advantages of biocatalysis are the absence of potential threat of contamination resulting from metals in catalysts and negative environmental impact.

Degussa Fine Chemicals is one example of fine chemical companies that heavily invested in biocatalysis with its hydantoinase technology to produce L-amino acids. This

technology starts from D,L-hydantoins that can be produced by easy, inexpensive and standard chemistry. Hydantoinases convert hydantoins to carbamoylamino acids, with amino acids as products when acted upon by carbamoylases. Hydantoins racemize steadily and offer an attractive route to L- or D-amino acids as one enantiomer is consumed, the remaining one racemizes and 100% of one enantiomer is theoretically produced. The route to D-amino acids is well established and widely used while a complementary path to L-amino acids had not been available.

In collaboration with California Institute of Technology, Degussa has developed a fairly selective L-hydantoinase by directed evolution of a wild-type hydantoinase that prefers D-hydantoins. Degussa uses the enzyme in conjunction with a racemase, which catalyzes hydantoin racemization and an extremely selective L-carbamoylase, all housed in modified *Escherichia coli* cells. The whole-cell biocatalyst digests a wide variety of raw material to make a range of products. Amino acids that has been produced at industrial scale include L-methionine, L-norleucine, L-2-aminobutyric acid and L-3-(3′-pyridyl)alanine.

Daicel Chemical Industries applied biocatalyst technology in the area of chiral alcohol. A recently discovered R-specific secondary alcohol dehydrogenase from *Pichia finlandica* now complements the S-specific enzyme from *Candida parapsilosis*, discovered in 1995. With these two enzymes, Daicel is now able to supply both enantiomers of a chiral secondary alcohol from the same ketone substrate.

CSIR Bio/Chemtec has developed a process to produce *l*-menthol from the readily available *m*-cresol. Alkylation of *m*-cresol generates thymol and hydrogenation of thymol yields four pairs of diastereomers: ±-menthol, ±-isomenthol, ±-neomenthol and ±-

neoisomenthol. Acylation of this mixture using a stereoselective lipase yields *l*-menthyl acetate in 96% minimum enantiomeric excess(ee). *l*-Menthyl acetate is separated from the unreacted isomers by distillation and hydrolysis yields *l*-menthol.

DSM Fine Chemicals produced an enantiopure secondary alcohol by dynamic kinetic resolution using a stereoselective lipase in multiton-per-year capacity. A ruthenium catalyst with proprietary ligands racemize both enantiomers. At the same spot, a stereoselective lipase converts only one enantiomer to an ester in high yield and greater than 99% ee. The ester is inert to the metal complex and does not racemize. Hydrolysis to the enantiopure alcohol is nearly quantitative.

As biocatalysis gains ground in chiral chemicals production, research in asymmetric chemical synthesis continues unabated. One active area is immobilization of asymmetric homogeneous catalysts. Asymmetric homogeneous catalysts are difficult to use in large scale runs. They are not reusable and tend to contaminate the desired products. Immobilization could solve this problem and open up fine chemicals production to continuous processing.

Synetix Chiral Technologies is among the companies that develop and commercialize catalysts-immobilizing technologies. Its technology is based on rigid porous solid formed by controlled hydrolysis of tetraethylorthosilicate in the presence of triethoxysilane or a triethoxyaluminium salt which provides linking group. Further chemistry on the resulting powder anchors the catalyst metal or ligands through electrostatic or covalent interactions with the linking groups. The anchored catalyst can be added directly to a reaction mixture or packed in a fixed bed through which substrate and reagents pass. Strong binding of the catalyst to the support prevents metal leaching into product.

Johnson Matthey is another company that is commercializing catalyst immobilization. Preformed asymmetric homogeneous catalysts, the metal and its coordinated ligands, are anchored onto various supports (such as alumina, silica or clay) by using heteropolyacids such as phospotungstic acid as anchoring agents. Asymmetric hydrogenation catalysts immobilized this way are at least as active and selective as the homogeneous versions, some are reusable for up to 15 times. Catalyst leaching is not observed.

This technology complements Johnson Matthey's FibreCat technology, based on anchoring catalysts to a polymer fiber backbone. Four series of fiber-anchored catalyst are already commercially available: palladium catalysts for carbon-carbon cross-coupling, rhodium catalysts for hydrogenation, osmium catalysts for cis-hydroxylations and ruthenium catalysts for selective oxidations. Even though the development of FiberCat is intended to bind expensive ligands and metals and to recover them after the chemistry is complete, yet it increases environmental stability. Pyrophoric ligands such as *tert*-butyl phosphines become stable when anchored and osmium tetroxide, originally volatile and highly toxic, can be handled like a nontoxic material.

No work has been done with asymmetric reactions although Johnson Matthey has shown that FibreCat osmium catalysts convert octane to dihydroxyoctane, chiral modifiers have not yet been used. Meanwhile research in chiral ligands continues to be very productive. (R)-DTBM SegPhos, developed by Takao Saito and coworkers at Takasago International Corp., is a new addition to the company's portfolio of SegPhos ligands {(4,4′-bi-1,3-benzodioxole)-5,5′-diyl-bis-(diarylphospine)s}. Under dynamic kinetic resolution conditions, ruthenium-(R)-DTBM SegPhos reduces the carbonyl group of

racemic α-benzamido-β-ketoesters to form only one of four possible isomers in greater than 98% diastereomeric excess and greater than 99% enantiomeric excess.

Also from Takasago are nine new chiral diphospine ligands from rhodium-catalyzed asymmetric hydrogenation of olefins based on three structure types: SegPhos, BeePhos{1,2-bis(2-alkyl-2,3-dihydro-1*H*-phosphindol-1-yl)benzenes} and UCAP{1-(2,5-dialkylphospholano)-2-(diarylphosphino)-benzenes or 1-(dialkylphosphino)-2-(2,5-dialkylphospholano)benzenes}. These catalysts are being applied to olefins that are enantioselectively difficult to reduce. Reactions are carried out at 30 ºC rather than at cryogenic temperatures with moderate pressure, sometimes as low as 13.6 lb per sq in.

In other works on asymmetric hydrogenations, Zumu Zhang, an associate professor at Pennsylvania State University and the chief technology officer of Chiral Quest, State College, Pa., has prepared ortho-subsituted BINAPO ligands {1,1'-bi-2-naphthylbis(diphenylphosphinite)s}. The ligands become more effective than the unsubstituted versions because the ortho-substitution restricts the orientation of aryl groups joined to phosphorus atoms. The new ligands have been used in ruthenium-catalyzed asymmetric hydrogenation of β-aryl-substituted β-(acylamino)acrylates to β-aryl-substituted β-(acylamino)esters at up to 99% ee.

For rhodium-catalyzed hydrogenations of α-(acylamino)acrylic acid derivatives and α-arylenamides, Zhang offers TangPhos, a 1,2-bisphospholane named after graduate student Wenjun Tang. The ligand, which has chiral phosphorus atoms, was designed with conformational rigidity in mind as well. Enantioselectivities of up to 99% and turnovers of up to 10000 have been achieved with the ligand.

In Germany, Bayer AG's fine chemicals business group has developed a new synthesis for its proprietary Cl-MeO-BIPHEP ligands {5,5′-dichloro-6,6′-dimethoxybiphenyl-2,2′-diyl}-bis(diphenylphosphine)s}. These ligands deliver greater than 98.7% enantioselectivity in asymmetric hydrogenations of carbonyl groups and carbon-carbon double bonds. The method enables a wide spectrum of alkyl groups to be introduced allowing fine tuning of the catalyst beyond what was possible before.

In other developments, Sumitomo Chemical is now making chiral cyclopropane carboxylic acids based on addition of a diazoacetate to a terminal alkene catalyzed by dimeric rhodium triphenylacetate. Yields of up to 90% are achieved with highly functionalized substrates. The reaction produces a racemate, but it is practical because of Sumitomo's library of phenethylamine resolving agents. Enantiopurities of at least 98% are achieved.

At SNPE, the inversion of configuration that occurs in bimolecular nucleophilic substitutions is being used to prepare chiral 2-chloropropionates. When methyl(S)-(-)-2-(chlorocarbonyloxy)propionate—made by phosgenation of methyl(S)-(-)-lactate—decomposes in the presence of hexabutylguanidinium chloride hydrochloride, methyl(R)-(+)-2-chloropropionate is formed in up to 90% yield and up to 98% ee. Continuous attack by chloride ion on other side of the substitution site can occur, resulting in a racemate, but continuous removal of the inversion product prevents that from happening.

These few examples hardly convey the breadth of recent advances in chiral technologies despite the industry's sluggish prospect. Many fine chemicals companies are ready for the challenges of chiral manufacture, however poor outlook for their customers at the moment (Rouhi, 2002).

2.2. Chromatographic Separation

Chromatographic separation utilizes the difference in sorption equilibria of components in a feed under contact with a suitable stationary phase. This stationary phase is usually a porous or granular solid which in some cases may be coated with a liquid substrate. The stationary and mobile phase being used depends on the type of application and the properties of the mixture to be separated.

In chromatography, the selection of stationary phase and mobile phase is very important. The choice of mean particle size of the stationary phase depends on the distribution coefficients of the components to be separated, the viscosity of the solution and the optimization between maximum throughput and the desired final product purity. In order to achieve a good separation, the particle size range must be very narrow, i.e. over 95% of the resin must be within 20% of the mean particle size (Ganetsos and Barker, 1992).

In addition to its powerful separation potential, the chromatographic operation is not energy intensive, versatile and does not involve any phase change making it the most suitable technique for bioseparation.

2.2.1. Elution Chromatography

The chromatographic principle was first conceived and tested by operating in a batch-wise mode: introducing a pulse of feed into a column packed with adsorbent solid with a continuous flow of carrier fluid. The components are stratified in the column by selective adsorption and desorption on the solid, forcing them to breakthrough at the end of the column at different times. The least adsorbed components, often referred as raffinate, will

emerge earlier than its counterparts (most strongly adsorbed), mostly known as extract. The process is, however, only suitable for batch production for small amount of feedstock.

The selection of packing material is important, not only on a physicochemical basis (mostly the selectivity) but also on mechanical basis. The use of large particles and/or large particle size distribution is not recommended as they combine high pressure and low efficiency. The presence of very fine dust is particular harmful to the process due to the resulting high column back pressure effect.

This technique was targeted toward the separation of chemicals that were not readily or economically produced by any other method, such as flavors and fragrances, petrochemicals (i.e. pentene isomers) and pharmaceuticals. Abcor (in Massachusetts) has successfully employed this technique for commercial separation of petrochemicals namely aromatic isomers *m*-xylene and *p*-xylene (Ryan and O'Donnel, 1968) and Asahi Chemical Industries (Japan) for separation of *p*-xylene and ethylbenzene by means of zeolite-desorbent system (Seko et al. 1982).

In the field of flavors, several leading groups are known to use chromatography such as Finnish Sugar for the desugarization of beet molasses (Hongisto, 1977; Heikkilä, 1983), Amino GmbH (Hongisto, 1977) and Suddeutsche Zucker AG in Germany (Munir, 1976) for purification of beet or cane molasses. Another leading group in the application of batch chromatography is Elf Aquitaine, in association with the Société de Recherches Techniques et Industielles (SRTI) of France (Bonmati et al., 1980). In 1979, a production scale Elf-SRTI batch system to purify perfume ingredients and flavor chemicals from terpene feedstocks was commissioned at the SCM Corporation Glidden Division Plant in Jacksonville, Florida.

The advantage of batchwise/elution chromatography is that it is directly scalable from an analytical separation. Yet, there are several disadvantages such as generation of considerable amounts of organic eluent wastes, significant product dilution and long elution times for recovery of pure products from the column (Schulte and Strube, 2001). Another drawback of this technique is relatively low throughput, when compared to SMB chromatography, making the latter preferable from economical point of view since the enantioselective resins are a significant portion of the cost of chromatography systems (Francotte, 2001).

In batch process, either the eluted components must be fully resolved (i.e. very long column) or the overlapping fraction must be removed. It involves alternate supply of sample mixture and desorbent solvent to the bed of adsorbent particles. Repetitive feed injection and continuous recycling of the overlapping parts are employed in production scale, resulting in up to 40% of the injected sample being recycled.

Scaling up might introduce problems like non-uniform liquid distribution causing flow irregularities such as tailing (Colin et al., 1990). This problem can be resolved by applying a variety column baffle systems to enhance radial mixing and maintain a narrowband profile laying the horizontal plane. This baffle system, however, creates another problem especially when it comes to backwashing, regenerating or repacking the column. It is also difficult to accommodate any swelling or shrinking of the resin.

Recent application has nullified the use of baffle in which uniform flow is achieved by running the system at optimal flow rates, temperature and solute concentration thereby allowing viscosity control and density gradients. The use of short and wide column is preferred in biochemical application. The selection of the stationary phase is of major

concern than column design because it must exhibit strong specific affinity to the components to be separated.

2.2.2. Continuous Crosscurrent Chromatography

In crosscurrent chromatography, the chromatographic bed moves perpendicularly to the direction of fluid motion within the bed. The retention time differences of the feed components are transformed into physical displacements so that each component may be withdrawn continuously at fixed and characteristic distances away from the feed point. The two-dimensional flow pattern is in contrast with the conventional batch system and the process is a steady state operation occurring in the axial and circumferential directions.

The concept of cross flow chromatography was attempted previously in at least three different operational modes. Initial effort on this system was introduced by Martin (1949) in which an annular chromatograph rotates with respect to a feed stream and product withdrawal points. The annular space between two concentric cylinders is packed with adsorbent solid for continuous separations. The annulus rotates around its center while the feed is injected continuously through an immersed pipe. Carrier fluid is fed axially through the annular bed and uniformly to all parts while the bed is slowly rotated. In this way, the molecules that travel with the mobile phase move vertically down the bed and circumferentially, and those with the stationary phase move circumferentially relative to the feed pipe. Therefore each component emerges at different location depending on its retention time and rotation rate of the annulus.

Dinelli et al. (1962) rotated a series of vertical columns on a circular pitch as a carousel at speeds between 1 and 50 revolutions per hour to separate volatile mixtures by gas-solid chromatography. The carrier gas traveled down the column with feed being injected successively into columns as they passed a fixed feed port. Very high product purity (99.9%) was achieved in the separation of cyclohexane-benzene mixtures using tricresyl phosphate as the solid phase at 200 cm^3/h throughput.

Giddings (1962) showed that the use of this annular approach can avoid some inherent disadvantages of batch type large scale systems. Improved capacity is achieved by increasing cross sectional area while keeping annulus width narrow enough to avoid losses in resolution due to packing non-uniformities, experienced in batch column with diameters greater than 25 mm. Properly spaced multiple feed points could increase capacity by having the last component of a feed mixture exit from the column just prior to the first component of a second feed stream.

Fox et al. (1969) extended the application of this annular system to the separation of biological mixtures. They purified cow heart myoglobin and separated skim milk proteins from lactose and salt using molecular sieve gels. The arising operating problem, due to low throughput, in the gravity-fed device is difficulty in obtaining uniform flow throughout the entire annulus.

The separation of nickel and cobalt from synthetic process liquor was investigated using 1 M ammonium carbonate eluent by Scott et al. (1976). They pressurized rotating annular chromatograph using an air line to provide constant over pressure. The annulus was 13 mm wide and 500 mm long with an outside diameter of 284 mm fabricated from Plexiglas.

Begovich and Sisson (1983) investigated the ion exchange separation of zirconium and hafnium from a sulfate feed solution. Nuclear reactor-grade zirconium (<0.01% hafnium by weight) and hafnium (<1% zirconium) have been previously prepared using cation exchange resin in the pressurized continuous annular chromatograph. The device is adaptive to large scale operation and able to separate many components.

Howard et al. (1988) investigated the separations of aqueous fructose, glucose and sucrose solutions in a 600 mm laboratory scale continuous rotating chromatograph using calcium-exchanged Dowex 50W-X8 resin. Complete resolution of fructose-glucose mixtures was achieved.

Another design of crosscurrent chromatography was reported as in the work of Sussman and Huang (1967). The device, known as radial flow continuous chromatograph, uses two rotating disk placed closely together and coated with a thin layer of solvent. Carrier fluid and feed are introduced at the center of the disks and cross flow separation occurs due to disk rotation and radial flow of the carrier fluid. The application of this system is limited by its low output, due to capacity of a single disk system. Larger systems employing multiple disks are possible to improve productivity, but the device suffers from mechanical rotation.

Tuthill (1970) operated a cross flow chromatographic device by continuous injection of multicomponent feed into the corner of a rectangular slab packed with adsorbent and changing the direction of carrier flow at right angles. As a result, the products move to different positions at the end of the slab. The inability to use very fine chemical, due to excessive pressure drop, has limited the separation efficiency of this device.

The continuous crosscurrent chromatographic device has been shown to operate effectively as a preparative chromatograph. Continuous feed injection and product withdrawal makes it more superior than the conventional batch system. Cross-flow systems have no restriction to the number of components to be separated. Its modification, carried out by holding the bed stationary and rotating nozzles and product collectors, has several advantages in terms of operating cost (lower power requirements compared to rotating the whole annular packed bed) and better scale-up potential. The system can be used to continuously separate multicomponent solution and/or concentrate single component solution.

2.2.3. Continuous Countercurrent Chromatography

The idea of developing large scale continuous chromatographic process, applying countercurrent contact between fluids and selecting appropriate chromatographic packing has emerged in the past half decade. The main rationale behind countercurrent contact between mobile and stationary phase is enhanced driving force for separation. The feed stream is introduced into the center containing the least strongly adsorbed species, which travels with the mobile phase and is withdrawn from the top of the column, and the more strongly adsorbed species, which travels with the solid phase and is stripped at the bottom part of the column.

In countercurrent process, the solute concentration profiles need only to be partially resolved within the chromatographic column to allow collection of pure products at the respective outlets. In this way, the entire separating power of this system can be exploited effectively, permitting severe overloading by batch cocurrent standards and enabling

higher throughputs per unit volume of resin. Most of the counter-flow systems are restricted to two components separation at a time or multi component separation of feed into two parts, followed by further separation to recover each single component.

Two categories have been identified in this area depending on whether the bed has been physically moved or the stationary-phase movement is simulated by mechanical means: the true moving bed systems and the simulated moving bed systems. The true moving bed systems appeared first in which the packing flowed under gravity while the mobile phase traveled counter current in a vertical column. The simulated moving bed is subsequently developed to overcome mechanical difficulties (non uniform flow) and operating cost problem (moving the entire packing) due to movement of solids.

2.2.3.1. True Moving Bed Chromatography

True Moving Bed is a continuous chromatographic process whose principle has been adopted in Simulated Moving Bed process in which liquid and solid phase flow in opposite direction. For production processes, the productivity of the classical (batch) chromatography is too small and the consumption of solvents is too high. Therefore, true moving bed chromatography was invented as an approximation to a continuous counter-current operation. The concrete example of a True Moving Bed system is given in Hypersorption process by Union Oil Company in California, USA (Berg, 1946, 1951; Kehde et al., 1948). The technique was first applied for gas separation with activated carbon as solid phase flowing continuously downward through a rising gas stream containing methane, hydrogen, ethylene and other gases lighter than ethane.

In the area of bioseparation, Barker et al. (1992) use a 12-column preparative semi-continuous counter current chromatographic bioreactor separator in biosynthesis of dextran from sucrose in the presence of enzyme dextransucrase and the continuous production of maltose from modified starch. They are able to overcome viscosity problems and displacement of Ca^{2+} from the resin but product contamination were encountered after 50 hours of operation due to formation of levan and glucose. For maltose production, high purity maltose can be produced while keeping enzyme usage as low as 50% of the theoretical requirement for a conventional batch bioreactor.

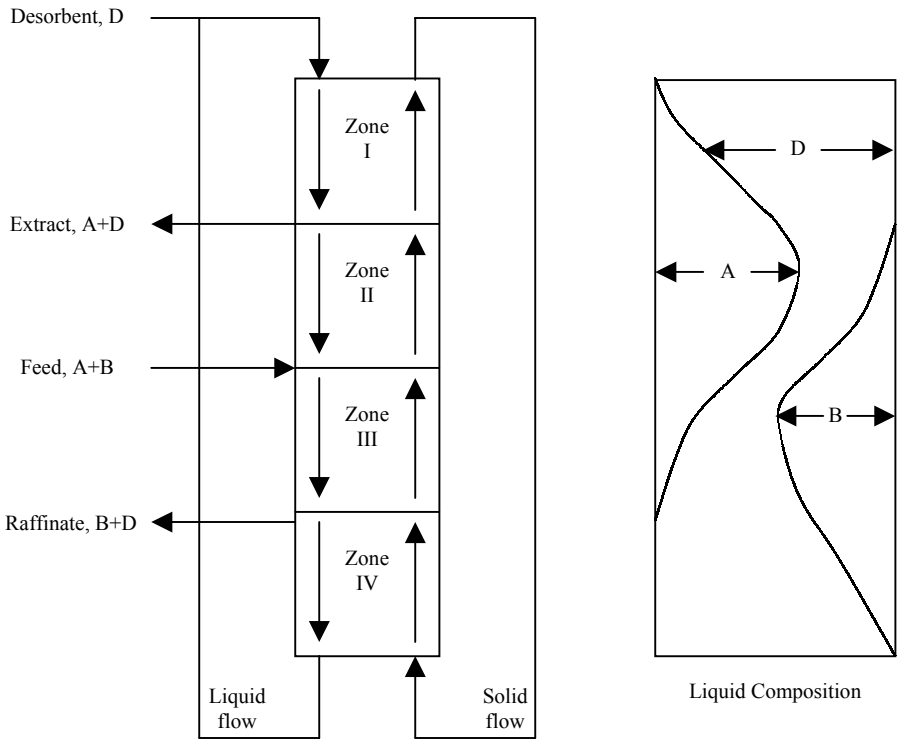

Figure 2.2 Schematic diagram of TMB chromatographic process

The main principle of this system is adjusting the relative velocity between the descending stationary phase and the ascending mobile phases to ensure that the more retained species move down the column and the less retained species move up the column.

Schematic representation of TMB process is depicted in Figure 2.2 for binary separation of species A and B, with A selectively adsorbed in the solid phase. Feed is continuously injected into the middle of the system with two product withdrawal ports: the extract port, rich in the strongly adsorbed species A and the raffinate port, rich in the weakly adsorbed species B. Continuous recovery of relatively pure products is achieved with appropriate regulation of internal liquid and solid flow rates thus eliminating the drawback of species dilution and low adsorbent utilization encountered in batch chromatography.

There exist four intrinsic zones in the bulk of the system and the governing role that allows chromatographic separation of any of two species is detailed as follows:

1. Zone I (Desorption of A), is between point of eluent injection and extract withdrawal. The solid entering zone I contains the more retained component A and as the fresh desorbent D stream flows in the opposite direction with the solid phase, component A are displaced by desorbent and a portion of liquid leaving this zone is withdrawn as extract and the remainder flows to zone II as reflux. In other words, zone I allows solid regeneration.
2. Zone II (Desorption of B), is between point of feed injection and extract withdrawal. At the fresh feed point, the upward flowing solid adsorbent contains the quantity of component A that was adsorbed in zone I. However, the pores will also contain a large amount of B, because the adsorbent has just been in contact with fresh feed. The liquid entering the top of zone II contains no B, only component A and D. In this way, component B is gradually displaced from the pores of A and as the adsorbent moves up through zone II. At the top of zone II the pores will contain only A and D.

3. Zone III (Adsorption of A), is between the point of feed injection and raffinate withdrawal. As fresh feed flows down through zone III, countercurrent to the solid adsorbent flowing upward, component A is selectively adsorbed from the feed into the pores of the adsorbent. At the same time, the desorbent is desorbed from the pores of the adsorbent to the liquid stream in order to provide room for component A in the pores.
4. Zone IV (Desorption of D), is where the feed components in zone III are segregated from extract in zone I. At the top of zone I, the adsorbent pores are completely filled with D. The liquid entering the top of zone IV consists of B and D. It is possible to prevent the flow of component B into zone I and avoid contamination of the extract by properly regulating the flow rate of zone IV.

This TMB approach, despite persistent work on moving system of this type, suffers from mechanical problem such as inconsistent flow caused by solids circulation, low mass transfer coefficient at uneven column packing, solid attrition due to shear forces and low mobile phase velocities to prevent bed fluidization. Low temperature distillation replaces this technique due to economical consideration after all.

In further development, the solid bed is kept stationary in practical applications and the continuous movement of solid phase is simulated by a periodic shift of inlet and outlet ports in the direction of mobile phase flow yielding Simulated Moving Bed Chromatography as described in the following sub chapter.

2.2.3.2. Simulated Moving Bed Chromatography

The SMB concept was introduced to solve practical difficulties arising from mechanical problem: solid movement in a transient TMB unit. It is a technical realization of a countercurrent adsorption process in which the counter-currency between mobile and stationary phases is accomplished without physical movement of the solid. The essential element in SMB operation is rotary valves (Broughton and Gerhold, 1968) or a number of conventional two-way valves (Marteau et al., 1994), which allows periodic shifting the position of feed, desorbent, extract and raffinate lines along the bed, and a pumparound pump to circulate liquid through the adsorbent chamber. The specific location of inlet (feed and desorbent) and outlet ports (extract and raffinate) divide the entire system into four zones, each assuming a certain role. In general, most of the benefits of a countercurrent operation can be achieved by subdividing the adsorbent into a number of static beds and regularly moving all inlet and outlet ports simultaneously one column forward in the direction of liquid flow at fixed time interval.

An SMB-plant consists of a number of chromatographic columns (usually 8 - 24) the input streams to which are switched periodically in order to approximate the countercurrency in true moving bed chromatography. In the limit of an infinite number of columns and short switching periods, the operating mode comprises a real countercurrent process. The operation of an SMB process is complicated and requires a careful choice of many parameters, in particular of the various flow rates and of the switching times. The process has nonlinear dynamic characteristics and it may drift away slowly such that after some hours, a breakthrough of a substance in the wrong stream will occur. As the SMB process is using little energy and can separate difficult mixtures, e.g. substances which

only differ in the geometric orientation (left and right hand molecules), it is becoming popular as a separation technique for low volume high price chemicals.

In the latest development, chemical industry has developed numerous processes based on the use of adsorption and some of the most recent ones are based on the use of chromatographic principles. This is the case of separation process based on the simulated moving bed principle. Initially developed for the extraction of a few specific compound from complex mixtures, such as paraxylene from reforming streams or fructose from corn syrup, these processes are beginning to compete with the simple processes evolved from direct scaling up of the lab procedures. Currently, overloaded elution for production rates below 500 ton/year and simulated moving bed for production rates above 10.000 ton/year are dominating the field, apparently leaving a serious gap in between.

The schematic diagram of SMB operation loop can be visualized in Figure 2.3 below:

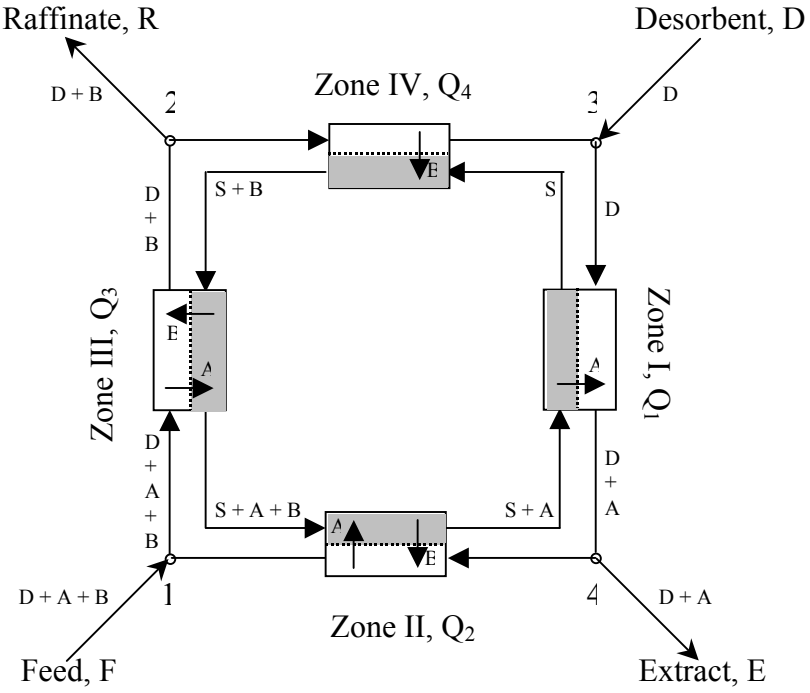

Figure 2.3 Adsorption-desorption diagram of SMB process

The general case of simulated counter-current process is that the movement of solid is simulated by successive switching of the feed and product positions at timed interval. The hypothetical velocity of solid phase is the ratio of length of column of each section and the switching time. The process shows a cyclic behavior, in the absence of disturbances, in which the profile at the end of the interval is equal to that at the beginning of the interval shifted one column in forward direction. In general, the simulated system does not reach a steady state in the time interval between successive switching due to the disturbances introduced each time a switching is made. The stationary regime of this process is a cyclic steady state, attained after several switching, in which an identical transient during each period between two valve switches takes place in each section. The system exists at a new transient behavior regardless of the state of the system had been in just before the switching.

The installation allows a continuous production by chromatographic separation by simulating the displacement of the counter-current bed of the eluent phase. The simulation is done by sequenced displacement of the injection points, from one column to another, upstream to the eluent phase. During this lapse of time, the chromatographic profile migrates in the same direction as the fluid inside the separator. A pseudo steady state mode allows continuous collection of raffinate and extract at specified yield and purities.

The desorbent liquid is selected so as to possess a boiling point significantly different from those of the feed components. The desorbent must also be capable of displacing the feed components from the pores of the adsorbent and conversely, the feed components must be able to displace the desorbent from the pores of the adsorbent. Therefore the desorbent must be chosen in such a way to be able to compete with the feed components

for any available active pore space in the adsorbent, solely on the basis of concentration gradients.

The actual liquid flow rate within each of the four zones is different, due to injection and withdrawal of the net streams. Both the concentration profiles as well as the zones position moves toward the adsorption chamber. The overall liquid circulation rate is controlled by the pumparound pump, which should operate at four different flow rates, depending on which zone is passing through the pump.

Even though SMB lends itself to production scale better than elution chromatography due to its continuous operating modes, it requires more development time and is sensitive to dead volume effects which must be accurately quantified and modeled (Schulte and Strube, 2001). Despite these disadvantages, several contract manufacturers and pharmaceutical companies such as Novasep, UPT and Merck have invested heavily in SMB technology, treating it as cost effective production scale enantioseparation technique (Juza et al., 2000; Francotte, 2001; Schulte and Strube, 2001).

2.3. Application of SMB Technology

Preparative chromatography is gaining more interest from wide range of industry both for product development as well as commercial production. It can be classified into two categories: batch or continuous modes. Even though the batch or elution chromatography mode has found the largest number of applications up to now (Colin et al., 2001), SMB chromatography as a continuous process is more attractive due to its advantages in terms of productivity and eluent consumption (Nicoud et al., 1993; Schulte et al., 1996) or in terms of chiral stationary phase (Rekoske, 2001).

Most applications of SMB process are developed with liquid mobile phases but extensions to gas phase (Mazzotti et al., 1996a; Tonkovich and Carr, 1996; Biressi et al., 2000a) and supercritical liquids (Depta, et al., 1999; Denet et al., 2001) were reported. The main advantage of gas phase operation is higher effective selectivity of the adsorbent since the non-selective hold-up in the macropores is very much smaller (Morbidelli et al., 1986) but higher energy cost and axial dispersion might shift the application to liquid phase operation. Both cases, however, are of great importance to industry and academic research since the separated mixture is solvent free, thus avoiding further post-processing operations.

The SMB process is applied over a wide range of product including petrochemical, food/flavor/fragrance, biotechnology, pharmaceutical and fine chemical with scale of the processes differs by several orders of magnitude. Brief applications of this technology will be discussed in the following section.

2.3.1. Petrochemical Industry

The fundamental work of Broughton (UOP, Des Plaines, IL, USA) in the early 1960's (Broughton and Gerhold, 1961) had opened the application of SMB chromatography in the petrochemical industry in which several million tons of product per year are produced using mainly zeolites as the solid phase thereafter. It was patented as the Sorbex process for the separation of *para*-xylene from C_8 hydrocarbons mixture on 100000 tons/yr scale. Recent application of this technology in the area of petrochemical industry includes the fractionation of C_5-C_6 paraffin (Mazzotti et al., 1996a) and the product separation of both

Table 2.3 Moving bed application in petrochemical industry

No.	Process	Application	Adsorbent	Contacting system	Regeneration	References
1.	Hypersorption	C_2H_4 from refinery gas	Activated carbon	Dense moving bed	Stream stripping	Berg, 1946, 1951 Kehde et al., 1948
2.	Arosorb	aromatics and saturates separation from cracked naphtha	Silica gel	8-column SMB	Displacement (pentane desorbent)	Eagle and Rudy, 1950
3.	Aromax	*para*-xylene from C_8 aromatics	X or Y zeolite	3-section SMB cascade	Heavy aromatic desorbent	Otani, 1973
4.	Molex	linear/branched paraffins	5A zeolite	Sorbex	Light naphtha desorbent	Broughton, 1968 Broughton and Carson, 1969
5.	Olex	Olefins from saturated isomers	CaX or SrX	Sorbex	Heavy naphtha	Broughton and Berg, 1969
6.	Parex	*para*-xylene from C_8 aromatics	Sr-BaY K-BaX	Sorbex	*para*-diethyl benzene	Broughton et al., 1970
7.	Ebex	Ethylbenzene from C_8 aromatics	NaY	Sorbex	Toluene	De Rosset et al., 1978

linear chain hydro-carbons from branched and cyclic hydrocarbon as well as alkenes from alkanes.

The Sorbex process developed by UOP for numerous industrially separation works on the same principle as the SMB system even though the actual configuration is somewhat different. Instead of being contained in discrete beds separated by switch valves, the desorbent is contained in a single bed with subdivision into several sections. Brief information about Sorbex family processes are tabulated in Table 2.3 summarizing its application in petrochemical area.

Another adaptation of SMB chromatography is used in converting natural gas into useful chemical feedstock. Tonkovich et al. (1993) used simulated countercurrent moving bed chromatographic reactor (SCMCR) in the oxidative coupling of methane to form ethane and ethylene (C_2). In general, it is difficult to obtain C_2 yields in excess of 20 to 25% but the rapid separation of oxygen, methane and C_2 products that occur in the SCMCR gives 65% methane conversion, 80% C_2 selectivity and C_2 yield slightly better than 50% with Sm_2O_3 catalyst at temperature about 1000 ºK.

2.3.2. Food and Flavor Industry

The very first application of chromatography is in the extraction and purification of complex mixtures of vegetal origin (Tswett, 1954). Nevertheless, chromatography has been identified as very expensive separation process and therefore its application is limited to the separation of biomolecules, where no other methods were suitable. Continuous effort on making chromatography as a powerful separation method has led to SMB chromatography, which can produce even low-value product at very good economy.

Most carbohydrates such as glucose, fructose, etc are chiral and chiral biological receptors might interact differently with the two enantiomers of a chiral flavor, fragrance or drug thus resulting in a different biological activity. For example, one enantiomer of limonene tastes like an orange while the other tastes like lemon. One enantiomer of vitamin C is an antioxidant, where as the other has almost no effects on human. The success of SMB chromatography in handling the separation of very difficult mixtures has paved the way to its application in food industry. This took place shortly after the famous merit in petrochemical industry when industrial plants started to use Sarex process (Broughton et al., 1977), the Sorbex version for fructose-dextrose separation, since 1977.

Many publications about carbohydrate separation using SMB process with regard to modeling, simulation and design strategies (Ching and Ruthven, 1985a, b, 1986; Hassan et al., 1995; Ma and Wang, 1997; Wooley et al., 1998; Azevedo and Rodrigues, 2001). Fructose-glucose systems have linear isotherms over a wide concentration range that they act as suitable test mixture for development of analytical and numerical solutions for performance prediction and design purposes. Most of the experimental investigation in fructose-glucose separation (Hashimoto et al., 1983a; Ching and Ruthven, 1985b, 1986; Mallman, 1998) used twelve columns more than 1 m to overcome or accommodate mass transfer resistance and dispersion effects into single non-ideality parameter.

A comprehensive summary of SMB chromatography in the food industry are given in Table 2.4, particularly in the production of mono- and oligosaccharides (Kawase et al., 2001). Another development includes the use of pseudo-simulated moving bed chromatography in the production of raffinose from beet molasses (Sayama et al., 1992) and in

Table 2.4 Moving bed application in food industry

#	Application	Raffinate Product	Extract Product	Adsorbent	Contacting system	Desorbent	References
1.	Fructose from glucose-fructose	Glucose	Fructose	Ca^{2+} resin	8-column, 4-section SMB	Water desorbent	Gembicki et al., 1997
2.	Fructose from glucose-fructose	Glucose	Fructose	CaY	Sorbex	Water	Broughton et al., 1977 Bieser and de Rosset, 1977
3.	Fructose from glucose-fructose	Glucose	Fructose	Ca^{2+} resin	3-section SMB	Water	Barker and Ching, 1980
4.	Xylose-arabinose from xylose-arabinose-glucose	Xylose	Arabinose	Ca^{2+} resin	4-zone SMB	Water	Balannec and Hotier, 1993
5.	Glutathione-glutamic acid	Glutathione	Glutamic acid	H^{+} resin	4-zone SMB	HCl	Maki, 1993
6.	Trehalulose-fructose	Trehalulose	Fructose	Ca^{2+} resin	12-column, 4-zone SMB	Water	Nicoud, 1998
7.	Lactosucrose production	Lactosucrose	Glucose	Cation exchange resin	12-column, 4-zone SMBR	Water	Kawase et al., 2001
8.	Dextran-fructose	Dextran	Fructose	Ca^{2+} resin	12-column, 4-zone SMB	Water	Coelho et al., 2002

the recovery of raffinose, sucrose, glucose and betaine from beet molasses mixture (Masuda et al., 1993).

Application in flavor industry involves the use of integrated reaction-separation in a SCMCR or SMBR unit. The widest class of reaction to which reactive chromatography can be applied is esterification reaction, either catalyzed by acidic ion exchange resins (Sardin and Villermaux, 1979; Kawase et al., 1996; Mazzotti et al., 1997b) or by immobilized enzymes (Mensah and Carta, 1999; Migliorini et al., 2000). These applications utilize polarity difference between the two products, ester and water, for separation on many different adsorbent.

2.3.3. Pharmaceutical and Fine Chemical Industry

The healthcare sector has recently outperformed the overall market in an unfavorable market environment. One of the reasons behind this development is that industry leaders have given solid results. Another positive sentiment regarding the industry is that many analysts see an increase in drug application and approvals due to delay of several new drugs in the previous years. While most of these drugs are synthesized stereospecifically, the advent of powerful analytical and process scale separation techniques gives downstream process developers more options when the drugs are still in research pipeline. These options allow drug companies to evaluate a greater number of potentially less expensive synthesis methods and can present significant cost savings in the overall drug discovery process (Juza et al., 2000).

Crystallization serves as the cheapest available method in general thanks to its low energy consumption and only enantiomerically pure seed crystals are required (Profir and

Table 2.5 Chiral separation on SMB technology

#	Synthetic name, 'trade name', therapeutic or substance class	Column number and size (length x ID, mm)	CSP and mobile phase	Amount of CSP (g)	Selecti-vity (approx)	ee (%) in extract	ee (%) in raffi-nate	Specific productivity (kg/kg/day)	References
1.	5,6,11,12-Tetrahydro-2,8-dimethyl-5,11-methanodibenzo[b,f][1,5]diazocin, 'Tröger base', chiral nitrogen model compound	8 (250 x 4.6)	MCTA Ethanol	15	2.0	97.4	96.4	0.006	Seebach et al., 1998
2.	(1-Aza-bicyclo-[2,2,2]-oct-3-yl)-methoxyimino-acetonitril, agonist at muscarinic receptors	8 (105 x 26)	Chiralpack AD Hexane/isopropanol (95:5, v:v)	240	1.9	97.8	99.5	0.260	Guest, 1997
3.	2-[(Dimethyl-amino)-methyl]-1-(3-methoxy-phenil)-cyclohexanol, 'Tramadol', analgesic	12 (100 x 21.2)	Chiralpack AD Benzene/isopropanol/diethylamine (95:5:0.1, v:v:v)	240	2.1	99	>99.8	0.600	Cavoy et al., 1997
4.	5-(1,2,3,4-Tetra-hydro-quinoline-6-yl)-6-methyl-3,6-dihydro-1,3,4-thiadiazine-2-one, 'EMD53986', pharmaceutical intermediate	8 (54 x 26)	Chiraspher Ethyl acetate/ethanol (95:5, v:v)	90	3.3	99	73.8	0.17	Devant et al., 1997

Table 2.5 Chiral Separation on SMB Technology (Cont'd)

5.	3-(2-Methoxy-phenoxy)-1,2-propane-diol, 'Guai-fenesin', antitussive	16 (60 x 21)	Chiralcel OD Heptane/ethanol (65:35, v:v)	201	2.4	98.8	99.2	0.080	Francotte and Richert, 1997
6.	(E)-(3R,5S,6E)-7-[2-Cyclopropyl-4-(4-fluoro-phenyl)-quinolin-3-yl]-3,5-dihydroxy-6-heptenoic acid, 'DOLE', pharma-ceutical intermediate	8 (100 x 100)	Chiralcel OF Hexane/isoprop anol(50:50, v:v)	3770	1.35	94.4	99.4	0.270	Nagamatsu et al., 1999
7.	2,2'-Dihydroxy-1,1'-binaphtol, intermediate for chiral catalysts	8 (105 x 26)	DNBPG Heptane/isopro panol (72:28, v:v)	250 (ml)	1.4	89	97.8	0.03 (kg/l/day)	Pais et al., 1997b
8.	D,L-Threonine, amino acid	12 (1000 x 25.4)	Chirosolve-L-proline Acetic acid (0.05 M) Copper acetate (0.125 μM)	2800 (ml)	1.6	98	98	0.005 (kg/l/day)	Fuchs et al., 1992a
9.	2-Chloro-1-(difluoromethoxy)-1,1,2-trifluoro ethane, 'Enflurane', 'Ethrane' inhalation anesthetic	8 (800 x 15)	γ-Cyclodextrin nitrogen	280 (ml)	1.34	98.4	98.4	0.026 (kg/l/day)	Juza et al., 1998

Matsuoka, 2000). It is usually used in the generic drug market where manufacturing cost pressures are important and large quantities of stereoisomers are being processed (Mc Coy, 2001). Though enantioselective chromatography is more expensive, it consumes less time than crystallization and is readily scaleable to production levels from analytical data. Mostly there are two techniques in production scale enantioseparation namely batchwise and simulated moving bed (Francotte, 2001).

The application of SMB chromatography in the area of pharmaceutical is tabulated in Table 2.5 (Juza et al., 2000). Even though most of the SMB applications in pharmaceutical area have been conducted in liquid phase, the gas phase enantioseparation has been performed (Juza et al. 1998). A modified pilot unit designed for the separation of hydrocarbons was used for the separation of the enantiomers of the chiral inhalation anesthetic enflurane but they end up with low productivity and purity due to high operating temperature (T = 50 ºC). Relatively high purity can only be obtained for one outlet stream but complete separation (both pure outlet streams) has never been obtained. They, however, demonstrate that appropriate GC-SMB separation performance can be attained by properly adjusting the flow rate ratio, m_2-m_3.

A capillary electrophoresis study for the separation of Piperoxan enantiomers based on difference in electrophoretic mobilities may be the latest application analog to SMB technology in the area of enantioseparation. Thome and Ivory (2002) used sulfated β-cyclodextrin as chiral selector to optimize the buffer conditions, which produce the maximum peak separation time between the two enantiomer of Piperoxan, and chiral selector concentration. They find out that the enantiomers can be forced to move counter-currently within the vortex stabilized apparatus by imposing a fluid flow opposite the

direction of electromigration. Relatively pure enantiomer can be collected by configuring the vortex stabilized electrophoresis apparatus with a feed port at the middle of the chamber axis and offtake ports near the cathode and anode.

2.3.4. Protein Separation

All amino acids, with the exception of glycine, are chiral in nature. Another example of chiral protein is the essential component of life itself, such as proteins and DNA. They are constructed from optically active building blocks. However, it is remarkable (although not yet fully understood) that, contrary to artificially synthesized molecule, all naturally occurring amino acids in living organisms have the same handedness. Chromatography has been proven to be the important protocol for purification of difficult molecules like protein, particularly pharmaceutical protein, at production scale due to attainable high purity level.

Simulated moving bed chromatography has been employed for fractionation of various small volume expensive compounds like biotechnological and pharmaceutical products. It has been successfully applied in the purification of monoclonal antibodies (Gottschlich and Kasche, 1997), separation of amino acid (Maki, 1993; van Walsem and Thompson, 1997; Wu et al., 1998), and antibiotics (Jensen et al., 2000). Advantages of SMB include higher efficiency during separation of like molecules and reduced both solvent as well as buffer consumption (Jensen et al., 2000).

Most published work on protein chromatography was largely concerned with process description. There are four different types of chromatography in the area of protein separation: ion-exchange chromatography, affinity chromatography including hydrophobic

interaction chromatography, size exclusion or gel filtration chromatography and reversed phase chromatography. These techniques can be used alone or in combination at different stages of the process. Reversed phase chromatography is the least commonly used because the organic solvent, which is added to the aqueous element, tend to denature the protein. Size exclusion chromatography is the most often used but it is unable to separate protein of different charge, unless they are of different size.

Size-exclusion chromatography remains a regular technique in the production of biopharmaceutical proteins (Leaver et al., 1987). It is a low efficiency technique due to limited selectivity of the resin material for the target protein or contaminants. High resolution can be attained by using larger ratio of sorbent material to feed volume to overcome the small differences in the distribution coefficients of each component. Product dilution is common and recycling of product fractions is needed to achieve high purity at reasonable yield and this will lead to increased desorbent and resin consumption.

Size-exclusion chromatography in SMB has been applied both in the fractionation of dextran polymers (Ruthven and Ching, 1989) and modeling/optimization of protein separation (Houwing, 2003) as well as in the desalination of a single protein feed stream (Hashimoto et al., 1988). Gottschlich and Kasche (1997) used affinity SMB chromatography to isolate antibodies at 90% yield. They concluded that the recovery of two zones SMB depends on extract purity and the addition of two purging steps between adsorption/desorption steps can increase yield. Reversed-phase SMB chromatography has been used by Jensen et al. (2000) to optimize the purification of nystatin and the separation of bovine insulin in terms of solvent consumption while ion-exchange SMB chromatography has been used for process fine-tuning (van Walsem and Thompson,

1997; Houwing et al., 2002b), modeling (Houwing et al., 2002b, 2003) and optimization (Houwing et al., 2002a).

There are two different operating modes for protein separation using SMB chromatography: the isocratic mode (Houwing et al., 2002a, 2003) and the gradient mode (Jensen et al., 1997; Houwing et al., 2002a, 2002b, 2003). The main difference relative to isocratic operation is that the salt concentration (Houwing et al., 2002b, 2003) or solvent strength (Jensen et al., 2000) is increased during the separation, either gradually or step-wise. Yu and Wang (1989) had previously developed a general rate equation model to simulate the column dynamics in which the effects of axial dispersion, film and intraparticle diffusion, size exclusion, non-linear isotherm and variable separation factors were incorporated. The model gives good prediction with experiment result and extendable to ion exchange, adsorption and size exclusion systems. Scaling up procedure should be considered after such a preliminary work in this area.

2.4. Optimization of Simulated Moving Bed

SMB chromatography was developed in order to minimize the amount of solvent waste generated and maximize process throughput per gram of resin by eluting multiple column simultaneously and recycling the eluent. Nowadays, the development and optimization of SMB process usually start after the choice concerning suitable mobile and stationary phases has been made. Then the established theories are adapted to identify attractive operating conditions (Ruthven and Ching, 1989; Charton and Nicoud, 1995; Mazzotti et al., 1997a; Ma and Wang, 1997; Heuer et al., 1998; Gentilini et al., 1998; Zhong and Guiochon, 1996, 1998)

Process industry is usually aimed at maximizing production capacities while at the same time improving or at least, maintaining the product quality. Trade-off between the two requirements often exists and this phenomenon is particularly true and not avoidable in enantiomeric separation using simulated counter-current chromatography (Strube et al., 1999), where product purities are crucial due to relatively stiff regulatory specification.

High product purity is particularly the most critical requirement in drug manufacture. In the simulated countercurrent enantiomeric separation of SB-553261 and 1,1′-bi-2-naphtol racemates, some variable contradict with each other. Operating conditions may be used as decision variable to optimize one performance parameter yet at the same time it turns out to be unfeasible on the basis of different considerations. In this case, optimal design of SMB process was explored for both throughputs as well as desorbent consumption rate and product purity.

2.4.1. Optimization Algorithm

A comprehensive optimization study using a state-of-the-art optimization technique, Genetic Algorithm will be carried out in this work. Genetic Algorithm is a non-traditional search and optimization method (Holland, 1975; Goldberg, 1989; Deb, 1995) that is well known in engineering optimization. This algorithm is essentially based on the mechanism of natural selection and genetics involving randomized but structured information exchange and survival of the fittest. It works with a population of points on a probabilistic platform requiring only the magnitude of hypothesis fitness value to evolve the next generation during the search therefore the algorithm does not require gradient information during the search, which may lead conventional algorithm trapped in local optima.

The main principle of Non Dominated Sorting Genetic Algorithm is almost similar to the general Genetic Algorithm. A set of population of chromosome is randomly generated and these chromosomes are sorted into several fronts according to their fitness values. One chromosome is dominated by the other chromosome if their real fitness value is worse than that other chromosome. These inferior chromosomes are then assigned a dummy fitness value which is directly proportional to their real fitness value and inversely proportional to their relative dimensionless distance between that particular chromosome and other chromosome (niche count). These dummy fitness values will help these inferior chromosomes to survive in the roulette wheel selection procedure so they will not disappear in the early stages. Thus, diversity of chromosomes in the mating pool is maintained and the algorithm might not converge to the wrong solution.

The method of Genetic Algorithm used in this project is very versatile and applicable to almost any other engineering applications. The sorting and sharing mechanism introduced in Elitist Non-dominated Sorting Genetic Algorithm (Deb et al., 2002) has paved the way to multi-objective optimization which simultaneously leading to Pareto optimal solution. Pareto optimal solution emerges when there exist two objectives which contradicts one another. Any attempts to improve one objective function will jeopardize the other. The Pareto-set narrows down the choices and helps to guide a decision-maker in selecting a desired operating point (called the preferred solution) from among the (restricted) set of Pareto-optimal points, rather than from a much larger number of possibilities (Bhaskar et al., 2000).

The Elitist Non-dominated Sorting Genetic Algorithm has proved to give better convergence criteria (Deb et al., 2002) as it maintains the concept of elitism in which the

good population is preserved by introducing dummy fitness value and later characterized in several fronts. The best populations are located in the first front and treated as the automatic qualifier for subsequent generation while the fronts of population with lower fitness value is preserved to maintain genetic variety. The recent modification with jumping genes (Kasat et al., 2002) has improved the diversity of hypothetic mating pool leading to much better spreading of solution and increased convergence speed. The jumping gene operations adapt a modified mutation operator, borrowing from the concept of jumping genes in natural genetics. Kasat et al. (2002) used NSGA-II-JG for the optimization of an industrial fluid catalytic cracking unit and reported Pareto optimal solutions in significantly less number of generations.

The optimization study in this project is aimed at improving productivity for certain product purity requirement. A wide variety of other problem can, indeed, be formulated and solved depending upon one's interest.

2.4.2. Optimization Work on SMB

The optimization works in open literature usually describe empirical investigation and few theoretical studies. It is desired that theoretical discussions are able to place empirical observations into proper perspective. In this case, the systematic use of computer program covering various model of SMB chromatography is mandatory for theoretical investigation of optimization problems. The use of numerical approach in optimization is preferred in optimization because experimental investigation is expensive but the model has to be reliable i.e. the physico-chemical data must be carefully quantified (Guest, 1997;

Kaspereit et al., 2002). The selection of suitable model for specific separation should be taken seriously (Ruthven and Ching, 1989; Guiochon, 2002).

The design problem of a SMB process rely on appropriate setting of both internal liquid flow rates in each zone as well as solid flow rate to obtained certain separation task. The process performance is characterized by purity, recovery, solvent consumption and adsorbent productivity. Any optimization work begins with the selection of objective function. The objective function in industrial perspective will be product cost. The common objective function in academic studies is production rate (Guiochon et al., 1994; Biressi et al, 2000). The optimization works reported in literature include single objective and multi objective which will be discussed in the following.

2.4.2.1. Single Objective Optimization

Some studies in the area of simulated moving bed optimization employ single (scalar) objective function by incorporating several objectives with weightage factors (Storti et al., 1988, 1995; Wu et al., 1998; Dünnebier and Klatt, 1999; Karlsson et al., 1999). These approaches, however, is not efficient and has the possibility of losing certain optimal solutions when the non convexity of the objective function arise due to a duality gap, which is difficult to be examined for complex real-life problems.

In the area of pharmaceutical SMB separation, optimization work is started by the study to investigate the best stationary phase and mobile phase combination (Kruglov, 1996; Schulte et al., 1997; Guest, 1997; Kartozia et al., 2002). In particular, Schulte et al. (1997) used specific productivity to compare the performance of different chiral stationary phase and found that this is largely affected by several parameters i.e. selectivity, number

of plates, saturation capacity, particle size, retention, solubility and viscosity. To focus only one or some of these parameters may be misleading and it is difficult to choose optimum combination only from experience. Optimization study of this type serve as good basis for the next study to determine the optimum operating condition for separation i.e. switching time, column number and distribution, volumetric flow rates, column dimension, etc.

Kruglov et al. (1996) carried out optimization on the SCMCR for oxidative coupling of methane after preliminary evaluation on different adsorbent. Hydrophobic carbon molecular sieve is chosen due to its methane storing capability and efficient handling of the OCM effluent separation. They used switching time and methane/oxygen ratio in the make-up feed as decision variable to maximize the overall C_2 selectivity.

Biressi et al. (2000b) proposed an optimization procedure to maximize specific productivity, defined as mass of racemate per unit time and volume of adsorbent, with purity and pressure drop as constraint. The algorithm is used in illustrative non-linear separation in which only three pieces of information is required: adsorption isotherm, Van Deemter equation and one pressure drop equation. Column distribution in each section and feed concentration is fixed during the search while column length and section, internal flow rates and switching time is employed as decision variables. After the optimization study, they also explored the effect of purity constraint, particle size and feed concentration to the optimal design parameter and found out that specific productivity can be increased by lowering purity constraint, using relatively small particle size and increasing feed concentration (in this case asymptotic value of specific productivity will

be reached at elevated feed concentration). Practical reasons avoid the use of these last three parameters as decision variables.

In the field of protein separation, Houwing et al. (2002a) compare the optimum performance between isocratic and gradient operation for azeotropic separation of dilute mixture of bovine serum albumin and yeast protein on Q-Sepharose FF using NaCl as salt (Houwing et al., 1999). In addition to the common objective function appeared in most isocratic operation, i.e. maximizing throughput or minimizing desorbent consumption, they introduced salt consumption as additional objective as a result of gradient operation. The salt may have large implications on the process economy, possibly via environmental regulations. The optimization is carried out numerically using "constr" optimization function in Matlab 5.2. They considered three cases of single objective function including maximization of throughput by changing feed salt concentration, maximization of throughput and minimization of desorbent consumption (both by changing inlet salt concentration) and minimization of salt consumption by changing inlet salt concentration. Inlet salt concentration is actually the salt concentration in the lower sections. Houwing et al. (2003) also performed optimization on protein fractionation, this time by SMB size exclusion chromatography using two objective functions, purity/recovery and productivity.

Dünnebier et al. (1999) have tried a staged sequential optimization algorithm, which consists of two loops: the inner and outer loop, on several case studies like enzymatic sucrose inversion (Meurer et al., 1996) and synthesis of β-phenethylacetate (Kawase et al., 1996) based on SMB process. The inner loop is calculated by direct dynamic simulation in which the constraints are evaluated by integration of elution profiles while the outer

loop is solved by standard SQP algorithm in which the required gradients are evaluated by perturbation methods. Toumi et al. (2002) extend the application of this algorithm to Varicol system in which, like the previous study, two case study were used namely trytophan and phenylalanine separation on a poly-4-vinylpyridine resin (Wu et al., 1998) and glucose-fructose separation on an ion-exchange resin (Jupke et al., 2000). Minimized desorbent and maximized throughput are achieved for the former and latter case confirming the robustness of the algorithm but the selection of cost as objective function limit the applicability of the obtained optimum results because cost is time and site specific.

Toumi et al. (2003) compared the optimum performance of SMB and Varicol process for the separation of propanolol isomers on Chiralpak AD. They used the same optimization algorithm (Dünnebier et al., 1999) which leads to a complex mixed integer non linear program (MINLP). The objective function chosen in the study is the maximization of feed throughput at purity (greater than 98%) and pressure drop constraint (equal to 20 bar). They later verified their finding by performing experiment at the optimal operating point suggested by the study and found that experimental purities were 2-6% less than the prediction. They also highlighted the failure of equilibrium theory used in SMB in predicting the separation behavior of varicol process. The optimization also proved that Varicol allow more production than the conventional SMB process at the same number of column or Varicol need one column less than SMB for the same separation duty due to the flexible switching strategy at small number of column.

2.4.2.2. Multi Objective Optimization

Only a few multi objective optimization studies are reported in the open literature. The first article will be the one reported by Zhang et al. (2002a) in which dominated sorting genetic algorithm is used in numerical optimization of SCMCR process for MTBE synthesis. They used equilibrium dispersive model with linear adsorption isotherm to describe the solute concentration in the solid phase. They executed 3 multi objective cases and found that the selection of operating parameter for SCMCR is not straightforward. The economical operation of an SCMCR process depends on by many factors according to dictating objective and other process specification i.e. purity, conversion, etc.

Zhang et al. (2002b) also reported the first multiobjective optimization in the area of enantioseparation of chiral drug. They used experimentally validated mixing cell model (Ludemann-Hombourger et al., 2000) to simulate and optimize the separation of 1,2,3,4-tetrahydro-1-naphtol racemic mixture. They performed both single and multi objective optimization and compared the performance of SMB and Varicol process. Two cases of multiobjective optimization were presented and it was found that Varicol operation lead to better performance compared to conventional SMB process. Optimum points are explained using equilibrium theory (Storti et al., 1995) by plotting in the m-operating plane.

2.5. Update on Moving Bed Technology

Traditional SMB as a powerful technology undergo incessant modification which brings improvement to its performance. These modification strategies do not breach the essence of countercurrent movement between the two phases and usually is applied to

further enhance the separation power, efficiency and applicability by incorporating reaction (SMBR), increasing process flexibility (Varicol), changing process geometry (ternary SMB and pseudo SMB) and applying gradient mode of operation (SF-SMB) which will be discussed in the following overview.

2.5.1. Reactive SMB

The concept of simultaneous reaction and separation might be the first introduced to SMB system as early as 1960's by the work of Roginskii et al. (1961) and Magee (1963). The idea emerged to overcome the limitation of a reversible reaction where conversion rate is dictated by chemical equilibrium in which Gibbs free energy is at the minimum at a given temperature. Reactive distillation processes for examples have gained strong interest in the chemical industry, particularly in the production of ester (Agreda, 1986), ether (Isla and Irazoqui, 1996) and alcohol (Gonzales and Fair, 1997; Gonzales et al., 1997). Another way to integrating reaction and separation is to combine a chemical or biochemical reaction with a chromatographic separation.

Reactive SMB is a realization of unit operation which ability to accommodate continuous reaction with countercurrent contact for enhanced separation. It enables increased conversion, direct collection of pure products and driving the selectivity of a complex reaction (Falk and Seidel-Morgenstern, 1999). This device work under similar principle with SMB, the only difference is the composition of the feed (usually reactant at certain stoichiometric ratio) and the duality function of the stationary phase (as adsorbent and catalyst). The application of reactive simulated moving bed has been reported for more than two decades ago when Zabransky and Anderson (1977) conducted zeolite

catalyzed alkylation reaction. Different types of reaction is also reported: isomerization A ↔ B (Hashimoto et al., 1983b), decomposition reaction A ↔ B + C (Fricke et al., 1999), esterification A + B ↔ C + D (Mazzotti et al., 1996b; Kawase et al., 1996, 2001), alkylation A + B ↔ C + D (Kawase et al., 1999) and (de-)hydrogenation A + B ↔ C (Ray and Carr, 1995)

Various applications, in term of system phases, have been reported both in the gas phase as well as in the liquid phase. Gas phase operations include the oxidative coupling of methane to form C_2 products (Tonkovich et al., 1993; Tonkovich and Carr, 1994). Another example will be in the hydrogenation of mesitylene (Ray and Carr, 1995; Bjorklund and Carr, 1995) in which better conversion relative to fixed bed system is achieved. Here, the more retained component is obtained from an auxiliary purge step without recycling the effluent stream to other sections in the unit. In most cases above, the reactive SMB is packed with two different solid particles, either mixed or layered, one serves as catalyst and the other as selective sorbent. Dual role resin, with ability to act as catalyst and adsorbent, is later commercialized in favor of liquid phase application.

Liquid phase reactions extend from acetic acid esterification catalyzed by sulfonated ion-exchange resins (Amberlyst 15). Mazzotti et al (1996b) used four section reactive SMB, in which one of the reactant (ethanol) is used as solvent, under open-loop conditions with pure acetic acid in the feed. They observe complete conversion of acetic acid with good separation of the reaction products. This system exhibits a rather rich dynamic behavior (Mazzotti et al., 1997b) due to the dual role played by the resin, as a catalyst and as a selective sorbent. Kawase et al. (1996) used the same stationary phase for esterification of phenethyl alcohol but this time a non-reactive solvent, 1,4-dioxane, is

used. They come up also with complete conversion and product withdrawal in pure but diluted form. Other liquid phase applications reported in literature is the production of resin intermediate (Kawase et al., 1999) and oligosaccharide (Kawase et al., 2001) using 3- and 4-zone SMB respectively.

2.5.2. Ternary and Pseudo-SMB

Ternary and pseudo SMB are essentially an attempt to overcome the limitation of classical SMB process, i.e. inability to separate multi component mixtures, by applying flow rate/column/sequence adjustment but still maintaining SMB framework. There are four different types of modification reported in literature. The first is done by alternating two different adsorbents in the four zones configuration (Hashimoto et al., 1993) for the separation of starch-glucose-NaCl mixture or by varying working flow rates with respect to time within a switching period (Kearney and Hieb, 1992).

The second type of modification consists of adding a fifth zone and modifying the elution strength within the five zones (Nicoud, 1999) or keeping the same desorbent within the entire configuration (Navarro et al, 1997). The third type will be feed discontinuity and switching column adequately (Ching et al., 1994; Masatake and Tamura, 1996; Mata et al., 2001). The last type consists of having two SMB combined in a single unit (Kim et al., 1992; Chiang, 1998; Wooley et al., 1998, Nicolaos et al., 2001).

Navarro et al. (1997) used ternary SMB of type three in the simulation of sorbitol-xylitol-mannitol mixture separation. In this case, sorbitol is withdrawn as extract product, xylitol as intermediate and mannitol as raffinate. They use axial dispersed flow model for 5 zones SMB (as depicted in Figure 2.4) with 1/2/2/2/1 configuration. With individual

feed concentration used in the simulation is 100 g/l each, they can achieve theoretical purities of 58%, 38% and 94% of extract, intermediate and raffinate respectively. Their work, however, still need to be validated experimentally.

Nicolaos et al. (2001) proposed ternary SMB with 4 different configurations for multicomponent mixture of M compound. Figure 2.5 correspond to 4+4 zone, 5+4 zone, 8-zone and 9-zone equivalent TMB configuration. These configurations are defined for KEY=1 in which component 1 is separated from the (M-1) component in the mixture. They assessed the performance of each configuration under certain objectives, i.e. minimum specific solvent consumption and maximum productivity for a given pressure drop, and found that the 5-zone TMB alone and the 8-zone TMB are unable to produce three pure compounds at a time. It was shown that 5+4 zone SMB is the most suitable in which the most difficult separation has to be performed by the second TMB. This might be attributed to different solid recirculation rate in the dual SMB.

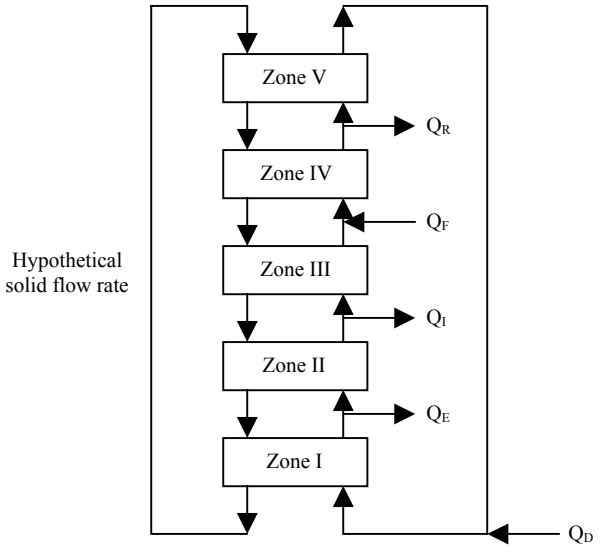

Figure 2.4 Ternary SMB with 5-Zone configuration

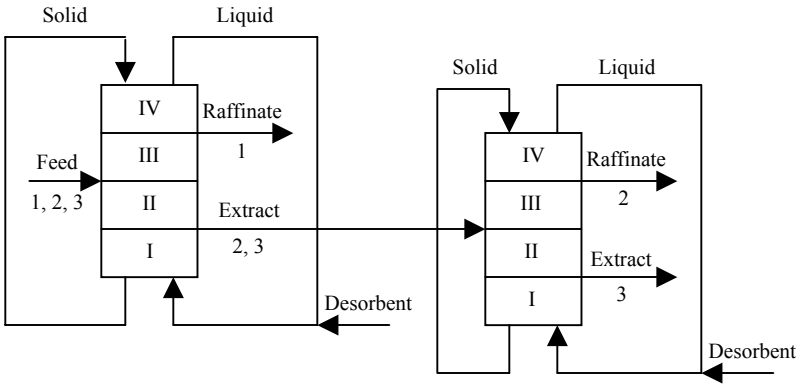

4+4 Zone TMB

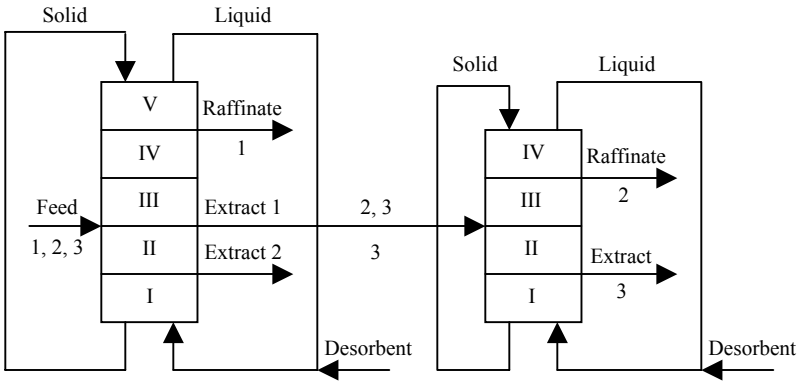

5+4 Zone TMB

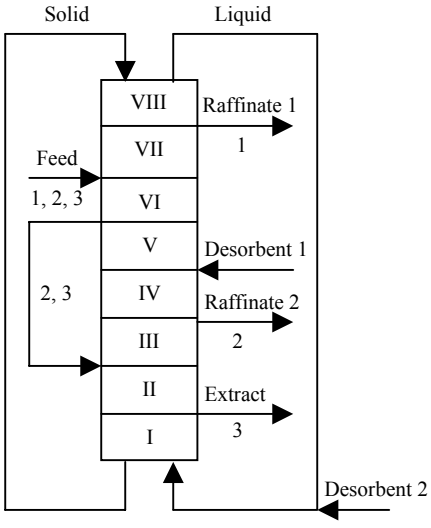

8 Zone TMB

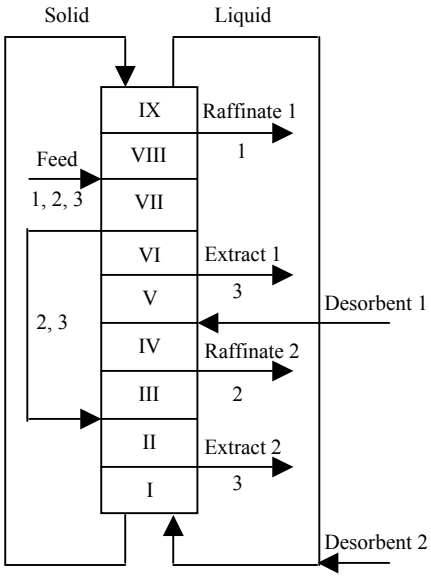

9 Zone TMB

Figure 2.5 Ternary multi zone SMB configuration

Another type of modification which belongs to the third type is pseudo SMB process. Pseudo SMB process is initially applied in sugar industry when Sayama et al. (1992) recover raffinose from beet molasses. The application was extended to multi component mixtures containing raffinose, sucrose, glucose and betaine (Masuda et al., 1993). The process is patented as JO SMB process and applied by the Japan Organo Company.

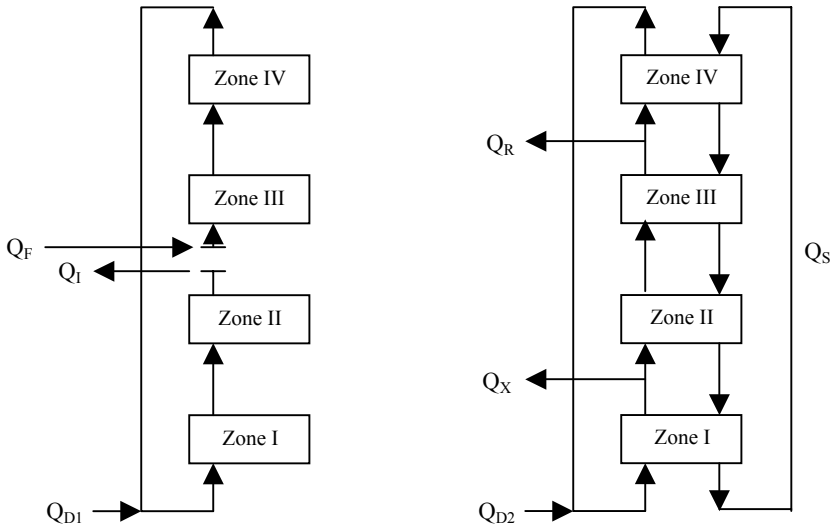

Figure 2.6 Pseudo 4-zone SMB configuration (JO process)

The cyclic process is split into two main steps as described in Figure 2.6 based on 4-zone TMB process. The first step consists of feed (Q_F) and desorbent (Q_{D1}) injection with continuous withdrawal of intermediate component B (Q_I) without solid recycling. The second step involves the recovery of the less retained component A and more retained component C in the raffinate and extract streams respectively at certain solid recycling rate, Q_S. Desorbent is supplied, at different flow rate from that of the first step (Q_{D2}), in the absence of feed. Component B is located downstream of the feed point at the end of this step. The development of concentration profile is visualized in Figure 2.7 as follows:

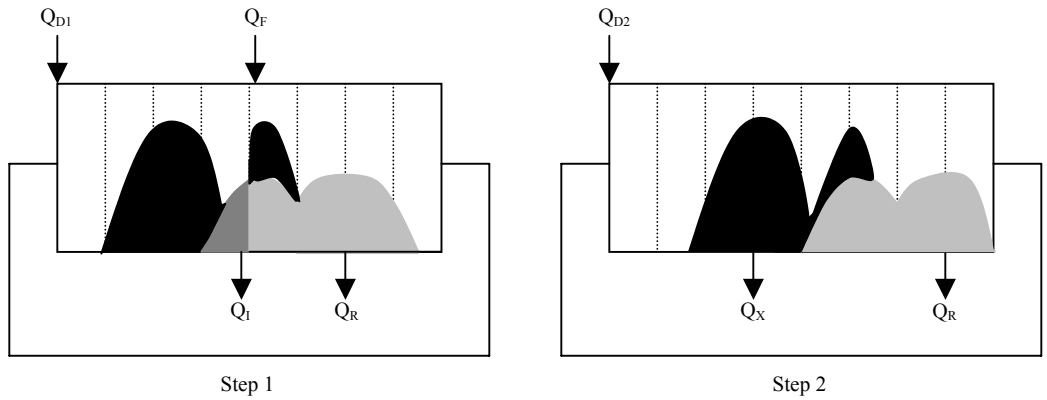

Figure 2.7 Pseudo 4-zone SMB concentration profile (JO process)

Mata et al. (2001) performed modeling and simulation of pseudo SMB for the separation of undisclosed ternary mixture. The first step is modeled as a series of preparative chromatographic column while the second step is modeled as pseudo TMB without feed. All internal flow rates were calculated based on propagation velocity of species concentrations and system constraints. They analyzed the effect of operating conditions (during step 1 and 2) and mass transfer coefficient on the process performance.

2.5.3. Supercritical Fluid-SMB Chromatography

The idea to use pressure gradient in SMB operation derived from fact that each zone of the unit plays different separation role and tuning elution strength in different zones in the unit can enhance separation performance. The working principle in SF-SMB operation is decreasing pressure gradient along the four zones of a SMB unit under supercritical condition to decrease elution strength. It is desired to apply highest pressure in zone I, whose task is to ensure complete regeneration of desorbent, because maximum desorbent strength is needed to elute the more retained component from the mobile phase. The concept has been observed for linear chromatographic conditions in which Henry's

constant of solute decreases as density of supercritical desorbent increases (Luffer et al., 1990) and for non-linear competitive condition (i.e. overloaded column) in which density of supercritical desorbent increases as adsorbed loading decreases. SF-SMB operation enables the use of pressure gradient throughout specific zones of the simulated moving bed thus adsorption is not depending on mobile phase only but also on the applied pressure.

Mostly CO_2 is used as mobile phase in subcritical (Fuchs et al., 1992b) and/or supercritical chromatography due to its low viscosity resulting higher column efficiency and ability to perform separation at increased flow rates. Other reasons include its low economical value, non-toxicity and non-flammability. CO_2 possess the potential to substitute organic solvents which is relatively more harmful in processing products related to human use i.e. food and pharmaceutical industry. SF-SMB operation also enables product withdrawal free of desorbent as the gaseous desorbent can be recycled after liquefaction in a condenser.

The coupling of supercritical fluid chromatography with SMB chromatography, however, is started by Clavier et al. (1996) when they successfully separate γ-linolenic ethyl ester (GLA) and docosahexaenoic ethyl ester (DHA) on C_{18} bonded silica by applying pressure gradient from 174 bar (in zone I) to 138 bar (in zone IV). In their operation, it is desired to apply the maximum elution strength in zone I, in which desorption of the more adsorbed component takes place, and minimum elution strength in zone IV, in which the less adsorbed component must be retained by the stationary phase. They varied the adsorption strength of the mobile phase by playing with pressure in the zones of SMB to enable higher feed load therefore increasing productivity. This is

because steeper fronts of internal concentration profile are achieved by pressure gradient operation.

An important factor to evaluate the choice of mobile phase for SF-SMB operation is the dependence of the solvation power to temperature and pressure. In supercritical region, the solvating power is a function of temperature and pressure and so is the affinity of a given solute to that particular supercritical fluid. The affinity of that solute for a given stationary phase is also a function of temperature (Perrut, 1994). The SF-SMB system is judged to be less feasible, relative to isocratic, if the solvation power is independent of temperature and pressure (for linear system) or pressure and modifier concentration (for non linear system). Denet et al. (2001) have shown this phenomena when they use SF-SMB to separate the isomers of tetralol (1,2,3,4-tetrahydro-1-naphtol, a chiral pharmaceutical intermediate. They observed strong impact on separation performance even though the absolute change in selectivity, defined as the ratio of Henry's constants of the two enantiomers, is relatively small. This is due to low separation factor (about 1.1) assuring SF-SMB is absolutely useful for this kind of separation. Productivity can be increased by almost three times, in comparison with isocratic operation, by rationalizing the unit behavior using triangle theory under linear and non-linear condition.

Rationale between SF-SMB with triangle theory is performed under linear (Mazzotti et al., 1997c) and non-linear systems (Di Giovanni et al., 2001). For linear system, it was found that the pure separation regime for supercritical system is no longer of triangular shape but either a truncated or full rectangle. The size of the regime has been shown to increase indicating that pressure gradient mode is in favor of separation compared to isocratic mode. The coordinates of optimum point (in terms of productivity, solvent

consumption, recovery and enrichment) has also shifted from isocratic optimum point in the direction much further away from the diagonal (Mazzotti et al., 1997c). For non-linear systems, different adsorption isotherm must be used in different zones of the unit. Linear isotherm of Henry's law type is used for low fluid phase concentration while Langmuir competitive isotherm is used for elevated concentration. In the frame of equilibrium theory, it was found that the linear and non-linear pure separation regions have different intersections with the diagonal. The pure separation regime for non-linear condition follows the triangular shape of an isocratic operation, especially at higher feed concentration, while the pure regime for linear condition still has the shape of a rectangle. The size of this region shrinks with increasing feed concentration as expected indicating that the separation task becomes increasingly difficult at higher feed load (Di Giovanni et al., 2001).

The limitation of this approach is the limited solvating power for elution of polar and large molecules (Schulte and Strube, 2001), particularly when CO_2 is used. These molecules are even difficult to be eluted on common stationary phases i.e. those based on silica. Only lipophilic compound exhibit high solubility in pure CO_2 but this problem can be handled by adding polar modifier such as alcohols (Fuchs et al., 1992a) although this attempt doesn't solve the entire problem. The presence of this modifier affects the mobile and stationary phase as it may increase the solvating power of the supercritical fluid while at the same time it can cause deactivation of the most active sites of the adsorbent which is responsible for solute retention. This phenomenon might affect solute retention time and peak shape under supercritical condition (Wright and Smith, 1986).

Another example of SF-SMB separation is the separation of phytol (3,7,11,15-tetramethyl-2-hexadecen-l-ol) isomers with trans-isomer is used as fixer in perfume industry (Depta et al., 1999). They used a dynamic model for SMB simulation to predict the region of complete separation taking into account different column configuration (4 and 8 total column) and compressibility of the mobile phase. Later, Peper et al. (2002) optimize the separation of R- and S- Ibuprofen using numerical model. The operating condition for the model is based on prior experiment using 40º C and pressure ranges from 17 – 14 MPa. 4.5% (wt) 2-propanol is used as modifier. They are able to increase productivity as high as 504 $g_{racemate}/kg_{solid}$/day with 99% raffinate purity. Johannsen et al. (2002) compared the process performance of bi-naphtol enantiomers separation on 10 different stationary phases. They found that the Kromasil CHI-DMB and Chiralcel OJ phase were the most suitable for the bi-naphtol system. Numerical optimization revealed that 6-column configuration (1/2/2/1) was sufficient for this separation. Further simulation and optimization study on phytol isomers using triangle theory leads to enhanced productivity up to 54 g_{feed}/l_{solid}/h. The earlier work of Pirkle et al. (1996) in examining some chiral stationary phases extensively over a wide range of temperature and mobile phase additives under sub/supercritical condition leads to better prospect of this system.

2.5.4. Varicol Process

Varicol is a new multicolumn continuous process which can be operated in all systems that is based on SMB platform (Adam et al., 2000; Ludemann-Hombourger et al., 2000). Similar to SMB process, Varicol consist of several number of column adequately connected in series with inlet or outlet ports between the columns. The difference is

asynchronous shift of these inlet/outlet ports thus it offers additional degrees of freedom, the subintervals after which the different ports are moved relative to the main period. This flexibility can be used to optimize the column distribution among the different zones. The column distribution is dynamic within the period, because lines are shifted at different times, allowing variation of zone length over time. Figure 2.8 describe the column evolution in a 4-sub interval Varicol process.

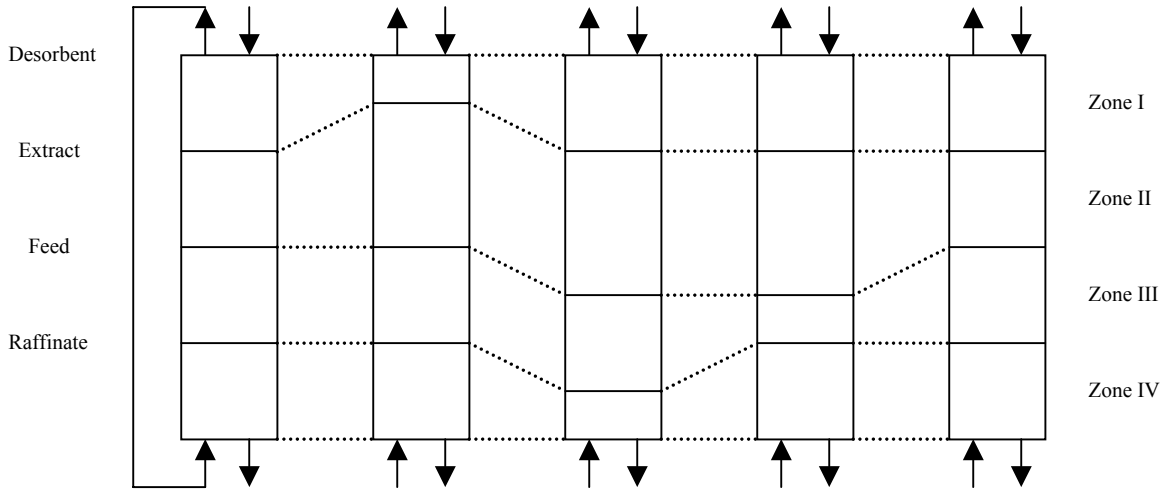

Figure 2.8 Switching sequence for 4-sub interval Varicol process

The average number of columns in different zones during one period is affected by the choice of these subintervals. The introduction of these parameters simplifies the process descriptions (Ludemann-Hombourger et al., 2000; Toumi et al., 2002) in which Varicol process is characterized by rational average number of column. The dynamic movement of inlet and outlet leads to obvious consequences in the design of Varicol unit. The two outlet lines must be connected to the recycling line before the eluent and feed lines as presented in Figure 2.9 below. In this way, contamination of product, when the number of column in zones II or III is zero, can be avoided. Likewise, the desorbent flow will not

contaminate the extract or raffinate line when the number of column is equal to zero in zone I or IV.

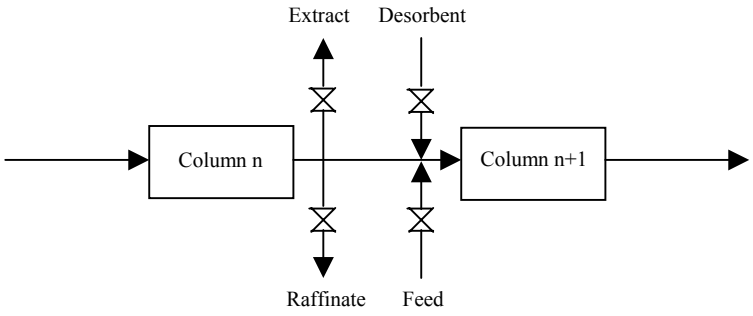

Figure 2.9 Varicol design connection

The first chiral separation performed using Varicol technology was reported by Ludemann-Hombourger et al. (2000) when they successfully isolated each isomer of 1,2,3,4-tetrahydro-1-naphtol from its racemic mixture. Toumi et al. (2002) demonstrated the ability of Varicol to give higher efficiency in terms of product per amount of solid phase using two theoretical cases with linear and non-linear adsorption isotherm behavior. They found out that even higher efficiency, relative to SMB, is observed in small number of column. This finding is further confirmed by Ludemann-Hombourger et al. (2002) in rigorous optimization of SB-553261 chiral racemate. They found that the same amount of feed can be treated using smaller number of column in which improved specific productivity is attained at the expense of higher desorbent consumption. Optimization attempt on this new technology was carried out for two important objectives in chiral separation: minimizing desorbent consumption (Toumi et al., 2002) and maximizing productivity (Toumi et al., 2002; Toumi et al., 2003).

2.5.5. SMB and Process Control

Until recently SMB plants are manually controlled by determining the set points of the operating parameters like flow rates and switching time. Process performance is assessed from the development of internal concentration profile or from the analysis of raffinate and extract product. Necessary adjustment to the set of operating parametric is simply introduced by manual setting. Some reason for this manual approach include the slow dynamic of chromatography processes, difficulty in applying online measurement and the inability to apply standard control algorithm to SMB process because its discrete nature.

Operation of SMB at the economical optimum point may result in high sensitivities to disturbances and operating parameter changes. Measurement of internal concentration profile is expensive and can only be installed at the outlet of the separation columns. Most processes are operated in the neighbourhood of optimum condition to avoid off-spec production and to ensure sufficient robust margins. The task to control SMB separation process to ensure a safe and economical operation at certain product specification at any time is challenging.

Recent research interest will be in the development of online process control devices to ensure the process operates within the theoretical optimal framework (Klatt et al., 2002) thus enabling direct control of the process. On-line detection methods (Marteau et al., 1994) enable direct measurement of internal concentration profile and allow parameter fitting to an underlying model. Model based process control algorithms are combined with online optimization to automatically control all operating parameters simultaneously to keep process performance as close to optimal condition as possible (Klatt et al., 2002). Instabilities of the process can be instantly detected and corrected by the control method.

Important precondition for these approaches are reliable and fast multicomponent process analytics (Mannschreck, 1992).

There are several strategies can be found in the area of automatic control of SMB chromatographic process. One example will be the control of the internal flow rates (Ando and Tanimura, 1986; Cohen et al., 1997; Hotier, 1998) which is difficult but can be treated as the basic layer for more advanced control approaches. Other authors suggest feedback control for certain operating variables, i.e. purity, yield, based on concentration measurements (Holt, 1995a, 1995b; Cansell et al., 1996; Couenne, 1999). They use Raman spectroscopy (Marteau et al., 1994) to measure the concentration at the outlet of the chromatographic column. Kloppenburg and Gilles (1999) used TMB model for geometric non-linear control to simulate the separation of C_8 aromatics hydrocarbon based on asymptotically exact input/ouput-linearization principle. This approach, however, lacks of reliability for system in which deviation between SMB dynamics and TMB approximation persists i.e. in process with low number of column. In the other hand, it is not easy to use SMB model due to its discrete component thus exhibits complex hybrid dynamics. Recently, Klatt et al. (2002) used dispersive SMB model for linear isotherm (Dünnebier et al., 1998) to optimize and control SMB process for fructose-glucose separation. This is because SMB model represents the complete process dynamic which is essential for model-based control approach. They propose two-layer control scheme in which optimal operating trajectory is calculated off-line by model-based dynamic optimization and control objective involves maintaining process on the optimal trajectory despite disturbances and plant/model mismatch. The identification models based on simulation data along the optimal trajectory are combined with a suitable local controller.

Demand for development in this area is growing with time. Effort to use model-based approach is focused on enantioseparation process (Haag et al., 2001). Another development from the control algorithm area, local linear ARX model was reported by Klatt et al. (2000) leading to the design of internal model controller. Natarajan and Lee (2000) combined the concepts of model predictive control and repetitive control. They applied balanced model reduction to SMB model leading to the design of repetitive model predictive controller. The combination of NARX model based on neural networks and non linear model predictive control is under investigation. In the area of online detection device, multiwave diode array UV and chiral polarimeter detector seem to be promising in the near future (Brandl et al., 1999). An automated, optimized and properly controlled process may save time in manufacturing and marketing of a new product. In case of pharmaceutical drug operation, short production time does not mean only economy of the drug itself but also the success or failure of the drug development.

Chapter 3 Simulated Moving Bed and Varicol Process

3.1. Schematic Diagram of SMB and Varicol Process

SMB system consists of cascade of columns arranged in a circular way. Each column is connected by a flexible valve injection and withdrawal ports. Columns are classified into four zones by two inlets (feed and desorbent) and two outlets (raffinate and extract) and loaded with resin that could be used both as catalyst and adsorbent. The discrete movements of the inlet and the outlet terminals of columns mimics solids flow in the opposite direction of liquid flow.

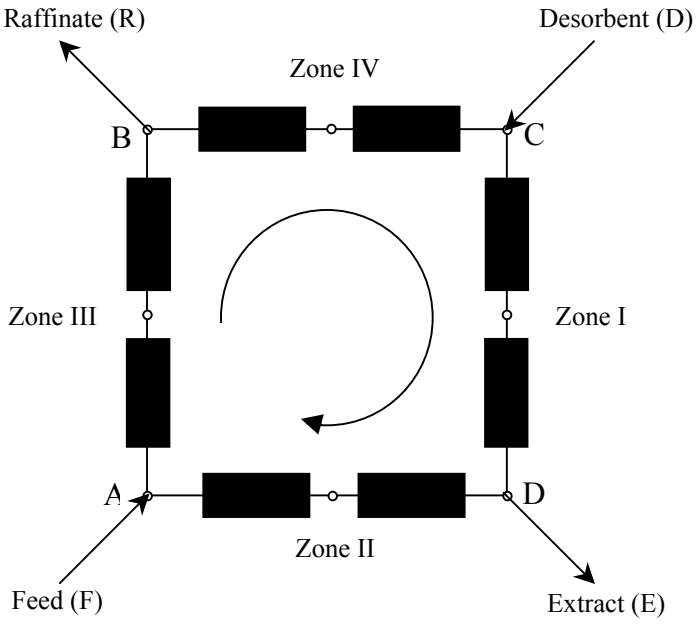

Figure 3.1 Schematic diagram of 4-zone 8-column SMB with 2 columns per zone

The key elements in SMB operations include the selection of an appropriate adsorbent and adjustment of internal flow rates. This is to ensure that the more retained species,

collected at the extract node, migrates with the stationary phase and the less retained species, withdrawn at the raffinate node, travels with the mobile phase. Comprehensive studies focusing the importance of adsorbent selection in order to maximize throughput (Schulte et al., 1997) and flow rates setting to ensure that each zone perform its specific role (Kawase et al., 1996) have been reported.

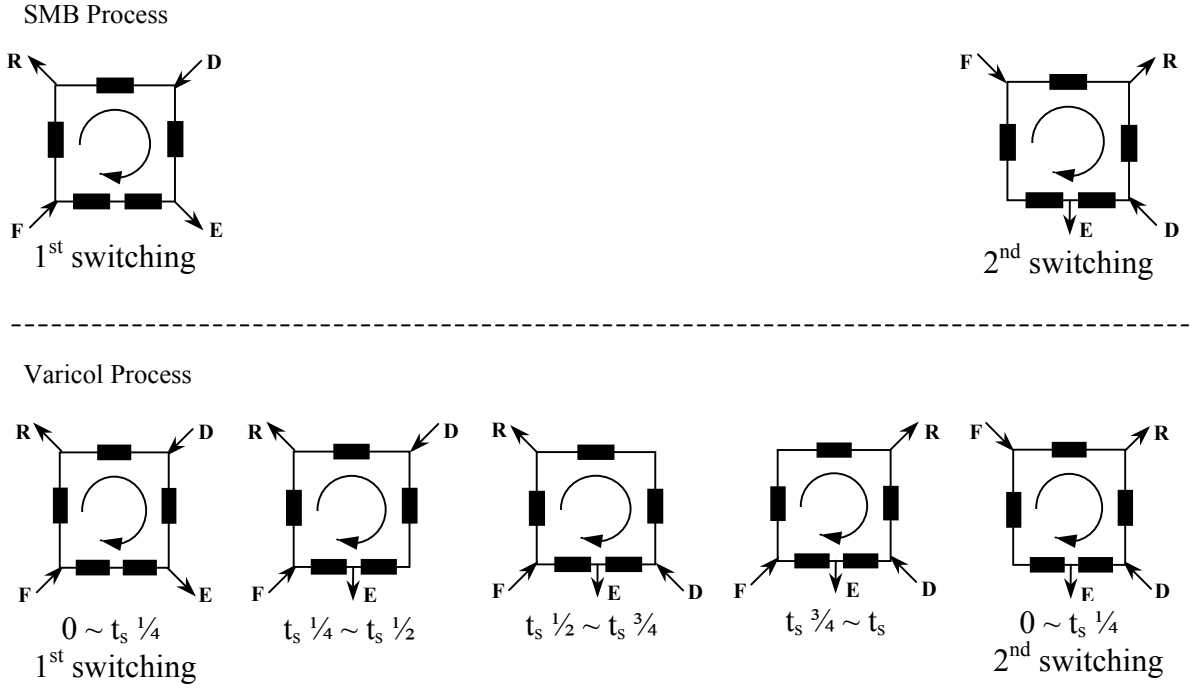

Figure 3.2 Switching profile of 4-zone 5-column SMB and Varicol processes

Varicol process (Adam et al., 2000) adopts similar apparatus in which the four terminal points are not shifted concurrently as in SMB operation. The overall switching time is divided into several subintervals and this number of subinterval depends on the magnitude of switching time due to operation feasibility. In fact, one column can be moved more than once during a switching period but the column configuration at the end of the switching interval returns to that attained by the SMB before the switching

operation. Figure 3.2 demonstrate switching development of 4-zone SMB in comparison with 4-subinterval Varicol process.

Table 3.1 Possible column configurations for SMB and Varicol processes

N_{col} = 4 (with 3-zone configuration)	0/1/1/2	1/0/1/2	1/1/1/1	1/2/1/0	2/1/1/0
	0/1/2/1	1/0/2/1	1/1/2/0	2/0/1/1	
	0/2/1/1	1/1/0/2	1/2/0/1	2/1/0/1	
N_{col} = 5	1/1/1/2	1/1/2/1	1/2/1/1	2/1/1/1	
N_{col} = 6	1/1/1/3	1/2/1/2	1/3/2/1	2/2/1/1	
	1/1/2/2	1/2/2/1	2/1/1/2	3/1/1/1	
	1/1/3/1	1/3/1/2	2/1/2/1		
N_{col} = 7	1/1/1/4	1/2/1/3	1/3/2/1	2/1/3/1	3/1/1/2
	1/1/2/3	1/2/2/2	1/4/1/1	2/2/1/2	3/1/2/1
	1/1/3/2	1/2/3/1	2/1/1/3	2/2/2/1	3/2/1/1
	1/1/4/1	1/3/1/2	2/1/2/2	2/3/1/1	4/1/1/1
N_{col} = 8	1/1/1/5	1/2/3/2	1/5/1/1	2/2/3/1	3/2/1/2
	1/1/2/4	1/2/4/1	2/1/1/4	2/3/1/2	3/2/2/1
	1/1/3/3	1/3/1/3	2/1/2/3	2/3/2/1	3/3/1/1
	1/1/4/2	1/3/2/2	2/1/3/2	2/4/1/1	4/1/1/2
	1/1/5/1	1/3/3/1	2/1/4/1	3/1/1/3	4/1/2/1
	1/2/1/4	1/4/1/2	2/2/1/3	3/1/2/2	4/2/1/1
	1/2/2/3	1/4/2/1	2/2/2/2	3/1/3/1	5/1/1/1

Each zone in SMB process accounts for specific function. Zone I, between the desorbent and the extract stream, allows solid regeneration by ensuring complete desorption of the more retained component from the solid phase. This helps to reduce contamination of the raffinate product as zone I becomes zone IV in subsequent switching. Zone II, the section between the extract and the feed injection point, is responsible for desorption of the less retained component off the adsorbent in order for the feed section has a head start. Zone III, the section between the feed and the raffinate nodes, is the adsorption zone for the more retained component to prevent this component from being conveyed by the mobile phase to the raffinate collection outlet. Solvent

regeneration takes place in zone IV, the section between the raffinate and the desorbent port, whose role is to ensure adsorption of the less retained component.

Subdivision of bed (or columns) results in numerous possible configuration of SMB and Varicol process. High number of total columns of a SMB, or Varicol, unit is preferred

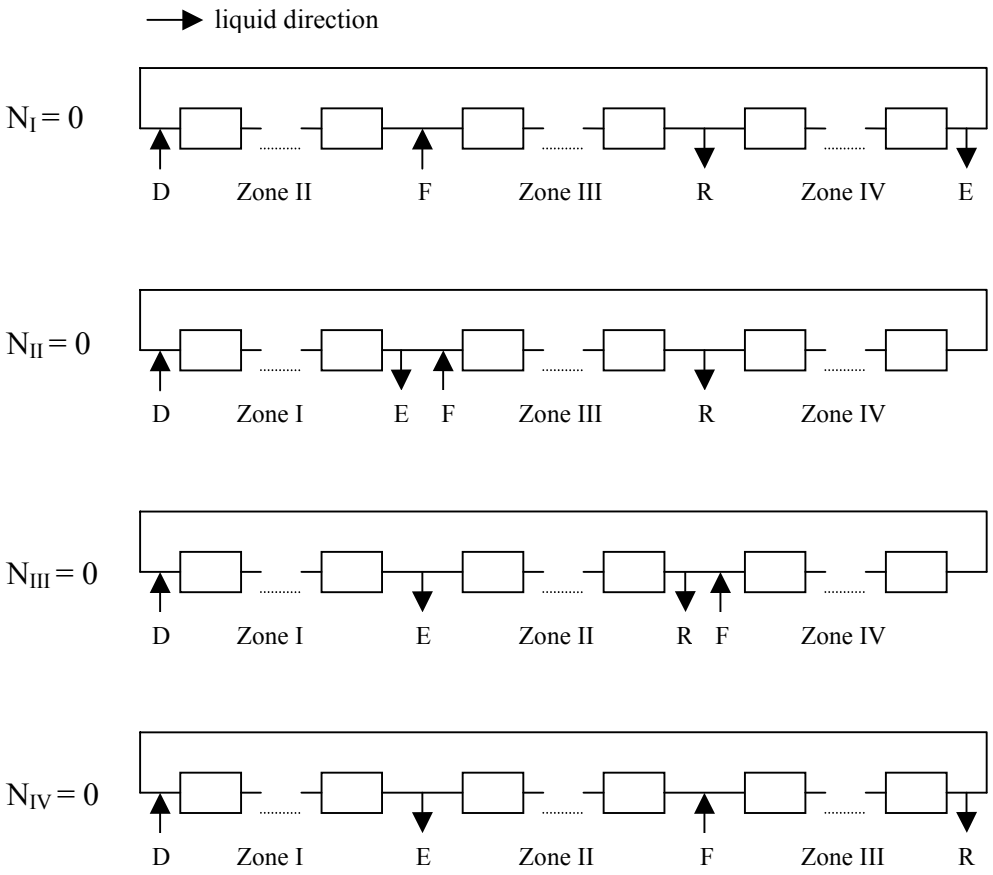

Figure 3.3 Schematic diagram of 3-zone 4-column SMB/Varicol process

as it allows more flexibility in column configuration thus introduces more degree of freedom in defining the right combinations of columns in respective zones. This effect is largely exercised by Varicol process, because it overcomes the rigidity of SMB in acquiring countercurrent motion between the mobile and the stationary phase. There are only 4 possible configurations for a 5-column SMB unit while in contrast, 11

configurations for 6-column setup. Table 3.1 spells out the detail of possible configurations for 4-zone setup, except for 4-column unit.

The principle of 3-zone SMB (Bjorklund et al., 2001) is applied to 4-column Varicol process as can be seen in Figure 3.3. The number of columns could take zero value for certain configurations. For illustration, configuration 2/1/1/0 results in the absence of zone IV while there are 2 columns in zone I and 1 column each for zone II and III to constitute 3-zone 4-column Varicol unit. This is particularly true for process in which the desired product has absolutely no or little affinity toward the adsorbent. Thus zone IV, whose main task is to prevent the less retained component from entering zone I, is no longer needed.

Chapter 4 Optimal Operation of Moving Bed Process for Chiral Drug Separation

4.1. Background of Enantio-Separation

Majority of the biologically active compounds such as flavors, nutrients, agrochemicals and pharmaceuticals are chirals and approximately more than 50 % of today's top selling drugs are single enantiomers. This phenomenon makes the stereoselective synthesis of chiral compounds is of substantial interest. The chiral drug industry soared through a major milestone in the past few years, as annual sales in this rapidly growing segment of the drug market surpassed $100 billion for the first time. This compound is now close to one third of all drugs sales worldwide. The industry's continuing growth is rooted, in part, in fundamental biochemistry. The biological messenger molecules and cell surface receptors that medicinal chemists try to affect are chiral, so drug molecules must match their asymmetry.

Over the course of ten years, the pharmaceutical industries realize the necessity to produce drugs in optically pure form. One important reason for the proliferation of the interest in chiral technologies and intermediates, which can yield optically pure therapeutics, is the FDA's policy statements commencing in 1992 regarding chiral drugs. It requires *in vitro* pharmacological studies to be conducted on both chiral forms of new or improved drugs submitted for evaluation. A similar, albeit slightly weaker, directive has been issued by the European Council for Proprietary Medicinal Products.

Another reason for producing single isomer drugs is the sales potential which hurtles past $100 billion as illustrated in Table 4.1 and shows no signs of slowing. The growth ra-

Table 4.1 Chiral drug global sales data

Drug Application	Global Sales ($ Millions)		
	1998	1999	2000
Cardiovascular	21,906	24,805	26,012
Antibiotics/antifungal	19,756	20,907	23,265
Hormones/endocrinology	12,297	13,760	17,345
Cancer	8,006	9,420	13,360
Central nervous system	7,027	8,592	13,720
Hematology	6,730	8,580	11,445
Antiviral	6,131	7,540	13,446
Respiratory	4,305	5,087	8,795
Gastrointestinal	1,718	2,998	5,355
Ophthalmic	1,482	1,794	2,070
Dermatological	1,124	1,270	1,540
Analgesics	842	1,045	1,135
Vaccines	568	676	1,100
Other	7,947	8,527	7,425
Total	$99,389	$115,001	$146,013

Source: Technology Catalysts International Corp.

te for these sales has been about 20% for the last 5 years and it is predicted that 75% of synthetic pharmaceuticals will be chiral as of the year 2000. The regulatory requirements, market potential, recent technology advances and promising foreseeable prospect suggest that chiral technologies will become a very lucrative area of biopharmaceutical research

and commercialization. This is true not only for pharmaceutical companies that develop new drugs, but also for those that develop chiral intermediates, which are used subsequently in the synthesis of optically pure drugs.

4.2. Numerical Simulation of SMB and Varicol Process

In the open literature, the only reported results on the Varicol process are those of Ludemann-Hombourger et al. (Ludemann-Hombourger et al., 2000, 2002) for the enantioseparation of 1,2,3,4-tetrahydro-1-naphtol and the optical isomers of SB-553261 racemate using Chiralpak AD 20 μm as CSP. These experimental results will be used as a measure of reliability of the numerical approach in this study.

There are numerous different models can be applied to simulate the counter current moving bed chromatographic process but the mixing cell model is used in this work due to the usual conditions of high performance preparative chromatography (Golshan-Shirazi and Guiochon, 1994). The column is assumed as a cascade of ideal mixing cells. For each column of the process, the mass balance for each compound *i* in the mixing cell *k* during N^{th} switching period for SMB can be written as follows (Charton and Nicoud, 1995):

$$C_{i,k-1}^{(N)} = C_{i,k}^{(N)} + \left[\frac{t_o(\phi)}{J}\right]\frac{dC_{i,k}^{(N)}}{dt} + \left[\frac{1-\varepsilon_0}{\varepsilon_0}\right]\left[\frac{t_0(\phi)}{J}\right]\frac{d\overline{C}_{i,k}^{(N)}}{dt} \qquad 0 \le t \le t_s \qquad (4.1)$$

The mass balance equation for component *i* in mixing cell k during the M^{th} switching period for Varicol will be:

$$C_{i,k-1}^{(N,M)} = C_{i,k}^{(N,M)} + \left[\frac{t_o(\phi)}{J}\right]\frac{dC_{i,k}^{(N,M)}}{dt} + \left[\frac{1-\varepsilon_0}{\varepsilon_0}\right]\left[\frac{t_0(\phi)}{J}\right]\frac{d\overline{C}_{i,k}^{(N,M)}}{dt} \qquad (4.2)$$

$0 \le t \le t_s$; M = 1, 2, 3 or 4

in which C and $\overline{C}$ are the concentration in the mobile and stationary phase respectively, J is the theoretical number of cells in the column and $t_0(\phi)$ is the zero retention time of the column in section ϕ (I, II, III or IV) and is given by

$$t_0(\phi) = \frac{\varepsilon V_{col}}{Q_{(\phi)}} \tag{4.3}$$

$Q_{(\phi)}$ is the volumetric flow rate in the column in section ϕ and ε is the column external porosity, used as 0.43. The boundary conditions used to simulate the process is based on periodic regime of the process meaning that the boundary conditions are changing over time corresponding to the position of the different lines. Initial condition is derived from the fact that the column is empty as the process initializes then:

$$C_{i,k}^{(N=0)} = C_{i,k}^{0} = 0 \tag{4.4}$$

Boundary condition is derived from the mass balance at the inlet node of each zone in SMB. When the desorbent stream is connected at the inlet of zone I, the resulting mass balance will be:

$$C_{i,first}^{(N)}\Big|_{\phi=I} = \frac{(Q_I - Q_D)C_{i,last}^{(N)}\Big|_{\phi=IV}}{Q_I} \tag{4.5}$$

When extract product is withdrawn at the end of zone I, the mass balance at the beginning of zone II will give:

$$C_{i,first}^{(N)}\Big|_{\phi=II} = C_{i,last}^{(N)}\Big|_{\phi=I} \tag{4.6}$$

The mass balance when the feed stream is connected to the inlet of section III will give:

$$C_{i,first}^{(N)}\Big|_{\phi=III} = \frac{Q_{II}C_{i,last}^{(N)}\Big|_{\phi=II} + Q_F C_i^F}{Q_{III}} \tag{4.7}$$

The mass balance at the beginning of zone IV when raffinate product is withdrawn at the end of zone III will be:

$$C_{i,first}^{(N)}\Big|_{\phi=IV} = C_{i,lasi}^{(N)}\Big|_{\phi=III} \tag{4.8}$$

The raffinate concentration of component *i* is simply equal to its concentration at the last cell of section III, while the extract concentration is its concentration at the last cell of section I. The internal flow rates Q_I, Q_{II}, Q_{III} and Q_{IV} can be simply computed if the measurable quantities Q_F, Q_E, Q_R and Q_D are known. Each time switching operation is performed, a new BVP has to be solved. The detail of derivation is given in Appendix A.

The resulting first order differential equations were solved using DIVPAG (based on Gear's algorithm) in IMSL library. The aim of this mathematical model is to study how the disturbances ignited by periodical switching procedure are propagated along the system. Some important process performance parameter introduced here are:

$$\text{Purity (Pur)} = 100 \cdot \frac{\int_0^{t_S} C_{i,\phi}^{(N)}\big|_{z=L}\, dt}{\int_0^{t_S} \sum_{i=R,S} C_{i,\phi}^{(N)}\big|_{z=L}\, dt} \tag{4.9}$$

$$\text{Productivity (Pr)} = (Q_\phi - Q_{\phi+I}) \int_0^{t_s} C_{i,\phi}^{(N)}\big|_{z=L}\, dt \tag{4.10}$$

$$\text{Recovery (Rec)} = 100 \times \frac{(Q_{\phi} - Q_{\phi+I}) \int_0^{t_S} C_{i,\phi}^{(N)}|_{z=L} dt}{Q_F C_i^F} \tag{4.11}$$

$$\text{Solvent Consumption (SC)} = \frac{Q_D}{\sum_{i=R,S} (Q_{\phi} - Q_{\phi+I}) \int_0^{t_S} C_{i,\phi}^{(N)}|_{z=L} dt} \tag{4.12}$$

where i = component-*I* (R-enantiomer for extract product, S-enantiomer for raffinate product), ϕ = zone in SMB (I for extract product, III for raffinate product).

4.3. Calculation of Theoretical Number of Plate

The separation was carried out at 25 °C on Chiralpak AD with an average particle size of 20 μm whose void fraction is calculated based on the productivity data given by Ludemann-Hombourger et al (2002) as clearly described in Appendix B. Molecular structure of SB-553261 is given as follows :

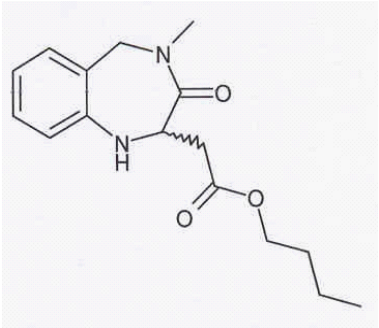

Figure 4.1 Molecular structure of SB-553261

Desorbent will be a mixture of acetonitrile-methanol 80/20 (v/v) and at the rate of 1.5 ml/min, the retention times of the R-enantiomer and S-enantiomer are 5.78 minutes and 8.89 minutes respectively. The chromatogram, resulting from elution experiment,

corresponding to an analytical injection of the racemic mixture into a 10 mm I.D. column is shown as follows:

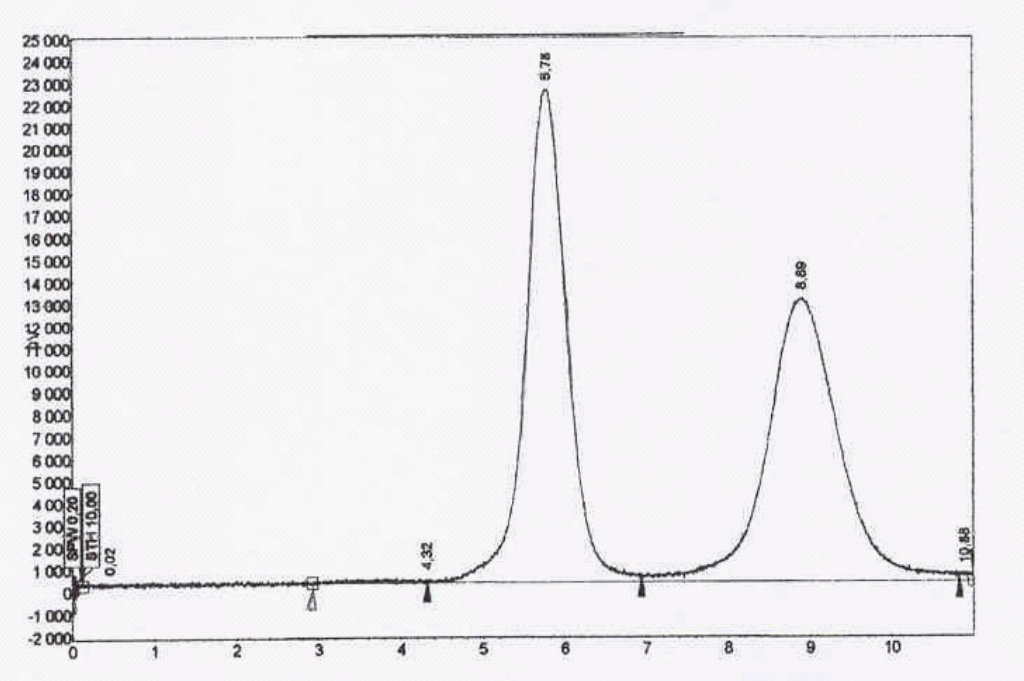

Figure 4.2 Breakthrough curve during single column experiment (pulse injection at Q = 1.5 ml/min, V_{inj} = 10 µl, C_{inj} = 1 g/l, UV detection λ = 310 nm)

The number of plate requirement is first determined by means of the column hydrodynamic data given by Ludemann-Hombourger et al. (2002) as follows:

$$H_1 = 6 \cdot 10^{-5} + 1.63 \cdot 10^{-3} u \quad \text{(SI unit)} \tag{4.13}$$

$$H_2 = 6 \cdot 10^{-5} + 2.64 \cdot 10^{-3} u \quad \text{(SI unit)} \tag{4.14}$$

Since Q = 1.5 ml/min and A = 0.7854 cm^2 then u = 1.9099 cm/min. The number of plate can be easily calculated by dividing the length of single column by the HETP and we obtain 2553 plate according to eq. (4.13) and 1588 plate according to eq. (4.14). This

result, however, can not be used since it will consume massive computation time for simulation and we opt for different method to determine this parameter.

Desty et al. (1963) provide another way of calculating the number of plate requirement by taking into account the retention time of a single enantiomer and the base peak width of its chromatogram according to the following correlation:

$$N_{eff} = 16\left(\frac{t_R'}{w_b}\right)^2 \tag{4.15}$$

with t_R' is the adjusted retention time, defined as the solute total elution time minus the retention time of an unretained peak (hold-up time), and w_b is the base peak width, defined as the bar segment of the peak base and projected on to the time or volume axis. By examining the chromatogram in Figure 4.2, we obtain for the S-enantiomer and R-enantiomer respectively:

$$N_{eff} = 16\left(\frac{5.78}{1.1}\right)^2 = 442 \tag{4.16}$$

and

$$N_{eff} = 16\left(\frac{8.89}{1.8}\right)^2 = 390 \tag{4.17}$$

In later stage, simulation was run using the average value of 400 but it was found that 120 plates are enough to give good prediction to the SMB profile as given by the author as it is unwise to obtain slightly better accuracy at the expense of high computation time. The validation of this decision can be visualized in the following figure.

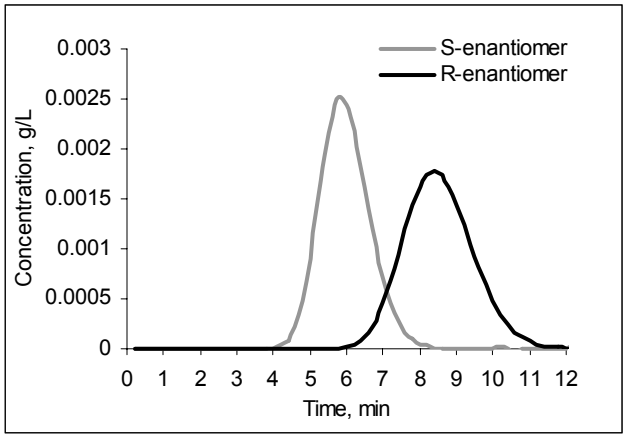

Figure 4.3 Simulated elution profile for enantioseparation of SB-553261

Retention times of the R-enantiomer and S-enantiomer in Figure 4.3 are ~5.8 minutes and ~8.5 minutes respectively, thus simulation with 120 plates has been proven to provide result close to experiment.

4.4. Model Validation

The experimental condition tabulated in Table 4.2 is taken from the work of Ludemann-Hombourger et al. (2002). Few overloaded injections were given to determine the adsorption isotherm and classical optimization procedure is employed in estimating the isotherm parameters (Nicoud and Seidel-Morgenstern, 1996). Liquid and adsorbed phase equilibrium is well represented using a modified competitive Langmuir adsorption as in Table 4.2.

C_i and $\overline{C_i}$ are the concentration of species i in the mobile phase and stationary phase respectively. Component 1 and 2 refer to S- and R-enantiomer respectively. The number of theoretical plate used in the entire study is 120 which have been verified in Section 4.3. It is desired to use experimental condition of 5-column Varicol (Q_I = 17.49 ml/min) as the

Table 4.2 Column specification and adsorption isotherm for SMB experiment used by Ludemann-Hombourger et al. (2002)

Column dimension	10 mm ID and 81 mm bed length	
Feed Concentration	$C_{F1} = C_{F2} = 32$	(g/l)
Adsorption isotherm	$\overline{C_1} = 1.35 \cdot C_1 + \frac{0.294 \cdot C_1}{1 + 0.0338 \cdot C_1 + 0.1696 \cdot C_2}$	(g/l)
	$\overline{C_2} = 1.17 \cdot C_2 + \frac{1.509 \cdot C_2}{1 + 0.0338 \cdot C_1 + 0.1696 \cdot C_2}$	(g/l)
Pressure drop / column	$\Delta P / L = 2.5 \cdot 10^9 \cdot u$	(SI Unit)
Column efficiency	$H_1 = 6 \cdot 10^{-5} + 1.63 \cdot 10^{-3} \cdot u$	(SI Unit)
	$H_2 = 6 \cdot 10^{-5} + 2.64 \cdot 10^{-3} \cdot u$	(SI Unit)

reference conditions in order to compare the performance of 4-column Varicol, 5-column SMB and 5-column Varicol. This is because the high recovery reported for 5-column Varicol experiment which indicates the ease of performing experiment at the given setting and it will help experimental verification towards optimum result obtained in this work.

Table 4.3 summarizes the result when the model is further verified at this setting. It can be seen that the simulation result is somewhat different from the experimental result as not all details about the 5-column experimental configuration was published in Ludemann-Hombourger et al. (2002). Further validation is given for 6-column SMB (Figure 4.4) to prove the reliability of the model in predicting the system behavior as well as in finding the optimum process operating condition.

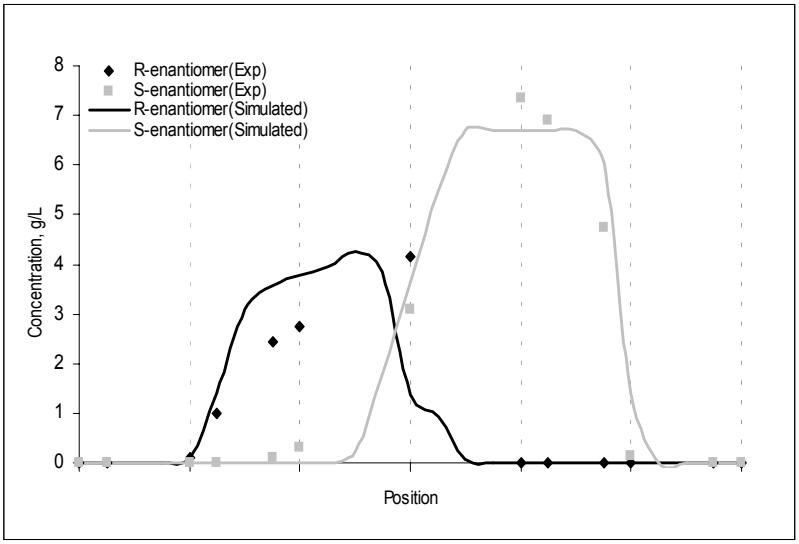

Figure 4.4 Concentration profile on 6-column SMB (N_{plate} = 120, Q_1 = 15.3 ml/min, Q_F = 0.3 ml/min, Q_R = 1.79 ml/min, Q_D = 8.55 ml/min, t_s = 1.11 min, 1/2/2/1 setup)

Table 4.3 Performance comparison for 5-column, 4-subinterval Varicol process

Process Parameter	Reference (L-H et al., 2002)	This work
Q_1 (ml/min)	17.49	
Q_E (ml/min)	7.59	
Q_F (ml/min)	0.3	
Q_D (ml/min)	9.78	
t_s (min)	0.925	
L_{col} (cm)	8.1	
χ	0.95/1.85/1.5/0.7	1/1.75/1.5/0.75*
Calculated Parameter		
PurR (%)	99.7	99.988
PurE (%)	96.8	99.057
RecR (%)	96.8	99.697
RecE (%)	99.9	98.598
Pr ($g_{product}$/day)	13.413	13.706
SC ($m^3_{desorbent}/kg_{product}$)	1.05	1.028

* Varicol switching sequence: J/J/L/I

4.5. Sensitivity Study

The purpose of sensitivity study is to determine the respond of the objective function when incremental changes are applied to a particular variable while the other variables remain fixed. These variables include the variables that appear in both the objective function as well as in the constraints. These studies might serve as a source of information about the upper and or lower limit of a specific variable, in case it has the potential to be used as decision variables.

The variables which are considered affecting the optimal objective function in this system are switching time (t_s), feed flow rate (Q_F), raffinate flow rate (Q_R) and desorbent flow rate (Q_D). In this sensitivity study, two objective functions which play a key role in the chiral separation process performance will be used, namely productivity and purity. Furthermore, we will observe how the complex interplay between these variables affects the magnitude of the objective function.

The purity in this work is defined as the ratio of concentration of one enantiomer to the total concentration of both enantiomers while productivity is defined as grams of specific enantiomer in product line per day as in eq. (4.9) and (4.10) respectively. This is for easy comparison with the works of Ludemann-Hombourger et al. (2002).

4.5.1 The Effect of Switching Time

Switching time as a measure of solid velocity will indisputably possess an apparent impact on productivity and purity as depicted in Figure 4.5(a) and (b). Productivity of both enantiomer is used as the objective function in Figure 4.5(a) and this figure informs us that the productivity of raffinate and extract contradict each other at the range of 0.8 -

1.2 min. With the increase of switching time, PrR increases but PrE decreases due to insufficient Q_D. The purity tends to increase from t_s = 0.8 min to 1 min and decreases subsequently. The behavior of purity below and beyond t_s = 1 min can be easily understood if the relative velocity of the two components to be separated are considered.

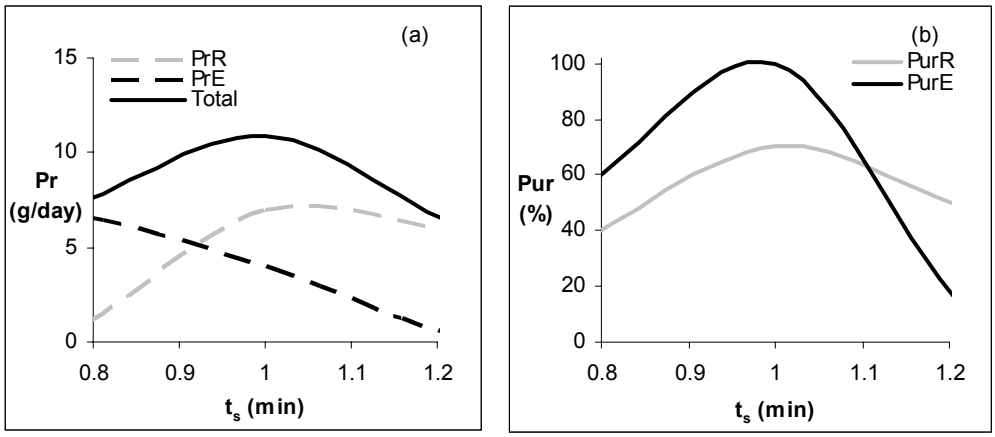

Figure 4.5 Sensitivity study: (a) Plot of productivity vs switching time (b) Plot of purity vs switching time

The countercurrent separation of the components is achieved by appropriately specifying the internal flow rates in the columns and the switching time. Petroulas et al. (1985) defined for true countercurrent moving bed chromatographic reactor (CMCR) a parameter, σ_i, called relative carrying capacity of the solid relative to the fluid stream for any component i as

$$\sigma_i = \frac{1-\varepsilon}{\varepsilon} NK_i \frac{u_S}{u_g} = \delta_i \frac{u_S}{u_g} \tag{4.18}$$

where u_s and u_g are respectively solid phase and fluid phase velocity. They showed that to achieve countercurrent separation between the two components, one must set σ greater than 1 for one (species move with the solid phase) and less than 1 (species move with the

fluid phase) for the other. When $\sigma = 0$, it represents fixed bed. Ray et al. (1994) re-defined the above parameter, σ, by replacing the solid-phase velocity, u_s, in CMCR by a hypothetical solid phase velocity, ζ, defined as $\zeta = L_{col}/t_s$. They found, both theoretically (Ray et al., 1994) and experimentally (Ray and Carr, 1995), that simulation of the countercurrent movement between two components can be achieved when redefined σ's were set such that it is greater than 1 for one and less than 1 for the other component. It was observed that for the reference run, countercurrent separation occurs ($\sigma > 1$ for one component and $\sigma < 1$ for the other) around t_s equal to 1, while both components travel co-currently ($\sigma > 1$ for $t_s < 1$ min and $\sigma < 1$ for $t_s > 1$ min) spoiling the separation and thereby, the purity. An illustrative example in the calculation of relative velocity of each species in zone II can be found in Appendix C and the result is tabulated in Table 4.4 below, in which the best separation performance takes place when the relative velocity reaches the maximum value indicating the two species travel in opposite direction, the less retained component travel with the mobile phase and the more retained component travel with the stationary phase. The optimum value of switching time is characteristic to the respective system and it depends on the internal flow rate and column configuration.

Table 4.4. Relative velocity of each species in zone II at various switching time for enantioseparation of SB-553261 racemate

t_s	δ		σ		V		
(min)	δ_S	δ_R	σ_S	σ_R	V_S	V_R	ΔV
0.8	2.1793	3.5512	0.752725	1.226576	1.525216	1.31797	0.207246
0.925	2.1793	3.5512	0.651005	1.060822	1.383668	-0.168453	1.552121
1.2	2.1793	3.5512	0.501817	0.817717	1.975157	0.504852	1.470305

4.5.2 The Effect of Feed Flow Rate

Figure 4.6 shows that up to feed flow rate of 2.5 ml/min, productivity increases and purity decreases as the feed flow rate increases. The phenomena emerging from the figure are explicable as productivity will increase as increasing feed flow rate will supply more component to be processed but the separation task becomes more difficult resulting in decreased purity. Feed flow rate, however, does not significantly affect the purity at the feed range beyond 2.5 ml/min.

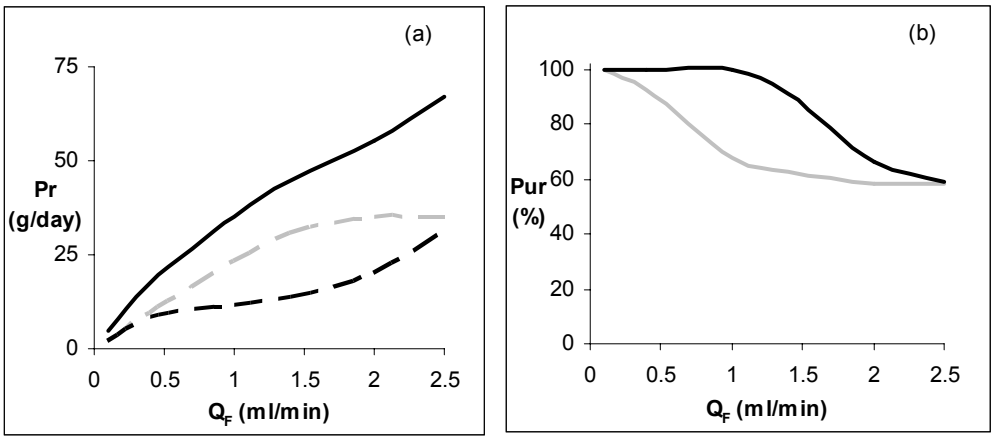

Figure 4.6 Sensitivity study: (a) Plot of productivity vs feed flow rate (b) Plot of purity vs feed flow rate

Figure 4.6 tells us that no separation can occur at high feed rate indicating that the incoming feed will simply eluted out of the column. The trend, however, reveals that we can at least maintain desired high purity at low feed rate and real optimization problem can be exercised by using feed flow rate as the objective function with purity in the penalty term to see how high the feed rate can be maximized at a certain high purity requirement.

4.5.3 The Effect of Raffinate Flow Rate

A contradictive relation between variables can be seen in the relation between purity and or productivity with raffinate flow rate (Figure 4.7) when it is used as decision variables. In studying the effect of raffinate flow rate, the extract flow rate is automatically adjusted to compensate the change of raffinate flow rate in order to satisfy mass balance of the system.

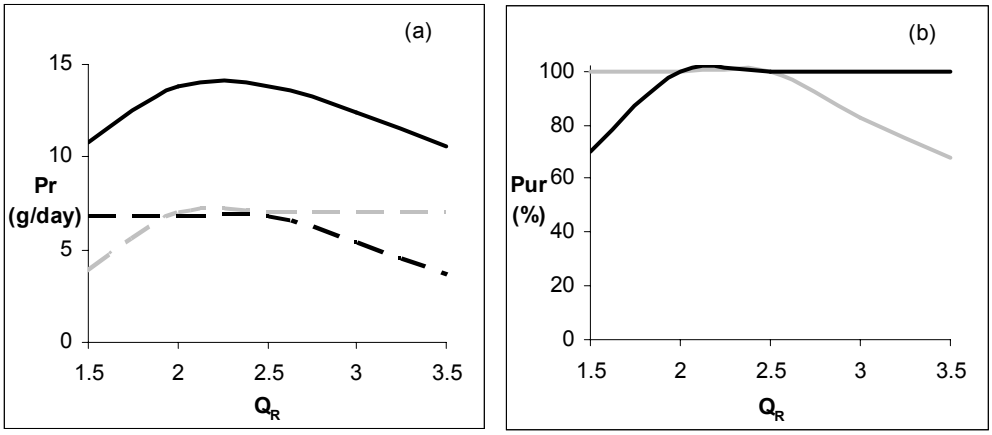

Figure 4.7 Sensitivity study: (a) Plot of productivity vs raffinate flow rate (b) Plot of purity vs raffinate flow rate

Any increase in raffinate flow rate beyond a certain point will reduce the raffinate purity while alternately, increase the extract purity. Figure 4.8 (grey represents S-enantiomer and black represents R-enantiomer) shows the steady-state concentration profiles inside the columns under the following conditions: Q_I = 17.49 ml/min, Q_F = 0.3 ml/min, L_{col} = 8.1 cm and χ = 1/2/1/1. At lower raffinate flow rates, Q_R = 1.5 ml/min, the raffinate concentration is high. Although some portions of less retained component appear in the extract withdrawal port, but no trace of the more retained component is found near the raffinate withdrawal port. This explains the high raffinate purity and low extract purity at lower raffinate flow rate. The reduction of liquid flow rates in Zone II and III causes the

more retained component to be selectively adsorbed in zone IV, thereby instigating mobile phase concentration build-up of the less retained component in zone IV. This concentration is high enough to be transferred from zone IV to zone I due to recycle, and subsequently, appear at the extract withdrawal port polluting the extract product. Raffinate

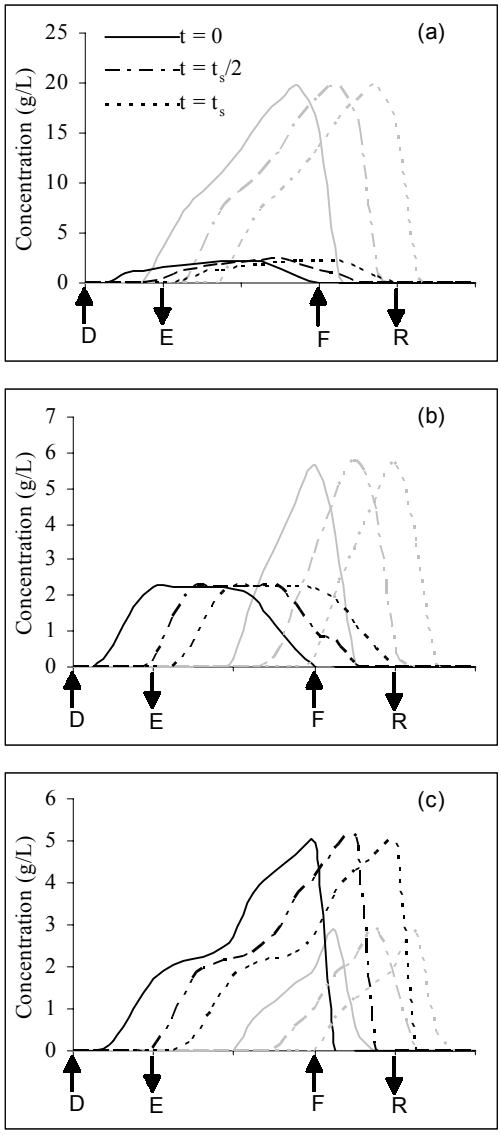

Figure 4.8 Effect of raffinate flow rate on steady state concentration profile for 5-column SMB. (a) Q_R = 1.5 ml/min, (b) Q_R = 2.5 ml/min, (c) Q_R = 3.5 ml/min

productivity is low at this point but gradually increases up to a fixed value with the increase of raffinate flow rate. However, the extract productivity decreases as some of the more retained component appears in the raffinate withdrawal port due to increasing raffinate purity.

4.5.4 The Effect of Desorbent Flow Rate

The effect of desorbent flow rate is examined over a relatively wider range to see if there is any possibility of improvement. The productivity of raffinate and extract contradict each other within the entire range as shown in Figure 4.9(a).

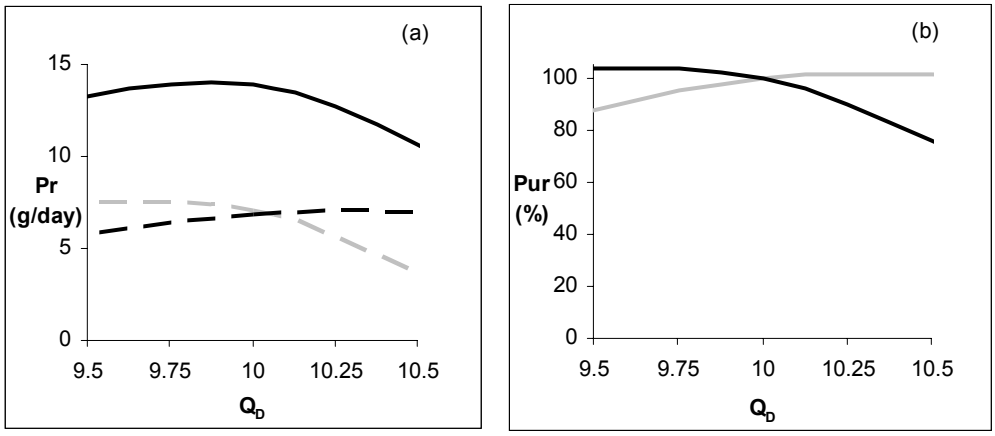

Figure 4.9 Sensitivity study: (a) Plot of productivity vs desorbent flow rate (b) Plot of purity vs desorbent flow rate

It can be understood that as desorbent flow is increased up to 10 ml/min, the effect of desorbent is exercised mainly in zone I. There is enough desorbent to wash the more retained component off the adsorbent and most of them will emerge at the extract line rather than the raffinate line. This also explains why the productivity of the more retained component at the extract line increases as the desorbent flow rate increases. Consequently, purity remains and productivity increases steadily. This is mainly due to the huge linear

velocity of the desorbent causing the desorbent to travel very fast in section I that there is enough time for it to wash the more retained component off the adsorbent At desorbent flow rate beyond 10 ml/min, all the retained component is completely diluted by the excess desorbent and extract productivity will reach its asymptotic value. The excess desorbent, however, reduces raffinate productivity by carrying the less retained component toward the extract line thus polluting the extract stream.

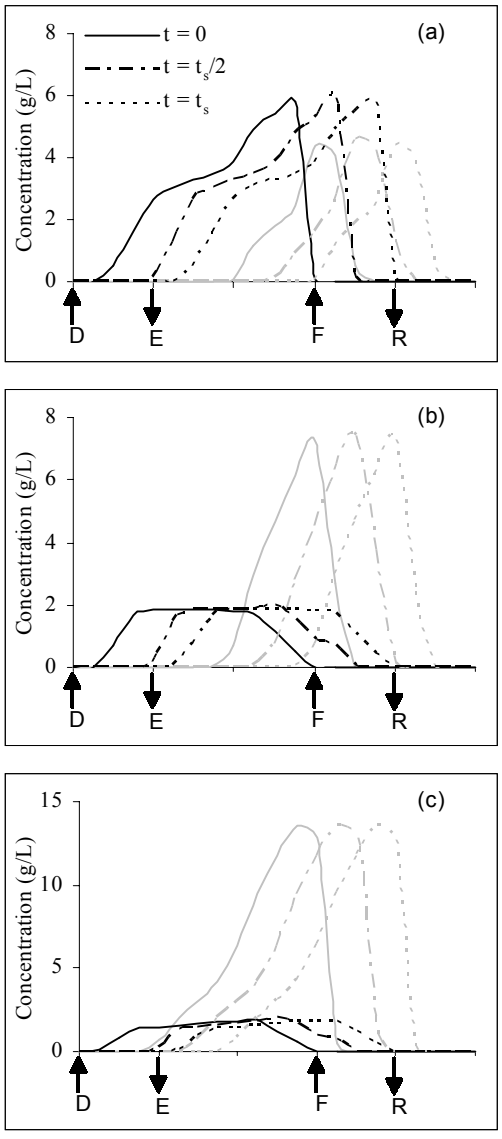

Figure 4.10 Effect of desorbent flow rate on steady state concentration profile for 5-column SMB. (a) Q_D = 9.5 ml/min, (b) Q_D = 10 ml/min, (c) Q_D = 10.5 ml/min.

Figure 4.9 (b) indicates that the highest purity for both streams can be achieved when the desorbent flow rate is around 10 ml/min. The trend is further comprehended when the effect of desorbent flow rates on the steady state concentration profiles are examined (Figure 4.10). Figure 4.10 uses similar conditions as those used in Figure 4.8. When desorbent flow rate is less than 10 ml/min, the strongly adsorbed component is not completely washed out of zone I and it breaks through at the raffinate port when it becomes zone III in subsequent switching. When the desorbent flow rate is greater than that is required for purging, it will simply lower the extract purity.

This preliminary study is very important since it provides us a lot of information such as the range of decision variables that enable high purity separation, i.e. ts between 0.8 – 1.2 min and relatively low feed rate. This study inadvertently reveals the infeasible region for separation such as ts beyond 1 min, feed rate beyond 2.5 ml/min and eluent beyond 10 ml/min because no high purity enantiomer can be obtained from these regions. This study also helps identifying the most sensitive parameter which might affect the process and the complex interaction between parameters in moving bed chromatography.

4.6. Single Objective Optimization

The first optimization work in this study is the single objective optimization and is meant to compare the result with the work of Ludemann-Hombourger et al.(2002). The objective function formulated in this study is based in view of economic consideration as maximizing the amount of feed will raise more income and minimizing eluent consumption will suppress process expenses.

4.6.1. Case 1. Single Objective Optimization: Maximization of throughput

In general, purity will decrease as feed flow rate is increased making the separation task much more difficult. In order to test whether the feed flow rate can be increased without jeopardizing the purity requirement, and to test the optimization procedure based on GA, the following optimization problem was solved:

$$\text{Max} \qquad I = Q_F\,[Q_F, Q_R, t_s, \chi] \tag{4.19}$$

$$\text{Subject to PurR and PurE} \geq \text{Experimental value (in L-H et al., 2002)} \tag{4.20}$$

The chosen objective function was the maximization of the feed flow rate, Q_F, subject to target purities of extract, PurE and raffinate, PurR streams greater than experimental reported values by Ludemann-Hombourger et al. (2002). Four decision variables were used for this optimization study as indicated in eq. (4.19): feed flow rate, Q_F, raffinate stream flow rate, Q_R, switching time, t_s and column configuration, χ. In order to be able to compare our results with those of Ludemann-Hombourger et al. (2002), four cases were solved (see Table 4.5) corresponding to the experimental values for flow rates Q_I and Q_D used in their work with respect to 6-column SMB and 4, 5 and 6 columns Varicol respectively. Since only four flow rates could be selected independently, while the other four were determined by mass balance equations at points 1-4 (see Figure 3.1), the remaining two flow rates (in this case, Q_F and Q_R) were used as decision variables. The third decision variable was the switching time t_s, which clearly had a strong influence on the purity of the outlet streams (see Figure 4.5). The bounds for t_s lie between the breakthrough times of the two components for a specific CSP.

Table 4.5 Optimization attributes used in single objective optimization

Problem		Objective	Constraints	Decision variables
Case 1	SMB / Varicol	Max Q_F	PurR and PurE ≥ Experimental value (in L-H et al., 2002)	$0.3 < Q_F < 0.7$ ml/min $1 < Q_R < 10$ ml/min $0.4 < t_s < 1.2$ min χ [See Table 3.1]
Case 2	SMB / Varicol	Min Q_D	PurR and PurE ≥ Experimental value (in L-H et al., 2002)	$4 < Q_D < 12$ ml/min $0.5 < Q_R < 10$ ml/min $0.4 < t_s < 1.2$ min χ [See Table 3.1]
Fixed Variables: $L_{col} = 8.1$ cm				
a	$N_{col} = 4$, $Q_1 = 21.3$ ml/min	Case 1: $Q_D = 13.06$ ml/min, Case 2: $Q_F = 0.3$ ml/min		
b	$N_{col} = 5$, $Q_1 = 17.5$ ml/min	Case 1: $Q_D = 9.78$ ml/min, Case 2: $Q_F = 0.3$ ml/min		
c	$N_{col} = 6$, $Q_1 = 15.3$ ml/min	Case 1: $Q_D = 8.55$ ml/min, Case 2: $Q_F = 0.3$ ml/min		
d	$N_{col} = 6$, $Q_1 = 15.3$ ml/min	Case 1: $Q_D = 9.05$ ml/min, Case 2: $Q_F = 0.33$ ml/min		

The fourth decision variable used was the column configuration (χ). For a fixed number of total columns (N_{col}), there exists number of possible column configurations. In a SMB system, there is only one column configuration, which is fixed with time. However, there are many possible column configurations in Varicol process depending on the number of sub-time intervals. In order to somehow restrict this variety, we considered here only 4-sub-time interval Varicol process, assuming that in each subinterval the unit could take any one of the configurations possible for the SMB unit as listed in Table 3.1. For example, for a 5-column SMB process, χ = J indicates the column configuration 1/2/1/1. Whereas, for a 4-subinterval 5-column Varicol process, χ = I-J-I-K indicates that

the sequence of column configurations I-J-I-K is used within the 4-subinterval global switching period (Table 4.6). In terms of time average column length, this corresponds to

Table 4.6 Optimum column configuration for SMB and Varicol process for chiral drug separation

N_{col}	χ	Column	χ	Column	χ	Column	χ	Column	χ	Column
4	A	0/1/2/1	B	0/2/1/1	C	1/1/1/1	D	1/1/2/0	E	1/2/1/0
	F	2/0/1/1	G	2/1/1/0						
5	H	1/1/1/2	I	1/1/2/1	J	1/2/1/1	K	2/1/1/1	L	1/2/2/0
6	M	1/1/1/3	N	1/1/3/1	O	1/1/2/2	P	1/2/2/1	Q	2/1/1/2
	R	1/3/1/1	S	2/1/1/2	T	2/1/2/1	U	2/2/1/1	V	

the configuration 1.25/1.25/1.5/1. The optimization formulation, the bounds of the decision variables, constraints, and the fixed parameter values used were summarized in Table 4.5. In order to get meaningful optimum solutions, the bounds for the decision variables were estimated using the equilibrium theory (Storti et al., 1995; Mazzotti et al., 1997) and sensitivity analysis of the model.

For 4-column Varicol process, there will be 13 possible column configurations (Refer to Table 3.1) but this number reduces as there are only 7 optimum column configurations for 4-column Varicol as suggested in Table 4.6. Preliminary study showed that steady state condition could not be achieved when the number of column in zone III (between the feed port and raffinate withdrawal port) was set to zero. Therefore every configuration involving zero column in zone III will not be examined throughout the study. Steady state operation can be achieved for the rest of the configuration even though they give

reasonably low purity but it might benefit of high productivity and low eluent consumption. The best purity was given by 1/1/1/1 configuration while the best productivity was given by 1/0/2/1 configuration.

4.6.2. Case 2. Single Objective Optimization: Minimization of desorbent consumption

In order to reduce operating cost, minimization of desorbent flow rate was selected as objective function. Desorbent is needed in chromatographic column to desorb (purge) the strongly adsorbed component and it has significant impact on purity of the extract stream. It is desirable to see how far the desorbent requirement can be reduced (thereby reducing operating cost) without sacrificing the required purity. Hence, we solved the following optimization problem:

$$\text{Min} \qquad I = Q_D\,[Q_D, Q_R, t_s, \chi] \tag{4.21}$$

$$\text{Subject to PurR and PurE} \geq \text{Experimental value (in L-H et al., 2002)} \tag{4.22}$$

Similar four decision variables were used as in case I except Q_D which is a decision variable in this case while Q_F is fixed (see Table 4.5). Yet again, four cases was considered (see Table 4.5) corresponding to the experimental values of flow rates Q_I and Q_F used in the work of Ludemann-Hombourger et al. (2002) with respect to 6-column SMB and 4, 5 and 6 columns Varicol respectively.

In solving constrained optimization using Genetic Algorithm, penalty methods have been mostly used with large value of constant, R. The constraints that are handled here is inequality constraint and bracket operator penalty term is not used in this case as mostly

suggested since it is not needed to penalize all the feasible points due to the relative importance of the magnitude of objective function rather than constraint violation.

Instead, a modified infinite barrier penalty is used since it penalizes only the infeasible point and takes the following form:

$$\Omega = R\left[(g_i - c_i) - \left|g_i - c_i\right|\right] \tag{4.23}$$

with R as penalty term (in this case 1000 is used), c_i is the purity requirement for separation and g_i represents the purity obtained from simulation. As can be examined from the above form, the penalty term assigns no penalty to feasible points since for feasible points, (g_i-c_i) will be equal to its absolute value so in this case, Ω will be zero. In the case of infeasible points, (g_i-c_i) will be negative because $g_i < c_i$ and its absolute value is subtracted from that negative term and then multiplied by the penalty parameter, R so a penalty proportionate to constraint violation is assigned to the objective function.

Thus the objective function will be of the form:

$$P_{(x)} = Q_F + R\sum_{i=1}^{2}\left[g_i - c_i) - \left|g_i - c_i\right|\right] \tag{4.24}$$

$$P_{(x)} = \frac{1}{1+Q_D} + R\sum_{i=1}^{2}\left[(g_i - c_i) - \left|g_i - c_i\right|\right] \tag{4.25}$$

Non Dominated Sorting Genetic Algorithm is designed for maximization problem making transformation is necessary to convert maximization problem into minimization problem and transformation of the form $I = \frac{1}{1+I}$ is used in all related minimization pro-

Table 4.7 Single objective optimization results

Performance Parameter	4-column Varicol			4-column SMB	
	L-H et al., 2002	Case 1a	Case 2a	Case 1a	Case 2a
Q_1 (ml/min)	21.3	21.3	21.3	21.3	21.3
Q_F (ml/min)	0.3	0.56 (+86%)	0.3	0.46 (+53%)	0.3
Q_D (ml/min)	13.06	13.06	8.09 (-38%)	13.06	10.11 (-23%)
Q_R (ml/min)	4.58	5.50	3.90	5.25	1.66
t_s (min)	0.8	0.60	0.60	0.70	0.77
χ (-)	0.85/1.5/1.15/0.5	A/D/D/E	C/C/D/F	C	C
Q_E (ml/min)	8.78	8.11	4.49	8.27	6.97
PurR (%)	99.6	99.85	99.75	99.98	99.99
PurE (%)	96.6	99.00	97.40	98.95	97.08
Y(g_{prod}/g_{CSP}/day)	0.906	1.698	0.918	1.431	0.913
RecR (%)	87.8	100	97.68	100	97.43
RecE (%)	99.9	98.90	98.57	98.73	97.64
SC (m^3/kg_{prod})	1.392	0.750	0.859	0.889	1.080

Table 4.7 Single objective optimization results (Cont'd)

Performance Parameter	5-column Varicol			5-column SMB	
	L-H et al., 2002	Case 1b	Case 2b	Case 1b	Case 2b
Q_1 (ml/min)	17.5	17.5	17.5	17.5	17.5
Q_F (ml/min)	0.3	0.51 (+70%)	0.3	0.46 (+54%)	0.3
Q_D (ml/min)	9.78	9.78	5.71 (-42%)	9.78	6.24 (-36%)
Q_R (ml/min)	2.49	4.96	1.89	2.05	0.89
t_s (min)	0.93	0.74	0.72	0.91	0.75
χ (-)	0.95/1.85/1.5/0.7	I/J/I/K	H/K/K/K	J	J
Q_E (ml/min)	7.59	5.33	4.12	8.19	5.65
PurR (%)	99.7	99.94	99.83	99.97	99.94
PurE (%)	96.8	99.28	99.85	99.17	99.33
Y(g_{prod}/g_{CSP}/day)	0.725	1.271	0.747	1.149	0.745
RecR (%)	96.8	100	100	100	99.83
RecE (%)	99.9	98.71	99.29	98.65	99.33
SC (m^3/kg_{prod})	1.05	0.600	0.596	0.664	0.653

Table 4.7 Single objective optimization results (Cont'd)

Performance	6-column SMB			6-column Varicol	
Parameter	L-H et al., 2002	Case 1c	Case 2c	Case 1c	Case 2c
Q_1 (ml/min)	15.3	15.3	15.3	15.3	15.3
Q_F (ml/min)	0.3	0.43 (+44%)	0.3	0.46 (+54%)	0.3
Q_D (ml/min)	8.55	8.55	5.57 (-35%)	8.55	5.40 (-37%)
Q_R (ml/min)	1.79	3.39	1.39	3.23	1.57
t_s (min)	1.11	0.89	0.87	0.90	0.83
χ (-)	P	P	P	N/P/T/T	O/N/T/T
Q_E (ml/min)	7.06	5.60	4.47	5.78	4.13
PurR (%)	99.6	99.98	99.97	100	99.91
PurE (%)	95.6	99.92	99.33	99.66	99.43
Y(g_{prod}/g_{CSP}/day)	0.60	0.91	0.62	0.98	0.62
RecR (%)	85	100	99.86	100	99.90
RecE (%)	99.9	99.08	97.98	98.98	99.43
SC (m^3/kg_{prod})	0.922	0.613	0.586	0.576	0.565

Table 4.7 Single objective optimization results (Cont'd)

Performance	6-column Varicol			6-column SMB	
Parameter	L-H et al., 2002	Case 1d	Case 2d	Case 1d	Case 2d
Q_1 (ml/min)	15.3	15.3	15.3	15.3	15.3
Q_F (ml/min)	0.33	0.53 (+59%)	0.33	0.50 (+50%)	0.33
Q_D (ml/min)	9.05	9.05	5.60 (-38%)	9.05	5.72 (-37%)
Q_R (ml/min)	1.89	4.46	1.29	2.36	1.20
t_s (min)	1.11	0.84	0.85	1.04	0.88
χ (-)	1/2.25/2/0.75	T/T/R/U	S/T/P/T	P	P
Q_E (ml/min)	7.49	5.11	4.64	7.19	4.85
PurR (%)	99.7	99.95	100	100	99.99
PurE (%)	95.6	99.66	99.60	99.49	99.60
Y(g_{prod}/g_{CSP}/day)	0.664	1.104	0.696	1.031	0.683
RecR (%)	85.1	100	100	100	100
RecE (%)	99.9	99.33	99.20	96.60	99.02
SC (m^3/kg_{prod})	0.888	0.533	0.532	0.571	0.544

blem. In this problem, inequality constraint is used rather than equality constraint due to the stringent condition imposed by equality constraint in finding adequate solution.

In total there are 6 variables in chiral separation process so if in the first two single objective cases, 3 variables are fixed then we have 3 degree of freedom. Likewise, we will have 4 degree of freedom if 2 variables are fixed in the last case. The lower and upper bounds for each decision variables is obtained from the sensitivity study.

Flow rate in section I, Q_I was chosen as fixed variables because Q_I was the highest flow rate in SMB process and by fixing Q_I, it would not violate the pressure drop constraint along the column as defined in Table 4.2. Volume of adsorbent, V_{col} was chosen as fixed variables to correspond to the experiment carried out by Ludemann-Hombouger, et. al. (2002), whose experimental data and results were used in this work.

Table 4.7 compares the optimum results obtained with GA for both cases 1 and 2 with that of the experimental results of Ludemann-Hombourger et al. (2002). It is seen that the GA optimization leads to a larger feed flow rate (for case 1) and smaller desorbent flow rate (for case 2) for 6-column SMB and 4, 5 and 6 columns Varicol compared to the reported results. The table also lists the optimum values of Q_R, t_s, and column configuration (χ) as well as calculated values of extract flow rate (Q_E), product purity (Pur), recovery (Rec), yield (Y), and solvent consumption (SC). From Table 4.7 it can be seen that optimization leads to an optimum Q_F = 0.56 ml/min, an increase of 86% over the experimental Q_F of 0.3 for the 4-column Varicol system. Similarly, when desorbent flow rate (Q_D) is minimized, an optimum Q_D = 8.1 ml/min was obtained, a decrease of 38% over the experimental Q_D of 13.06 for the 4-column Varicol system. An average improvement of about 55% in the amount of feed (throughput) can be handled while about

30-40% savings of desorbent requirement (although not simultaneously) without sacrificing product purities.

It is observed that the optimum switching time for the Varicol process is smaller than that of SMB. Varicol offers more flexibility, and therefore, does not require long residence time as in SMB. The optimum column distribution (χ) for the 4-column Varicol process is χ = A/D/D/E (which corresponds to 0.75/1.25/1.75/0.25) for case 1, while χ = C/C/D/F (≡1.25/0.75/1.25/0.75) for case 2. It shows that more columns are needed in zone 3 for case 1 and in zone 1 for case 2. Table 4.7 also reveals that improvement in Varicol over SMB is more obvious when the total number of columns is less, which imparts that Varicol offers more flexibility at relatively small number of columns. Note that in Table 4.7, shaded cells represent optimum values and the numbers in bracket for Q_F and Q_D are % improvement over the experimentally reported results.

These comparisons, relative to single-objective optimization problems show the reliability and efficiency of genetic algorithm (GA) in finding optimal operating conditions, which compare well with previous literature results and actually lead to improved values of the objective functions. The unique capabilities and superiority of the GA will clearly appear later when considering multi-objectives optimization problems.

4.7. Multi-Objectives Optimization

Multi-objectives optimization problems arise when several objectives are entailed from the system and they usually appear to contradict with one another. The fact that a certain objective can not be improved without forfeiting the others will lead to the concept

Table 4.8 Optimization attributes used in multi-objectives optimization

Problem		Obj. funct.	Constraints	Decision variables	Fixed variables
Case 3	SMB / varicol	Max PrR Max PrE	PurR > 90% PurE > 90%	$8 < Q_D < 15$ ml/min $2 < Q_R < 10$ ml/min $0.3 < t_s < 1$ min $3 < L_{col} < 7$ cm χ [See Table 3.1]	Q_1=17.49 ml/min $Q_F = 0.3$ ml/min $N_{col} = 4$ or 5
Case 4	SMB / varicol	Max PurR Max PrR	PurR > 90% PurE > 99%	$8 < Q_D < 15$ ml/min $2 < Q_R < 10$ ml/min $0.3 < t_s < 1$ min $3 < L_{col} < 7$ cm χ [See Table 3.1]	Q_1=17.49 ml/min $Q_F = 0.3$ ml/min $N_{col} = 4$ or 5
Case 5	SMB / varicol	Max PurE Max PrE	PurR > 99% PurE > 90%	$8 < Q_D < 15$ ml/min $2 < Q_R < 10$ ml/min $0.3 < t_s < 1$ min $3 < L_{col} < 7$ cm χ [See Table 3.1]	Q_1=17.49 ml/min $Q_F = 0.3$ ml/min $N_{col} = 4$ or 5
Case 6	SMB / varicol	Max Q_F Min Q_D	PurR > 99% PurE > 99%	$0.2 < Q_F < 0.45$ ml/min $5 < Q_D < 12$ ml/min $1 < Q_R < 5$ ml/min $0.3 < t_s < 1$ min χ [See Table 3.1]	Q_1=17.49 ml/min $L_{col} = 8.1$ cm $N_{col} = 4$ or 5
Case 7	SMB / varicol	Max PrR Max PrE Min L_{col}	PurR > 90% PurE > 90%	$8 < Q_D < 15$ ml/min $2 < Q_R < 10$ ml/min $0.3 < t_s < 1$ min $3 < L_{col} < 7$ cm χ [See Table 3.1]	Q_1=17.49 ml/min $Q_F = 0.3$ ml/min $N_{col} = 4$ or 5
Case 8	SMB / varicol	Max PrR Max PrE Min Q_D	PurR > 90% PurE > 90%	$8 < Q_D < 15$ ml/min $2 < Q_R < 10$ ml/min $0.3 < t_s < 1$ min χ [See Table 3.1]	Q_1=17.49 ml/min $Q_F = 0.3$ ml/min $L_{col} = 8.1$ cm $N_{col} = 4$ or 5

of Pareto optimal solution in which all the solutions are equally good and non-dominating each other. Numerous multi-objectives optimization problems can be formulated and they are vital particularly in the design of a new system. Process economy governs the formulation of objective function as tabulated in Table 4.8.

4.7.1. Case 3. Two Objectives Optimization: Maximization of raffinate and extract productivity

In two objectives optimization, productivity of raffinate and extract were employed as objective function with raffinate flow rate, eluent flow rate, switching time and column configuration as decision/dependent variables. Purity of both streams greater than 90% served as inequality constraint and was incorporated in the same way as in the previous case. The process parameter in case 1b single objective optimization was used in this multi-objectives optimization: Q_1 = 17.49 ml/min and Q_F = 0.3 ml/min.

Relative performance of 4-column Varicol, 5-column SMB and 5-column Varicol is assessed under the same condition and the result can be observed in Figure 4.11 where each point in the Pareto set corresponds to a set of decision variables. It is clearly shown that 5-column Varicol offers more room for improvement indicated by the size of the Pareto set, followed by 5-column SMB and 4-column Varicol. The optimum configuration for 4-column Varicol in the Pareto set is χ = B-B-C-F which means the column configuration is 1/1/1/1 for the first two subinterval followed by 1/2/1/0 for the third sub interval and 2/1/1/0 for the last sub interval. The optimum column configuration for 5-column SMB is χ = I which is essentially 1/2/1/1 configuration and this is similar to experimental column configuration.

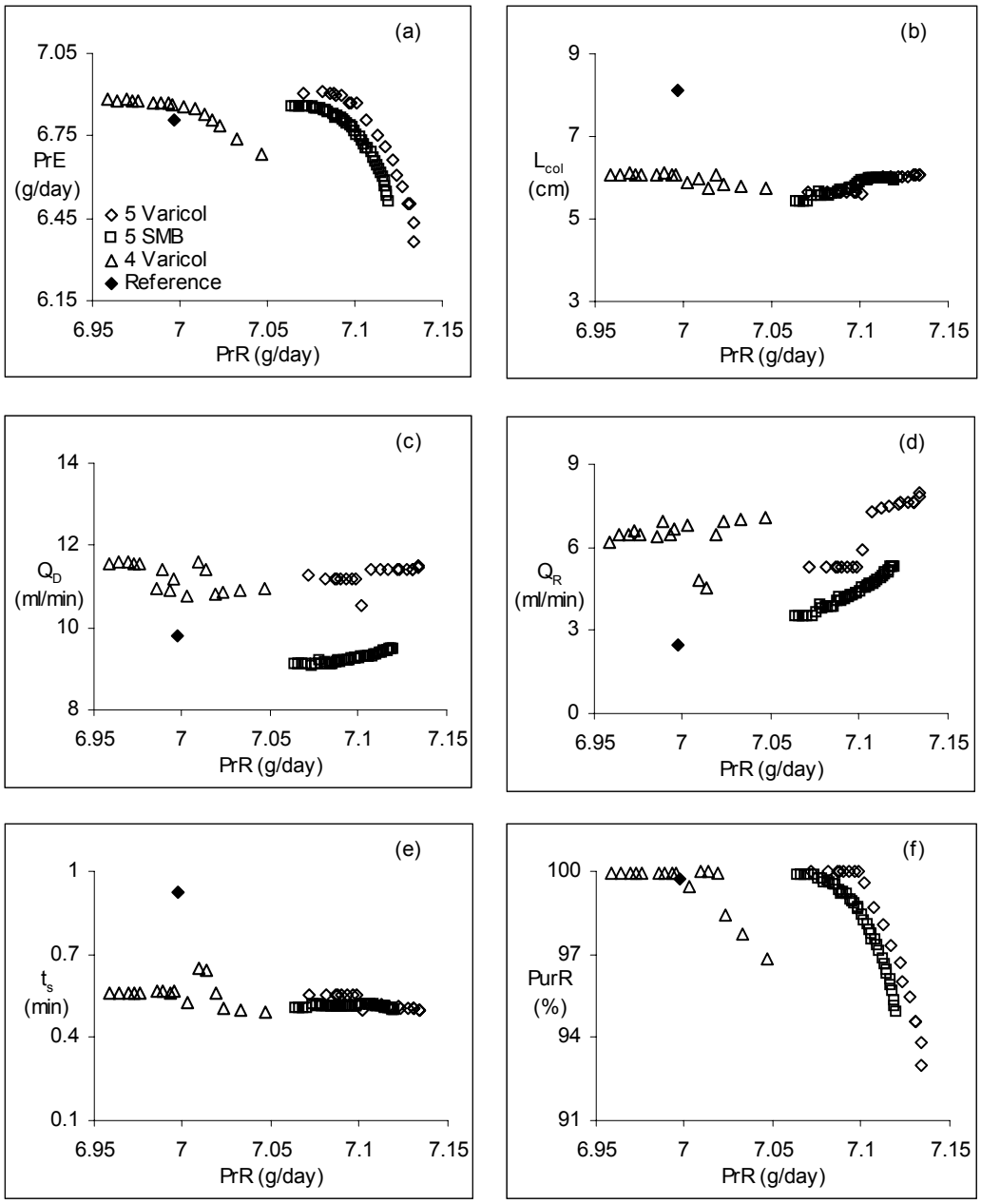

Figure 4.11 Pareto optimal solution and plot of decision variables (case 3) for SMB and Varicol systems

Significant transition from 4-column Varicol to 5-column SMB is observed, especially in terms of raffinate productivity but 5-column SMB slightly suffers in terms of extract productivity. It can be seen that the experiment is almost performed in the optimum range

for 4-column Varicol suggested in this study. Improved productivity of both stream is achieved with 5-column Varicol with χ = H-I-J-J indicating more column is needed in section III (between the feed and raffinate withdrawal port) during the early sub switching and similarly, one more column is needed in section I (between the eluent port and the extract withdrawal port) during the last subswitching. Purity of extract product achieved in this case is greater than 99% thus is not shown in Figure 4.11 while other operating parameter is kept constant for the sake of fair comparison.

4.7.2. Case 4. Two Objectives Optimization: Maximization of raffinate purity and productivity

Simultaneous maximization of purity and productivity of raffinate stream for a given feed flow rate is subjected to a constraint that the purity of extract stream must be greater than 99%. High product purity is typically an important requirement in drug manufacture although for a binary mixture with a low separation factor ($K_A/K_B < 1.15$), the high purity requirement entails high cost and low throughput. In this case optimal design of SMB and Varicol processes were performed at the design stage. Table 4.8 lists the objective function, constraints, decision variables and fixed parameter values used in this study. Five decision variables (Q_D, Q_R, t_s, L_{col}, χ) were used in the optimization study. Since Q_F and Q_1 (this comes directly from fixing the maximum allowable pressure drop in the system) were fixed, only two other flow rates (among Q_D, Q_R, Q_E, Q_2, Q_3 and Q_4) could be determined independently. We selected Q_D and Q_R as the two decision variables. Switching time (t_s), length of each column (L_{col}) and distribution (for SMB) and sequence (for Varicol) of columns were selected as the other decision variables.

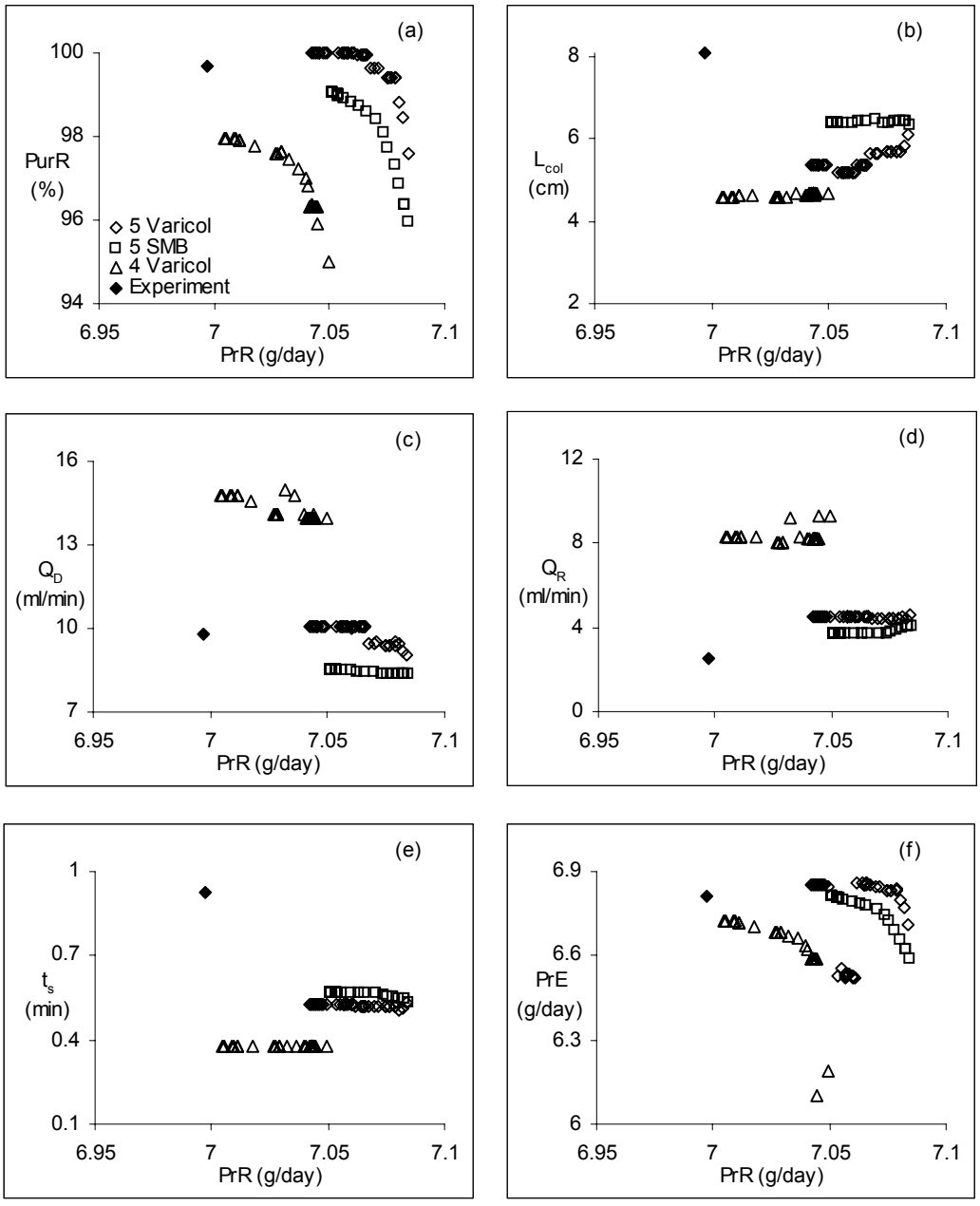

Figure 4.12 Pareto optimal solution and plot of decision variables (case 4) for SMB and Varicol systems

Relative performance of 4-column Varicol, 5-column SMB and Varicol was assessed under the same conditions and the result is shown in Figure 4.12. The Pareto optimal solution obtained represents the maximum possible productivity and purity of raffinate

streams. The benefit of multi-objectives optimization study is evident upon observing the wide range of operating points available in the optimal Pareto set. If conventional techniques were used, we would have been able to predict only one point at a time on the Pareto optimal curves, by fixing either one and maximizing the other.

The figure clearly shows that 5-column Varicol offers more room for improvement indicated by the magnitude of the Pareto set, followed by 5-column SMB and 4-column Varicol. The maximum attainable productivity and purity of raffinate stream in a 4-column Varicol system are less than that could be obtained in a 5-column SMB. In other words, the increase achieved in a 5-column SMB system is due to the increase of one column (which implies a 25% increase of stationary phase) outweighs the improvement attainable due to the increase in flexibility in a 4-column 4-subinterval Varicol system, which on the other hand does not imply any additional cost. Each point on the Pareto set corresponds to a set of decision variables.

The optimum configuration for 4-column 4-subinterval Varicol in the Pareto set is χ = B-A-D-D, which means the column configuration, is 0/2/1/1 for the first sub-interval, 0/1/2/1 for the second sub-interval followed by 1/1/2/0 for the last two sub-intervals. This corresponds to average column configuration of 0.5/1.25/1.75/0.5. The optimum column configuration for 5-column SMB is χ = J, which is essentially 1/2/1/1, while for 5-column Varicol it is χ = I-I-J-J, which corresponds to 1/1.5/1.5/1. Significant transition from 4-column Varicol to 5-column SMB and finally to 5-column Varicol is observed indicating the difficulty in obtaining high extract product purity (>99%). The optimum column distribution for both 4 and 5-column Varicol process indicates that zone II (between the extract withdrawal port and the feed entry port) and zone III (between the feed and

raffinate withdrawal port) is critical in maximizing the productivity and purity of the raffinate product. This is expected as the primary job for zone II and zone III is to desorb less strongly adsorbed component and retain more strongly adsorbed component.

4.7.3. Case 5. Two Objectives Optimization: Maximization of extract purity and productivity

The optimization problem studied in this case is exactly similar to case 4 except it is done for maximization of productivity and purity of extract stream subject to purity of raffinate stream greater than 99%. Low purity product can be obtained in large amount while high purity product ends up in small quantity. Case 4 and 5 co-exist in this study as adequate information about the relative importance of raffinate and extract product is not available and this dilemma can be resolved by assuming the two products are of equal importance.

The Pareto set in Figure 4.13 shows that 5-column Varicol maintains its narrow dominance over 5-column SMB and 4-column Varicol, and concurrently confirms the previous finding that it is relatively easier to satisfy high raffinate purity constraint than high extract purity. This is because the less adsorbed component is always moving with the mobile phase. The optimum column configuration for 4- and 5-column Varicol are χ = C-C-E-G (≡1.25/1.25/1/0.5) and χ = H-J-J-K (≡1.25/1.5/1/1.25) respectively while the same for 5-column SMB is χ = K (≡2/1/1/1).

The optimal column configuration for 4- and 5-column Varicol requires more columns in zone I (between the desorbent and extract port) and II (between the feed and extract withdrawal port) as the extract is the product of interest. This is in line with the role of zo-

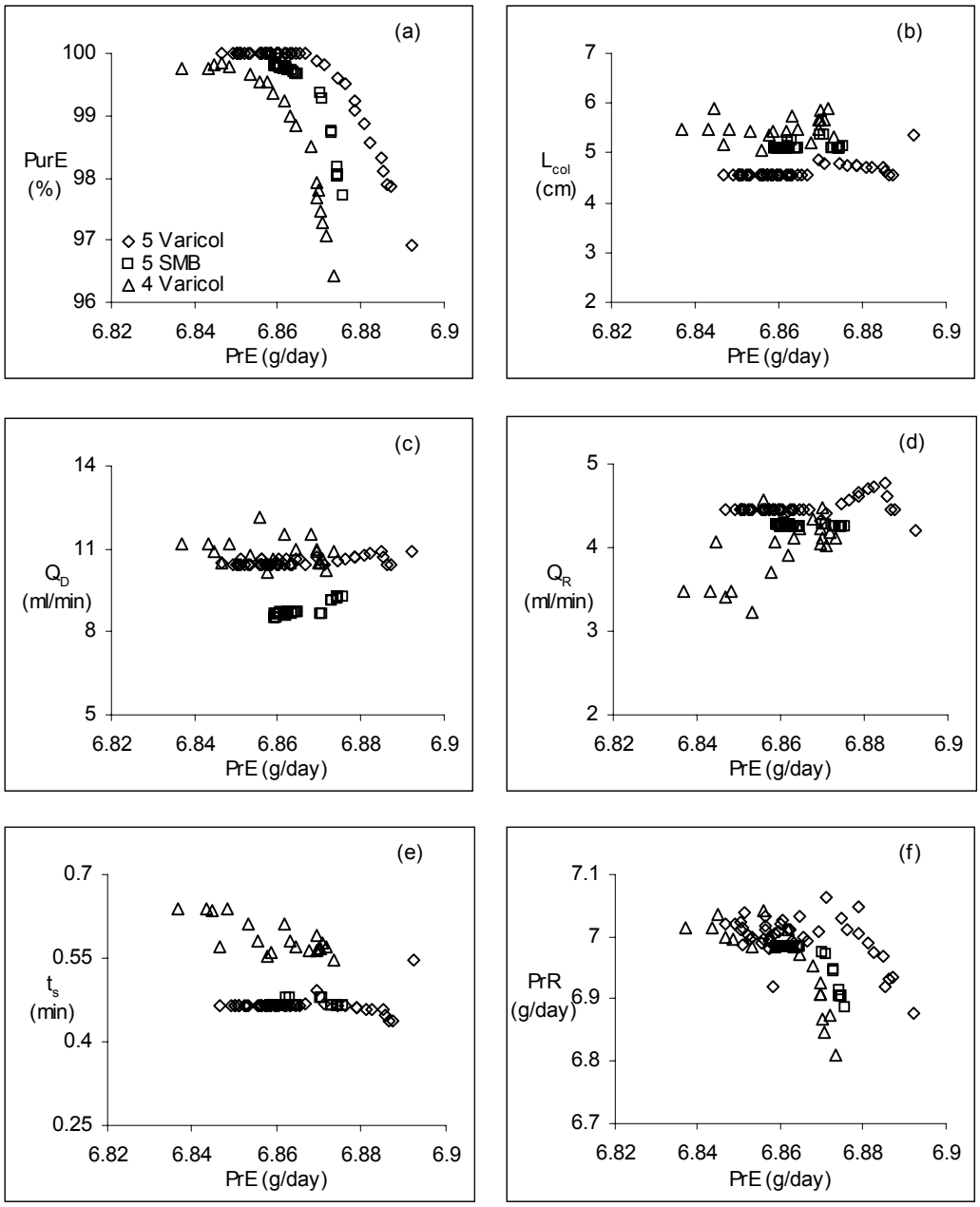

Figure 4.13 Pareto optimal solution and plot of decision variables (case 5) for SMB and Varicol systems

ne II, assuring complete desorption of the less strongly adsorbed component from the adsorbent, as the adsorbent has just been in contact with fresh feed in zone III. Subsequently, the desorbent will desorbs the more strongly component from the adsorbent

thus more column is needed in zone I. As expected, figure 4.13 shows desorbent flow rate increases as extract productivity increases while raffinate flow rate is slightly scattered as this variable was found to be less sensitive, in line with previous finding that pure raffinate stream is easier to obtain, towards the objective functions.

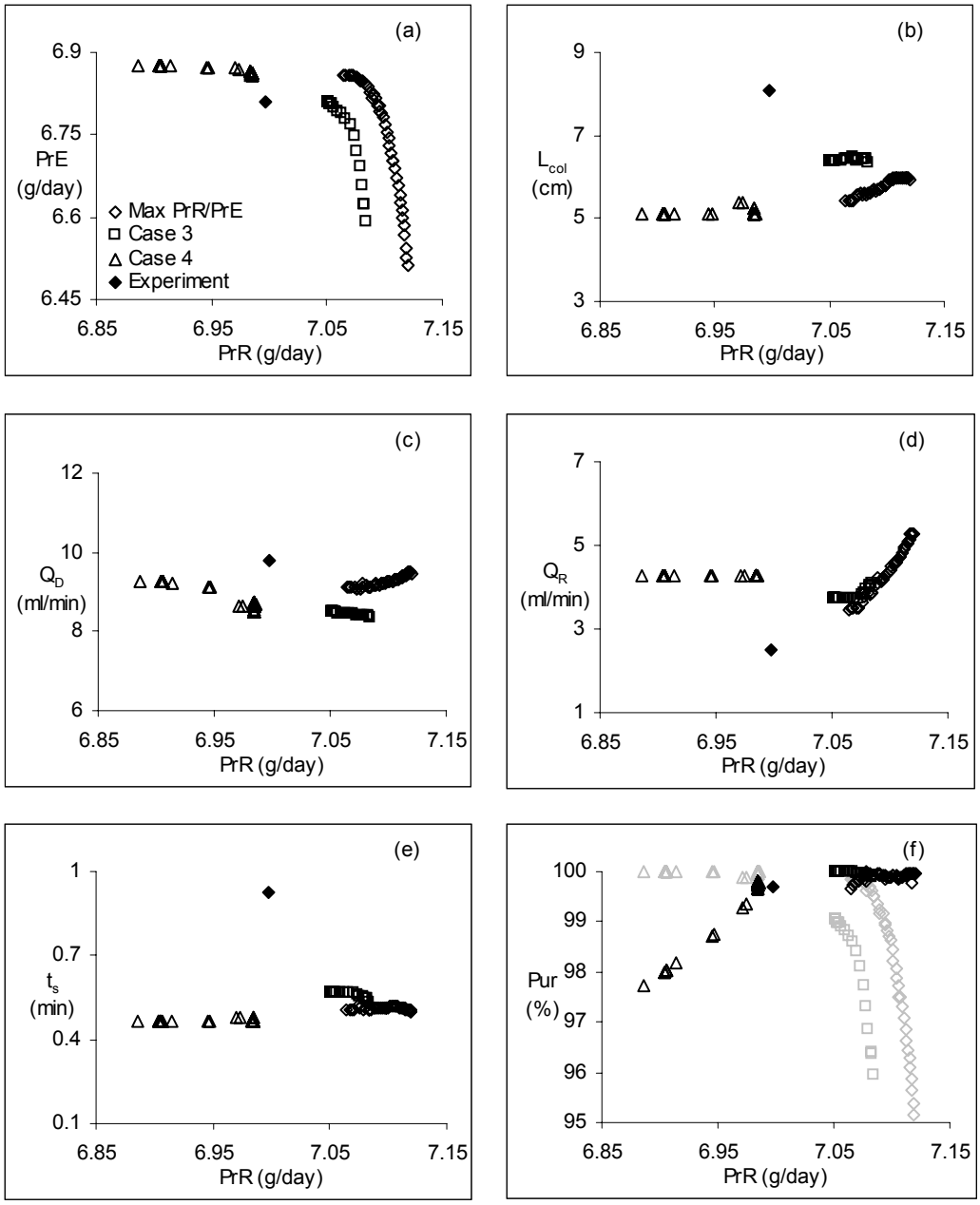

Figure 4.14 Pareto optimal solution and plot of decision variables (comparison between case 3, case 4 and case 5) for SMB and Varicol systems

The decision variables in Figure 4.13 demonstrate much similar trend in which desorbent flow rate increases as extract productivity increases. In addition, a comparison between case 3, case 4 and case 5 for 5-column SMB is illustrated in Figure 4.14 where case 3 exhibits relatively higher raffinate and extract product over case 4 but only higher raffinate productivity over case 5. The Pareto for case 3 is optimized under 90% minimum purity requirement and gives better result at relatively close decision variable given it has more lenient purity constraint (Refer to Table 4.8).

4.7.4. Case 6. Two Objectives Optimization: Maximization of throughput and minimization of desorbent consumption

Another case of multi-objectives optimization is formulated in view of economic consideration. In this case optimal process operation conditions were determined to reduce operating costs by minimizing desorbent flow rate while increasing revenue by increasing productivity through maximization of feed flow rate for product purities greater than a specified value.

The choice of the two objective functions, as in Table 4.8, enables to maximize production using minimum solvent for product purities greater than 99% of both extract and raffinate streams for 5-column SMB and 4 and 5-column Varicol systems. Similar to earlier cases, Q_1, the column flow rate in zone I, was fixed at 17.49 ml/min to keep the maximum system pressure drop constant, and the total CSP used was also fixed by fixing L_{col} = 8.1 cm and N_{col} = 4 or 5. The dependence of pressure drop on liquid flow rate is shown in Table 4.2 and the fact that zone I has the highest flow rate of all zones have

necessitated the need to set Q_1 to keep the system working within the maximum tolerable pressure drop.

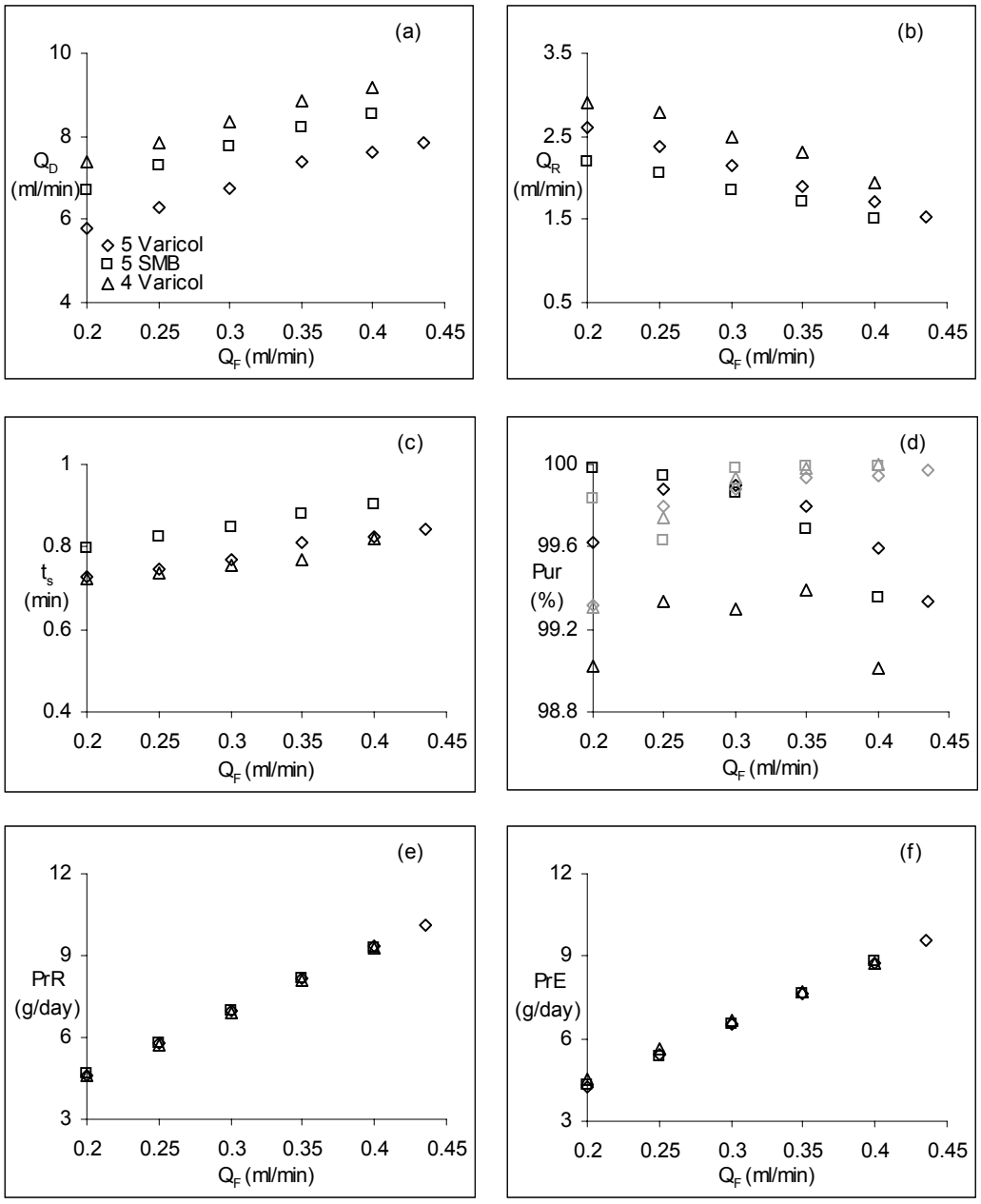

Figure 4.15 Pareto optimal solution and plot of decision variables (case 6) for SMB and Varicol systems

The details of the optimization formulation together with the bounds used for the decision variables are reported in Table 4.8. Note that the two variables (Q_F and Q_D) appear in the objective functions as well as in decision variables. The Pareto optimal solutions (Q_F vs Q_D) and the values of the associated decision variables are shown in Figure 4.15. The Pareto shown in the figure indicate that both the SMB and Varicol processes need to increase desorbent consumption in order to increase throughput. Secondly, for similar conditions, the Varicol process consumes less desorbent (Q_D) than an equivalent SMB process for the same feed flow rate, Q_F; or for similar desorbent consumption, the Varicol process can treat more feed. Thus, it is confirmed and quantified that the flexibility due to the non-synchronous shift of the input/output ports in a Varicol process achieves the same desired target purity with less eluent and/or treats more feed. Increasing desorbent consumption compensates the increase in amount of feed to be treated as the separation task becomes for difficult. More desorbent is needed to ensure sufficient desorption of the strongly adsorbed component from the adsorbent. The optimum column configuration for 4-column Varicol is C-B-C-D (≡0.75/1.25/1.25/0.75) while for 5-column SMB is H (≡1/1/1/2) and for 5-column Varicol is I-H-K-J (≡1.25/1.25/1.25/1.25). The trends are expected as more desorbent is needed when the feed flow rate is increased. Again, 5-column Varicol outweigh 4-column Varicol and 5-column SMB and it conveys that 5-column Varicol consume less desorbent or for the same amount of desorbent, it can treat more feed compared to 4-column Varicol and 5-column SMB.

4.7.5. Case 7. Three Objectives Optimization: Maximization of raffinate and extract productivity and minimization of solid requirement

Three objectives optimization is formulated in view of economic consideration related to the investment involved in every chiral separation process. The dilemma of high initial cost has motivated the needs of increasing productivity at low fixed cost. Thus, an additional objective function is needed to compensate the increase in productivity that is, minimizing solid requirement. This is similar to minimizing column length (at fixed column ID) as amount of CSP required for separation is directly related to the volume of column. The fixed and decision variable for three objective optimization are essentially similar to those of previous two objectives optimization.

The Pareto set represented in Figure 4.16 is showing consistency with the previous one in terms of the size of the Pareto (Figure 4.11). Another similarity is the tendency that 5-column SMB perform in raffinate productivity and suffer in extract productivity relative to 4-column Varicol even though this indication is not quite obvious in the previous case. The column configuration for 4-column Varicol and 5-column Varicol are also similar but there are two unique column configurations that constitute the Pareto set for 5-column SMB. The upper part of the Pareto set is generated by χ = J indicating more column in zone 1 (between eluent port and extract withdrawal port) is needed to increase extract productivity and the lower part is given by χ = I similar to case II. Time and again, 5-column Varicol displays its superiority over 5-column SMB and 4-column Varicol. Purity of raffinate product achieved in this case is greater than 99% and in all optimization result presented in this work, the decision variable demonstrate similar trend such as raffinate flow rate increases as raffinate productivity increases.

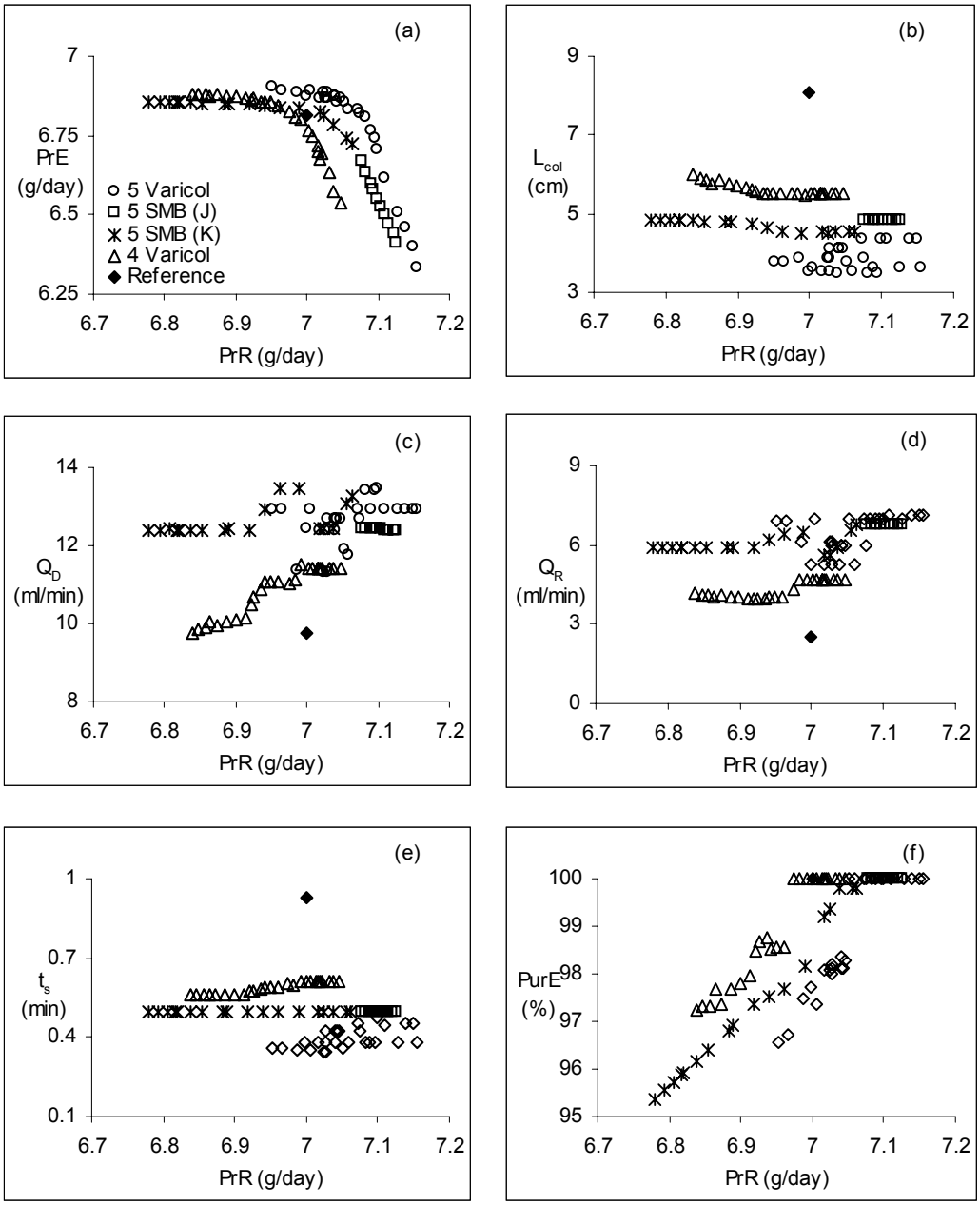

Figure 4.16 Pareto optimal solution and plot of decision variables (case 7) for SMB and Varicol systems

4.7.6. Case 8. Three Objectives Optimization: Maximization of raffinate and extract productivity and minimization of desorbent consumption

The problem formulation for case 7 and 8 looked similar in which the only difference comes from the third objective function. The third objective function in case 7 represents the minimization of fixed cost yet this time, it represents the minimization of operating cost. Case 7 and 8 exist concurrently to provide the decision maker and or operator more options in operating the system as cost information is site and time specific.

The Pareto optimal solution for 4-column Varicol, 5-column SMB and 5-column Varicol interestingly converge to the same solution as displayed in Figure 4.17. In general, increased desorbent consumption will follow the increase in total number column because it also implies the increase of adsorbent involved in the separation. The behavior of the system in the region of limited desorbent could be understood as 4-column Varicol tends to attain higher productivity at reasonable desorbent while 5-column SMB/Varicol prefers to minimize their desorbent consumption due to their originally high productivities. This phenomenon can be justified if new definition, namely desorbent consumption per column (Q_D/column), is used over the course of the separation. Figure 4.17(b) shows comparable magnitude of Q_D/column for 4-column Varicol, 5-column SMB and 5-column Varicol.

Another interesting finding is the sensitivity of the decision variables for each solution obtained using this specific objective function. Small changes made toward any decision variable will cause significant deviation in the objective function in Figure 4.17(a). This can be understood as desorbent is critical in enantioseparation and all points in Figure 4.17(a) are obtained in the condition of limited presence of desorbent. Figure

4.17(f) shows the common feature in every chromatographic separation: the ease of obtaining raffinate product at higher purity relative to extract product. Column configura-

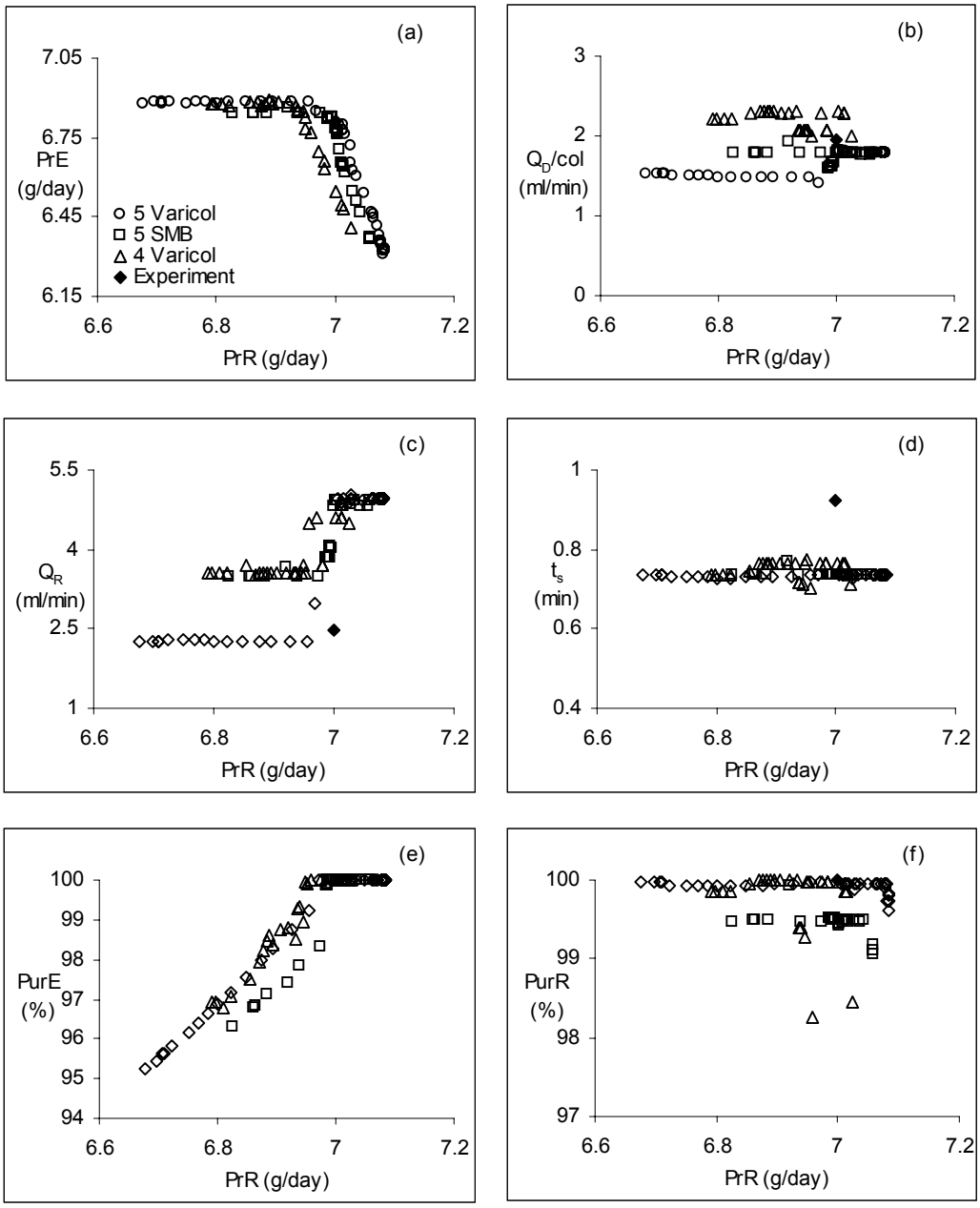

Figure 4.17 Pareto optimal solution and plot of decision variables (case 8) for SMB and Varicol systems

tion for 4-column Varicol is 1/1/1/1, 1/1/1/1, 1/2/1/0 and 2/1/1/0 while for 5-column SMB is 1/2/1/1. Switching sequence of 1/1/2/1, 1/2/1/1, 2/1/1/1 and 2/1/1/1 constitute the Pareto for 5-column Varicol in Figure 4.17. The optimization results, however, indicates that similar productivity can be achieved at relatively lower desorbent requirement compared to that used in the experiment.

4.8. Pure Separation Regime for Binary Separation

For better understanding of the reliability of the optimization results it is worthwhile to discuss the results using equilibrium theory applied to countercurrent chromatography (Storti et al., 1995). They showed that the unit behavior could be explained in terms of the flow rate ratio parameters relative to the four zones of the unit:

$$m_j = \frac{Q_j t_s - V_{col}\varepsilon}{V_{col}(1-\varepsilon)}, \qquad j = 1 \sim 4 \tag{4.26}$$

In particular, the flow rate ratio parameter m_1 has to be larger than a critical value (σ_i in eq. (4.18) to be less than 1 for both components) in order to achieve complete regeneration of the solid phase from the strongly adsorbed (heavy) component, while m_4 has to be smaller than a critical value ($\sigma_i > 1$ for both components) in order to achieve complete regeneration of the liquid phase from the weakly adsorbed (light) component. Once both such conditions are satisfied, it is possible to identify in the (m_2-m_3) parameter plane a triangular region, which includes all pairs of values leading to complete separation ($\sigma > 1$ for one component and $\sigma < 1$ for the other), i.e., the two components are recovered pure in the extract and in the raffinate, respectively. This region, which depends only on the adsorption isotherms and also feed concentration, has been calculated and represented

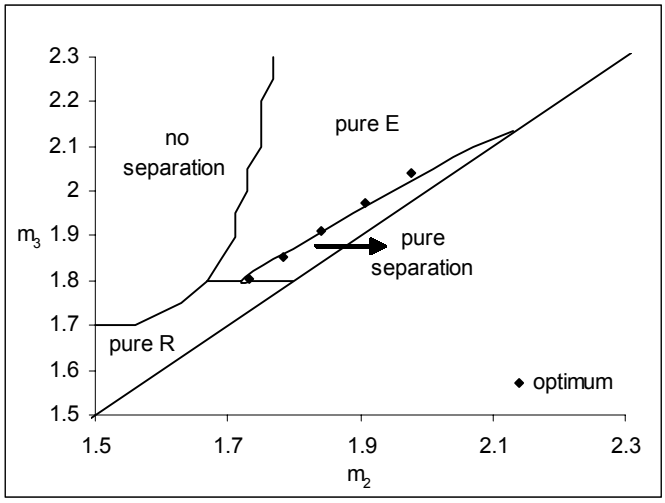

Figure 4.18 Optimum operating regime in m_2-m_3 plane for enantioseparation of SB-553261 racemate using 5-column SMB (case 6)

in Figure 4.18 for 5-column SMB and in Figure 4.19 for 5-column Varicol process. In the upper right region, with respect to that of complete separation, a pure extract stream is obtained, while the raffinate is polluted. In the lower left region, only the raffinate and not extract is obtained pure. Finally, it is worth pointing out that the distance from the diagonal of a point in the (m_2 - m_3) plane is directly proportional to productivity and inver-

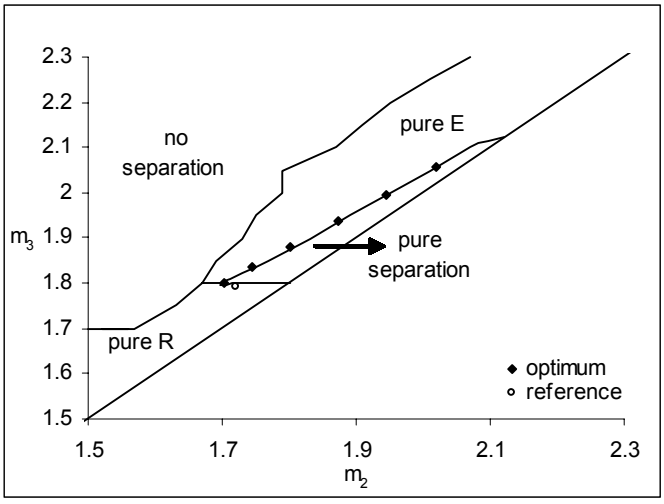

Figure 4.19 Optimum operating regime in m_2-m_3 plane for enantioseparation of SB-553261 racemate using 5-column Varicol (case 6)

sely proportional to desorbent requirement. The vertex of the complete separation triangular region gives thus the optimal operating point with respect to such two process performances.

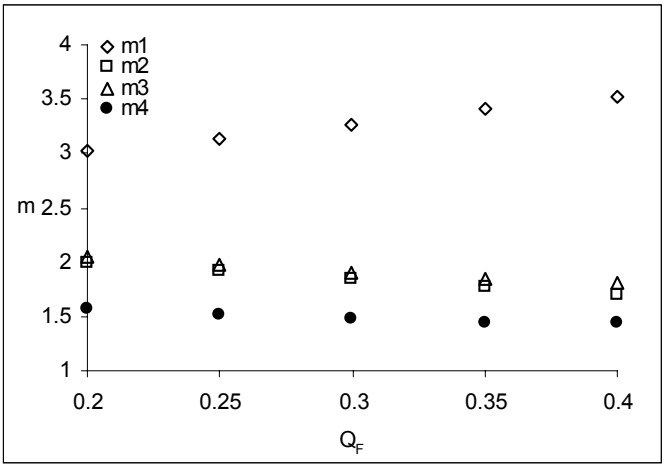

Figure 4.20 m operating plane for enantioseparation of SB-553261 racemate using 5-column SMB (case 6)

In order to interpret the results of the optimization, the optimal values of the decision variables in Figure 4.15 have been re-plotted in terms of the four flow rate ratio parameters, m_j, as shown in Figure 4.20 for 5-column SMB and Figure 4.21 for 5-column

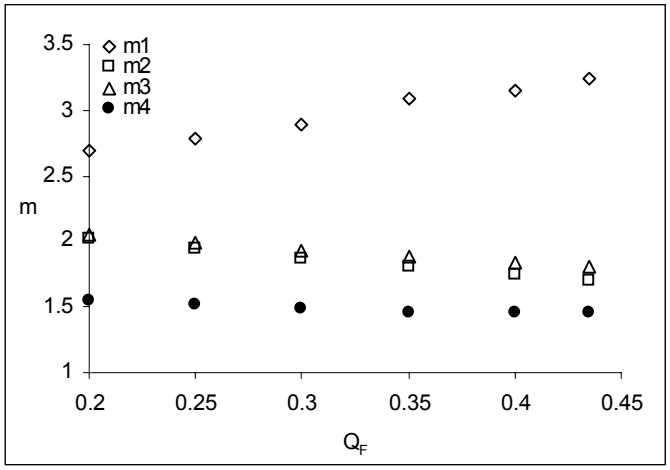

Figure 4.21 m operating plane for enantioseparation of SB-553261 racemate using 5-column Varicol (case 6)

Varicol process, respectively. Both figures reveal that all operating points on the Pareto correspond to a substantially constant value of m_1, in agreement with equilibrium theory, which predict a constant lower bound for such parameter. Only for the points corresponding to the higher feed flow rate we observe an increase of m_1. This is due to the necessity to improve the solid regeneration in zone I in order to avoid that the heavier component entering zone IV and then pollutes the raffinate. This indicates that zone I is critical in controlling the purity in the raffinate as production increases. It is better to control the regeneration of the solid from the heavy component in zone I. On the other hand, m_4 undergoes smaller changes, indicating that zone IV is much less critical to achieve the desired separation performance in the particular case under examination.

It is seen that the values of m_2 and m_3 obtained in each case do change very little as the feed flow rate increases. This is consistent with the equilibrium theory result, which indicates that the optimal operating point (the vertex of the triangle) is independent of the feed and eluent flow rates. Moreover, the values of m_2 and m_3 should not vary a lot, according to equilibrium theory, which would see them constant and corresponding to the vertex of the complete separation region. However, due to dispersion phenomena, same change in m_2 and m_3 is observed, and actually they both tend to decrease, as moving along the Pareto.

Switching time increases as feed flow rate increases (see Figure 4.15) because one has to increase the residence time in order to achieve high purity separation. The increase in switching time initiates the increase of m_1 at fixed value of Q_1. The declining value of m_2 and m_3 is expected, as the internal flow rates tend to decrease with the increase of feed flow rate. This phenomenon is consistent with the increase in switching time (Figure 4.15)

as contact between fluid phase and solid phase has to be maximized as the separation becomes more and more difficult. The reduction of flow rate in zone IV is merely the net effect of increasing desorbent consumption as the feed flow rate increases. The reduced flow rate compensates the increase in switching time (eq. 4.26) and it contributes to the decrease of m_4. The value of m_1 for 5-column Varicol is somewhat smaller than that of SMB due to the smaller switching time while the magnitude of m_2, m_3 and m_4 for both systems are more or less similar.

The comparison of m values in Figure 4.20 and 4.21 between SMB and Varicol systems also explain the ability of the latter to handle more feed than SMB process at the same size of triangle. As a consequence of the fact that the performance of the separation (i.e. the flow rate ratio parameter values) remains substantially constant for all the operating points along the Pareto, also the optimal column configuration remains the same both for the 5-column SMB and the 4- and 5-column Varicol processes, and equal to 1/1/1/2, 0.75/1.25/1.25/0.75 and 1.25/1.25/1.25/1.25 respectively. Note that the flexibility of Varicol in distributing the column in the various zones of the unit allows making such a transition more smoothly and following closer the separation needs, than the SMB process. This justifies the improvement in its performance.

Figure 4.18 and 4.19 show the location of each optimum point within the m_2-m_3 plane for 5-column SMB and Varicol respectively. The complete separation region with 99% purity requirement forms a triangle with the maximum amount feed which can be handled is precisely located at the vertex of the triangle. The optimum points (stretching along one side of the triangle) move toward the vertex as the feed flow rate increases. The fact that optimum points lie on the border of the triangle is expected as the optimum point will opt

to move away from the diagonal line. Both reveal that the size of the triangle is relatively small, indicating the difficulty level for the enantioseparation and even though the size of the triangle is almost similar, Varicol can treat up to Q_F = 0.435 ml/min, slightly more amount of feed than SMB (Q_F = 0.4 ml/min) at 5-column configuration. Figure 4.18 and 4.19 explicitly show that the complete separation region is independent of the feed flow rate. It is worth observing that the interpretation above, based on equilibrium theory basic concepts, helps to rationalize the results of the optimization procedure, which when plotted in terms of the original variables (i.e. Figure 4.15) appear a bit confusing

4.9. The Effect of Sub-interval and Partial Feed Operation

Optimized results of SMB and Varicol, both single objective as well as multi objectives, process have shown that Varicol process performed better than the traditional SMB process due to flexibility of the former. The enhanced performance of n-column Varicol process, however, never emulate that of (n+1)-column SMB process. This is because the advantage of having one extra column and therefore more solid phase for higher purity and increased productivity. It is theoretically possible to further boost Varicol performance by manipulating its flexibility or applying partial feed operation.

Sub-interval operation introduces more additional degree of freedom to the system. A more flexible allocation of stationary phase to each of the four zones can be attained adjusting to each local separation task. It might happen that a smooth transition is necessary for a certain column configuration before shifting to another. Optimization formulation in case 3 (objective function, fixed and decision variable, upper and lower

bounds, etc.) are used, with further subdivision of switching interval, to illustrate the concept.

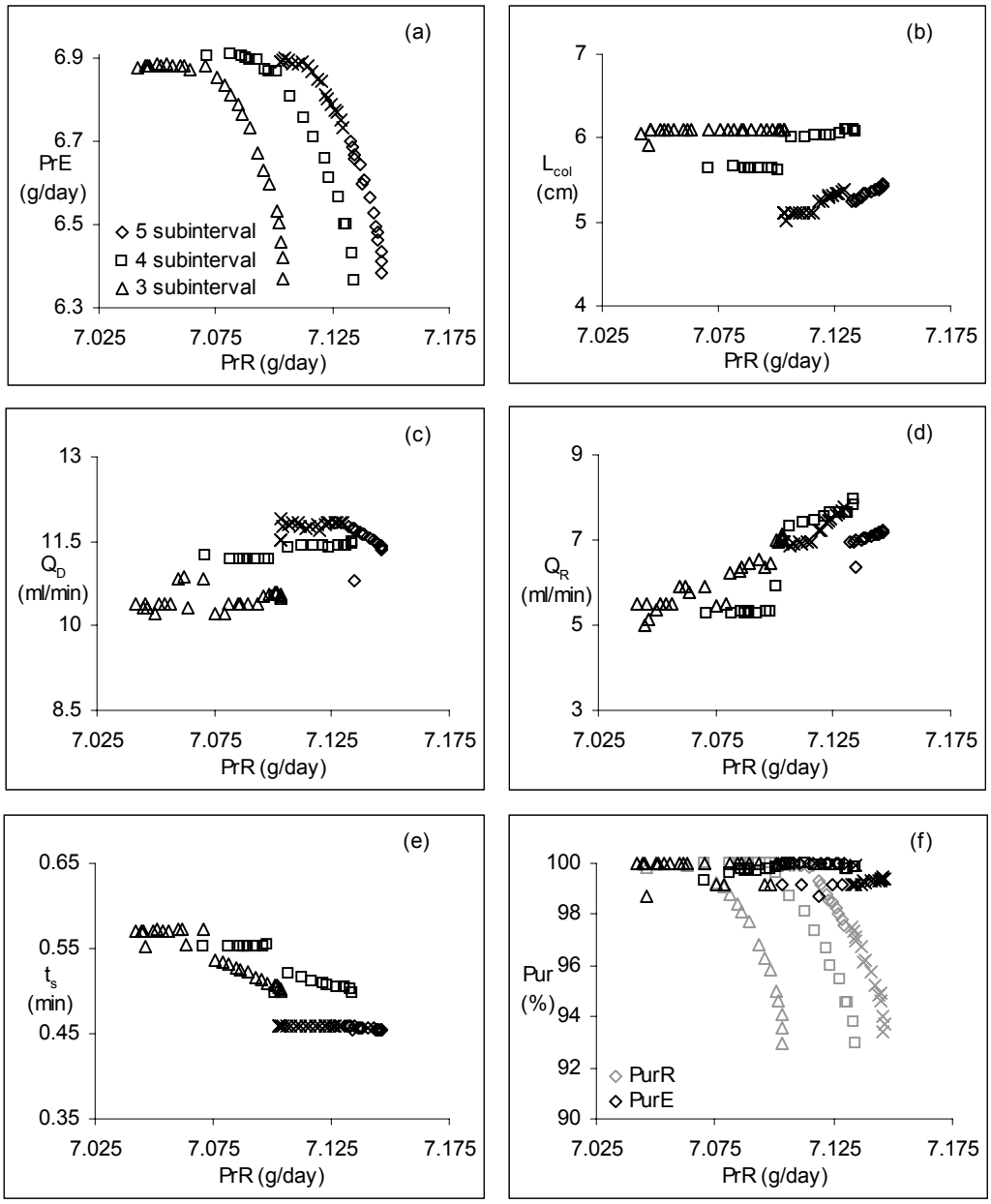

Figure 4.22 The effect of subinterval for 5-column Varicol (case 3)

Figure 4.22 showed the effect of sub-switching interval, onto 4-zone Varicol process, with maximum productivity as the objective function. The optimal switching sequence for

3-subinterval is I/J/K while for 4-subinterval it consists of I/J/K/K. The upper part of 5-subinterval Pareto is given by I/J/K/K/K while the lower part is made of J/I/J/J/J. This column distribution can be expounded that more column in zone III is mandatory in the early switching for sufficient feed loading and extra column in zone I is necessary in the latter period to regenerate the considerably saturated adsorbent.

The switching distribution at higher subinterval suggests that column regeneration is more critical during the whole process. The improvement at higher subinterval is marginal thus proper consideration is required, especially at extremely small magnitude of switching time.

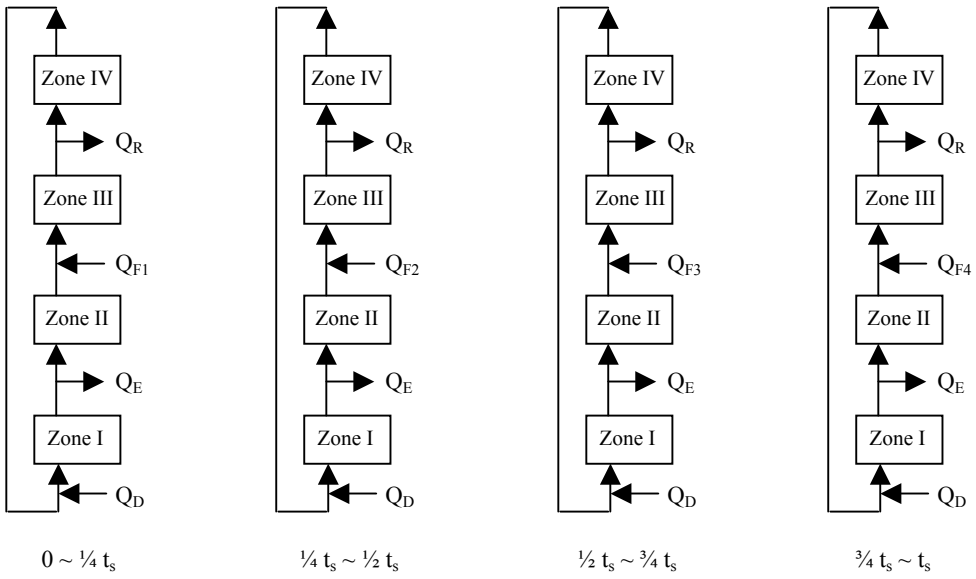

Figure 4.23 Discrete feed operation for 5-column 4-interval SMB process

Another distinct adaptation to SMB and Varicol process is the asynchronous introduction of feed to the system. The idea is essentially similar to application of solvent gradient (Jensen et al., 2002) as the highest strength is needed in zone I where solid regeneration takes place. This concept, referred here as discrete feed operation, was first

introduced by Kearney and Hieb (1992) followed by flow rate optimization (Kloppenburg and Gilles, 1999) and comparison with total feed operation (Zang and Wankat, 2002).

In discrete feed operation, the system is fed at discrete interval to allow proper allocation due to the idea that the highest portion of feed should be given, i.e. in the absence of separation, at early switching period. Like sub-interval operation, discrete feed operation introduces more degree of freedom than constant feed operation. Optimization formulation in case 3 is used as reference, i.e. constant feed operation, in this study. Extract flow rate is allowed to adjust according the mass balance constraint while the total amount of feed per unit time is kept constant, with switching time is discretized into 4 interval, according to

$$[Q_F \cdot t_s]_{total} = [Q_{F1} + Q_{F2} + Q_{F3} + Q_{F4}]_{discrete} \cdot ¼\, t_s \tag{4.27}$$

Figure 4.24 summarize the optimum result for both 5-column 4-interval SMB and Varicol in comparison with constant feed operation for case 3-optimization formulation. High extract purity is obtained for all systems; therefore it is not plotted in Figure 4.24. Length of column is fixed for fair comparisons. Yet two values, one for SMB and another for Varicol system, are used, which were obtained from the optimization earlier.

For SMB system, low value of L_{col} (~5.58 cm) leads to two configurations: K for the upper part of the Pareto for discrete operation (solid black triangle) and J for the middle part (empty black triangle). Column sequence J/K/K/K is obtained for shorter column Varicol (~6.02 cm). SMB column distribution for higher value of L_{col} (~5.98 cm) is I as indicated by solid grey triangle and Varicol switching sequence is given by J/J/K/K at

column length about 6.09 cm. It can be seen that discrete feed operation leads to higher values of objective function.

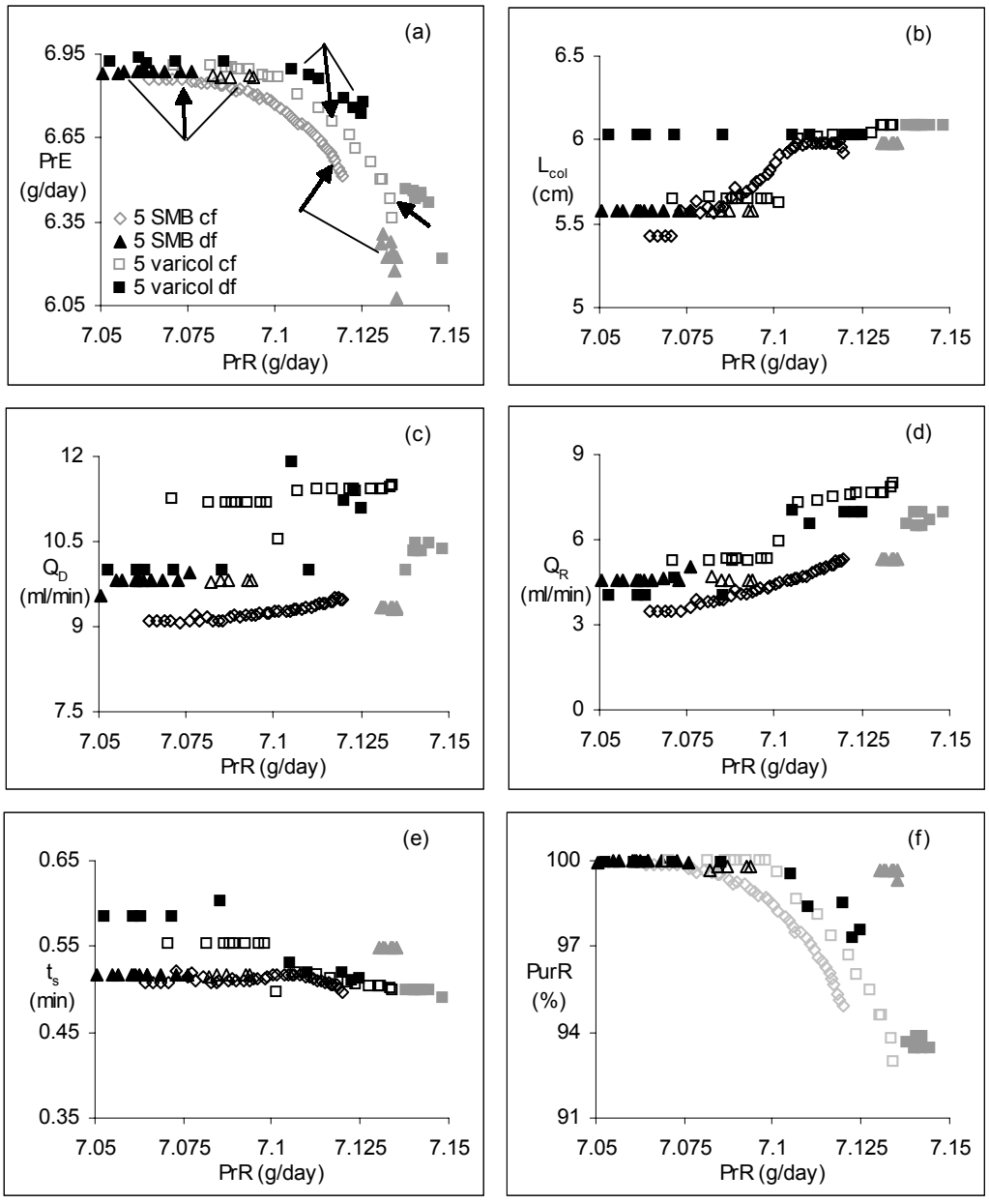

Figure 4.24 Comparison between discrete feed and constant feed operation for 5-column 4-interval SMB and Varicol processes (case 3)

The average feed flow rate was 0.3 ml/min for both constant feed and discrete feed operations in Figure 4.24 while feed distribution for discrete feed operation, for shorter column length, is given in Figure 4.25 indicating that the highest feed load is required at the first interval and the requirement plunges almost to nothing for the 2nd interval. Feed loading shoots up again, at the third interval for SMB and at the fourth interval for varicol,

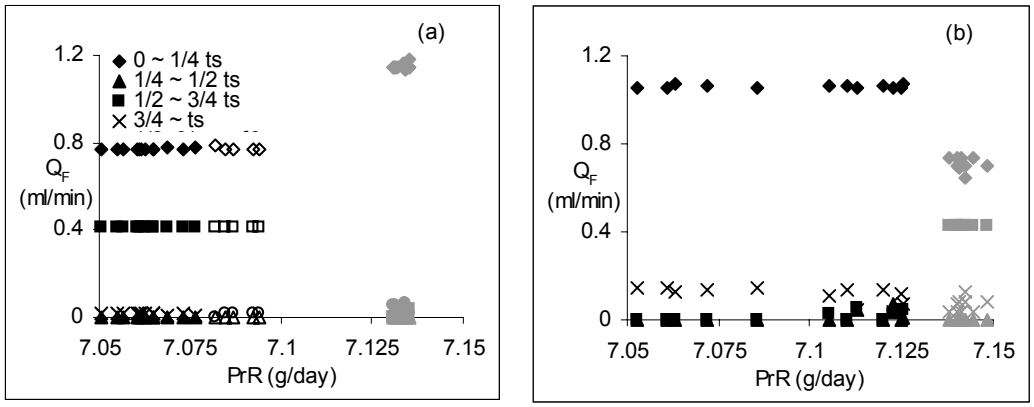

Figure 4.25 Feed profile for discrete feed and constant feed operation for 5-column 4-interval SMB and Varicol processes (case 3)

but this time the amount is less than the initial loading. Different feed loading behavior is observed for longer column. The highest feed rate is applied at the first interval and immediately sinks at the next subinterval for SMB system while feed behavior for longer column Varicol repeats feed behavior for shorter SMB (see Figure 4.25). This finding is obvious as there is no separation takes place at the beginning of the interval thus higher feed flow is necessary to initiate loading. The loading process is relaxed when sufficient amount of feed presents in the system as it focuses on separation task. This cycle repeated again for the third and last sub interval at smaller magnitude due to reduced capacity of the adsorbent in treating the previous load.

An extreme improvement is expected for more complicated system i.e. integrated reactor-separator system as task distribution is more obvious in such system. The process scenario will be high feed loading at the initial interval, medium loading at the middle interval as reaction takes place and low loading at the end of the interval for separation. This result clearly shows the advantage of applying discrete/gradient operation and still could be further enhanced by applying discrete desorbent flow rate as well.

Chapter 5

Optimization Study for Continuous Chromatographic Separation of a Chiral Intermediate

5.1. The Application of 1,1'-bi-2-naphtol

The development of a highly enantioselective chiral catalysts for asymmetric synthesis has encouraged strong interest among scientists to resolve racemic mixture of these potential catalysts into its optically pure form. The catalytic asymmetric carbon-carbon bondforming reactions are the most popular in the field of asymmetric catalysis (Noyori, 1994). A number of remarkably effective catalysts have been synthesized from chiral alcohol, making it the highly valuable intermediates for the manufacturing of chiral pharmaceuticals and agricultural products. Several highly enantioselective catalyst from alcohol derivatives have been reported in the literature such as β-amino alcohol (Noyori et al., 1990), pyrrolidinylmethanols (Soai et al., 1987), 1,3-dioxolan-4,5-dimethanol/DINOL (Schmidt and Seebach, 1991) and 1,1'-bi-2-naphtol/BINOL (Kitajima et al., 1996). The later is preferred due to its distinctive features: BINOL ligands contain hard oxygen atoms that is used to coordinate with hard metal centers such as Al(III), Ti(IV), Zn(II) and Ln(III) to produce highly enantioselective Lewis acid catalyst for many asymmetric organic transformations such as Diels-Alder reactions (Maruoka et al., 1988; Maruoka and Yamamoto, 1989; Terada et al., 1991; Bao et al., 1993), Michael additions (Tomioka et al., 1989; Jansen and Feringa, 1990), Mukaiyama aldol-ene reactions (Mikami and Matsukawa, 1993) and glyoxylate-ene reactions (Van der Meer and Feringa, 1992; Terada et al. 1994). BINOL and its derivatives have been regarded as important chirality source

for many chemical processes. The C_2-symmetric chiral 1,1'-bi-2-naphtol is also used as chiral auxiliaries in stoichiometric and catalytic asymmetric synthesis such as aza Diels-Alder reactions (Hattori and Yamamoto, 1992), enantioselective protonations (Ishihara et al., 1994), nitroaldol reactions (Sasai et al., 1992), hydroformylations (Sakai et al., 1993; Nozaki et al., 1997), alkylation (Chan et al., 1997), oxidations (Komatsu et al., 1993; Reetz et al., 1997), enantioselective reduction of ketone (Noyori et al, 1984a, 1984b; Suzuki et al. 1990) and epoxidations (Bougauchi, 1997). Optically active binaphthyl derivatives have been applied in host-guest chemistry, molecular recognition and enantioselective chromatography separation (Helgeson et al., 1974; Lehn et al., 1978; Sogah and Cram, 1979; Lingenfelter et al., 1981; Artz et al., 1985; Castro et al., 1989). BINOL derivatives have been used to control the stereochemistry of polymer structures in polymerization processes (Okamoto and Nakano, 1994; Nakano and Sogah, 1995).

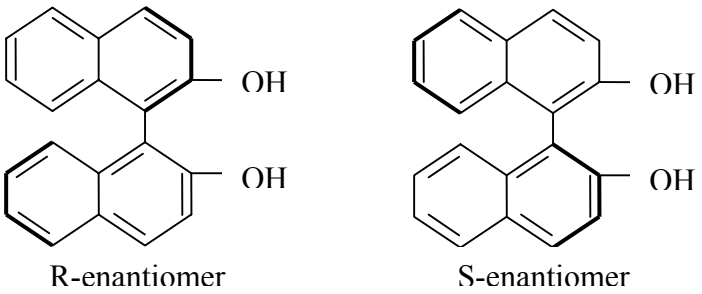

Figure 5.1 Molecular structure of 1,1'-bi-2-naphtol optical isomer

The 1,1'-bi-2-naphtol molecule is classified as axially chiral molecule due to restricted rotation of the two naphthalene rings. The single bond joining the two aromatic ring systems can not rotate freely. Both enantiomers of 1,1'-bi-2-naphtol serve important application in asymmetric reactions such as asymmetric reductions (Noyori et al., 1984b;

Suzuki et al., 1990), asymmetric alkylation (Fuji et al., 1990; Maglioli et al., 1992), asymmetric induction (Whitesell, 1989) and asymmetric catalysis (Maruoka et al., 1988; Bao et al., 1993). They are also found useful in synthesis of chiral macrocycles (Lehn et al., 1978; Sogah and Cram, 1979) or as a chiral host for optical resolution and chiral shift reagent for the determination of optical purity and absolute configurations of a wide range of chiral compound. BINOL has a remarkable enantio-differentiating property but its application is dictated by the cost of this material due to complexity encountered in obtaining it in optically pure form. Methods for preparation of optically active BINOL are well reported in literature ranging from classical resolution to enzymatic hydrolysis of their derivatives such as fractional crystallization of diastereomeric cyclic phosphate ester derivatives (Jacques and Fouquay, 1988; Truesdale, 1988; Tamai et al., 1990; Gong et al., 1991; Brunel and Buono, 1993; Fabbri et al., 1993), enzymatic hydrolysis of the diester of 1,1'-bi-2-naphtol (Kazlauskas, 1989, 1991), resolution through inclusion complexes (Kawashima and Hirayama, 1990; Tanaka et al., 1993; Toda et al., 1994; Hu et al., 1995) and enantioselective oxidative coupling of 2-naphtol in the presence of chiral amines (Smrcina et al., 1993; Nakajima et al., 1995). Some of these methods will only give one pure enantiomer, either R or S, thus requiring some modification in the resolution procedure and or chiral resolving agent. Chow et al. (1996) have pointed out that they fail to resolve 4,4'-dibromo-1,1'-bi-2-naphtol using Toda's procedure although the same method is able to resolve 1,1'-bi-2-naphtol in good optical purity. The unsubstituted 1,1'-bi-2-naphtol could be resolved using enzymatic method but poor solubility of the 4,4'-dibromo derivative in the medium lead to another failure. Expensive chiral sources and complicated experiment parts are also leaving scientist a challenge to come up with a

more simple and practical method with good reproducibility. Moreover, the need to produce in synthetic scale is another important factor that should come into consideration in choosing the appropriate method to prepare BINOL in considerably high purity.

Several practical resolutions of BINOL by chromatography employing chiral stationary phase are developing rapidly. Racemic mixture of 1,1'-bi-2-naphtol can be synthesized from its starting material (2-naphtol) catalyzed by copper(II) catalyst in air (Noji et al., 1994). This is followed by optical resolution by isolating one species from its racemic mixture, usually involving the use of resolving agent

5.2. Mathematical Model of SMB and Varicol Process

There are two ways of simulating the SMB (Ruthven and Ching, 1989): the first, known as equivalent True Moving Bed (TMB) approach, which represents each of the four sections as counter-current bed and solid moves with a velocity, u_s (which is equivalent to the ratio of bed length (L_{col}) to the switching time of an actual SMB process). The solid moves counter-currently in relation to the fluid phase and the problem is reduced to writing the pertinent mass balance equations for each of the species involved in each of the four countercurrent sections, together with the global mass balance around the eluent, extract, feed and raffinate port. Steady state condition is indicated with stationary internal profiles and constant product concentrations. The second, known as actual SMB approach, represents the system as an array of fixed beds connected in series with moving boundary conditions at regular time intervals. The steady state is actually a periodic condition with moving internal profiles at a definite pattern. The product

concentration varies within a period despite similar cycle averages to that of TMB approach and this is known as cyclic steady state.

Dispersive plug flow models are used in this study to simulate 4-zone SMB behavior with linear driving force approximation to describe the mass transfer kinetics between the two phases. The dispersive plug flow model assumes rapid mass transfer across the column thus implying one dimensionality of the system that concentration and velocities are radially homogeneous but it accounts for a finite extent of axial dispersion. Axial dispersion was taken into account for the mobile phase while plug flow was considered for the stationary phase. The mass balance for each component of a racemic mixture can be expressed by convection-dispersion PDEs as described below.

Mass balance of component i in the mobile phase:

$$\frac{\partial C_{i,j}^{(N)}}{\partial t} + \frac{(1-\varepsilon)}{\varepsilon} k[q_{i,j}^{*(N)} - q_{i,j}^{(N)}] = D_j \frac{\partial^2 C_{i,j}^{(N)}}{\partial z^2} - v_j \frac{\partial C_{i,j}^{(N)}}{\partial z} \tag{5.1}$$

Mass balance of component i in the stationary phase:

$$\frac{\partial q_{i,j}^{(N)}}{\partial t} = k[q_{i,j}^{*(N)} - q_{i,j}^{(N)}] \tag{5.2}$$

Initial condition,

when N = 0,

$$C_{i,j}^{(0)} = 0 \tag{5.3}$$

when $N \geq 0$,

$$C_{i,j}^{(N)} = C_{i,j+1}^{(N-1)} \qquad \text{for j = 1, } (N_{col} - 1) \tag{5.4}$$

$$C_{i,j}^{(N)} = C_{i,1}^{(N-1)} \qquad \text{for j = } N_{col} \tag{5.5}$$

Boundary Condition,

Desorbent port,

$$C_{i,j}^{(N)}\Big|_{z=0} = \frac{(v_j - v_E)C_{i,j-1}^{(N)}\big|_{z=L}}{v_j} \tag{5.6}$$

Feed port,

$$C_{i,j}^{(N)}\Big|_{z=0} = \frac{(v_j - v_F)C_{i,j-1}^{(N)}\big|_{z=L} + v_F C_F}{v_j} \tag{5.7}$$

Extract/Raffinate port,

$$C_{i,j}^{(N)}\Big|_{z=0} = C_{i,j-1}^{(N)}\big|_{z=L} \tag{5.8}$$

The assumptions made in the modeling of SMB process are:

1. The process is isothermal

2. Mobile phase velocity is constant throughout the process
3. Negligible compressibility of the mobile phase
4. Porous and spherical particle for the stationary phase are uniform in size
5. Negligible concentration gradient in the radial direction of the bed
6. Local equilibrium exist for each component between the pore surface (monolayer) and the stagnant fluid phase inside the macropore
7. Dispersion coefficients of all components are independent of concentration

The model consider the influence of a finite column efficiency as a small correction but the validity of this model is confirmed when the column efficiency is high such as in the case of RPLC of small molecules of moderate polarity. The adsorption equilibrium isotherms (Nicoud and Seidel-Morgenstern, 1993; Nicoud, 1995) are given by the following expressions:

$$q_A^* = \frac{2.69C_A}{1+0.0336C_A+0.0466C_B} + \frac{0.1C_A}{1+C_A+3C_B} \tag{5.9}$$

$$q_B^* = \frac{3.73C_A}{1+0.0336C_A+0.0466C_B} + \frac{0.3C_A}{1+C_A+3C_B} \tag{5.10}$$

The PDEs from the above mass balance equations with all accompanying adsorption isotherms, initial and boundary conditions were solved using the method of lines (Schiesser, 1991). The PDEs are discretized in space using Finite Difference Method to convert it into a set of several-coupled ODE-IVPs. The resulting stiff ODE of initial value kind was solved using DIVPAG subroutine in IMSL library based on Gear's algorithm.

5.3. Model Validation

The model is verified by comparing with the experimental and simulation results reported by Pais et al. (1997a, 1997b, 1998). The experimental conditions used by them are tabulated in Table 5.1 and the comparative results are shown in Table 5.2 to Table 5.5. The results show that our SMB model under predicts the experimental result in terms of purity while the simulation results reported by Pais et al. (1997a, b, 1998) over predicts at similar operating conditions.

Table 5.1 Experimental and simulation process parameter for enantioseparation of 1,1'-bi-2 naphtol racemate

Parameter	Table 5.2	Table 5.3	Table 5.4	Table 5.5
L_{col}, cm	10.5	10.5	10.5	10.5
Column ID, cm	2.6	2.6	2.6	2.6
ε	0.4	0.4	0.4	0.4
C_F, g/l	2.9	2.9	2.9	2.9
Q_1, ml/min	56.83	56.83	56.83	56.83
Q_E, ml/min	16	17.98	16	17.98
Q_R, ml/min	9.09	7.11	9.09	7.11
Q_F, ml/min	3.64	3.64	3.64	3.64
Q_D, ml/min	21.45	21.45	21.45	21.45
t_s, min	See Table 5.2	2.75	See Table 5.4	See Table 5.5
χ	2/2/2/2	See Table 5.3	2/2/2/2	See Table 5.5

Table 5.2 Comparison between experimental (Pais et al., 1997a) and simulation result for enantioseparation of 1,1'-bi-2 naphtol racemate at various switching time

Run		t_s	Pur(%)		Rec(%)		SC(l/g)		Y(g/h/l_s)	
		min	E	R	E	R	E	R	E	R
	Exp.		74	93.8	96	66.6	2.47	3.57	2.27	1.58
1	Pred.[1]	2.55	76.8	92.3	-	-	-	-	-	-
	Pred.[2]		71.7	90.9	94.1	63.2	2.53	3.76	2.23	1.5
	Exp.[1]		93	96.2	97.3	91.6	2.44	2.59	2.31	2.17
2	Pred.[1]	2.75	95.4	97.6	-	-	-	-	-	-
	Pred.[2]		91.7	96.3	96.4	92	2.46	2.58	2.29	2.18
	Exp.[1]		95.6	95.4	95	96.1	2.48	2.45	2.27	2.3
3	Pred.[1]	2.80	97.4	98.2	-	-	-	-	-	-
	Pred.[2]		94.5	96.4	96.4	95.1	2.47	2.5	2.28	2.26
	Exp.[1]		91.5	70.9	61.5	94.7	3.86	2.51	1.46	2.24
4	Pred.[1]	3.05	97.9	85.8	-	-	-	-	-	-
	Pred.[2]		96.4	79.2	74.1	97.9	3.21	2.43	1.76	2.32

[1] Pais et al. (1997a)
[2] This work

The resulting concentration profiles are also compared with the experimental and the simulation results reported by Pais et al. (1998). Figure 5.2 demonstrate that the experimental and the simulated concentration profiles based on the operating conditions used in Pais et al. (1998) are comparable, and therefore, reliability of the SMB model in predicting the internal concentration profiles.

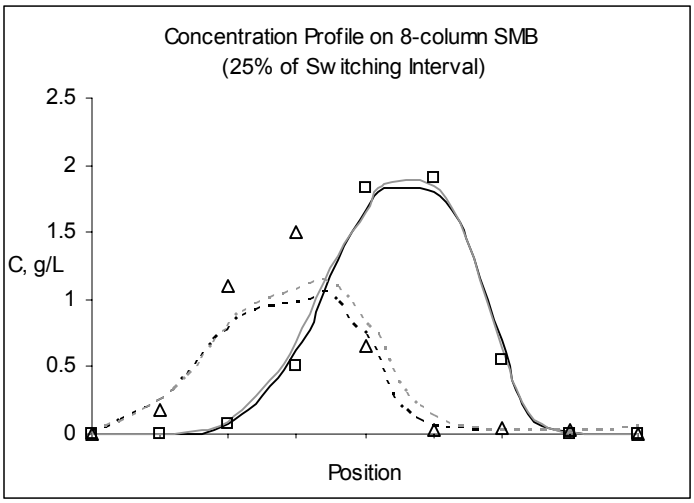

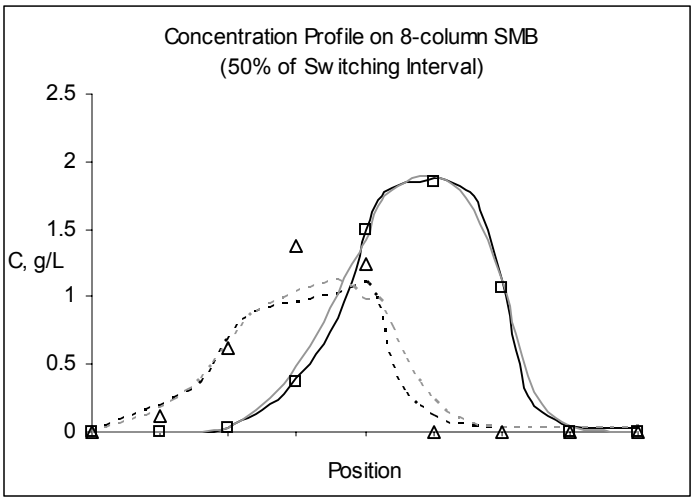

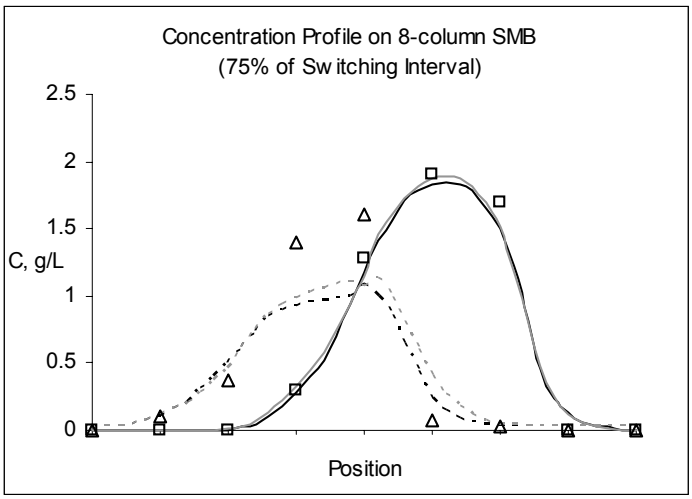

Figure 5.2 Experimental and simulated concentration profile on 8-column SMB based on operating parameter in Pais et al., 1998 (symbol: experiment, black: simulation by Pais et al., grey: simulation by this work)

Table 5.3 Comparison between Experimental (Pais et al., 1997a) and simulation result for enantioseparation of 1,1'-bi-2 naphtol racemate at various column configurations

Run		χ	Pur(%)		Rec(%)		SC(l/g)		Y(g/h/l_s)	
			E	R	E	R	E	R	E	R
A	Exp.[1]	2/2/2/2	93	96.2	97.3	91.6	2.44	2.59	2.31	2.17
	Pred.[1]		95.4	97.6	-	-	-	-	-	-
	Pred.[2]		91.7	96.3	96.4	92	2.46	2.58	2.29	2.18
B	Exp.[1]	1/3/3/1	94.8	95	97.1	96.8	2.45	2.45	2.3	2.29
	Pred.[1]		97	94.5	-	-	-	-	-	-
	Pred.[2]		93	91.7	91.7	94.2	2.59	2.52	2.17	2.23
C	Exp.[1]	1/2/4/1	92.6	95.2	97.5	94.5	2.44	2.52	2.31	2.24
	Pred.[1]		94.6	94.3	-	-	-	-	-	-
	Pred.[2]		89.2	91.5	91.9	90	2.59	2.64	2.18	2.13

[1] Pais et al. (1997a)
[2] This work

Table 5.4 Comparison between experimental (Pais et al., 1997b) and simulation result for enantioseparation of 1,1'-bi-2 naphtol racemate

Run		t_s	Pur(%)		Rec(%)		SC(l/g)		Y(g/h/l_s)	
		min	E	R	E	R	E	R	E	R
1	Exp.[1]	172	94.5	98.9	99.1	94.1	2.37	2.5	2.37	2.25
	Pred.[2]		91	98.2	98	90.9	2.42	2.62	2.32	2.15
2	Exp.[1]	165	93	96.2	97.3	91.6	2.44	2.59	2.31	2.17
	Pred.[2]		91.7	96.3	96.4	92	2.46	2.58	2.29	2.18

[1] Pais et al. (1997b)
[2] This work

Table 5.5 Comparison between experimental (Pais et al., 1998) and simulation result for enantioseparation of 1,1'-bi-2 naphtol racemate

Case		t_s min	χ	α	*Pe*	Pur(%)	
						E	R
SMB4	Exp.[1]	6	1/1/1/1	36	2000	89.7	95.3
	Pred.[2]					86.7	91.3
SMB8	Exp.[1]	3	2/2/2/2	18	1000	95.9	98.7
	Pred.[2]					95.1	96.7
SMB12	Exp.[1]	2	3/3/3/3	12	667	96.8	99.1
	Pred.[2]					96.5	97.6

[1] Pais et al. (1998)
[2] This work

5.4. Sensitivity Analysis

SMB chromatography utilizes operating variables which have different effect on the separation performance. Some variables may exercise insignificant effect while other may dictate the overall process performance in distinctive way. It is of particular interest to study the effect of switching time (t_s), raffinate flow rate (Q_R), desorbent flow rate (Q_D) and number of columns in any particular zone ($N_Ø$) on the purity and the productivity of the enantiomers collected at the raffinate and extract ports. Purity and productivity, as process performance parameter, is chosen as the two objective functions due to their vital role in assessing the viability of chiral separation process.

The sensitivity analysis is performed by varying one variable at a time keeping all other variables fixed, mostly at values at which the experiment was done. At this end, it may provide rudimentary information whether the experiments are carried out within the

optimum framework. The information, however, is premature to be regarded as optima as intricate interaction between each decision variable introduces adversity to such stochastic optimization procedure.

5.4.1. The Effect of Switching Time

Figure 5.3 (a) and (b) represent the impact to separation performance when switching time is varied keeping all other parameters constant at the reference value listed in Table 5.1. In general, switching time is directly linked to solid phase velocity, and therefore, the residence time of the components within the columns. Increasing switching time will lower the solid velocity thereby increasing residence time of the component as switching time is inversely proportional to solid velocity. Hence, increase of switching time will allow enough time for the components to be positioned along the raffinate and extract withdrawal port just before the switching operation is performed.

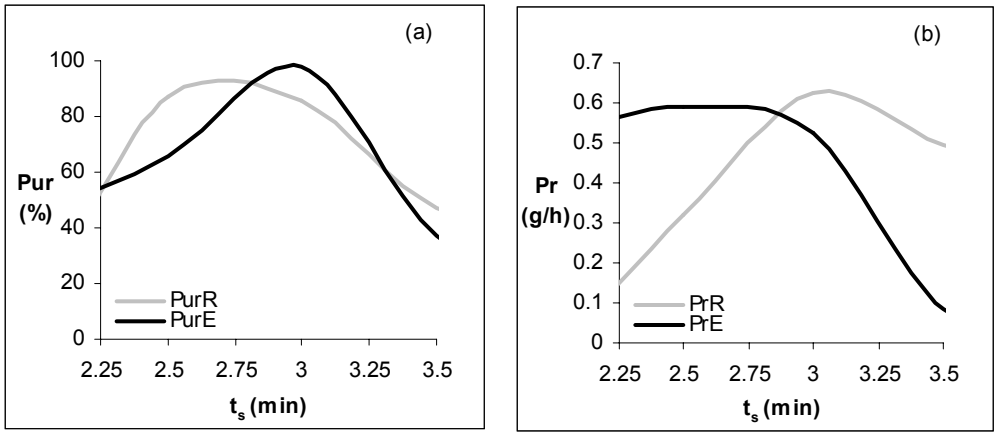

Figure 5.3 The effect of switching time on purity and productivity

The purities of both enantiomers, however, deteriorate when the switching time is increased beyond 3 minutes. It can be seen from Figure 5.3(b) that the components tend to move with the mobile phase rather than with the stationary phase and it contributes to the increase of raffinate productivity. An interesting phenomenon from Figure 5.3(a) is that there are two apexes: one for raffinate purity and another for extract purity. This finding indicates that it is difficult to obtain both enantiomers at high purity by merely regulating the switching time. Similar phenomenon is depicted in Figure 5.3(b) as the maximum productivity of both components can not be achieved at a single value of switching time.

5.4.2. The Effect of Feed Flow Rate

Figure 5.4 demonstrate almost linear relationship between purity and productivity when the feed flow rate is varied over the range of 3 to 6 ml/min. In examining the effect of feed flow rate, the extract stream is allowed to adjust to the changes of feed flow rate according to the mass balance causing the increase of extract flow rate as feed flow increases.

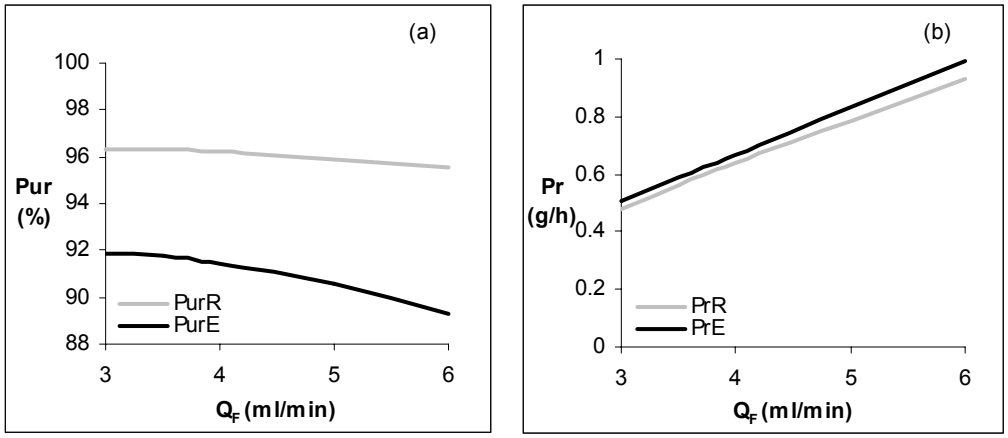

Figure 5.4 The effect of feed flow rate on purity and productivity

The experimental feed flow rate is 3.64 ml/min and it is interesting to study the behavior of the system under high feed loading. The trend in Figure 5.4 is as expected: purity deteriorates at elevated feed flow rate as the separation task becomes more intense but productivity rises due to the increasing availability of both enantiomers in the entire system.

5.4.3. The Effect of Raffinate Flow Rate

The figure below represents the effect of raffinate flow rate on the productivity of less retained component in raffinate stream and that of more retained component in the extract port. The decreased productivity of more retained component in the extract stream is reasonable at sufficiently high raffinate flow rate as some of the strongly adsorbed component emerge at the raffinate port thus less extract product is collected.

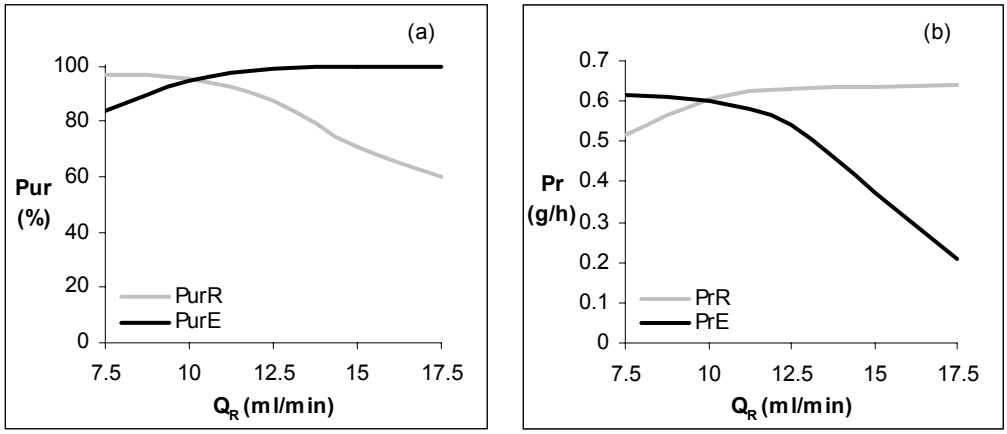

Figure 5.5 The effect of raffinate flow rate on purity and productivity

The increased raffinate flow rate results in higher raffinate productivity. The decline of raffinate purity, however, is a consequence of the accumulation of more retained component in the raffinate line due to reduced amount of this component removed from

the extract line. The reduced flow rate in the section between raffinate withdrawal port and the desorbent inlet port forces component in this section to be conveyed toward the raffinate line and pollutes the raffinate product stream.

5.4.4. The Effect of Desorbent Flow Rate

The effect of desorbent flow rate helps to improve the quality of separation as its role is to remove the more retained component from the stationary phase. Purity and productivity of both component improve as the desorbent flow rate increases up to 20 ml/min then they exhibit contradictive behavior beyond 20 ml/min. Figure 5.6(a) demonstrate that the more retained component is effectively removed from the adsorbent as desorbent flow rate rises to 20 ml/min. This also helps in increasing raffinate purity, as the columns are clean to begin with. However, at a relatively very high mobile phase velocity (desorbent flow rate greater than 20 ml/min), purity decreases as high desorbent flow rate, causes some of the less retained component to emerge at the extract port.

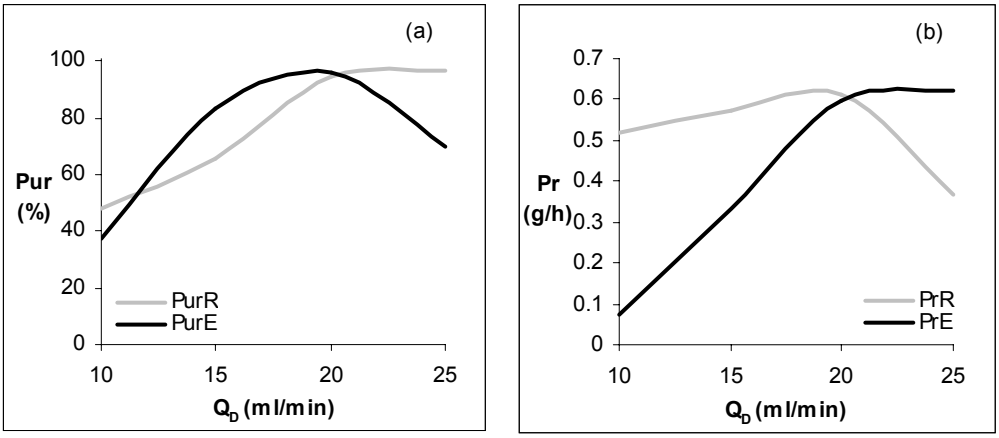

Figure 5.6 The effect of desorbent flow rate on purity and productivity

This explains the deteriorating extract purity and raffinate productivity at the condition of excess desorbent (wash out condition). The high mobile phase velocity is in favor of raffinate purity as it ensures that no strongly adsorbed component travel to raffinate withdrawal port to contaminate raffinate product stream as observed in Figure 5.6(a). The excess desorbent completely wash the more retained species off the adsorbent in zone I thereby extract productivity attain a steady value at fixed amount of feed.

5.4.5. The Effect of Number of Column

Figure 5.7(a) and (b) portray the effect of number of column in zone I on the purity and the productivity of both product streams. In examining the effect of number of columns, all process parameters were kept constant at the experimental setting listed in Table 5.1 except the switching time. It can be seen that varying number of columns in zone I will affect raffinate purity only, while changes are hardly seen for productivity.

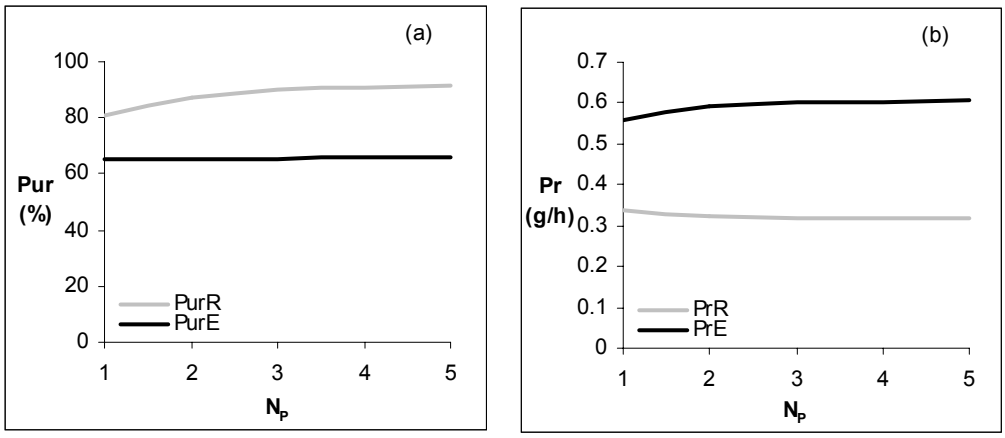

Figure 5.7 The effect of number of column in zone I on purity and productivity

The role of zone I is to ensure perfect desorption of the more retained component and Figure 5.7(a) shows that since the desorbent is present in sufficient amount, the extract

purity can not be improved further by varying the number of column in zone I. Increasing number of column in zone I will assure complete desorption of the more retained component in this zone thus helps in avoiding the contamination of raffinate stream.

The influence of number of columns in zone II can be visualized in Figure 5.8 where improvement can be achieved by increasing the number of columns in zone II. This zone is responsible for desorption of the less retained component and it can be seen that zone II is important in improving purity and productivity for this enantioseparation.

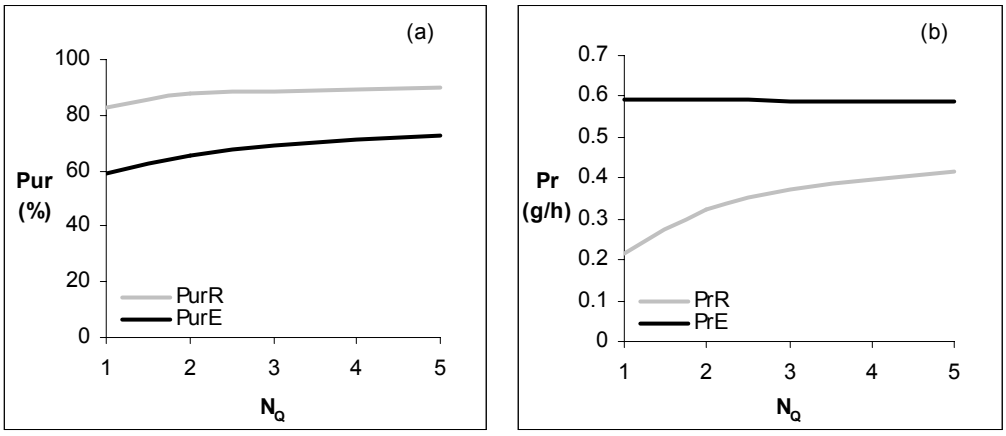

Figure 5.8 The effect of number of column in zone II on purity and productivity

Improved extract purity is obvious as increasing the number of column in zone II will increase residence time thus allowing more time for the less retained component to be desorbed from the pores of the adsorbent. Hence, the columns in zone II will be free from the less retained component when zone II becomes zone I in the next switching. The liquid entering zone III will be rich in less retained component, as a result of improved desorption of this component in zone II, resulting in higher purity and productivity of raffinate stream.

Figure 5.9(a) and (b) is showing variation of number of columns in zone III, and it indicates that the number of columns in zone III more or less exhibits similar effect on the separation performance as that of zone I. Zone III involves mainly in adsorption of the strongly adsorbed component thus improved raffinate performance is expected from varying the number of columns in this zone.

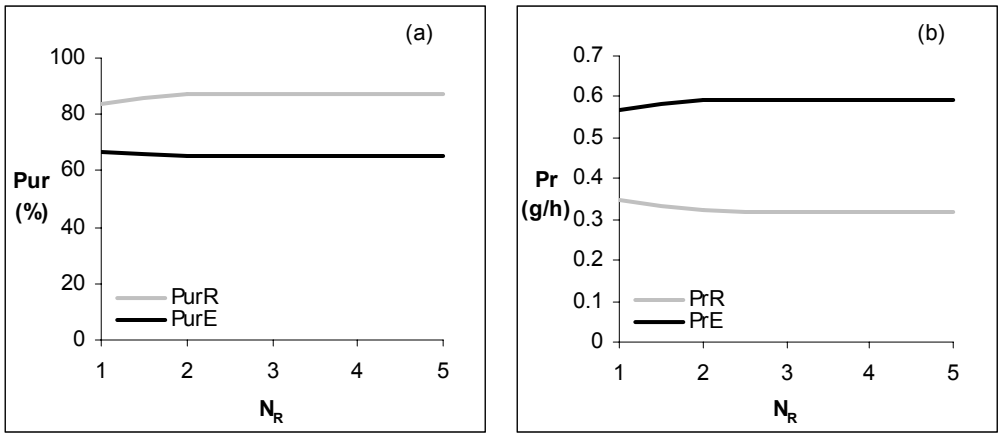

Figure 5.9 The effect of number of column in zone III on purity and productivity

Raffinate purity indeed shows slight increasing trend but no significant changes can be observed in productivity thus Figure 5.9(b) implies that one column in zone III is enough for the separation to take place.

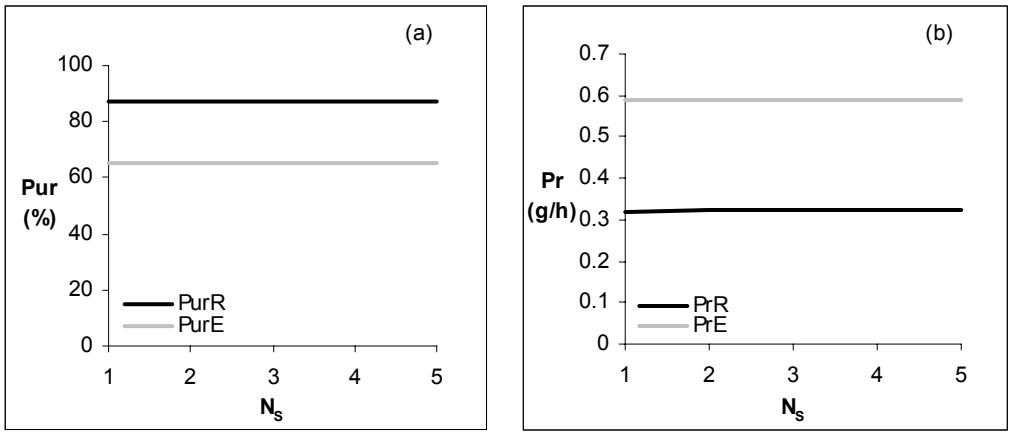

Figure 5.10 The effect of number of column in zone IV on purity and productivity

The impact of the last zone in 4-zone SMB is well described in Figure 5.10 where insignificant effect on the purity and the productivity was observed when the number of column in zone IV was varied. The liquid entering zone IV is rich in less retained component thus the role of zone IV is to mainly ensure removal of desorbent from adsorbent. This will make the adsorbent pores available for adsorption of less retained component and prevent them from entering zone I to contaminate extract stream. Enhanced performance in the extract stream is therefore expected but it turns out that this zone IV is insensitive.

5.5. Optimization Study

The optimization problem for simulated counter-current process is to find the optimum switching time, internal flow rates and column configuration to satisfy specified purity or productivity requirement. As has been shown previously in the sensitivity analysis, some variables contradict each other i.e. high feed load increase productivity at the expense of high desorbent consumption rate and relatively lower product purity making this system prone to multi-objectives optimization study. Optimization study of simulated moving bed has been reported in the open literature is the work of Storti et al. (1988, 1995), Dunnebier and Klatt (1999), Karlsson et al. (1999), Wu et al. (1999) employing a weightage factor to convert several objective functions into one objective function. In this study, first single objective function optimization is performed to test whether the optimization algorithm can result in improved solution compared to the experimental results reported by Pais et al. (1997a, 1997b, 1998). Multi-objectives optimization is carried out to provide decision makers with set of solutions which will

enable them to choose the appropriate operating condition suitable to certain circumstances.

5.5.1 Single Objective Optimization

In order to test the optimization procedure, single objective optimization study was performed to compare the result of this work with those reported by Pais et al (1997a), which were obtained by simulation-optimization without following any systematic optimization procedure. The first hypothesis made at the initial stage of this work is that there exists at least one of the operating variables in the experimental work reported by Pais et al. (1997a) that can still be improved. Single objective optimization study, as tabulated in Table 5.6, is first carried out before multi-objectives optimization studies.

5.5.1.1. Case 1. Single Objective Optimization: Maximize feed flow rate

The purpose of single objective optimization study is to find out whether process performance can be improved maintaining at least the same quality of separation. In most enantioseparation process, purity is regarded as the important parameter, and it will decrease as feed flow rate is increased or as desorbent flow rate is decreased. In the first case of single objective optimization, it is desired to see how high the feed flow rate can be increased maintaining a predefined purity. The optimization problem formulated for SMB and Varicol is described as follows:

$$\text{Max} \qquad I = Q_F[Q_F, Q_R, t_s, \chi] \tag{5.11}$$

$$\text{Subject to PurR and PurE} \geq \text{Experimental value (in Pais et al., 1997a)} \tag{5.12}$$

The desired purity is used as an inequality constraint and its value is targeted to be greater than the reported experimental purity. The total number of column is kept constant to enable direct comparison with the existing system. The flow rate in zone I is also treated as fixed variable to ensure the whole system working below the allowable pressure drop range.

Table 5.6 Single objective optimization attributes used in the enantioseparation of 1,1'-bi-2 naphtol racemate

Problem		Objective Function	Constraints	Decision variables
Case 1	SMB	Max Q_F	PurR and PurE ≥ Experimental value (Pais et al., 1997a)	$3.5 < Q_F < 4$ ml/min $1 < Q_R < 10$ ml/min $2 < t_s < 4$ min χ [See Table 3.1]
	Varicol			
Case 2	SMB	Min Q_D	PurR and PurE ≥ Experimental value (Pais et al., 1997a)	$18 < Q_D < 21$ ml/min $1 < Q_R < 10$ ml/min $2 < t_s < 4$ min χ [See Table 3.1]
	Varicol			
Fixed Variables: $L_{col} = 10.5$ cm, $N_{col} = 8$, $Q_I = 56.83$ ml/min				
Case 1: $Q_D = 21.45$ ml/min			Case 2: $Q_F = 3.64$ ml/min	

Incorporating modified infinite barrier penalty function, similar to eq. (4.24) and (4.25), to the objective function develops the optimization code and a large penalty weightage is used to penalize only the unfeasible points.

5.5.1.2. Case 2. Single Objective Optimization: Minimize desorbent flow rate

The desorbent flow rate minimization is chosen as the objective function as it serves as one component that constitutes the total cost of separation. Desorbent is needed in chromatographic column to desorb the most strongly adsorbed component from the adsorbent thus reducing the desorbent flow rate will have significant impact on the process performance especially purity. It is required to see how low the desorbent can be used at the limit of achieving a definite purity requirement.

The following formulation for SMB and Varicol processes is considered:

$$\text{Min} \qquad I = Q_D[Q_D, Q_R, t_s, \chi] \tag{5.13}$$

$$\text{Subject to PurR and PurE} \geq \text{Experimental value (in Pais et al., 1997a)} \tag{5.14}$$

The details of optimization formulation (objective function, constraints, fixed variables and bounds for each decision variables) are well summarized in Table 5.6. Column configuration is employed as one of the decision variables and its optimum value is tabulated in Table 5.7. It is worth to note that 4 sub-intervals are used in Varicol process due to the magnitude of switching time. There are 20 and 35 possible configurations for 7-column and 8-column Varicol systems respectively.

Table 5.7 Optimum column configuration for SMB and Varicol processes for enantioseparation of 1,1'-bi-2 naphtol racemate

N_{col}	χ	Column	χ	Column	χ	Column	χ	Column	χ	Column
7	A	1/1/2/3	B	1/1/3/2	C	1/2/2/2	D	1/2/3/1	E	1/3/1/2
	F	1/3/2/1	G	2/1/3/1	H	2/2/1/2	I	2/2/2/1	J	2/3/1/1
	K	3/1/2/1								
8	L	1/2/2/3	M	1/3/2/2	N	1/3/3/1	O	2/1/3/2	P	2/2/2/2
	Q	2/2/3/1	R	2/3/2/1	S	3/2/2/1				

The result of single objective optimization is summarized in Table 5.8 in which the reference value presented was used for SMB experimental study while the optimized value is given for both SMB and Varicol system. Shaded column represents optimum values of objective function and decision variables and the number in bracket are percentage improvement over experimental results. Optimum result clearly exhibits improvement as expected. Higher feed rate or lower desorbent flow rate is achieved relative to experimental value for the SMB process.

Table 5.8 Single objective optimization result in the enantioseparation of 1,1'-bi-2 naphtol racemate

Process Parameter	8-column SMB			8-column Varicol	
	Ref.	case 1	Case 2	case 1	case 2
Q_1(ml/min)	56.83	56.83	56.83	56.83	56.83
Q_E(ml/min)	16	19.40	19.53	18.49	17.16
Q_R(ml/min)	9.09	5.74	5.39	6.65	6.83
Q_F(ml/min)	3.64	3.69(+1.26%)	3.64	3.69(+1.47%)	3.64
Q_D(ml/min)	21.45	21.45	21.28(-0.82%)	21.45	20.35(-5.15%)
t_s(min)	2.75	3.00	3.03	2.96	2.93
L_{col}(cm)	10.5	10.5	10.5	10.5	10.5
χ(-)	P	L	L	L/NP/M	L/M/P/O
PurR(%)	96.2	96.20	96.22	96.2	96.39
PurE(%)	93	93.00	93.06	93.00	93.05
RecR(%)	91.6	92.55	91.55	93.01	93.3
RecE(%)	97.3	95.98	95.93	96.07	95.98
SCR(l/g)	2.59	2.54	2.56	2.52	2.44
SCE(l/g)	2.44	2.45	2.44	2.44	2.37
YR(g/h/l_s)	2.17	2.22	2.17	2.24	2.21
YE(g/h/l_s)	2.31	2.30	2.27	2.31	2.28

This improvement can be achieved by reducing internal liquid flow rates and pseudo solid velocity (implicitly enclosed in Table 5.8). This phenomenon is evident as it is desirable to enhance the countercurrent contact between the mobile and the stationary phase by increasing the residence time of the component along the column, at high feed flow rate. The column configuration is L for SMB and L/N/P/M for Varicol.

Desorbent flow rate can be minimized up to 0.82 % and 5.15 % for SMB and Varicol respectively by significantly increasing internal liquid flow rate, although the solid flow rate was slightly changed from the reference value. This fact is understandable, as high liquid internal flow rate will ensure that adsorption-desorption in each zone attained satisfactorily at the condition of minimum desorbent flow rate. Optimization result displayed in Table 5.8 shows only slight improvement over the reference value in terms of operating variable such as purity, recovery, solvent consumption and specific yield. The result obtained in this work shows that there is not much room for improvement with single objective function. However, it shows the ability of genetic algorithm to locate the better optimal (global optima) solution of this system.

5.5.2. Multi-Objectives Optimization

SMB operating variables often affect the performance in conflicting ways making single objective optimization not sufficient for real-life industrial design. Hence, multi-objectives optimization is essential for SMB and Varicol systems particularly when it is desired to satisfy more than one criterion, for example, purity and productivity of one particular stream. Multi-objective optimization will lead to the concept of Pareto, a set of

Table 5.9 Multi objective optimization attributes used in the enantioseparation of 1,1'-bi-2 naphtol racemate

Problem		Obj. funct.	Constraints	Decision variables	Fixed variables
Case 3	SMB / varicol	Max PurR Max PurE	PurR > 90% PurE > 90%	$18 < Q_D < 35$ ml/min $5 < Q_R < 15$ ml/min $2 < t_s < 4$ min $8 < L_{col} < 13$ cm χ [See Table 3.1]	$Q_1 = 56.83$ ml/min $Q_F = 3.64$ ml/min $N_{col} = 7$ or 8
Case 4	SMB / varicol	Max PrR Max PrE	PurR > 90% PurE > 90%	$18 < Q_D < 35$ ml/min $5 < Q_R < 15$ ml/min $2 < t_s < 4$ min $8 < L_{col} < 13$ cm χ [See Table 3.1]	$Q_1 = 56.83$ ml/min $Q_F = 3.64$ ml/min $N_{col} = 7$ or 8
Case 5	SMB / varicol	Max PurR Max PrR	PurR > 90% PurE > 95%	$18 < Q_D < 35$ ml/min $5 < Q_R < 15$ ml/min $2 < t_s < 4$ min $8 < L_{col} < 13$ cm χ [See Table 3.1]	$Q_1 = 56.83$ ml/min $Q_F = 3.64$ ml/min $N_{col} = 7$ or 8
Case 6	SMB / varicol	Max PurE Max PrE	PurR > 95% PurE > 90%	$18 < Q_D < 35$ ml/min $5 < Q_R < 15$ ml/min $2 < t_s < 4$ min $8 < L_{col} < 13$ cm χ [See Table 3.1]	$Q_1 = 56.83$ ml/min $Q_F = 3.64$ ml/min $N_{col} = 7$ or 8
Case 7	SMB / varicol	Max Q_F Min Q_D	PurR > 95% PurE > 95%	$3 < Q_F < 6$ ml/min $18 < Q_D < 35$ ml/min $5 < Q_R < 15$ ml/min $2 < t_s < 4$ min χ [See Table 3.1]	$Q_1 = 56.83$ ml/min $Q_F = 3.64$ ml/min $N_{col} = 7$ or 8
Case 8	SMB / varicol	Max PrR Max PrE Min Q_D	PurR > 90% PurE > 90%	$18 < Q_D < 35$ ml/min $5 < Q_R < 15$ ml/min $2 < t_s < 4$ min $8 < L_{col} < 13$ cm χ [See Table 3.1]	$Q_1 = 56.83$ ml/min $Q_F = 3.64$ ml/min $N_{col} = 7$ or 8
Case 9	SMB / varicol	Max PrR Max PrE Min L_{col}	PurR > 90% PurE > 90%	$18 < Q_D < 35$ ml/min $5 < Q_R < 15$ ml/min $2 < t_s < 4$ min $8 < L_{col} < 13$ cm χ [See Table 3.1]	$Q_1 = 56.83$ ml/min $Q_F = 3.64$ ml/min $N_{col} = 7$ or 8

equally good non-dominated solution, in which one objective can be improved at the cost of the other objective function.

Product purity, as a supreme separation feature, has been frequently used to measure the feasibility of a separation method. The purity of both enantiomer of 1,1'-bi-2-naphtol has been shown earlier to contradict each other in sensitivity analysis. Purity optimization serves as a good problem to introduce the concept of non-dominating solution as represented in Pareto Set. Minimum purity of 90% is used to penalize infeasible points during the search.

5.5.2.1. Case 3. Multi-objectives Optimization: Maximize raffinate and extract purity

The optimization problem formulated is to maximize the purity of the raffinate and the extract streams simultaneously. The choice of decisions was based on the ease of operating the process conveniently. In this case, purity is treated both as constraint (in order to have products with purity greater than a specified value) as well as objective function. The Pareto for 7-column SMB and Varicol, and 8-column SMB are compared in Figure 5.11. Two problems are formulated for 8-column SMB, one with L_{col} as decision variable, and the other with fixed L_{col} to enable direct comparison between optimum results at existing design and to measure the dependency of purity with respect to column length.

The figure shows that 7-column SMB with optimal configuration [χ = C (1/2/2/2)] can only achieve medium range of purity while 7-column Varicol can achieve better purity. The column switching sequence for 7-column Varicol is A/C/C/D and this is equivalent with 1/1.75/2.25/2 which is very close to the SMB optimal configuration. Varicol process,

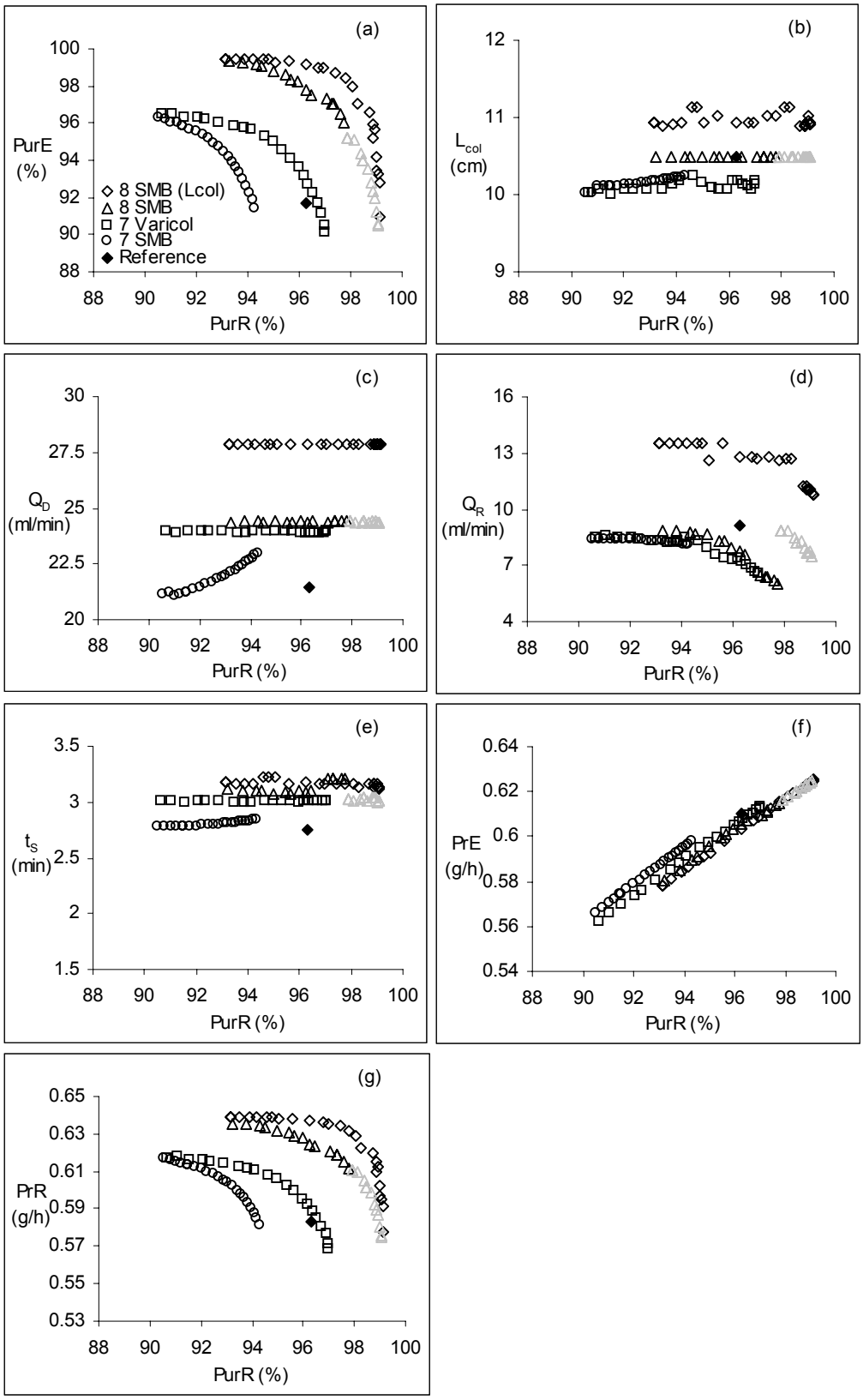

Figure 5.11 Multi-objectives optimization results (case 3) for SMB and Varicol

gives relatively higher purity, as expected, than 7-column SMB especially in the raffinate stream. The experimental purity obtained for 8-column SMB (Pais et al., 1997a) lies near the 7-column Varicol (See Figure 5.11). Purity in this case was found to depend on the length of column and desorbent rate. Higher product purity is possible for 8-column SMB especially when the length of column is allowed to vary at the expense of high desorbent flow rate.

For optimization at existing design, the Pareto set for 8-column SMB consists of two unique configurations. For the upper part (higher extract purity, black triangle) the optimal configuration is M (χ = 1/3/2/2) while for the lower part (higher raffinate purity, gray triangle) it is R (χ = 2/3/2/1). When the column length was allowed to vary, the Pareto shifted towards even higher purity and the optimum column configuration obtained was R (χ = 2/3/2/1) for the entire Pareto range.

Figure 5.11(a) shows that zone I is less important at low raffinate purity but is vital for high raffinate purity. This is understandable as the task of zone I is to ensure smooth desorption of the more retained component to be eluted at the extract withdrawal port, so that the liquid eluting from zone I is rich in the more retained component. The task of zone II is to ensure desorption of the less retained component from the adsorbent to the liquid phase. With increasing number of columns in zone II, the liquid entering zone III will be richer in the less retained component and this will increase the driving force for the more retained component in zone III to be adsorbed in the solid phase. This phenomenon will help the system to attain high raffinate purity.

5.5.2.2. Case 4. Multi-objectives Optimization: Maximize raffinate and extract productivity

The specific ability of SMB chromatography to separate difficult mixtures has secured it to be the popular method to handle small volume expensive chemicals. Both enantiomers of 1,1'-bi-2-naphtol are of equal importance, depending on its application. The productivities of raffinate and extract streams have been shown to contradict in sensitivity analysis, and therefore, they serve as a good objective function leading to Pareto optimal solution. If conventional optimization techniques were used, we would be able to predict only one point at a time on the Pareto optimal curves by fixing one of the productivity values and maximizing the other. This effort will consume considerable computation time but the results would be more meaningful.

The problem formulation is almost similar to case 3 (Table 5.9) but the objective function is modified to incorporate productivity. The purity constraint in this case was set to be greater than 90% to acquire more feasible solutions. Productivities of both streams are used as objective function with raffinate flow rate, desorbent flow rate, switching time, length of column (except in one of the two cases for 8-column SMB) and column configuration as decision variables. Like the previous cases, all variables except length can be manipulated in optimization at design stage when L_{col} is relaxed.

The column configurations for upper (black square, symbols) and lower part (grey square, symbols) of Pareto for 7-column Varicol are G/F/I/I and E/F/I/I respectively. The reference experimental point is achieved by 8-column SMB with configuration P (2/2/2/2). Two column configurations constitute the Pareto for 8-column SMB with fixed length. The upper part (black triangle) is achieved by S (3/2/2/1) and the lower part (grey

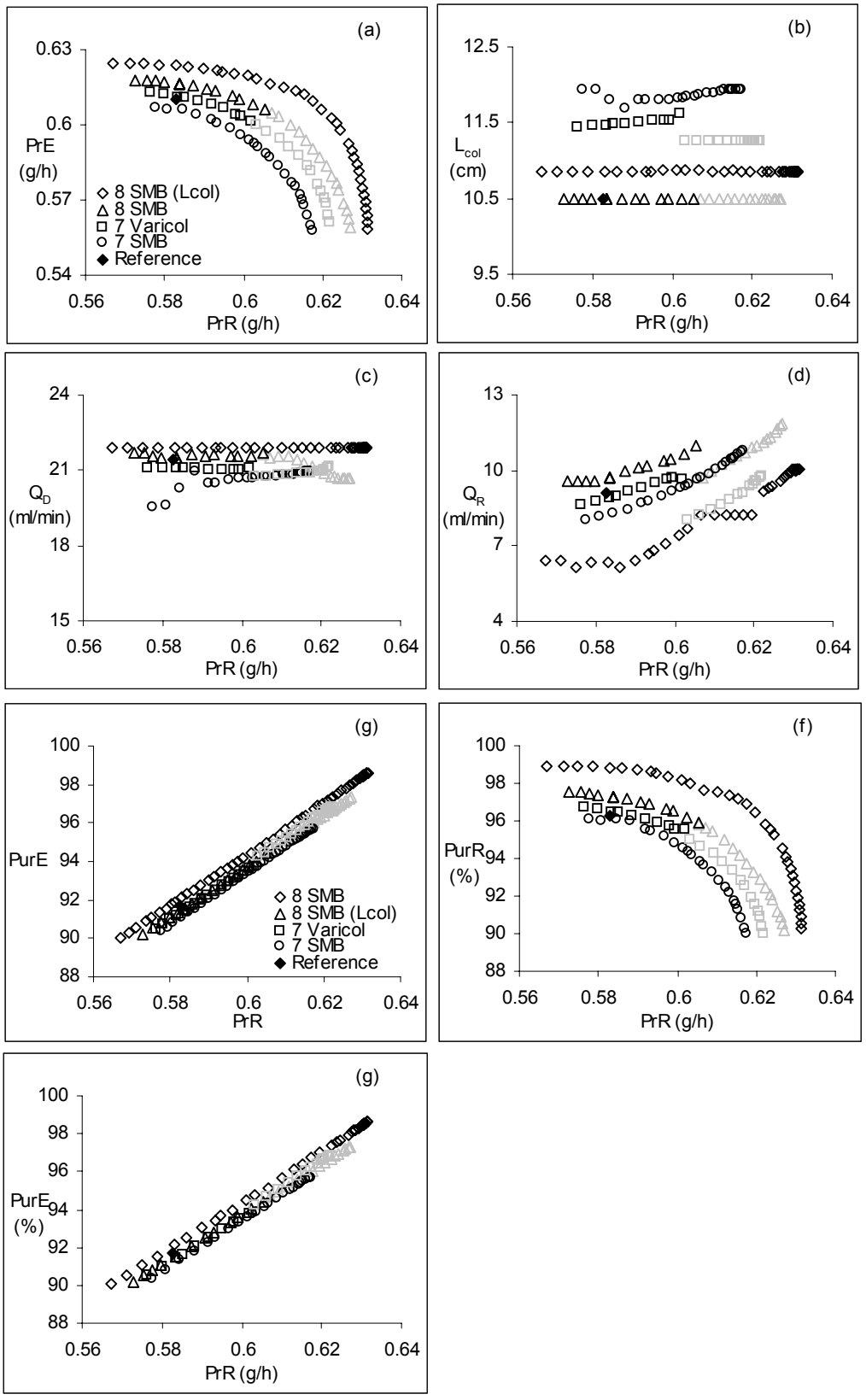

Figure 5.12 Multi objective optimization results (case 4) for SMB and Varicol

triangle) by R (2/3/2/1) configuration. The column configuration when length is used as decision variable is P (2/2/2/2), same as the reference experimental configuration. The two different column configurations that constitute 8-column SMB Pareto (Figure 5.12) when length is fixed can be understood as extract productivity is more dominant than the raffinate productivity (at the upper part of the Pareto), zone I requires an extra column to increase elution of the more retained component from the adsorbent. On the contrary, the extract productivity is more inferior to the raffinate productivity at the lower part of the Pareto, hence zone II, as explained earlier, need more columns to enrich the mobile phase with raffinate product.

5.5.2.3. Case 5. Multi-objectives Optimization: Maximize raffinate purity and productivity

The combination of (S)-1,1'-bi-2-naphtol and $Ti(O\text{-}i\text{-}Pr)_4$ is found to be highly enantioselective for the reaction of aromatic aldehydes (Moore and Pu, 2002). Nonetheless, the (S)-1,1'-bi-2-naphtol is deemed to be more superior than its (R) counterpart when used as chiral ligand in alkylation of a variety of aromatic aldehydes to chiral alcohol (Chan et al., 1997).

In this case, the objective functions are formulated based on the two qualities of raffinate stream: purity and productivity. These two parameters have been shown to contradict each other in our earlier sensitivity analysis. The extract purity constraint of greater than 95% is used to avoid the loss of the more retained component in the raffinate line. There is no sub-case in which the L_{col} is fixed because the length of column for 8-column SMB converges around its design value used in the experiment. The optimum re-

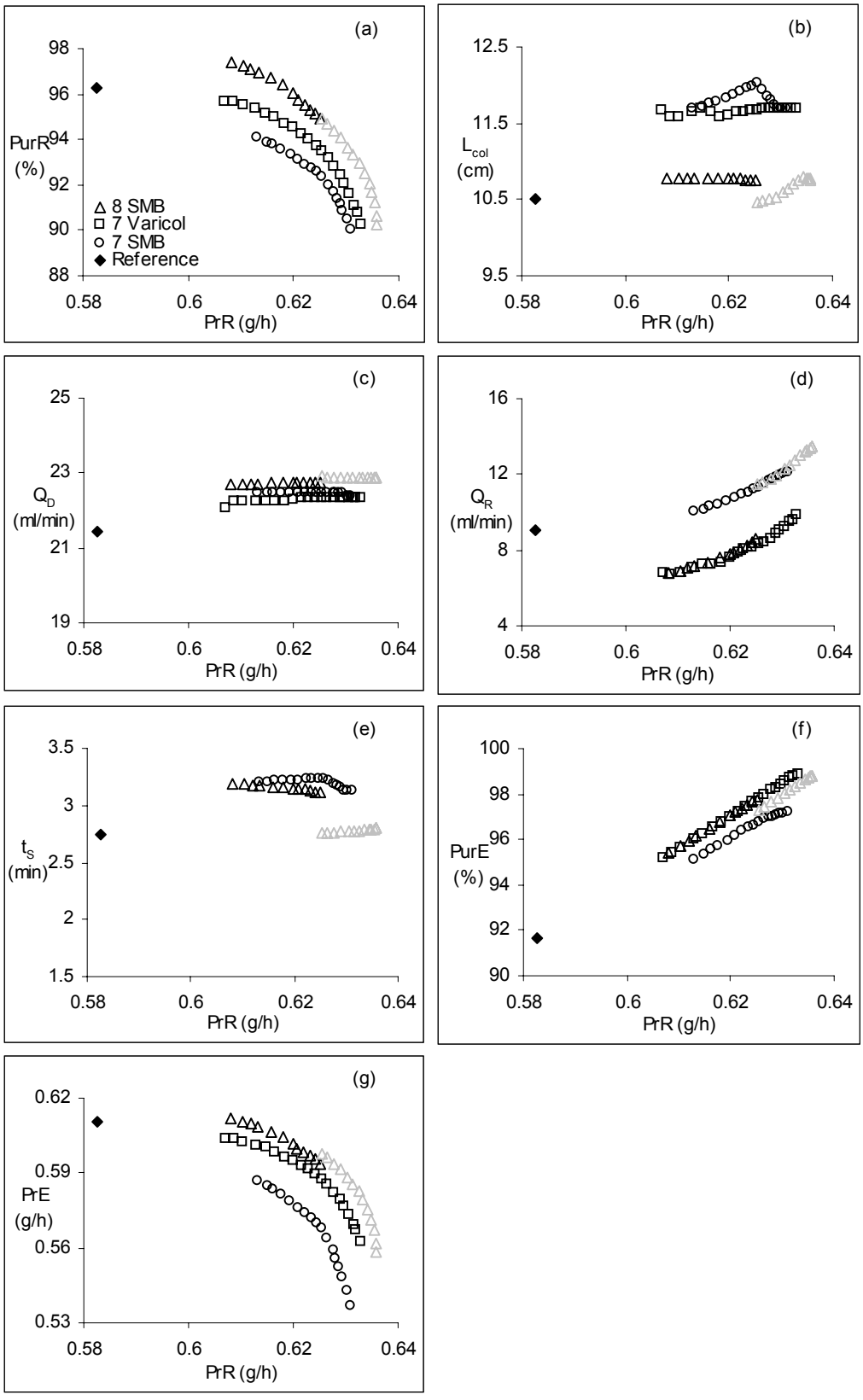

Figure 5.13 Multi-objectives optimization results (case 5) for SMB and Varicol

sult of case 5 is well represented in Figure 5.13 in which extreme improvement over experimental (reference) value is achieved even under stringent extract purity constraint. The column configuration for 7-column SMB is D (2/3/2/1) and the switching sequence for 7-column Varicol is C/C/E/F, which corresponds to 1/2.5/1.75/1.75. The Pareto optimal solution for 8-column SMB is given by two column configurations: the upper part (black triangle) is by P (2/2/2/2) whilst the lower part (grey triangle) is given by R (2/3/2/1). This result shows the significance of zone II over the other zones in dictating the quality of raffinate product. It has been mentioned earlier that more columns in zone II will enrich the liquid stream-entering zone III with the less retained component and raffinate product quality will improve with the aid of zone III.

The total length of the separation column is comparable between 7-column SMB, 7-column Varicol and 8-column SMB as depicted in Figure 5.13(b). Increased desorbent consumption rate as in Figure 5.13(c) is the outcome of enhanced quality of raffinate product and to satisfy the extract purity requirement. The plot of constraint as depicted in Figure 5.13(f) points out that no feasible points are lost. The smaller Pareto size for 7-column SMB in Figure 5.13(a) is due to the fact that each terminal point of the Pareto is dictated by purity constraint. The upper edge is governed by extract purity constraint [PurE $\geq$ 95%, see Figure 5.13(f)] and the lower edge is controlled by raffinate purity constraint [PurR $\geq$ 90%].

5.5.2.4. Case 6. Multi-objectives Optimization: Maximize extract purity and productivity

(R)-1,1'-bi-2-naphtol is found useful mostly in polymeric application. Its derivative is used in tandem asymmetric reactions (Yu et al, 2000). Copolymer catalyst synthesized from (R)-1,1'-bi-2-naphtol or BINOL and 2,2'-bis(diphenylphosphino)-1,1'-binaphtyl or BINAP, either in individual or combination state, demonstrate outstanding stereoselectivity in asymmetric addition to aldehydes or in hydrogenation of ketones. Later, (R)-1,1'-bi-2-naphtol is used as the starting material to produce chiral polymer catalyst, poly(R)-binaphtol. Instead of merely giving high yields and selectivity, this new chiral catalyst can be recovered and reused without losing its enantioselectivity (de Vains, 2001).

The fixed and decision variables are almost similar to the previous case. Raffinate purity greater than 95% is employed as a constraint to maintain the recovery of the more retained component in the extract stream. Similar to case 5, there are only 3 sub-cases in this case as the decision variable L_{col}, when used as decision variables, converges nearly to design length of 10.5 cm. The Pareto solution for 7-column SMB, 7-column Varicol and 8-column SMB is given in Figure 5.14(a) with similar trend as before in which the 8-column SMB was found to be more superior to 7-column Varicol and 7-column SMB.

The reference value for 8-column SMB experimental result reported by Pais et al.(1997a), is achieved by using 7-column Varicol with B/D/I/G (1.5/1.5/2.75/1.25 in average) column configuration for the upper part of the Pareto (black square, Figure 5.14a) while D/F/K/I (1.75/2/2.25/1) for the lower part (grey square). The 7-column SMB is given by G configuration (2/1/3/1) and 8-column SMB by P (2/2/2/2). It is obvious that

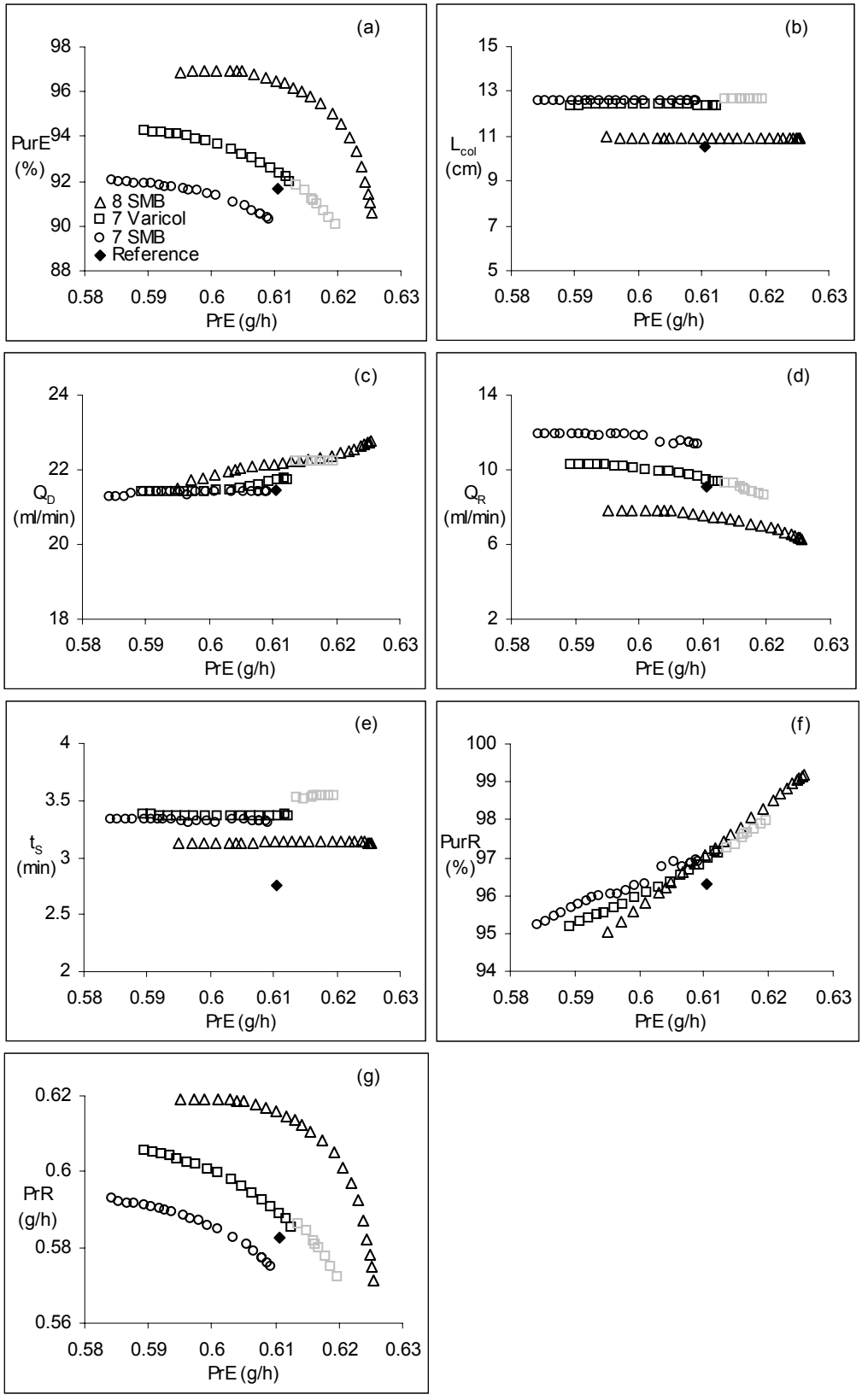

Figure 5.14 Multi-objectives optimization results (case 6) for SMB and Varicol

zone I and III are critical for extract product and this is understandable considering the roles of zone I and III. The role of zone III is to ensure adsorption of the more retained component onto the adsorbent while zone I is responsible for its desorption from the adsorbent. The two column configuration that constitute 7-column Varicol Pareto Set exhibit similar trend as it starts with allowing more column in zone III (to capture the more retained component in the adsorbent) and followed by giving extra column in zone I in the subsequent switching (to wash off the more retained component from the adsorbent).

Comparison between Figure 5.13 and Figure 5.14 implies that raffinate product is easier to obtain than the extract product due to the narrow distance between each Pareto in Figure 5.13(a) relative to the Pareto in Figure 5.14(a). Besides, slight increase of decision variables in Figure 5.13(b)-(e) is able to improve the objective function significantly even under extract purity requirement greater than 95%. The improved objective function in Figure 5.14(a), however, is achieved with decision variables close to the experimental value[Figure 5.14(b)-(e)]

5.5.2.5. Case 7. Multi-objectives Optimization: Maximize feed and minimize desorbent rate

One important case in any enantioseparation is the simultaneous maximization of throughput (capacity) and minimization of desorbent consumption. In general, desorbent consumption will increase as the feed load increases as the separation task becomes more difficult.

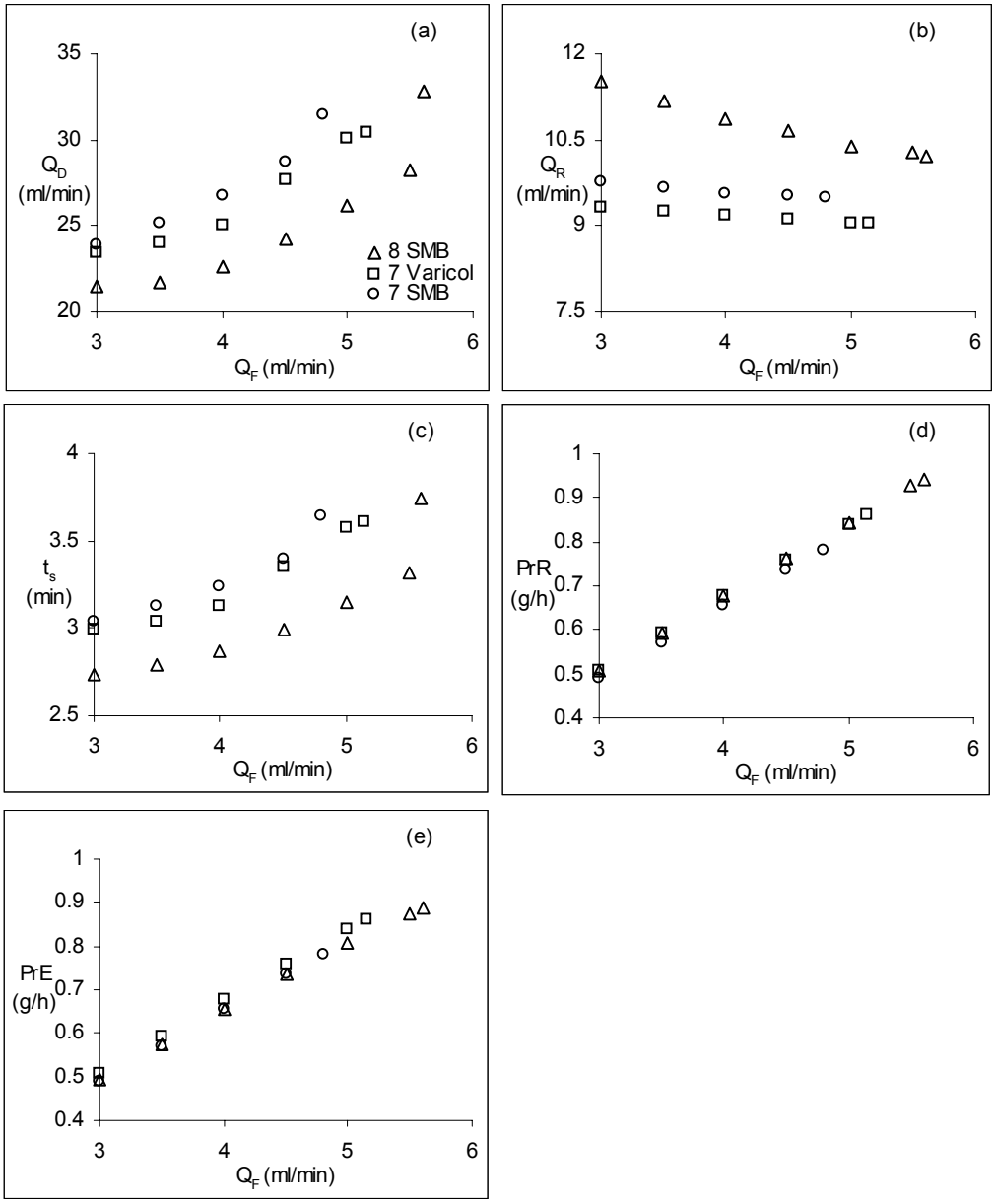

Figure 5.15 Multi-objectives optimization results (case 7) for SMB and Varicol

Length of column will not be used as decision variables to avoid infinite (multiple) optimal solution. The introduction of length of column as decision variable will create an open-ended problem as productivity will increase as length of column increases. It is more worthwhile to find out the maximum productivity that can be reached for a definite

column length. Purity constraint is chosen to be greater than 95% to accommodate commercial market requirement.

The column configuration for 7-column SMB is I (2/2/2/1) while for 8-column SMB is Q (2/2/3/1). The sequence for 7-column Varicol is B/C/C/D, which is equal to 1/1.75/2.5/1.75 in terms of average column within a switching interval. It clearly shows that more columns are needed in the feed zone as no separation occurs during the first sub-switching interval. When sufficient amount of feed is present in the system, separation is needed straight away, therefore more column are required in zone II rather than in zone III. The number of columns in zone III is relaxed to allow enough time for separation to take place but it is still important as zone II and zone III are responsible for separation in SMB. Zone IV, whose role is to prevent raffinate product from entering zone I, become less important at the end of the interval as most of the components have been separated in the first 3 sub-switching and the sequence repeated.

Pareto set in Figure 5.15(a) shows that 7-column SMB and Varicol are able to tolerate feed load up to 4.8 and 5.15 ml/min while 8-column SMB feed limit stands at 5.6 ml/min. Any attempt to extend feed flow rate below this limit result in contaminated extract product meaning extract purity constraint is violated. Switching time increases with feed flow rate as residence time should be increased when separation task become more difficult. Productivity of raffinate and extract will increase and this is marked by the increasing raffinate flow rate at higher feed loading. The decision variables in this case have arranged themselves in such a way to anticipate the increasing task of separation.

5.5.2.6. Case 8. Multi-objectives Optimization: Maximize raffinate and extract productivity and minimize desorbent rate

Three objectives optimization is formulated in view of economic consideration related to investment and operating cost involved in chiral separation process. One of the advantages of SMB chromatography over elution chromatography is the ability to achieve higher productivity at lower solvent consumption. The dilemma of high separation cost has motivated the needs of increasing throughput while simultaneously reducing operating cost as low as possible. Due to the way the original NSGA code has been written, the third objective function is considered by taking reciprocal value of desorbent flow rate because minimization is essentially the inverse of a maximization problem.

The performance of 7-column and 8-column SMB, and 7-column Varicol is compared with an additional case where the length of the 8-column SMB was fixed as a measure of improvement that can be made over the existing design. Figure 5.16(a) and (b) show that treating column length (L_{col}) as decision variable can improve the system performance. In contrast to case 4, the Pareto optimal solution for 7-column Varicol is not able to emulate the reference experimental value and this is expected because of introduction of the third objective function, which renders more restriction to the system. The decision variables of 7-column Varicol in Figure 5.16(c) and (d) pointed out the ability of optimization package in finding optimal solutions even when discontinuity persists. The optimum column configurations are C (1/2/2/2) for 7-column SMB and Q (2/2/3/1) for 8-column SMB while the flexible 7-column Varicol is given by 2 sets of configuration: the upper part by I/F/I/I and the lower part by C/C/F/I. The column configurations follow the previous trend

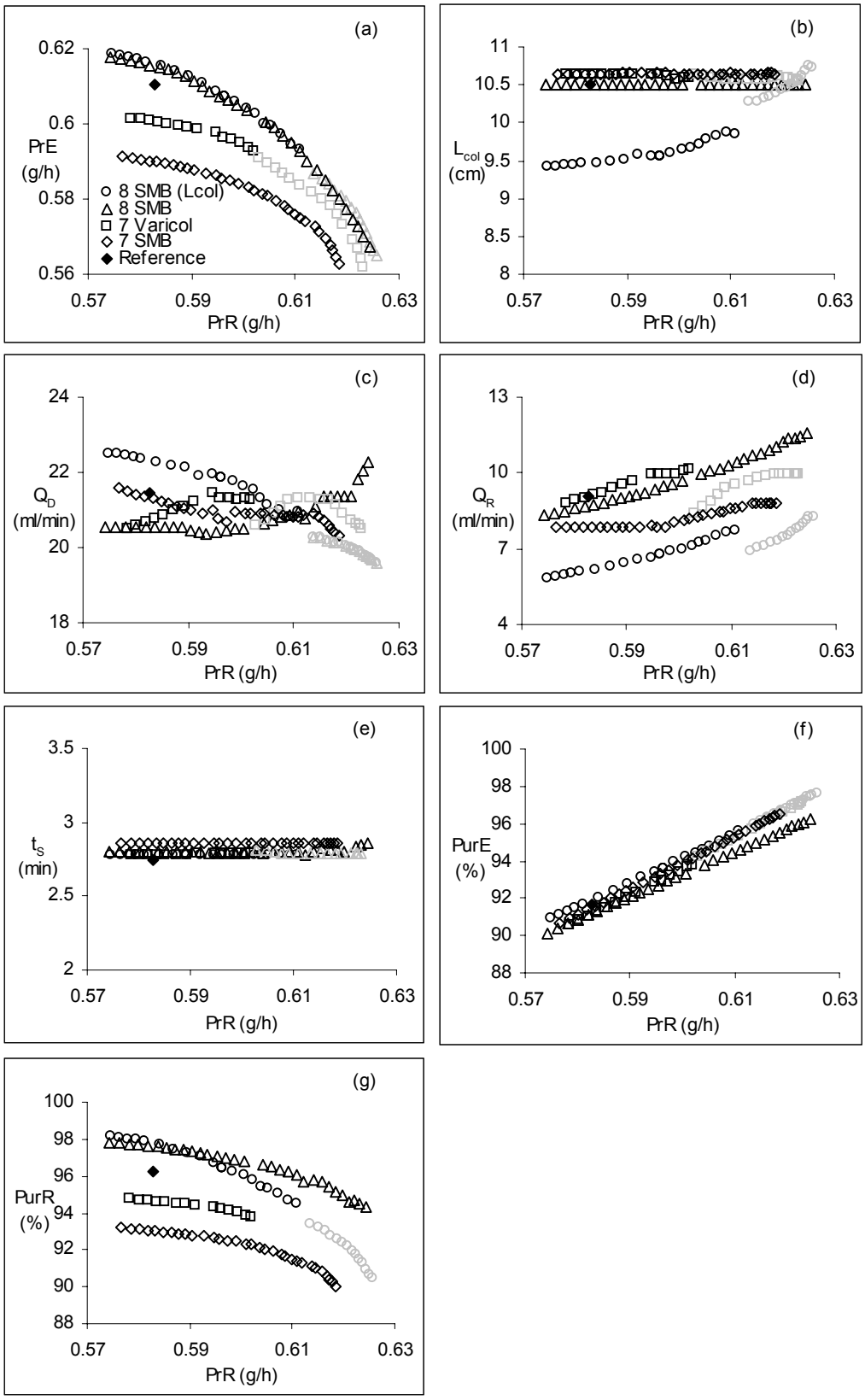

Figure 5.16 Multi-objectives optimization results (case 8) for SMB and Varicol

noting that zone I is more likely for extract stream (upper configuration is equal to 1.75/2.25/2/1) and zone IV is crucial for raffinate product (lower configuration correspond to 1.25/2.25/2/1.5). This is further justified as the optimal column configurations obtained are P (2/2/2/2) and M (1/3/2/2) for the upper and lower part of the Pareto for 8-column SMB when length was allowed to vary. Zone I clearly makes a great impact on the performance of extract product while zone IV is essentially responsible for the desorption of the desorbent from the adsorbent. In this way, zone IV allows more time for adsorption for the strongly adsorbed component into the pores of adsorbent, particularly when zone IV become zone III in the next switching cycle. We notice similar trends for column configuration in all optimization run: zone I and III control the separation for the extract product and zone II and IV are responsible for the raffinate product.

5.5.2.7. Case 9. Multi-objectives Optimization: Maximize raffinate and extract productivity and minimize column length

The next case of three objectives optimization is another effort to facilitate SMB chromatography to become an ultimate separation method by minimizing the capital cost of separation. Length of column is directly related to the amount of chiral stationary phase (which is quite expensive) needed to perform the separation. Thus, the additional objective function is needed to compensate the increase in productivity and it is incorporated in the same way as in case 8.

The optimum results for case 9 are well represented in Figure 5.17(a)-(g). As the length of column is used as one of the objective functions, there will be only 3 sub-cases in the problem formulation. The bounds, constraints, fixed and decision variables for case

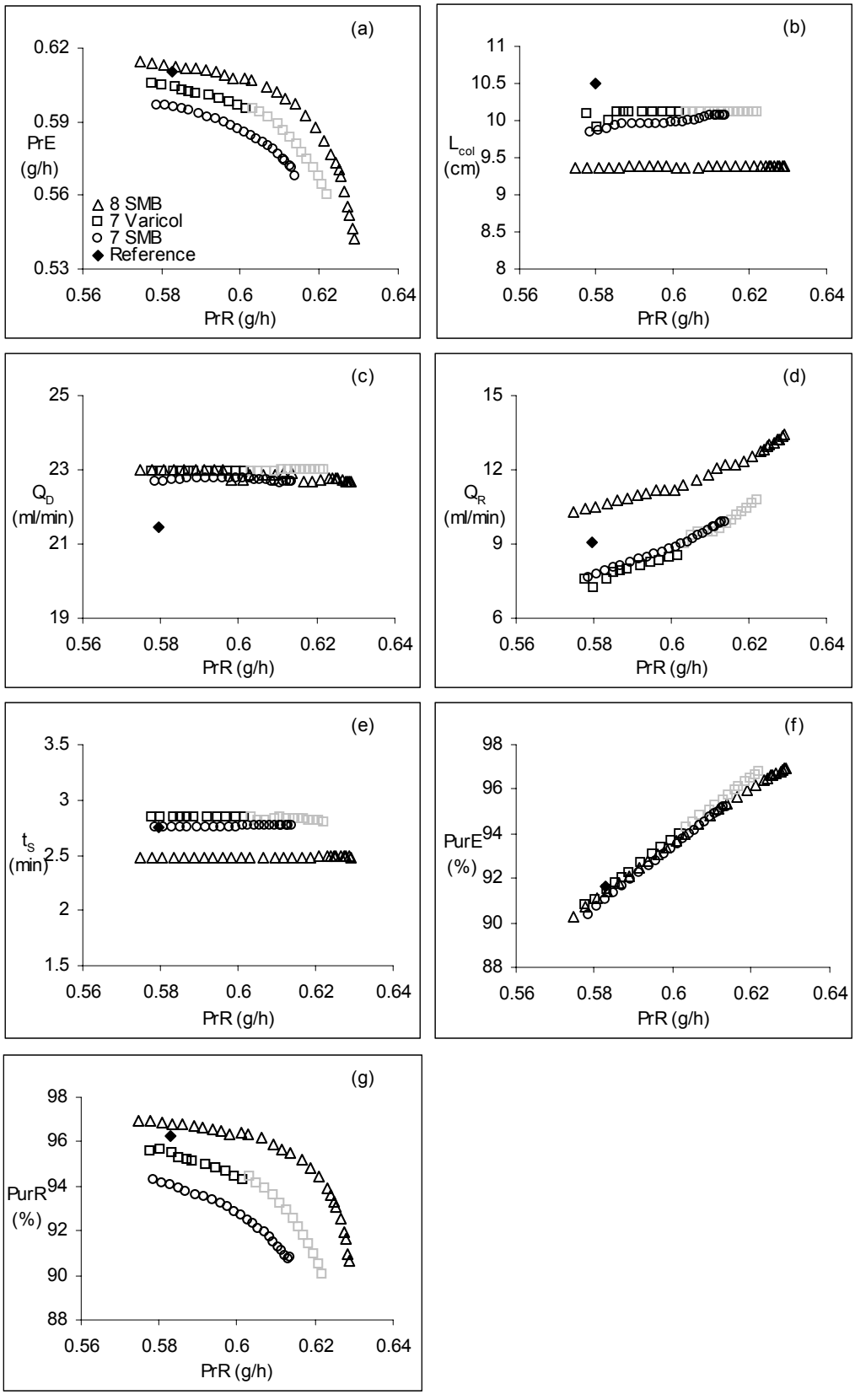

Figure 5.17 Multi-objectives optimization results (case 9) for SMB and Varicol

9 are essentially similar to those in case 8 while the modified additional objective function is augmented in the same fashion as before. The optimal column configuration for the Pareto for 7-column SMB is given by F (1/3/2/1) while for 8-column SMB it is Q (2/2/3/1).

Column configuration of C/D/F/J constitutes the upper part of Varicol Pareto while the lower part is governed by C/D/I/J. Overall, all the Pareto optimal solutions shown in Figure 5.17 are slightly inferior to those of Figure 5.12 but trade off is obtained for the length of column as portrayed in Figure 5.17(b) where no single optimum length higher than the experimental length is used.

Direct comparison between Figure 5.16(a) and 5.17(a) indicates that both Pareto are marginally equal and it implies two analogous consequences: lower desorbent flow rate is required for longer column while higher desorbent flow rate is needed if the columns are shorter. The decision maker reserves full right to decide which is more economically viable, saving fixed cost by using smaller amount of chiral stationary phase or lowering operating cost by using less desorbent.

Chiral separation process by moving bed chromatography becomes more economically attractive with the information presented in case 8 and case 9 thus offering more challenges to kick off new dimension in both designing more competitive separation process as well as establishing universal recognition.

5.6. Complete Separation Region

An attempt to use triangle theory with linear adsorption isotherm and ideal model has been done for the separation of 1,1'-bi-2-naphtol using 4-column SMB by Lai and Loh

(2002). The points in complete separate region were utilized to run SMB experiment and to predict the good separation region under non-linear equilibrium and mass transfer effects. Triangle theory is also used in this study to verify the optimization result under non-linear equilibrium with linear mass transfer approximation for case 3 (8-column SMB, fixed column length).

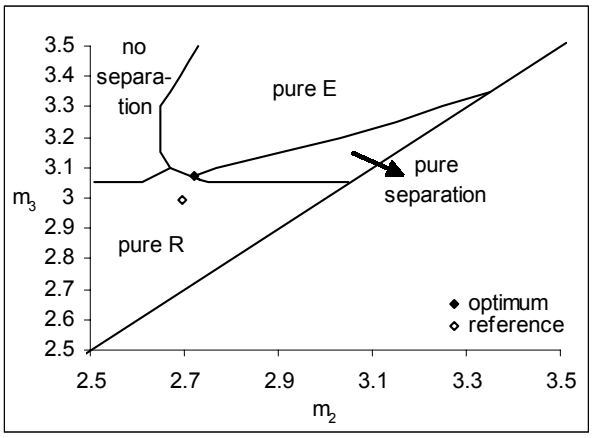

Figure 5.18 Plot of binary separation plane for optimization case 3

Figure 5.18 demonstrates agreement with the triangle theory for binary separation in which the pure separation region (purity requirement greater than 97%) is in triangular form with optimum point is located at the vertex of the obtuse triangle. The experimental point is located in the pure raffinate region. The fact that optimum point should always be located at the vertex of the triangle is obvious as optimization in SMB system is actually a matter of flow rate regulation in each zone so as to attain counter current movement of the two separating species.

The relative velocity of the species is calculated by virtue of the relative carrying capacity as defined by Petroulas et al. (1985) with all the required parameter in its calculation is tabulated in Table 5.10. It can be seen that both enantiomers move counter-

currently in zone II, III and IV in which separation take place while both species travel with the liquid phase in zone I ($\sigma>>1$) in which column regeneration takes place.

Table 5.10 Condition for counter-currency for case 3 in each SMB zone for enantioseparation of 1,1′-bi-2-naphtol racemate

Zone in SMB	δ		σ		V		
	δ_S	δ_R	σ_S	σ_R	V_S	V_R	ΔV
Zone I	4.035	5.595	0.510634	0.708054	1.041017	0.474596	0.566421
Zone II	4.035	5.595	0.824862	1.143768	0.250317	-0.122229	0.372546
Zone III	4.035	5.595	0.74752	1.036524	0.450776	-0.053733	0.504509
Zone IV	4.035	5.595	0.894959	1.240965	0.145745	-0.202598	0.348343

The component, however, is not supposed to move counter-currently in zone IV as both components must travel with the solid phase due to desorbent regeneration. The counter-currency in this case emerged due to the lack of freedom in choosing the flow rate in zone IV. The flow rate in zone IV is related to the desorbent flow rate and the flow rate in zone I. This means better separation is possible if Q_I is treated as decision variables in case 3 but it is fixed in this particular case due to pressure drop constraint.

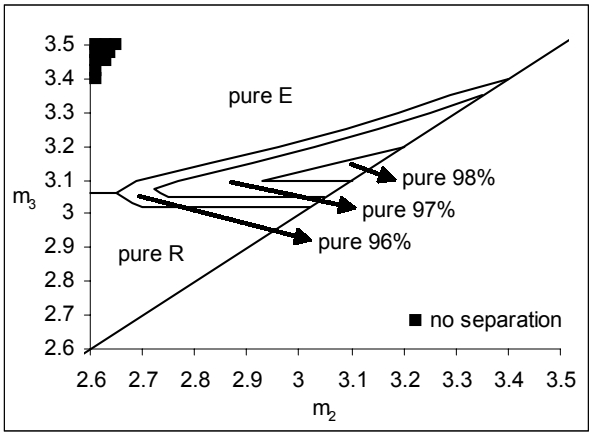

Figure 5.19 Plot of binary separation plane under various purity constraints

When purity constraint is made more stringent, the triangle region shrinks but its shape does not change as can be seen in Figure 5.19. It indicates that there exist numerous operating conditions to operate SMB that satisfy lower purity requirement. The optimal point should also move from one vertex to another as the triangle shrinks for more stringent separation.

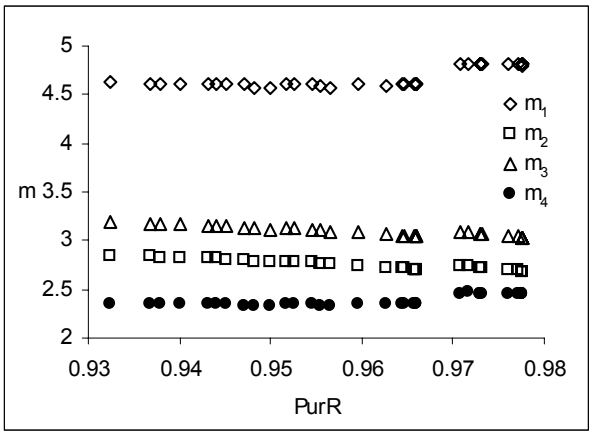

Figure 5.20 Plot of m flow rate parameter for all points in Pareto case 3

At extreme purity requirement, any attempt to disturb the operating condition away from the triangle will end up in either pure extract or pure raffinate region. Figure 5.20 shows the correlation between flow rate parameter and purity in case 3. Flow rate parameter is calculated according to eq. (4.26) in which the magnitude of m in each zone will only be a product of flow rate and switching time at certain column design.

The flow rate parameter in zone I, m_1 slightly increases with purity as one must maximize the contact between the mobile and stationary phase to accommodate high purity. This simply means an increase in residence of the separating species along the column at fixed liquid flow rate. The decrease of m_2 and m_3 is largely attributed to the decrease of flow rates in zone II and zone III respectively as the switching time for this

case only slightly increases as shown in Figure 5.11(e). It means solid phase dominates the separation in zone I while the liquid phase controls it in zone II and zone III.

The overall phenomenon in each zone in SMB is similar, high purity can be achieved by maximizing the contact between liquid and solid phase. It has been mentioned earlier that purity and productivity contradict each other thus raffinate flow rate will decrease to compensate the increase in raffinate purity. This explains the increase of m_4 as the flow rate in zone IV will be the difference between flow rate in zone III and raffinate flow rate. At high raffinate purity, the raffinate flow rate decreases drastically thereby the increase of m_4 is more apparent than that of low purity. Q_{IV} can also be defined as the difference between flow rate in zone I, Q_I and desorbent consumption, Q_D but since Q_I is fixed and Q_D slightly scattered, it can be concluded that m_4 is not governed by the latter. Flow rate parameter, as depicted in Figure 5.20, serves as a good tool to understand the phenomenon inside the moving Bed system.

5.7. The Effect of Flow Rate in Zone 1 (Q_1) on Countercurrent Separation

It has been discussed in the previous section that better separation is possible when both species travel countercurrently only in zone II and III. Specifically, both components should travel with the mobile phase in zone I to ensure perfect regeneration of the adsorbent from the more retained component because zone I will become zone IV in the subsequent switching. Likewise, they are preferred to travel with the stationary phase in zone IV for complete regeneration of the mobile phase from the less retained component.

Complete regeneration in zone IV is not attained for optimum results in case 3 (See Table 5.10) thus it is desired to reformulate optimization case 3 by treating Q_1 as decision

variable. The concept illustrated in this section is designated only for SMB system. The upper bound for this variable is selected so as to maintain column pressure drop still below the tolerable limit. All setting for other variables are kept similar to its original value in case 3 in which column length is not allowed to vary for the sake of fair comparison.

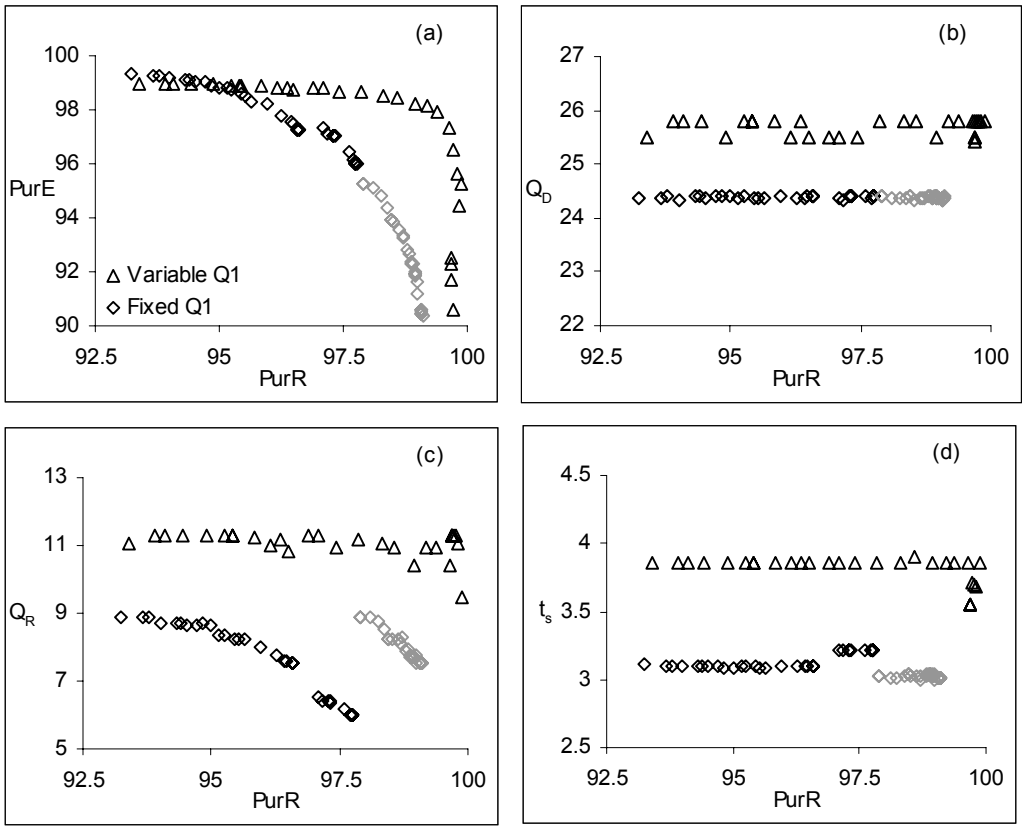

Figure 5.21 The effect of Q_1 on optimum points in case 3

Comparison between the new optimum results (in which Q_1 is a decision variable) with the old optima (fixed Q_1) is shown in Figure 5.21. Column configuration for the new Pareto is 2/2/3/1 while for the old Pareto it is composed of two configurations: 1/3/2/2 for the upper left of the Pareto and 2/3/2/1 for the lower right of the Pareto. Constant switching time is mainly attributed to fixed column length (10.5 cm) in this study. Purity

of extract stream for the new Pareto is somewhat smaller than the old one due to pressure drop constraint (direct impact on upper and lower bound of Q_1).

Despite the unique shape of the new Pareto for variable Q_1, it can be seen from Figure 5.21 that treating Q_1 as decision variable can bring about considerable improvement. Profile of flow rate in zone I (Q_1) is given in Figure 5.22. It can be seen that Q_1 has a slight declining trend with increasing raffinate purity. From the mass balance at the inlet of zone I, this is plausible because it implies that Q_4 is decreasing at constant desorbent rate as shown in Figure 5.21(b). Both components must travel with the solid phase thus internal flow rate in zone IV should be reduced according to eq. (4.18) described previously.

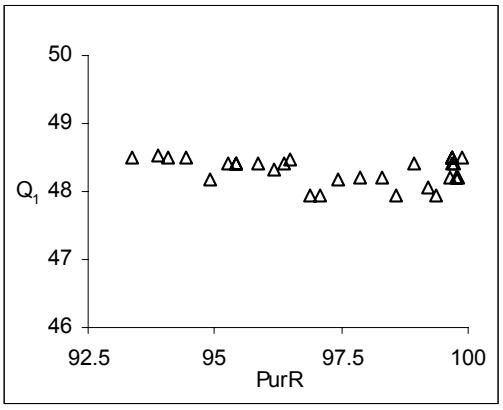

Figure 5.22 Profile of flow rate in zone I (Q_1) vs raffinate purity

The relative carrying capacity (σ) for a particular optimum point on the Pareto set for case 3 is given in Table 5.10 given previously. The details of calculation can be found in Appendix C. Although this point is one of the optimum points along the Pareto for case 3, it can be seen that task allocation is poor, as both component moves in the same direction in zone IV.

Similar calculations are done, for comparison, using an optimal point when Q_1 is varied and is summarized in Table 5.11. The tabulated results show that each zone in SMB system has now performed its specific role. Counter-currency only takes place in zone II and zone III in which $\sigma < 1$ for the weakly adsorbed component and $\sigma > 1$ for the strongly adsorbed component. In this way, better separation can be obtained due to additional degree of freedom enacted to the system.

Table 5.11 Condition for counter-currency for variable Q_1 in each SMB zone for enantioseparation of 1,1′-bi-2-naphtol racemate

Zone in SMB	δ		σ		V		
	δ_S	δ_R	σ_S	σ_R	V_S	V_R	ΔV
Zone I	4.035	5.595	0.523053	0.725274	0.863662	0.379802	0.483860
Zone II	4.035	5.595	0.82802	1.148147	0.196724	-0.129377	0.326100
Zone III	4.035	5.595	0.739939	1.026012	0.332888	-0.025421	0.358309
Zone IV	4.035	5.595	1.105089	1.532335	-0.090070	-0.348331	0.258261

Chapter 6 Conclusions and Recommendation

6.1. Optimal Operation of SMB and Varicol Processes for Chiral Drug Separation

First part of the thesis focuses on multi-objective optimization study for chiral drug separation. The work was initiated by modeling of published experimental study reported by Ludemann-Hombourger et al. (2002). This includes the determination of solid void fraction and theoretical number of plates for the separation of SB-553261, the development of breakthrough curves from single column experiment and numerical modeling of SMB and Varicol process. Moreover, the model was modified to describe 4-column Varicol, adapted from the concept of 3-zone SMB.

The next phase of the work consisted of a sensitivity study using the experimentally verified simulation model. At this phase, it was found that many process parameters in SMB separation process contradict various performance indexes, which necessitates an optimization study for this system. This study also revealed that experimental results reported by Ludemann-Hombourger et al. (2002) is not too far from the optimum solution, but the complex interplay between decision variables was not studied thoroughly.

Single objective optimization was subsequently carried out to test the optimization algorithm based on genetic algorithm. An adaptation of genetic algorithm, namely, non-dominated sorting genetic algorithm with jumping genes, was used in obtaining Pareto optimal solutions. Several numerical parameters that include selection of random seed, mutation and crossover probability, penalty parameter, etc were involved. It was found that optimum results are much better for all sets of experimental results reported by Ludemann-Hombourger et al. (2002). In two objectives functions, i.e. simultaneous maximization of

feed flow rate and minimization of desorbent flow rate, it was found that approximately 55% and 38% improvement can be achieved for the first and second objective function respectively. The next phase of the work was related to industrial design issues. Most industrial application involves several objectives and mostly these objectives are conflicting to each other. The solutions of these optimization problems are well summarized in all the Pareto Set obtained for different optimization formulations in chapter 4. Two objectives functions explored in this study include simultaneous maximization of raffinate and extract productivity, maximization of raffinate purity and productivity, maximization of extract purity and productivity, and finally the most prominent objectives in chiral drug industries: maximization of feed loading (capacity) and minimization of desorbent requirement. Three objectives optimization studies outlined simultaneous maximization of raffinate and extract productivity coupled with minimization of column length and/or minimization of desorbent requirement.

It was found that zone II and zone III were important to improve raffinate product quality (purity and productivity) while zone I and zone II were critical for extract product quality. No trend can be observed for the maximization of feed flow rate and minimization of desorbent rate except that that feed flow rate is linearly proportional to desorbent requirement, meaning more desorbent is required at higher feed loading capacity. In all optimization cases that involve simultaneous maximization of raffinate and extract productivity (including three objective optimization), it was found that zones I and II are critical.

The ranges for optimum decision variables are found to be away from those predicted by simple sensitivity study, indicating that multi-objectives optimization study is required. It was found that Varicol outperforms SMB process in all cases while enhanced performance is

achieved at relatively smaller number of columns. Extract flow rate is allowed to change in all cases of optimization according to mass balance constraint. Flow rate in zone I is fixed to a certain value in all cases of optimization to ensure pressure drop on the system is not excessive.

Finally, the optimum results have been examined for agreement with triangle theory by plotting in m_2-m_3 operation plane and all internal phenomena in each zone of the system has been explained using triangle theory. Moreover, further benchmarking on the effect of sub-interval and discrete feed operation has been applied to SMB and Varicol system. The concept mimics gradient operation in SMB operation and works by utilizing the additional degrees of freedom introduced to the system. Enantioseparation employing SMB technology may mostly be found at the preparative scale for the time being, due to the nature of chiral drug as small volume expensive material, but scale-up procedure is reported elsewhere (Zenoni et al., 2002).

6.2. Optimization Study of Continuous Chromatographic Separation of a Chiral Intermediate in SMB and Varicol System

The trend of chiral chemistry would be heading to catalytic asymmetric synthesis, which involves the use of chiral catalysts to accelerate the production of single enantiomer compounds for pharmaceutical use as well as wide ranges of other applications. This technique has been devised by three scientists: Monsanto retiree William S. Knowles and Professor Ryoji Noyori of Nagoya University in Japan for their work on catalytic asymmetric hydrogenation reactions, and Professor K. Barry Sharpless of Scripps Research Institute on catalytic asymmetric oxidations.

In general, there are two ways of producing pure enantiomeric from of a compound: conventional chemical synthesis and asymmetric synthesis. Both approaches have their own advantages and disadvantages. Conventional synthesis might end up with chirality element in the molecule but it is economically interesting. The method is suitable for compound whose counter species is not harmful or inactive. Asymmetric synthesis, on the other hand, can selectively produce certain species at high purity with the virtue of a chiral selector, which is very expensive. This method is less effective when both enantiomers of the compound are of equal importance.

In a bid to cover the increasing demand of (R)- and (S)-1,1'-bi-2-naphthol, SMB chromatography method seems promising due to ease of operation and high purity separation. The success of numerical model to quantify internal concentration profiles is also an encouraging factor to eliminate the hectic experimental work. SMB based model is used in all optimization work in this study which gives better agreement with experimental results compared to TMB based model (Pais et al. 1997a, b, 1998). Sensitivity study was also performed for this system with similar results as in the previous study with chiral drug separation but this time number of columns was also explored as decision variable.

Single objective function and multi-objectives function optimization were carried out to determine how much the process performance could be improved for the existing system. The optimization work on this topic was rather difficult as it involves large number of columns. Approximately 20 and 35 column configurations were possible for 7-column and 8-column configurations, and therefore, optimization work was quite tedious to ensure global optimality of all the solutions in Pareto Set. Optimum condition for maximization of feed flow rate was achieved by reducing internal liquid flow rates and pseudo solid phase velocity.

This is obvious, as residence time must be increased to enhance countercurrency. For minimization of desorbent flow rate, optimum condition required an increase in internal liquid flow rate, at almost fixed solid flow rate, to ensure sufficient adsorption-desorption mechanism at the condition of minimum solvent present in the system. The switching time for Varicol was smaller in magnitude than SMB due to more flexibility endowed by variation of solid velocity from one cycle of operation to another.

A distinct phenomenon noticed from multi-objectives optimization study was the effect of column configurations to the objective functions, which was not apparent in sensitivity study. Both purity and productivity hardly showed any changes when the number of columns of each zone was varied at fixed values of other operating parameters. Improvement could be attained, even though not as extreme as the previous case in chiral drug separation, by appropriate selection of column configurations. These optimum configurations, however, depended on the objective function being studied. There were 5 cases of two objective functions and 2 cases of three objective functions explored in this work. It was observed that zones II and IV were responsible for raffinate stream quality, while zones I and III were crucial for improving extract stream quality. Another plausible conclusion was, when comparing case 5 and case 6 in Chapter 5, that raffinate product was easier to obtain because slight disturbances in decision variables was able to drastically improve the objective function even under strict extract purity requirement.

For optimization involving three objectives, it was found that the Pareto Sets for two cases, maximization of raffinate and extract productivity and minimization of solid and/or solvent requirement, evaluated in this work are marginally equal. This phenomena lead to the following implication: little amount of solid phase demands more desorbent to achieve

optimal separation and vice versa. Optimum column configurations suggested in these two cases are also in agreement with those concluded previously. These pedestal results are useful as this information allow to understand in designing the operation as well as design of SMB and Varicol process and allows the decision maker to decide on the favorable operating condition which often depends on time, location and market conditions. Higher order multi-objectives optimization study i.e. higher than three objectives is felt unnecessary it may introduce too many conflicts among the objectives and thus is not practical in real life.

6.3. Recommendation for Future Work

The current work is limited to the merit of SMB and Varicol process for binary separation of chiral compounds, and therefore, it would be valuable if the scope for future work is extended to reactive system such as esterification, hydrogenation, etherification or isomerization reaction. This may exert more operating variables, e.g. feed concentration/ratio, as changes/disturbances applied will shift the equilibrium of a reversible reaction. Numerical model has also been established and verified for agreement with experimental studies for the production of bisphenol A, a resin intermediate, from phenol and acetone, and the synthesis of β-phenethyl acetate, used in fragrance industry. Kawase et al., 1999 reported experimental studies using 3-zone SMB unit without recycle for the production of bisphenol and experimental studies on 4-zone SMB unit with recycle for the synthesis of β-phenethyl acetate from β-phenethyl alcohol and acetic acid. Both products result from the reversible reactions and follow non-linear adsorption behavior on the solid phase, which has dual role, as adsorbent and catalyst. Optimization work on these reactive systems is expected to give

even more interesting results due to more complex conflicting behavior and process constraint.

Reactive system such as the organic synthesis of bisphenol A, entails many disturbances during operation. Problems like deteriorating resin activity (by adsorption of water), accumulation of by-product and inconsistent raw material quality might arise during operation. Automatic control is essential for implementation of this kind of systems. A static program based on Microsoft Visual Basic® has been developed to simulate the development of SMB internal concentration profile in the absence of disturbances. Further work, however, is still needed to convert this program to allow on-line simulation and optimization before providing output/response to the controller.

The future trend of SMB operation is in implementation of gradient operation which has been proven to allow both increased throughput, i.e. the volume of feed load per volume of adsorbent, as well as reduced desorbent consumption per feed volume. Hence, it is necessary to apply temperature gradient, particularly for reactive systems in which physico-chemical data for each compound such as in the esterification of β-phenethyl acetate is available in open literature (Yadav and Mehta, 1994). Examples of gradient operation reported in the literature include temperature gradient in sugar separation (Ching and Ruthven, 1986), pressure gradient in supercritical fluid chromatography (Mazzotti et al., 1997c), solvent gradients for enantio-separation of ionone (Abel et al., 2002) and salt gradient in protein separation (Houwing et al., 2002b).

REFERENCES

Abel, S., M. Mazzotti and M. Morbidelli. Solvent Gradient Operation of Simulated Moving Beds: I. Linear Isotherms, J. Chromatogr. A, *944*, pp. 23-39. 2002.

Adam, P., R.M. Nicoud, M. Baily and O. Ludemann-Hombourger. Process and Device for Separation with Variable Length, US Patent 6 136 198. 2000.

Agreda, V.H. Reactive distillation process for the production of methyl acetate, US Patent 4 435 595. 1986.

Ando, M. and M. Tanimura. Method for Controlling Simulated Moving Bed Systems, US Patent 4 599 115. 1986.

Artz, S.P., M.P. deGrandpre and D.J. Cram. Host-guest complexation. 33. Search for New Chiral Hosts, J. Org. Chem.*, 50*, pp. 1486-1496. 1985.

Azevedo, D.C.S. and A.E. Rodrigues. Fructose-Glucose Separation in a SMB Pilot Unit: Modeling, Simulation, Design, and Operation, AIChE J., *47*, pp. 2042-2051. 2001.

Balannec, B. and G. Hotier. From Batch To Countercurrent Chromatography. In Preparative and Production Scale Chromatography, ed by G. Ganetsos and P.E. Barker, pp. 301-357. New York: Marcel Dekker. 1993.

Bao, J., W.D. Wulff and A.L. Rheingold. Vaulted Biaryls as Chiral Ligands for Asymmetric Catalytic Diels-Alder Reactions, J. Am. Chem. Soc.*, 115*, pp. 3814-3815. 1993.

Barker, P.E. and C.B. Ching. Continuous Liquid Chromatographic Process for Separation of Fructose-Glucose Mixtures, Eur. Fed. Chem. Eng. Kemtek 5, Copenhagen, Denmark, 1980.

Barker, P.E., N.J. Ajongwen, M.T. Shieh and G.Ganetsos. Simulated Counter-Current Chromatographic Bioreactor-Separators. In Fundamental of Adsorption, ed by M. Suzuki, pp. 35-44. Tokyo: Kodansha. 1993.

Begovich, J.M. and W.G. Sisson. Continuous Ion Exchange Separation of Zirconium and Hafnium using an Annular Chromatograph, Hydrometallurgy, *10*, pp. 11-20. 1983.

Berg, C. Hypersorption Process for Separation of Light Gases, Trans. A.I.Ch.E., *42*, pp. 665-680. 1946.

Berg, C. Hypersorption Design: Modern Advances. Chem. Eng. Prog., *47*, pp. 585-591. 1951.

Bhaskar, V., S.K. Gupta and A.K. Ray. Applications of Multi-objective Optimization in Chemical Engineering, Rev. Chem. Eng., *16*, pp. 1-54. 2000.

Bieser, H.J. and A.J. de Rosset. Continuous counter-current separation of saccharides with inorganic adsorbents, 28th Starch Convention, Detmold, F.R.G. 1977.

Biressi, G., F. Quattrini, M. Juza, M. Mazzotti, V. Schurig and M. Morbidelli. Gas chromatographic simulated moving bed separation of the enantiomers of the inhalation anesthetic enflurane. Chem. Eng. Sci., *55*, pp. 4537-4547. 2000a.

Biressi, G., O. Ludemann-Hombourger, M. Mazzotti, R.M. Nicoud and M. Morbidelli. Design and Optimization of a Simulated Moving Bed Unit: Role of Deviations from Equilibrium Theory, J. Chromatogr. A, *876*, pp. 3-15. 2000b.

Bjorklund, M.C and R.W. Carr. The Simulated Counter-Current Moving Bed Chromatographic Reactor: A Catalytic and Separative Reactor, Catalysis Today, *25*, pp. 159-168. 1995.

Bjorklund, M.C, A.V. Kruglov and R.W. Carr. Further Studies of the Oxidative Coupling of Methane to Ethane and Ethylene in a Simulated Countercurrent Moving Bed Chromatographic Reactor, Ind. Eng. Chem. Res., *40*, pp. 2236-2242. 2001.

Bonmati, R.G., G. Chapelet-Letourneux and J.R. Margulis. Gas Chromatography – Analysis to Production, Chem. Eng., *Mar. 24*, pp.70-72. 1980.

Bougauchi, M., S. Watanabe, T. Arai, H. Sasai and M. Shibasaki. Catalytic Asymmetric Epoxidation of α,β-Unsaturated Ketones Promoted by Lanthanoid Complexes, J. Am. Chem. Soc., *119*, pp. 2329-2330. 1997.

Brandl, F., N. Pustet and A. Mannschreck. Applications of a Novel Type of Detector for Liquid Chromatography of Chiral Compounds, Int. Lab., *29*, pp. 10C-15C. 1999.

Broughton, D.B. and C.G. Gerhold. Continuous Sorption Process Employing Fixed Bed of Sorbent and Moving Inlets and Outlets, US Patent 2 985 589. 1961.

Broughton, D.B. Molex: Case History of a Process, Chem. Eng. Prog., *64*(8), pp. 60-65. 1968.

Broughton, D.B. and D.B. Carson. The Molex Process, Petrol. Refiner., *38*(4), pp. 130-134. 1969.

Broughton, D.B. and R.C. Berg. Olefins by dehydrongenation-extraction, Hydrocarb. Process., *48*(6), pp.115-120. 1969.

Broughton, D.B., R.W. Neuzil, J.M. Pharis and C.S. Brearley. The Parex process for recovering p-xylene. Chem. Eng. Prog., *66*, pp. 70-75. 1970.

Broughton, D.B., H.J. Bieser, R.C. Berg and E.D. Connel. High Purity Fructose via Continuous Adsorptive Separation, Suc. Belg., *96*, pp. 155. 1977.

Brunel, J.M. and G. Buono. A New and Efficient Method for the Resolution of 1,1'-binaphthalene-2,2'-diol, J. Org. Chem., *58*, pp. 7313-7314. 1993.

Cansell, F., G. Hotier, P. Marteau and N. Zanier. Method for Regulating a Process for the Separation of Isomers of Aromatic Hydrocarbons having 8 to 10 Carbon Atoms, US Patent 5 569 808. 1996.

Castro, P.P., T.M. Georgiadis and F. Diederich. Chiral Recognition in Clefts and Cyclophane Cavities Shaped by the 1,1'-binaphthyl Major Groove, J. Org. Chem., *54*, pp. 5835-5838. 1989.

Cavoy, E., M.-F. Deltent, S. Lehoucq and D. Miggiano. Laboratory - developed simulated moving bed for chiral drug separations. Design of the system and separation of Tramadol enantiomers, J. Chromatogr. A, *769*, pp. 49-57. 1997.

Chan, A.S.C., F. Zhang and C. Yip. Novel Asymmetric Alkylation of Aromatic Aldehydes with Triethylaluminium Catalyzed by Titanium·(1,1'-bi-2-naphtol) and Titanium·(5,5',6,6',7,7',8,8'-octahydro-1,1'-bi-2-naphtol) Complexes, J. Am. Chem. Soc., *119*, pp. 4080-4081. 1997.

Charton, F. and R.M. Nicoud. Complete design of a simulated moving bed, J. Chromatogr. A, *702*, pp. 97-112. 1995.

Ching, C.B. and D.M. Ruthven. An experimental Study of a Simulated Counter-Current Adsorption System: I. Isothermal Steady State Operation, Chem. Eng. Sci., *40*, pp. 877-885. 1985a.

Ching, C.B. and D.M. Ruthven. An experimental Study of a Simulated Counter-Current Adsorption System: II. Transient Response, Chem. Eng. Sci., *40*, pp. 887-891. 1985b.

Ching, C.B. and D.M. Ruthven. An experimental Study of a Simulated Counter-Current Adsorption System: IV. Non-Isothermal Operation, Chem. Eng. Sci., *41*, pp. 3063-3071. 1986.

Chow, H.-F., C.-W. Wan, M.-K. Ng. A Versatile Method for the Resolution and Absolute Configuration Assignment of Substituted 1,1'-Bi-2-naphtols, J. Org. Chem., *61*, pp. 8712-8714. 1996.

Clavier, J.Y., R.M. Nicoud and M. Perrut. A New Efficient Fractionation Process: The simulated Moving Bed with Supercritical Eluent. In High Pressure Chemical Engineering: Proc. of the 3rd International Symposium on High Pressure Chemical Engineering, October 1996, Zurich, Switzerland, pp. 429-434.

Coelho, M.S., D.C.S. Azevedo, J.A. Teixeira and A.E. Rodrigues. Dextran and Fructose Separation on an SMB Continuous Chromatography Unit, Biochem. Eng. J., *12*, pp. 215-221. 2002.

Cohen, C., R. Jacob, G. Bureau du Columbier and G. Hotier. Process for Regulating At Least One Fluid Flow Circulating in a Simulated Moving Bed Chromatographic Separation Loop, US Patent 5 685 992. 1997.

Colin, H., O. Ludemann-Hombourger and R.M. Nicoud. Recent Developments in Industrial High-Performance Preparative Chromatography, Pharma. Visions, pp. 26. Winter 2001

Colin, H., P. Hilaireau and J. De Tournemire. Liq. Chromatogr. Gas Chromatogr., *8*, pp. 302-304. 1990

Couenne, N., P. Duchenne, G. Hotier and D. Humeau. Method for Controlling with Precision a Process for Separating Constituents of a Mixture, in a Simulated Moving Bed Separation Systems, US Patent 5 902 486. 1999.

Crosby, J. Chirality in Industry, ed by A.N. Collins, G.N. Sheldrake and J. Crosby, pp. 2-66. Chichester: Wiley. 1992.

Davankov, V.A., A.A. Kurganov and T.M. Ponornareva, Enantioselectivity of complex formation in ligand-exchange chromatographic systems with chiral stationary and/or chiral mobile phases, J. Chromatogr., *452*, pp. 309-316. 1988.

de Rosset, A.J., R.W. Neuzil and D.J. Korous. Liquid Column Chromatography as a Predictive Tool for Continuous Counter-current Adsorption Separation, Ind. Eng. Chem. Process Des. Dev., *15*, pp. 261-266. 1978.

Deb, K. Optimization for Engineering Design: Algorithms and Examples, New Delhi: Prentice-Hall of India, pp. 290-320. 1995.

Deb, K. Multi-Objective Optimization Using Evolutionary Algorithms, Chicester: Wiley Interscience, pp. 1-497. 2001.

Deb, K., A. Pratap, S. Agarwal and T.A. Meyarivan. Fast and Elitist Multiobjective Genetic Algorithm: NSGA-II, IEEE Trans Evolutionary Computing, *6*, pp. 182-197. 2002.

Denet, F., W. Hauck, R.M. Nicoud, O. Di Giovanni, M. Mazzotti, J.N. Jaubert and M. Morbidelli. Enantioseparation through Supercritical Fluid Simulated Moving Bed (SF-SMB) Chromatography. Ind. Eng. Chem. Res., *40*, pp. 4603-4609. 2001.

Depta, A., T. Giese, M. Johannsen and G. Brunner. Separation of stereoisomers in a simulated moving bed-supercritical fluid chromatography plant. J. Chromatogr. A, *865*, pp. 175-186. 1999.

Desty, D.H., A. Goldup and W.T. Swanton, in *Lectures on Gas Chromatography-1962*, ed by H.A. Szymanski, pp. 105. New York: Plenum Press. 1963.

Devant, R.M., R. Jonas, M. Schulte, A. Keil, and F. Charton. Enantiomer separation of a novel Ca-sensitizing drug by simulated moving bed (SMB) chromatography, J. Prakt. Chem., *339*, pp. 315-321. 1997.

Di Giovanni, O., M. Mazzotti, M. Morbidelli, F. Denet, W. Hauck and R.M. Nicoud. Supercritical Fluid Simulated Moving Bed Chromatography. II. Langmuir Isotherm, J. Chromatogr. A., *919*, pp. 1-12. 2001.

Dinelli, D., S. Polezzo and M. Taramasso. Rotating Unit for Preparative-Scale Gas Chromatography, J. Chromatogr., *7*, pp. 477-484. 1962.

Dünnebier, G. and K.-U. Klatt. Optimal Operation of Simulated Moving Bed Chromatographic Processess, Comput. Chem. Eng., *23*, pp. S195-S198. 1999.

Dünnebier, G., I. Weirich and K.-U. Klatt. Computationally Efficient Dynamic Modeling and Simulation of Simulated Moving Bed Chromatographic Processes with Linear Isotherms, Chem. Eng. Sci., *53*, pp. 2537-2546. 1998.

Eagle, S. and C.E. Rudy. Separation and Desulfurization of Cracked Naphthas: Application of Cyclic Adsorption Process, Ind. Eng. Chem. *42*, pp. 1294-1299. 1950.

Fabbri, D., G. Delogu, O. De Lucchi. Preparation of Enantiomerically Pure 1,1'-binaphthalene-2,2'-diol and 1,1'-binaphthalene-2,2'-dithiol. J. Org. Chem., *58*, pp. 1748-1750. 1993.

Falk, T. and A. Seidel-Morgenstern. Comparison between a Fixed-Bed Reactor and a Chromatographic Reactor, Chem. Eng. Sci., *54*, pp. 1479-1485. 1999.

Fish, B. and R.W. Carr. An experimental study of the countercurrent moving bed chromatographic reactor, Chem. Eng. Sci., *44*, pp. 1773-1783. 1989.

Fox, J.B., R.C. Calhoun and W.J. Eglinton. Continuous Chromatography Apparatus: I. Construction, J. Chromatogr., *43*, pp. 48-54. 1969.

Francotte, E. and P. Richert. Applications of simulated moving-bed chromatography to the separation of the enantiomers of chiral drugs, J. Chromatogr. A, *769*, pp. 101-107. 1997.

Francotte, E.R. Enantioselective chromatography as a powerful alternative for preparation of drug enantiomers, J. Chromatogr. A., *906*, pp. 379-397. 2001.

Fricke, J., M. Meurer, J. Dreisörner and H. Schmidt-Traub. Effect of process parameters on the performance of a Simulated Moving Bed chromatographic reactor. Chem. Eng. Sci., *54*, pp. 1487-1492. 1999.

Fuchs, G., L. Doguet and D. Barth. Enantiomer fractionation of phosphine oxides by preparative subcritical fluid chromatography, J. Chromatogr. A, *623*, pp. 329-336. 1992b.

Fuchs, G., R.M. Nicoud and M. Bailly. Optical isomers purification with the simulated moving bed technology: Experimental and theoretical approaches, Proc. of the 9th International Symposium on Preparative and Industrial Chromatography "Prep 92", ed by Societe Francaise de Chimie, pp. 395-402. 1992a.

Fuji, K., M. Node and F. Tanaka. Complex-Induced Proximity Effects in Enolate Formation. Highly Diastereoselective α-Methylation of Binaphthyl Esters of Arylacetic Acid, Tetrahedron Lett., *31*, pp. 6553-6556. 1990.

Ganetsos, G. and P.E. Barker. Development in Large-Scale Batch Chromatography. In Preparative and Production Scale Chromatography, ed by G. Ganetsos and P.E. Barker, pp. 3-9. New York: Marcel Dekker. 1993.

Gembicki, S.A., A.R. Oroskar and J.A. Johnson. Adsorption, Liquid Separation. In Encyclopedia of Separation Technology I, ed by D.M. Ruthven, pp 172-196. New York: Wiley. 1997.

Gentilini, A., C. Migliorini, M. Mazzotti and M. Morbidelli. Optimal operation of simulated moving-bed units for non-linear chromatographic separations: II. Bi-Langmuir isotherm, J. Chromatogr. A., *805*, pp. 37-44. 1998.

Giddings, J.C. Theoritical Basis for a Continuous Large-Capacity Gas Chromatographic Apparatus, Anal. Chem., *34*, pp. 37-39. 1962.

Goldberg, D.E. Genetic Algorithm in Search Optimization and Machine Learning, Reading, Mass.:Addison-Wesley, pp.1-379. 1989.

Golshan-Shirazi, S. and G. Guiochon*,* Modelling of Preparative Liquid Chromatography, J. Chromatogr. A, *658*, pp. 149-171. 1994.

Gong, B., W. Chen and B. Hu. A New and Efficient Method for the Resolution of 2,2'-dihydroxy-1,1'-binaphthyl, J. Org. Chem*., 56*, pp. 423-425. 1991.

Gonzalez, J.C. and J.R. Fair. Preparation of tertiary amyl alcohol in a reactive distillation column. 1. Reaction kinetics, chemical equilibrium and mass transfer issues, Ind. Eng. Chem. Res., *36*, pp. 3833-3844. 1997.

Gonzalez, J.C., H. Subawalla and J.R. Fair. Preparation of' tertiary amyl alcohol in a reactive distillation column. 2. Experimental demonstration and simulation of the column, Ind. Eng. Chem. Res., *36*, pp. 3845-3853. 1997.

Gottschlich, N. and V. Kasche. Purification of monoclonal antibodies by simulated moving-bed chromatography, J. Chromatogr. A, *765*, pp. 201-206. 1997.

Guest, D.W. Evaluation of simulated moving bed chromatography for pharmaceutical process development. J. Chromatogr. A, *760*, pp. 159-162. 1997.

Guiochon, G. Preparative Liquid Chromatography, J. Chromatogr. A, *965*, pp. 129-161. 2002.

Guiochon, G., S.G. Shirazi and A.M. Katti. Fundamentals of Preparative and Nonlinear Chromatography, pp. 1-701. Boston: Academic Press. 1994.

Haag, J., A.V. Wouwer, S. Lehoucq and P. Saucez. Modelling and Simulation of a SMB Chromatographic Process Designed for Enantioseparation, Control Engineering Practice, *9*, pp. 921-928. 2001.

Hashimoto, K., S. Adachi and Y. Shirai. Continuous Desalting of Proteins with a Simulated Moving Bed Adsorber, Agric. Biol. Chem., *52*, pp. 2161. 1988.

Hashimoto, K., S. Adachi, H. Noujima and H. Maruyama. Models for the Separation of Glucose/Fructose Mixture Using a Simulated Moving-Bed Adsorber, J. Chem. Eng. Jpn., *16*, pp. 400-406. 1983a.

Hashimoto, K., S. Adachi, H. Noujima and Y. Ueda. A New Process Combining Adsorption and Enzyme Reaction for Producing Higher-Fructose Syrup, Biotechnol. Bioeng. , *25*, pp. 2371-2393. 1983b.

Hassan, M.M., A.K.M. Shamsur Rahman and K.F. Loughlin. Modelling of Simulated Moving Bed Adsorption System: A more Precise Approach, Sep. Tech., *5*, pp. 77-89. 1995.

Hattori, K. and H. Yamamoto. Asymmetric aza-Diels-Alder Reaction Mediated by Chiral Boron Reagent, J. Org. Chem., *57*, pp. 3264-3265. 1992.

Heikkilä, H. Separating Sugars and Amino Acids with Chromatopgraphy, Chem. Eng., *Jan. 24*, pp. 50-52. 1983.

Helgeson, R.C., J.M. Timko, P. Moreau, S.C. Peacock, M.M. Mayer and D.J. Cram. Models for Chiral Recognition in Molecular Complexation, J. Am. Chem. Soc., *96*, pp. 6762-6763. 1974.

Heuer, C., E. Küsters, T. Plattner and A. Seidel-Morgenstern. Design of the simulated moving bed process based on adsorption isotherm measurements using a perturbation method, J. Chromatogr. A, *827*, pp. 175-191. 1998.

Holland, J.H. Adaptation in Natural and Artificial Systems: An Introductory Analysis with Applications to Biology, Control and Artificial Intelligence. pp. 1-183, Ann Arbor: University of Michigan Press. 1975.

Holt, R.E. Control Process for Simulated Moving Bed para-Xylene Separation, US Patent 5 470 482. 1995a.

Holt, R.E. Control Process for Simulated Moving Bed Adsorbent Bed Separations, US Patent 5 457 260. 1995b.

Hongisto, H.J. Chromatographic Separation of Sugar Solutions: I. The Finn Sugar Molasses Desugarization Process, Int. Sugar J., *79*, pp. 100-104. 1977.

Hotier, G. Process for Simulated Moving Bed Separation with a Constant Recycle Rate, US Patent 5 762 806. 1998.

Houwing, J., H.A.H. Billiet, J.A. Wesselingh and L.A.M. van der Wielen. Azeotropic Phenomena During Separation of Dilute Mixtures of Proteins by Simulated Moving Bed Chromatography, J. Chem. Technol. Biotechnol., *74*, pp.213-215. 1999.

Houwing, J., H.A.H. Billiet and L.A.M. van der Wielen. Optimization of azeotropic protein separations in gradient and isocratic ion-exchange simulated moving bed chromatography, J. Chromatogr. A, *944*, pp. 189-201. 2002a.

Houwing, J, S.H. van Hateren, H.A.H. Billiet and L.A.M. van der Wielen. Effect of salt gradients on the separation of dilute mixtures of proteins by ion-exchange in simulated moving beds, J. Chromatogr. A, *952*, pp. 85-98. 2002b.

Houwing, J., H.A.H. Billiet and L.A.M. van der Wielen. Mass-Transfer Effects During Separation of Proteins in SMB by Size Exclusion, AIChE J., *49*, pp. 1158-1167. 2003.

Howard, A.J., G. Carta and C.H. Byers. Separation of sugar by continuous annular chromatography, Ind. Eng. Chem. Res., *27*, pp. 1873-1882. 1988.

Hu, Q.S., D. Vitharna and L. Pu. An Efficient and Practical Direct Resolution of Racemic 1,1´-bi-2-naphthol to Both of Its Pure Enantiomers, Tetrahedron: Asymmetry, *6*, pp. 2123-2126. 1995.

Ishihara, K., M. Kaneeda and H. Yamamoto. Lewis Acid Assisted Chiral Bronsted Acid for Enantioselective Protonation of Sylil Enol Ethers and Ketene Bis (trialkylsilyl) Acetals, J. Am. Chem. Soc., *116*, pp. 11179-11180. 1994.

Isla, M.A. and H.A. Irazoqui. Modelling, Analysis and Simulation of a Methyl *tert*-Butyl Ether Reactive Distillation Column, Ind. Eng. Chem. Res., *35*(8), pp. 2696-2708. 1996.

Jacques, J. and C. Fouquey. Enantiomeric (S)-(+)- and (R)-(-)-1,1′-Binaphthyl-2,2′-diyl Hydrogen Phosphate, Org. Synth., *67*, pp. 1-12. 1988.

Jansen, J.F.G.A. and B.L. Feringa. Enantioselective Conjugate Addition of Grignard Reagents to Enones Catalyzed by Chiral Zinc(II) Complexes, J. Org. Chem., *55*, pp. 4168-4175. 1990.

Jensen, T.B., T.G.P. Reijns, H.A.H. Billiet and L.A.M. van der Wielen. Novel Simulated Moving-Bed for Reduced Solvent Consumption, J. Chromatogr. A, pp. 149-162. 2000.

Johannsen, M., S. Peper and A. Depta. Simulated Moving Bed Chromatography with Supercritical Fluids for the Resolution of bi-naphtol enantiomers and phytol isomers, J. Biochem. Biophys. Methods, *54*, pp. 85-102. 2002.

Jupke, A., A. Epping, H. Schmidt-Traub and M. Schulte. Experimental Verification of a Process Model, Simulation and Optimisation of SMB Chromatography, SPICA, October 2000, Zurich, Switzerland.

Juza, M., M. Mazzotti and M. Morbidelli. Simulated-moving bed chromatography and its application to chirotechnology. Trends Biotechnol., *18*, pp. 108-118. 2000.

Juza, M., O. Di Giovanni, G. Biressi, V. Schurig, M. Mazzotti and M. Morbidelli. Continuous enantiomer separation of the volatile inhalation anesthetic enflurane with a gas chromatographic simulated moving bed unit, J. Chromatogr. A, *813*, pp. 333-347. 1998.

Karlsson, S., F. Pettersson and T. Westerlund. A MILP-Method for Optimizing a Preparative Simulated Moving Bed Chromatographic Separation Process. Comput. Chem. Eng., *23*, pp. S487-S490. 1999.

Kartozia, I., M. Kanyonyo, T. Happaerts, D.M. Lambert, G.K.E. Scriba and B. Chankvetadze. Comparative HPLC enantioseparation of new chiral hydantoin derivatives on three different polysaccharide type chiral stationary phases. J. Pharm. Biomed. Anal., *27*, pp. 457-465. 2002.

Kasat, R., D. Kunzru , D.N. Saraf and S.K. Gupta. Multiobjective Optimization of Industrial FCC Units Using Elitist Nondominated Sorting Genetic Algorithm, Ind. Eng. Chem. Res., *41*, pp 4765-4776. 2002.

Kaspereit, M., P. Jandera, M. Škavrada and A. Seidel-Morgenstern. Impact of Adsorption Isotherm Parameters on the Performance of Enantioseparation Using Simulated Moving Bed Chromatography, J. Chromatogr. A, *944*, pp. 249-262. 2002.

Kawase, M., T.B. Suzuki, K. Inoue, K. Yoshimoto and K. Hashimoto. Increased esterification conversion by application of the simulated moving bed reactor, Chem. Eng. Sci., *51*, pp. 2971-2976. 1996.

Kawase, M., Y. Inoue, T. Araki and K. Hashimoto. The simulated moving bed reactor for production of Bisphenol A, Catalysis Today, *48*, pp. 199-209. 1999.

Kawase, M., A. Pilgrim, T. Araki and K. Hashimoto. Lactosucrose Production Using a Simulated Moving Bed Reactor, Chem. Eng. Sci., *56*, pp. 453-458. 2001.

Kawashima, M. and A. Hirayama. Direct Optical Resolution of 2,2′-Dihydroxi-1,1′-binaphthyl, Chem. Lett., *12*, pp. 2299-2300. 1990.

Kazlauskas, R.J. (S)-(-)- and (R)-(+)-1,1′-bi-2-naphthol, Org. Synth., *70*, pp.60-67. 1991.

Kazlauskas, R.J. Resolution of Binaphtols and Spirobiindanols Using Cholesterol Esterase, J. Am. Chem. Soc., *111*, pp. 4953-4959. 1989.

Kearney, M.M. and K.L. Hieb. Time Variable Simulated Moving Bed Process, US Patent 5 102 553. 1992.

Kehde, A., K.G. Fairfield, J.C. Frank and L.W. Zhanstecher. Ethylene Recovery: Commercial Hypersorption Operation, Chem. Eng. Prog., *44*, pp. 575-578. 1984.

Kirkpatrick, F. Rev Up Patient Recruitment, Pharmaceutical Executive, April 1st, pp. 60-66. 2002.

Kishihara, S., S. Fujii, et al.. Continuous Chromatographic Separation of Palatinose and Trehalulose Using a Simulated Moving Bed Adsorber, J. Chem. Eng. Jpn., *22*, pp. 434-436. 1989.

Kitajima, H., K. Ito and T. Katsuki. Enantioselective Addition of Diethylzinc to Aldehydes Using 1,1′-Bi-2-naphthol-3,3′-dicarboxamide as a Chiral Auxiliary, Chem. Lett., *5*, pp. 343-344. 1996.

Klatt, K.-U., F. Hanisch and G. Dünnebier. Model-based Control of a Simulated Moving Bed Chromatographic Process for the Separation of Fructose and Glucose, J. Process Control, *12*, pp. 203-219. 2002.

Klatt, K.-U., G. Dünnebier, S. Engell and F. Hanisch. Model-Based Optimization and Control of Chromatographic Process, Comput. Chem. Eng., *24*, pp. 1119-1126. 2000.

Kloppenburg, E. and E.D. Gilles. Automatic Control of the Simulated Moving Bed Process for C8 Aromatics Separation using Asymptotically Exact Input/Output-Linearization, J. Process Contr., *9*, pp. 41-50. 1998.

Kloppenburg, E. and E.D. Gilles. A New Concept for Operating Simulated Moving-Bed Processes, Chem. Eng. Technol., *22*, pp. 813-817. 1999.

Komatsu, N., M. Hashizuma, T. Sugita and S. Uemura. Catalytic Asymmetric Oxidation of Sulfides to Sulfoxides with tert-Butyl Hydroperoxide Using Binaphtol as a Chiral Auxiliary, J. Org. Chem., *58*, pp. 4529-4533. 1993.

Kruglov, A.V., M.C. Bjorklund and R.W. Carr. Optimization of the Simulated Countercurrent Moving-Bed Chromatographic Reactor for the Oxidative Coupling of Methane, Chem. Eng. Sci., *51*, pp. 2945-2950. 1996.

Lai, S. and R. Loh. Quick method for the determination of the optimal operating conditions of a simulated moving bed unit, J. Liq. Chrom. & Rel. Technol., *25*(3), pp. 345-361. 2002.

Leaver, G., J.R. Conder and J.A. Howell. A method development study of the production of albumin from animal blood by ion exchange chromatography, Sep. Sci. Technol., *22* 2037-2059. 1987.

Lehn, J.-M., J. Simon and A. Moradpour. Synthesis and Properties of Chiral Macrotricyclic Ligands. Complexation and Transport of Chiral Molecular Cations and Anions, Helv. Chim. Act., *61*, pp. 2407-2418. 1978.

Lingenfelter, D.S., R.C. Helgeson, and D.J. Cram. Host-Guest Complexation. High Chiral Recognition of Amino Acid and Ester Guests by Host Containing One Chiral Element, J. Org. Chem., *46*, pp. 393-406. 1981.

Ludemann-Hombourger, O., R. M. Nicoud and M. Bailly. The "VARICOL" Process: A New Multicolumn Continuous Chromatographic Process, Sep. Sci. Technol., *35*(12), pp.1837-1838. 2000.

Ludemann-Hombourger, O., G. Pigorini, R. M. Nicoud, D. S. Ross and G. Terfloth, Application of the "Varicol" process to the separation of the isomers of the SB-553261 racemate, J. Chromatogr. A, *947*, pp. 59-68. 2002.

Luffer, D.R., W. Ecknig and M. Novotny. Physicochemical Model of Retention for Capillary Supercritical Fluid Chromatography, J. Chromatogr. A, *505*, pp. 79-97. 1990.

Ma, Z. and N.H.L. Wang. Standing Wave Analysis of SMB Chromatography: Linear Systems, AIChE J., *43*(10), pp. 2488-2508. 1997.

Magee, E.M. The course of a reaction in a Chromatographic Column, Ind. Eng. Chem. Fund., *2*, pp. 32-36. 1963.

Maglioli, P., O. De Lucchi, G. Delogu and G. Valle. Highly Diastereoselective Reduction and Addition of Nucleophiles to Binaphthol-protected Arylglyoxals, Tetrahedron: Asymmetry, *3*, pp. 365-366. 1992.

Maki, H. Separation of Glutathionine and Glutamic Acid using a Simulated Moving-Bed Adsorber System. In Preparative and Production Scale Chromatography, ed by G. Ganetsos and P.E. Barker, pp. 359-371. New York: Marcel Dekker. 1993.

Mallman, T., B.D. Burris, Z. Ma and N.-H.L. Wang. Standing Wave Design of Nonlinear SMB for Fructose Purification, AIChE J., *44*, pp. 2628-2646. 1998.

Mannschreck, A. Chiroptical Detection During Liquid Chromatography. 4. Applications to Stereoanalysis and Stereodynamics, Chirality, *4*, pp. 163-169. 1992.

Marteau, P., G. Hotier, N. Zanier-Szydlowski, A. Aoufi and F. Cansell. Advanced control of C_8 aromatics separation process with real-time multipoint on-line Raman spectroscopy, Process Control Qual., *6*, pp. 133-140. 1994.

Martin, A.J.P. Chromatographic Analysis: Summarizing Paper, Discuss. Faraday Soc., *7*, pp.332-336. 1949.

Maruka, K., T. Itoh, T. Shirasaka and H. Yamamoto. Asymmetric Hetero-Diels-Alder Reaction Catalyzed by a Chiral Organoaluminium Reagent, J. Am. Chem. Soc., *110*, pp. 310-312. 1988.

Maruoka, K. and H. Yamamoto. Generation of Chiral Organoaluminium Reagent by Discrimination of the Racemates with Chiral Ketone, J. Am. Chem Soc., *111*, pp. 789-790. 1989.

Masuda, T., T. Sonobe, F. Matsuda and M. Horie. Process for Fractional Separation of Multi-Component Fluid Mixture, US Patent 5 198 120. 1993.

Mata, V.G. and A.E. Rodrigues. Separation of ternary mixtures by pseudo-simulated moving bed chromatography, J. Chromatogr. A, *939*, pp. 23-40. 2001.

Mazzotti, M., R. Baciocchi, G. Storti and M. Morbidelli. Vapor phase SMB Adsorptive Separation of Linear/Nonlinear Paraffins, Ind. Eng. Chem. Res., *35*, pp. 2313-2321. 1996a.

Mazzotti, M., A. Kruglov, B. Neri, D. Gelosa and M. Morbidelli. A Continuous Chromatographic Reactor: SMBR, Chem. Eng. Sci, *51*, pp. 1827-1836. 1996b.

Mazzotti, M., G. Storti and M. Morbidelli. Optimal operation of simulated moving bed units for nonlinear chromatographic separations, J. Chromatogr. A, *769*, pp. 3-24. 1997a.

Mazzotti, M., B. Neri, D. Gelosa and M. Morbidelli. Dynamics of a chromatographic reactor: Esterification catalyzed by acidic resins, Ind. Eng. Chem. Res., *36*, pp. 3163-3172. 1997b.

Mazzotti, M., G. Storti and M. Morbidelli. Supercritical Fluid Simulated Moving Bed Chromatograpy, J. Chromatogr. A, *786*, pp. 309-320. 1997c.

Mc Coy, M. Making Drugs with Little Bugs, C&E News, *79*(21), pp. 37-43. 2001.

Mensah, P. and G. Carta. Adsorptive control of water with immobilized enzymes. Continuous operation in a periodic countercurrent reactor, Biotechnol. Bioeng., *66*, pp. 137-146. 1999.

Meurer, M., U. Altenhöner, J. Strube, A. Untiedt and H. Schmidt-Traub. Dynamic Simulation of a Simulated-Moving-Bed Chromatographic Reactor for the Inversion of Sucrose, Starch/Stärke, *48*, pp. 452-457. 1996.

Migliorini, C., M. Mazzotti and M. Morbidelli. Simulated moving bed units with extra column dead volume, AIChE J., *45*, pp. 1411-1422. 1999.

Mikami, K. and S. Matsukawa. Enantioselective and Diastereoselective Catalysis of the Mukaiyama Aldol Reaction: Ene Mechanism in Titanium-Catalyzed Aldol Reactions of Sylil Enol Ethers, J. Am. Chem. Soc., *115*, pp. 7039-7040. 1993.

Moore, D. and L. Pu, BINOL-Catalized Highly Enantioselective Terminal Alkyne Additions to Aromatic Aldehydes, Org. Lett., *0*, pp. A-C. 2002.

Morbidelli, M., G. Storti, S. Carra, G. Niederjaufner and A. Pontoglio. Study of a separation process through adsorption on molecular shieves application to a chlorotoluene isomer mixture, Chem. Eng. Sci., *39*, pp. 383-393. 1984.

Munir, M. Molasses Sugar Recovery by Liquid Distribution Chromatography. Int. Sugar J., *78*, pp.100-106. 1976.

Nagamatsu, S., K. Murazumi and S. Makino. Chiral separation of a pharmaceutical intermediate by a simulated moving bed process. J. Chromatogr. A, *832*, pp. 55-65. 1999.

Nakajima, M., K. Kanayama, I. Miyoshi, S.-i. Hashimoto. Catalytic Asymmetric Synthesis of Binaphthol Derivatives by Aerobic Oxidative Coupling of 3-Hydroxy-2-Naphthoates with Chiral Diamine-Copper Complex, Tetrahedron Lett., *36*, pp. 9519-9520. 1995.

Nakano, T. and D.Y. Sogah. Toward Control of Stereochemistry in GTP by a Rational Monomer Design. Cyclopolymerization of 2,2'-Bis-((methacryloyloxy)methyl)-1,1'-binaphthyl, J. Am. Chem. Soc., *117*, pp. 534-535. 1995.

Nandasana, A.D., A.K. Ray and S.K. Gupta. Applications of the Non-dominated Sorting Genetic Algorithm (NSGA) in Chemical Reaction Engineering, Int. J. Chem. Reactor Eng., *1*(*R2)*, pp. 1-16. 2003. www.bepress.com/ijcre/vol1/R2/

Natarajan, S. and J.H. Lee. Repetitive Model Predictive Control Applied to a Simulated Moving Bed Chromatographic System, Comput. Chem. Eng., *24*, pp. 1127-1133. 2000.

Nicoud, R.M., and A. Seidel-Morgenstern, Adsorption Isotherms: Experimental Determination and Application to Preparative Chromatography. In Simulated Moving Bed: Basics and Applications, ed by R.M. Nicoud, pp. 4. Nancy: Inst. National Polytechnique de Lorraine. 1993.

Nicoud, R.M., G. Fuchs, P. Adam, M. Bailly, E. Küsters, F.D. Antia, R. Reuille and E. Schmid. Preparative Scale Enantioseparation of a Chiral Epoxide: Comparison of Liquid Chromatography and Simulated Moving Bed Adsorption Technology, Chirality, *5*, pp. 267-271. 1993.

Nicoud, R.M. and A. Seidel-Morgenstern. Adsorption isotherms: Experimental determination and application to preparative chromatography, Isolation and purification 2, pp.165. 1996.

Nicoud, R.M. Simulated Moving Bed (SMB): Some Possible Applications for Biotechnology. In Bioseparation and Bioprocessing vol. 1, ed by G. Subramanian, pp. 3-39. Weinheim: Wiley-VCH. 1998.

Noji, M., M. Nakajima and K. Koga. A New Catalytic System for Aerobic Oxidative Coupling of 2-Naphthol Derivatives by the use of CuCl-Amine Complex: A Practical Synthesis of Binaphthol Derivatives, Tetrahedron Lett., *35*, 1994, pp. 7983-7984. 1994.

Noyori, R. Asymmetric Catalysis in Organic Synthesis, pp. 1-364. Wiley: New York, 1994.

Noyori, R., I. Tomino, Y. Tanimoto and M. Nishizawa. Asymmetric Synthesis via Axially Dissymmetric Molecules. 6. Rational Designing of Efficient Chiral Reducing Agents. Highly Enantioselective Reduction of Aromatic Ketones by Binaphtol-Modified Lithium Aluminium Hydride Reagents, J. Am. Chem. Soc., *106*, pp. 6709-6716. 1984a.

Noyori, R., I. Tomino, M. Yamada and M. Nishigawa. Asymmetric Synthesis via Axially Dissymmetric Molecules. 7. Synthetic Applications of the Enantioselective Reduction by Binaphtol-Modified Lithium Aluminium Hydride Reagents, J. Am. Chem. Soc., *106*, pp. 6717-6725. 1984b.

Noyori, R., S. Suga, K. Kawai, S. Okada, M. Kitamura, N. Oguni, M. Hayashi, T. Kaneko and Y. Matsuda. Enantioselective Addition of Diorganozincs to Aldehydes Catalyzed by β-Amino Alcohol, J. Organomet. Chem., *382*, pp.19-37. 1990.

Nozaki, K., N. Sakai, T. Nanno, T. Higashijima, S. Mano, T. Horiuchi and H. Takaya. Highly Enantioselective Hydroformylation of Olefins Catalyzed by Rhodium (I) Complexes of New Chiral Phosphine-Phosphite Ligands, J. Am. Chem. Soc., *119*, pp. 4413-4423. 1997.

Okamoto, Y. and T. Nakano. Asymmetric Polymerization, Chem. Rev., *94*, pp. 349-372. 1994.

Otani, S. Adsorption separates xylenes, Chem. Eng., *80*, pp. 106-107. 1973.

Pais, L.S., J.M. Loureiro and A.E. Rodrigues. Modelling, simulation and operation of a simulated moving bed for continuous chromatographic separation of 1,1'-bi-2-naphtol enantiomers, J. Chromatogr. A, *769*, pp. 25-35. 1997a.

Pais, L.S., J.M. Loureiro and A.E. Rodrigues. Separation of 1,1'-bi-2-naphtol enantiomers by continuous chromatography in simulated moving bed, Chem. Eng. Sci., *52*, pp. 245-257. 1997b.

Pais, L.S., J.M. Loureiro and A.E. Rodrigues. Modelling Strategies for Enantiomers Separation by SMB Chromatography, AIChE J., *44*, pp. 561-569. 1998.

Pasteur, L. Researches on the Molecular Asymmetry of Natural Organic Products, reprinted by The Alembic Club, pp. 7-46. Chicago: University of Chicago Press.1902.

Peper, S., M. Lübbert, M. Johannsen and G. Brunner. Separation of Ibuprofen Enantiomers by Supercritical Fluid Simulated Moving Bed Chromatography, Sep. Sci. Technol., *37*, pp. 2545-2566. 2002.

Perrut, M. Advances in Supercritical Fluid Chromatographic Processes, J. Chromatogr. A, *658*, pp. 293-313. 1994.

Petroulas, T., R. Aris and R.W. Carr. Analysis and Performance of a Countercurrent Moving-Bed Chromatographic Reactor, Chem. Eng. Sci., *40*, pp. 2233-2240. 1985.

Pirkle, W.H., D.W. House and J.M. Finn. Broad Spectrum Resolution of Optical Isomers Using Chiral High-Performance Liquid Chromatographic Bonded Phases, J. Chromatogr., *192*, pp. 143-158. 1980.

Pirkle, W.H., L.J. Brice and G.J. Terfloth. Liquid and subcritical CO_2 separations of enantiomer s on a broadly applicable polysiloxane chiral stationary phase, J. Chromatogr. A, *753*, pp. 109-119. 1996.

Profir, V.M. and M. Matsuoka. Processes and phenomena of purity decrease during the optical resolution of threonine by preferential crystallization, Colloids Surfaces, *164*, pp. 315-324. 2000.

Ray, A.K, R.W. Carr and R. Aris. The simulated countercurrent moving-bed chromatographic reactor - a novel reactor separator, Chem. Eng. Sci., *49*, pp. 469-480. 1994.

Ray, A.K. and R.W. Carr. Experimental Study of a Laboratory-Scale Simulated Countercurrent Moving Bed Chromatographic Reactor, Chem. Eng. Sci., *14*, pp. 2195-2202. 1995.

Reetz, M.T., C. Merk, G. Naberfeld, J. Rudolph, N. Griebenow and R. Goddard. 3,3′-dinitro-octahydrobinaphthol: A New Chiral Ligand for Metal-Catalyzed Enantioselective Reactions, Tetrahedron Lett., *38*, pp. 5273-5276. 1997.

Rekoske, J.E. Chiral Separations, AIChE J., *47*, pp. 2-5. 2001.

Roginskii, S.Z., M.I. Yanovskii and G.A. Gaziev. Cemical Reaction under Chromatographic Conditions, Dokl. Akad. Nauk SSSR (Engl. Transl.), *140*, pp. 771-776. 1961.

Rouhi, A.M. Chiral Roundup, C&E News, *80*(23), pp. 43-51. 2002.

Ruthven, D.M. and C.B. Ching. Counter-Current and Simulated Counter-Current Adsorption Separation Process, Chem. Eng. Sci., *44*, pp. 1011-1037. 1989.

Ryan, J.M., R.S. Timmins, and J.F. O'Donnell. Production Scale Chromatography. Chem. Eng. Prog., *64*(8), pp. 53-59. 1968.

Sakai, N., S. Mano, K. Nozaki and H. Takaya. Highly Enantioselective Hydroformylation of Olefins Catalyzed by New Phosphine-Phosphite-Rhodium(I) Complexes, J. Am. Chem. Soc., *115*, pp. 7033-7034. 1993.

Sardin, M. and J. Villermaux. Esteŕification catalyseé par une reśine ećhangeuse de cation dans un reácteur chromatographique, Nouveau Journal de Chimie, *3*, pp.225-235. 1979.

Sasai, H., T. Suzuki, S. Arai, T. Arai and M. Shibasaki. Basic Character of Rare Earth Material Alkoxides. Utilization in Catalytic Carbon-Carbon Bond-Forming Reactions and Catalytic Assymetric Nitroaldol Reactions, J. Am. Chem. Soc., *114*, pp. 4418-4420. 1992.

Sayama, K., T. Kamada, S. Oikawa and T. Masuda. Production of Raffinose: a New Byproduct of the Beet Sugar Industry, Zucherind., *117*, pp. 893. 1992.

Schiesser, W.E. The Numerical Method of Lines: Integration of Partial Differential Equation: ODEs, DAEs and PDEs. pp. 1-326, New York: Academic Press. 1991.

Schmidt, B. and D. Seebach. 2,2-Dimethyl-α,α,α′,α′-tetrakis(β-naphthyl)-1,3-dioxolan-4,5-dimethanol (DINOL) for the Titanate-Mediated Enantioselective Addition of Diethylzinc to Aldehydes, Angew. Chem. Int. Ed. Engl., *30*, pp. 1321-1323. 1991.

Schulte, M., J.N. Kinkel, R.M. Nicoud and F. Charton. Simulated Moving Bed (SMB). An efficient technique to producing optically active compounds on an industrial scale. Chem. Ing. Tech., *68*, pp. 670-683. 1996.

Schulte, M., R. Ditz, R.M. Devant, J.N. Kinkel and F. Charton. Comparison of the specific productivity of different chiral stationary phases used for simulated moving-bed chromatography, J. Chromatogr. A, *769*, pp. 93-100. 1997.

Schulte, M. and J. Strube. Preparative enantioseparation by simulated moving bed chromatography, J. Chromatogr. A, *906*, pp. 399-416. 2001.

Scott, C.D., R.D. Spence and W.G. Sisson. Pressurized, Annular Chromatograph for Continuous Separation, J. Chromatogr., *126*, pp. 381-400. 1976.

Seebach, D., M. Hoffmann, A.R. Sting, J.N. Kinkel, M. Schulte and E. Küsters. Chromatographic resolution of synthetically useful chiral glycine derivatives by high-performance liquid chromatography, J. Chromatogr. A, *796*, pp. 299-307. 1998.

Seko, M., H. Takeuchi, and T. Inada. Scale-up for Chromatographic Separation of p-xylene and ethylbenzene, Ind. Eng. Chem. Prod. Res. Dev., *21,* pp. 656-661. 1982.

Shibata, T., I. Okamoto and K. Ishii. Chromatographic Optical Resolution on Polysaccharides and Their Derivatives, J. Liq. Chromatogr., *9*, pp. 313-340. 1986.

Smrcina, M., J. Poláková, S. Vyskocil and P. Kocovsky. Synthesis of Enantiomerically Pure Binaphthyl Derivatives. Mechanism of the Enantioselective, Oxidative Coupling of Naphtols and Designing a Catalytic Cycle, J. Org. Chem., *58*, pp. 4534-4538. 1993.

Soai, K., A. Ookawa, T. Kaba and K. Ogawa. Catalytic Asymmetric Induction. Highly Enantioselective Addition of Dialkylzincs to Aldehydes Using Chiral Pyrrolidinylmethanols and Their Metal Salts, J. Am. Chem. Soc., *109*, pp. 7111-7115. 1987.

Sogah, G.D.Y. and D.J. Cram. Host Guest Complexation. 14. Host Covalently Bound to Polystyrene Resin for Chromatographic Resolution of Enantiomers of Amino Acid and Ester Salts, J. Am. Chem. Soc., *101*, p. 3035-3042. 1979.

Stinson, S.C. Chiral Drugs, C&E News, *78*(43), pp. 55-78. 2000

Stinson, S.C. Chiral Pharmaceutical, C&E News, *79*(40), pp. 79-97. 2001

Storti, G., M. Masi, R. Paludetto, M. Morbidelli and S. Carra. Adsorption Separation Processes: Countercurrent and Simulated Countercurrent Operations, Comput. Chem. Eng., *12*, pp. 475-482. 1988.

Storti, G., R. Baciocchi, M. Mazzotti and M. Morbidelli. Design of Optimal Operating Conditions of Simulated Moving Bed Adsorptive Separation Units, Ind. Eng. Chem. Res., *34*, pp. 288-301. 1995.

Strube, J., A. Jupke, A. Epping, H. Schmidt-Traub, M. Schulte and R. Devant. Design, Optimization and Operation of SMB Chromatography in the Production of Enantiomerically pure pharmaceuticals, Chirality, *11*, pp. 440-450. 1999.

Sussman, M.V. and C.C. Huang. Continuous Gas Chromatography, Science, *156*, pp. 974-976, 1967.

Suzuki, M., Y. Morita, H. Koyano, M. Koga and R. Noyori. Three-component Coupling Synthesis of Prostaglandins. A Simplified, General Procedure, Tetrahedron, *46*, pp. 4809-4822. 1990.

Tamai, Y., P. Heung-Cho, K. Iizuka, A. Okamura and S. Miyano. A Practical Method for Resolution of the Optical Isomers of 2,2′-Dihydroxy-1,1′-binaphthalene, Synth., *3*, pp. 222-223. 1990.

Tanaka, K., T. Okada and F. Toda. Separation of the Enantiomers of 2,2′-Dihydroxy-1,1′-binaphthyl and 10,10′-Dihydroxy-9,9′-biphenanthryl by Complexation with N-Alkylcinchonidinium Halides, Angew. Chem. Int. Ed. Engl., *32*, pp. 1147-1148. 1993.

Terada, M., K. Mikami and T. Nakai. Enantioselective Hetero-Diels-Alder Reaction with Glyoxylate Catalyzed by Chiral Titanium Complex: Asymmetric Synthesis of the Lactone Portion of Mevinolin and Compactin, Tetrahedron Lett.,*32*, pp. 935-938. 1991.

Terada, M., Y. Motoyama and K. Mikami. Diastereoselective and Enantioselective Glyoxylate-ene Reaction Catalyzed by New Class of Binaphthol-derived Titanium Complex, Tetrahedron Lett., *35*, p. 6693-6696. 1994.

Thome, B.and C.F. Ivory. Continuous fractionation of enantiomer pairs in free solution using an electrophoretic analog of simulated moving bed chromatography, J. Chromatogr. A, *953*, pp. 263-277. 2002.

Toda, F., K. Tanaka, Z. Stein and I. Goldberg. Optical Resolution of Binaphthyl and Biphenanthryl Diols by Inclusion Crystallization with n-Alkylchinconidium Halides. Structural Characterization of the Resolved Materials, J. Org. Chem., *59*, pp. 5748-5751. 1994.

Tomioka, K, M. Shindo and K. Koga. Novel Strategy of Using a C2 Symmetric Chiral Diether in the Enantioselective Conjugate Addition of an Organolithium to an α,β-Unsaturated Aldimine, J. Am. Chem. Soc., *111*, pp. 8266-8268. 1989.

Tonkovich, A.L., R.W. Carr and R. Aris. Enhanced C_2 Yields from Methane Oxidative Coupling by Means of a Separative Chemical Reactor, Science, *262*, pp. 221-223. 1993.

Tonkovich, A.L. and R.W. Carr. A Simulated Countercurrent Moving Bed Reactor for the Oxidative Coupling of Methane: Experimental Results, Chem. Eng. Sci., Chem. Eng. Sci., *49*, pp. 4647-4656. 1994.

Tonkovich, A.L. and R.W. Carr. Experimental Evaluation of Designs for the Simulated Countercurrent Moving Bed Separator, AIChE J., *42*, pp. 683-690. 1996.

Toumi, A., F. Hanisch and S. Engell. Optimal Operation of Continuous Chromatographic Process: Mathematical Optimization of the VARICOL Process, Ind. Eng. Chem. Res., *41*, pp. 4328-4337. 2002.

Toumi, A., S. Engell, O. Ludemann-Hombourger, R.M. Nicoud and M. Baily. Optimization of Simulated Moving Bed and Varicol Processes. J. Chromatogr. A., In Press. 2003.

Tswett, M.S., Tr. Protok., Varshav. Obshch. Estestvoistpyt. Otd. Biol., *14*. 1905. Reprinted and translated in G. Hesse, H. Weil, Michael Tswett's erste chromatographische Schrift, Woelm, Eschwegen. 1954.

Tuthill, E.J. A New Concept for the Continuous Chromatographic Separation of Chemical Species, J. Chromatogr. Sci., *8*, pp. 285-287. 1970.

Van der Meer, F.T. and F.L. Feringa. Catalytic Asymmetric Synthesis of Substituted Benzocyclo-alkenes via the Glyoxylate ene Reacytion, Tetrahedron Lett., *33*, pp. 6695-6696. 1992.

Van Walsem, H.J. and M.C. Thompson. Simulated moving bed in the production of lysine, J. Biotechnol., *59*, pp. 127-132. 1997.

Whitesell, J.K. C2 Symmetry and Asymmetric Induction, Chem. Rev., *89*, pp. 1581-1590. 1989.

Wooley, R., Z. Ma and N.H.L. Wang. A Nine-Zone Simulated Moving Bed for the Recovery of Glucose and Xylose from Biomass Hydrolyzate, Ind. Eng. Chem. Res., *37*(9), pp. 3699-3709. 1998.

Wright, B.W. and R.D. Smith. Investigation of polar modifiers in carbon dioxide mobile phases for capillary supercritical fluid chromatography, J. Chromatogr. A, *355*, pp. 367-373. 1986.

Wu, D.-J., Y. Xie, Z. Ma and N.-H.L. Wang. Design of Simulated Moving Bed Chromatography for Amino Acid Separations, Ind. Eng. Chem. Res., *37*, pp. 4023-4035. 1998.

Yadav, G.D. and P.H. Mehta. Heterogeneous Catalysis in Esterification Reactions: Preparation of Phenethyl Acetate and Cycrohexyl Acetate by using a Variety of Solid Acidic Catalysts, Ind. Eng. Chem. Res., *33*, pp. 2198-2208. 1994.

Yashima, E. and Y. Okamoto. Chiral Discrimination on Polysaccharides Derivatives, B. Chem. Soc. Jpn., *68*, pp. 3289-3307. 1995.

Yu, H., Q. Hu and L. Pu. The First Optically Active BINOL-BINAP Copolymer Catalyst: Highly Stereoselective Tandem Asymmetric Reactions, J. Am. Chem. Soc*., 122*, pp. 6500-6501. 2000.

Zabransky, R. and R. Anderson. Simulated Moving Bed Alkylation Process, US Patent 4 008 291. 1977.

Zang, Y. and P.C. Wankat. New SMB Operation Strategy-Partial Feed, Ind. Eng. Chem. Res., *41*, pp. 2504-2511. 2002.

Zenoni, G., F. Quattrini, M. Mazzotti, C. Fuganti and M. Morbidelli. Scale-up of analytical chromatography to the simulated moving bed separation of the enantiomers of the flavour norterpenoids α-ionone and α-damascone, Flavour and Fragrance Journal, *17*, pp. 195-202. 2002.

Zhang, Z., K. Hidajat and A.K. Ray. Multiobjective Optimization of Simulated Countercurrent Moving Bed Chromatographic Reactor for MTBE Synthesis, Ind. Eng. Chem. Res., *41*, pp. 3213-3232. 2002a.

Zhang, Z., K. Hidajat and A.K. Ray. Multiobjective Optimization of SMB and Varicol Process for Chiral Separation, AIChE J., *48*, pp. 2800-2816. 2002b.

Zhong, G. and G. Guiochon. Analytical Solution for the Linear Ideal Model of Simulated Moving Bed Chromatography, Chem. Eng. Sci., *51*, pp. 4307-4319. 1996.

Zhong, G. and G. Guiochon. Steady-State Analysis of Simulated Moving Bed Chromatography Using the Linear, Ideal Model, Chem. Eng. Sci., *53*, pp. 1121-1130. 1998.

List of Publications

Wongso, F., K. Hidajat and A. K. Ray. Application of Multiobjective Optimization in the Design of Chiral Drug Separators based on SMB Technology, Proc. of European Symposium on Computer Aided and Process Engineering (ESCAPE)-13, June 2003, Lappeenranta, Finland, pp. 1145-1150.

Wongso, F., K. Hidajat and A.K. Ray. Optimal Operating Mode of Simulated Moving Bed and Varicol Process for enantioseparation of SB-553261 racemate, submitted to Biotechnology and Bioengineering. 2003.

Wongso, F., K. Hidajat and A.K. Ray. Enhanced Performance of Moving Bed Technology for Continuous Separation of 1,1'-bi-2 naphtol racemate, submitted to Chemical Engineering Science. 2003.

Wongso, F., Hidajat, K., Ray, A.K., Utilizing SMB Behavior under Reactive System for Selective Conversion of Bisphenol A, to be submitted to Industrial and Engineering Chemistry Research. 2003.

APPENDIX A. Mixing Cell Model

$$C_{i,k-1}^{(N)} = C_{i,k}^{(N)} + \left[\frac{t_{0(\phi)}}{J}\right]\frac{dC_{i,k}^{(N)}}{dt} + \left[\frac{1-\varepsilon}{\varepsilon}\right]\left[\frac{t_{0(\phi)}}{J}\right]\frac{dq_{i,k}^{(N)}}{dt} \quad \text{for} \quad 0 \le t \le t_s \qquad \text{.....(A.1)}$$

where

$C_{i,k}^{(N)}$: concentration in the mobile phase for component i at column k and N^{th} switching

$q_{i,k}^{(N)}$: equilibrium concentration in the stationary phase for component i at column k and N^{th} switching

ε : porosity of the column packing

J : theoretical number of cells of the column (N_{plate})

$t_{0(\phi)}$: zero retention time ($\frac{V_{col}\varepsilon}{Q_i}$)

for component A

$$C_{A,k-1}^{(N)} = C_{A,k}^{(N)} + \left[\frac{t_{0(\phi)}}{J}\right]\frac{dC_{A,k}^{(N)}}{dt} + \left[\frac{1-\varepsilon}{\varepsilon}\right]\left[\frac{t_{0(\phi)}}{J}\right]\frac{dq_{A,k}^{(N)}}{dt} \qquad \text{.....(A.2)}$$

and

$$q_{A,k} = H_A C_{A,k} + \frac{NK_A C_{A,k}}{1 + K_A C_{A,k} + K_B C_{B,k}} \qquad \text{.....(A.3)}$$

for component B

$$C_{B,k-1}^{(N)} = C_{B,k}^{(N)} + \left[\frac{t_{0(\phi)}}{J}\right]\frac{dC_{B,k}^{(N)}}{dt} + \left[\frac{1-\varepsilon}{\varepsilon}\right]\left[\frac{t_{0(\phi)}}{J}\right]\frac{dq_{B,k}^{(N)}}{dt} \qquad \text{…….(A.4)}$$

and

$$q_{B,k} = H_B C_{B,k} + \frac{NK_B C_{B,k}}{1 + K_A C_{A,k} + K_B C_{B,k}} \qquad \text{…….(A.5)}$$

Then taking the derivative of eq.(A.5),

$$\frac{dq_{B,k}^{(N)}}{dt} = H_B \frac{dC_{B,k}^{(N)}}{dt} + \frac{NK_B \dfrac{dC_{B,k}^{(N)}}{dt}}{(1 + K_A C_{A,k}^{(N)} + K_B C_{B,k}^{(N)})} + NK_B C_{B,k}^{(N)} \left[\frac{-\left(K_B \dfrac{dC_{B,k}^{(N)}}{dt} + K_A \dfrac{dC_{A,k}^{(N)}}{dt}\right)}{(1 + K_A C_{A,k}^{(N)} + K_B C_{B,k}^{(N)})^2}\right] \qquad \text{…….(A.6)}$$

Substituting this derivative to eq.(A.4),

$$\left[\frac{J}{t_{0(\phi)}}\right]\left[C_{B,k-1}^{(N)} - C_{B,k}^{(N)}\right] = \frac{dC_{B,k}^{(N)}}{dt} + \left[\frac{1-\varepsilon}{\varepsilon}\right]\left[H_B + \frac{NK_B}{(1 + K_A C_{A,k}^{(N)} + K_B C_{B,k}^{(N)})} - \frac{NK_B C_{B,k}^{(N)} K_B}{(1 + K_A C_{A,k}^{(N)} + K_B C_{B,k}^{(N)})^2}\right]\frac{dC_{B,k}^{(N)}}{dt} - \left[\frac{1-\varepsilon}{\varepsilon}\right]\left[\frac{NK_B C_{B,k}^{(N)} K_A}{(1 + K_A C_{A,k}^{(N)} + K_B C_{B,k}^{(N)})^2}\right]\frac{dC_{A,k}^{(N)}}{dt}$$

…….(A.7)

Rearranging,

$$\frac{dC_{B,k}^{(N)}}{dt}=\frac{\left[\frac{J}{t_{0(\phi)}}\right]\left[C_{B,k-1}^{(N)}-C_{B,k}^{(N)}\right]+\left[\frac{1-\varepsilon}{\varepsilon}\right]\left[\frac{NK_BC_{B,k}^{(N)}K_A}{(1+K_AC_{A,k}^{(N)}+K_BC_{B,k}^{(N)})^2}\right]\frac{dC_{A,k}^{(N)}}{dt}}{\left[1+\left(\frac{1-\varepsilon}{\varepsilon}\right)H_B+\left(\frac{1-\varepsilon}{\varepsilon}\right)\frac{NK_B(1+K_AC_{A,k}^{(N)})}{(1+K_AC_{A,k}^{(N)}+K_BC_{B,k}^{(N)})^2}\right]} \qquad \text{…….(A.8)}$$

Similarly for component A, we first take the derivative of eq.(A.3) as follows:

$$\frac{dq_{A,k}^{(N)}}{dt}=H_A\frac{dC_{A,k}^{(N)}}{dt}+\frac{NK_A\frac{dC_{A,k}^{(N)}}{dt}}{(1+K_AC_{A,k}^{(N)}+K_BC_{B,k}^{(N)})}+NK_AC_{A,k}^{(N)}\left[\frac{-\left(K_B\frac{dC_{B,k}^{(N)}}{dt}+K_A\frac{dC_{A,k}^{(N)}}{dt}\right)}{(1+K_AC_{A,k}^{(N)}+K_BC_{B,k}^{(N)})^2}\right] \qquad \text{…….(A.9)}$$

Substituting this derivative to eq.(A.2), we obtain

$$\left[\frac{J}{t_{0(\phi)}}\right]\left[C_{A,k-1}^{(N)}-C_{A,k}^{(N)}\right]=\frac{dC_{A,k}^{(N)}}{dt}+\left[\frac{1-\varepsilon}{\varepsilon}\right]\left[H_A+\frac{NK_A}{(1+K_AC_{A,k}^{(N)}+K_BC_{B,k}^{(N)})}-\frac{NK_AC_{A,k}^{(N)}K_A}{(1+K_AC_{A,k}^{(N)}+K_BC_{B,k}^{(N)})^2}\right]\frac{dC_{A,k}^{(N)}}{dt}-\left[\frac{1-\varepsilon}{\varepsilon}\right]\left[\frac{NK_AC_{A,k}^{(N)}K_B}{(1+K_AC_{A,k}^{(N)}+K_BC_{B,k}^{(N)})^2}\right]\frac{dC_{B,k}^{(N)}}{dt}$$

…….(A.10)

Rearranging,

$$\frac{dC_{A,k}^{(N)}}{dt}=\frac{\left[\frac{J}{t_{0(\phi)}}\right]\left[1+\frac{1-\varepsilon}{\varepsilon}\left(H_B+\frac{NK_B(1+K_AC_{A,k}^{(N)})}{(1+K_AC_{A,k}^{(N)}+K_BC_{B,k}^{(N)})^2}\right)\right]\left[C_{A,k-1}^{(N)}-C_{A,k}^{(N)}\right]+\left[\frac{J}{t_{0(\phi)}}\right]\left[\frac{NK_AC_{A,k}^{(N)}K_B}{(1+K_AC_{A,k}^{(N)}+K_BC_{B,k}^{(N)})^2}\right]\left[C_{B,k-1}^{(N)}-C_{B,k}^{(N)}\right]}{\left[1+\frac{1-\varepsilon}{\varepsilon}\left(H_A+\frac{NK_A(1+K_BC_{B,k}^{(N)})}{(1+K_AC_{A,k}^{(N)}+K_BC_{B,k}^{(N)})^2}\right)\right]\left[1+\frac{1-\varepsilon}{\varepsilon}\left(H_B+\frac{NK_B(1+K_AC_{A,k}^{(N)})}{(1+K_AC_{A,k}^{(N)}+K_BC_{B,k}^{(N)})^2}\right)\right]-\left[\frac{NK_AC_{A,k}^{(N)}K_B}{(1+K_AC_{A,k}^{(N)}+K_BC_{B,k}^{(N)})^2}\right]\left[\frac{NK_BC_{B,k}^{(N)}K_A}{(1+K_AC_{A,k}^{(N)}+K_BC_{B,k}^{(N)})^2}\right]}$$

…….(A.11)

Boundary Condition,

At the eluent port,

$$C_{i,first}^{(N)}=\frac{(Q_1-Q_E)C_{i,last}^{(N)}}{Q_1}$$ …….(A.12)

At the feed port,

$$C_{i,first}^{(N)}=\frac{Q_2C_{i,last}^{(N)}+Q_FC_{i,F}^{(N)}}{Q_3}$$ …….(A.13)

Else,

$$C_{i,first}^{(N)}=C_{i,last}^{(N)}$$ …….(A.14)

APPENDIX B. Calculation of CSP usage & void fraction in SB-553261 separation.

Table B.1 Experimental Data on Productivity and Desorbent Consumption

	Productivity ($kg_{prod}/kg_{CSP}/day$)	Eluent Cons. ($m^3_{desorbent}/kg_{prod}$)	$Q_{Feed}/\overline{Q}$
6-column SMB 1/2/2/1	0.604	0.922	0.0369
6-column VARICOL <1>/<2.25>/<2>/<0.75>	0.664	0.888	0.0409
5-column VARICOL <0.95>/<1.85>/<1.5>/<0.7>	0.725	1.050	0.0297
4-column VARICOL <0.85>/<1.5>/<1.15./<0.5>	0.906	1.392	0.0233

Adapted from Ludemann-Hombouger et al (2002)

6 column SMB (Eluent Flow Rate : 8.55 ml/min)

$$\text{Product Flow Rate} = \frac{8.55\dfrac{ml}{\min}}{0.922\dfrac{m^3}{kg_{prod}}} \times 10^{-6}\,\frac{m^3}{ml} = 9.2733\cdot 10^{-6}\,\frac{kg_{prod}}{\min}$$

$$\text{CSP} = \frac{9.2733\cdot 10^{-6}\dfrac{kg_{prod}}{\min}}{0.604\dfrac{kg_{prod}}{kg_{CSP}day}\times 6column} \times 1000\,\frac{g_{CSP}}{kg_{CSP}} \times 24\,\frac{hr}{day} \times 60\,\frac{\min}{hr} = 3.6848\,\frac{g_{CSP}}{column}$$

6 column VARICOL (Eluent Flow Rate : 9.05 ml/min)

$$\text{Product Flow Rate} = \frac{9.05\dfrac{ml}{\min}}{0.888\dfrac{m^3}{kg_{prod}}} \times 10^{-6}\,\frac{m^3}{ml} = 1.0191\cdot 10^{-5}\,\frac{kg_{prod}}{\min}$$

$$\text{CSP} = \frac{1.0191\cdot10^{-5}\,\frac{kg_{prod}}{\min}}{0.664\,\frac{kg_{prod}}{kg_{CSP}day}\times 6column}\times 1000\,\frac{g_{CSP}}{kg_{CSP}}\times 24\,\frac{hr}{day}\times 60\,\frac{\min}{hr} = 3.6837\,\frac{g_{CSP}}{column}$$

5 column VARICOL (Eluent Flow Rate : 9.78 ml/min)

$$\text{Product Flow Rate} = \frac{9.78\,\frac{ml}{\min}}{1.05\,\frac{m^3}{kg_{prod}}}\times 10^{-6}\,\frac{m^3}{ml} = 9.3143\cdot10^{-6}\,\frac{kg_{prod}}{\min}$$

$$\text{CSP} = \frac{9.3143\cdot10^{-6}\,\frac{kg_{prod}}{\min}}{0.725\,\frac{kg_{prod}}{kg_{CSP}day}\times 5column}\times 1000\,\frac{g_{CSP}}{kg_{CSP}}\times 24\,\frac{hr}{day}\times 60\,\frac{\min}{hr} = 3.7\,\frac{g_{CSP}}{column}$$

4 column VARICOL (Eluent Flow Rate : 13.06 ml/min)

$$\text{Product Flow Rate} = \frac{13.06\,\frac{ml}{\min}}{1.392\,\frac{m^3}{kg_{prod}}}\times 10^{-6}\,\frac{m^3}{ml} = 9.3822\cdot10^{-6}\,\frac{kg_{prod}}{\min}$$

$$\text{CSP} = \frac{9.3822\cdot10^{-6}\,\frac{kg_{prod}}{\min}}{0.906\,\frac{kg_{prod}}{kg_{CSP}day}\times 4column}\times 1000\,\frac{g_{CSP}}{kg_{CSP}}\times 24\,\frac{hr}{day}\times 60\,\frac{\min}{hr} = 3.728\,\frac{g_{CSP}}{column}$$

It is assumed that the amount of CSP used in this separation is about 3.7 g CSP per column and this value is later used in the calculation of CSP void fraction according to the following relation ($\rho = 1 g/cm^3$):

$$\text{g CSP per column} = (1-\varepsilon)V_{col}$$

Since $V_{col} = 6.48\ cm^3$ then we obtain $\varepsilon = 0.43$

APPENDIX C. Calculation of σ and V_i

As defined by Petroulas et al. (1985) σ, the relative carrying capacity is defined as follows:

$$\gamma_i = K_i C_{iavg} \text{ and } \sigma_i = \delta_i \frac{u_s}{u_g}$$

$$\text{with } \delta_i = \frac{1-\varepsilon}{\varepsilon} NK_i \text{ and } V_i = u_g \frac{(1-\frac{\sigma_i}{1+\gamma_i})}{(1+\frac{\delta_i}{1+\gamma_i})}$$

at low concentration ($\gamma_i << 1$),

$$V_i = u_g \frac{(1-\sigma_i)}{(1+\delta_i)}$$

C.1. Calculation of σ and V_i used in Chapter 3

Data : ε = 0.43, L_c = 0.081 m, A = 7.854 x 10^{-5} m^2, NK_A = 1.644, NK_B = 2.679, K_A = 0.0338 and K_B = 0.1696

$$\delta_A = \frac{1-0.43}{0.43} 1.644 = 2.1793 \quad \text{and} \quad \delta_B = \frac{1-0.43}{0.43} 2.679 = 3.5512$$

The effect of switching time

C.1.1. ts = 0.8 min ($C_{i\,avg}$ = 4.6254 g/l)

Zone II, Q_{II} = 9.9 cm^3/min, u_{gII} = 12.60504 cm/min

$$\gamma_A = 0.0338 \cdot 4.6254 = 0.156339 \text{ and } \sigma_A = 2.1793 \frac{10.125 \frac{cm}{\min}}{29.31405 \frac{cm}{\min}} = 0.752725$$

$$V_A = 12.60504 \frac{(1 - \frac{0.752725}{1 + 0.156339})}{(1 + \frac{2.1793}{1 + 0.156339})} = 1.525216 \frac{cm}{\min}$$

$$\gamma_B = 0.1696 \cdot 4.6254 = 0.784468 \text{ and } \sigma_B = 3.5512 \frac{10.125 \frac{cm}{\min}}{29.31405 \frac{cm}{\min}} = 1.226576$$

$$V_B = 12.60504 \frac{(1 - \frac{1.226576}{1 + 0.784468})}{(1 + \frac{3.5512}{1 + 0.784468})} = 1.31797 \frac{cm}{\min}$$

$$\Delta V = V_A - V_B = 0.207246 \frac{cm}{\min}$$

C.1.2. ts = 0.925 min ($C_{i\ avg}$ = 0.75842 g/l)

Zone II, Q_{II} = 9.9 cm^3/min, u_{gII} = 12.60504 cm/min

$$\sigma_A = 2.1793 \frac{8.756754 \frac{cm}{\min}}{29.31405 \frac{cm}{\min}} = 0.651005$$

$$V_A = 12.60504 \frac{(1 - 0.651005)}{(1 + 2.1793)} = 1.383668 \frac{cm}{\min}$$

$$\sigma_B = 3.5512 \frac{8.756754 \frac{cm}{\min}}{29.31405 \frac{cm}{\min}} = 1.060822$$

$$V_B = 12.60504 \frac{(1 - 1.060822)}{(1 + 3.5512)} = -0.168453 \frac{cm}{\min}$$

$$\Delta V = V_A - V_B = 1.552121 \frac{cm}{\min}$$

C.1.3. ts = 1.2 min ($C_{i\,avg}$ = 0.21785 g/l)

Zone II, Q_{II} = 9.9 cm^3/min, u_{gII} = 12.60504 cm/min

$$\gamma_A = 0.0338 \cdot 0.21785 = 7.36333 \cdot 10^{-3} \text{ and } \sigma_A = 2.1793 \frac{6.75 \frac{cm}{\min}}{29.31405 \frac{cm}{\min}} = 0.501817$$

$$V_A = 12.60504 \frac{(1 - 0.501817)}{(1 + 2.1793)} = 1.975157 \frac{cm}{\min}$$

$$\gamma_B = 0.1696 \cdot 0.21785 = 3.694736 \cdot 10^{-2} \text{ and } \sigma_B = 3.5512 \frac{6.75 \frac{cm}{\min}}{29.31405 \frac{cm}{\min}} = 0.817717$$

$$V_B = 12.60504 \frac{(1 - 0.817717)}{(1 + 3.5512)} = 0.504852 \frac{cm}{\min}$$

$$\Delta V = V_A - V_B = 1.470305 \frac{cm}{\min}$$

C.2. Calculation of σ and V_i used in Chapter 4

Data: ε = 0.4, L_c = 10.5 m, A = 5.3093 cm^2, N_S = 80.0595, N_R = 80.0429, K_A = 0.0336 and K_B = 0.0466

$$\delta_S = \frac{1 - 0.4}{0.4} 2.69 = 4.035 \qquad \text{and} \qquad \delta_R = \frac{1 - 0.4}{0.4} 3.73 = 5.595$$

$$u_S = \frac{10.5 cm}{3.100572 \min} = 3.386472 \frac{cm}{\min}$$

C.2.1. Zone I

Q_I = 56.83 cm^3/min, u_{gI} = 10.703859 cm/min

$$\gamma_S = 0.0336 \cdot 0.0105 = 3.528 \times 10^{-4} \text{ (~0) and } \quad \sigma_S = 4.035 \frac{3.386472 \frac{cm}{\min}}{26.75965 \frac{cm}{\min}} = 0.510635$$

$$V_S = 10.703859 \frac{(1 - 0.510635)}{(1 + 4.035)} = 1.040336 \frac{cm}{\min}$$

$$\gamma_R = 0.0466 \cdot 0.0105 = 4.893 \times 10^{-4} \text{ (~0) and } \quad \sigma_R = 5.595 \frac{3.386472 \frac{cm}{\min}}{26.75965 \frac{cm}{\min}} = 0.708055$$

$$V_R = 10.703859 \frac{(1 - 0.708055)}{(1 + 5.595)} = 0.473834 \frac{cm}{\min}$$

$$\Delta V = V_S - V_R = 0.566502 \frac{cm}{\min}$$

C.2.2. Zone II

Q_{II} = 36.391195 cm^3/min, u_{g2} = 6.854236 cm/min

$$\gamma_S = 0.0336 \cdot 0.466 = 1.56576 \times 10^{-2} \text{ (~0) and } \quad \sigma_S = 4.035 \frac{3.386472 \frac{cm}{\min}}{17.13559 \frac{cm}{\min}} = 0.797429$$

$$V_S = 6.854236 \frac{(1 - 0.797429)}{(1 + 4.035)} = 0.275764 \frac{cm}{\min}$$

$$\gamma_R = 0.0466 \cdot 0.466 = 2.17156 \times 10^{-2} \text{ (~0) and } \quad \sigma_R = 5.595 \frac{3.386472 \frac{cm}{\min}}{17.13559 \frac{cm}{\min}} = 1.105729$$

$$V_R = 6.854236 \frac{(1 - 1.105729)}{(1 + 5.595)} = -0.109885 \frac{cm}{\min}$$

$$\Delta V = V_S - V_R = 0.385649 \frac{cm}{\min}$$

C.2.3. Zone III

$Q_{III} = 40.031195$ cm^3/min, $u_{g3} = 7.539825$ cm/min

$$\gamma_S = 0.0336 \cdot 1.8373 = 6.173328 \times 10^{-2} \text{ (~0) and } \quad \sigma_S = 4.035 \frac{3.386472 \frac{cm}{\text{min}}}{18.849563 \frac{cm}{\text{min}}} = 0.724919$$

$$V_S = 7.539825 \frac{(1 - 0.724919)}{(1 + 4.035)} = 0.411929 \frac{cm}{\text{min}}$$

$$\gamma_R = 0.0466 \cdot 1.8373 = 8.561818 \times 10^{-2} \text{ (~0) and } \quad \sigma_R = 5.595 \frac{3.386472 \frac{cm}{\text{min}}}{18.849563 \frac{cm}{\text{min}}} = 1.005186$$

$$V_R = 7.539825 \frac{(1 - 1.005186)}{(1 + 5.595)} = -0.005929 \frac{cm}{\text{min}}$$

$$\Delta V = V_S - V_R = 0.417858 \frac{cm}{\text{min}}$$

C.2.4. Zone IV

$Q_{IV} = 32.425336$ cm^3/min, $u_{g2} = 6.107271$ cm/min

$$\gamma_S = 0.0336 \cdot 0.46085 = 1.548456 \times 10^{-2} \text{ (~0) and } \quad \sigma_S = 4.035 \frac{3.386472 \frac{cm}{\text{min}}}{15.268178 \frac{cm}{\text{min}}} = 0.89496$$

$$V_S = 6.107271 \frac{(1 - 0.89496)}{(1 + 4.035)} = 0.12741 \frac{cm}{\text{min}}$$

$$\gamma_R = 0.0466 \cdot 0.46085 = 2.147561 \times 10^{-2} \text{ (~0) and } \quad \sigma_R = 5.595 \frac{3.386472 \frac{cm}{\text{min}}}{15.268178 \frac{cm}{\text{min}}} = 1.240967$$

$$V_R = 6.107271\frac{(1-1.240967)}{(1+5.595)} = -0.223146\frac{cm}{\min}$$

$$\Delta V = V_S - V_R = 0.350556\frac{cm}{\min}$$

APPENDIX D. Equilibrium Dispersive Model

$$\frac{dC_{i,k}^{(N)}}{dt}+\frac{1-\varepsilon}{\varepsilon}\frac{dq_{i,k}^{(N)}}{dt}+v\frac{dC_{i,k}^{(N)}}{dz}=D_L\frac{d^2C_{i,k}^{(N)}}{dz^2} \qquad \text{…….(D.1)}$$

$C_{i,k}^{(N)}$: concentration in the mobile phase for component I at column k and N^{th} switching

$q_{i,k}^{(N)}$: equilibrium concentration in the stationary phase for component i at column k and N^{th} switching

ε : porosity of the column packing

D_L : axial dispersion coefficient

v : mobile phase linear velocity ($\frac{Q_i}{\varepsilon A}$)

Langmuir adsorption isotherm,

$$\frac{dq_{i,k}^{(N)}}{dt}=k_i\left[q_{i,k}^{*(N)}-q_{i,k}^{(N)}\right] \quad \text{with} \quad q_{i,k}^{*(N)}=\frac{NK_iC_{i,k}^{(N)}}{1+K_iC_{i,k}^{(N)}+K_jC_{j,k}^{(N)}}+\frac{NK_i^{'}C_{i,k}^{(N)}}{1+K_i^{'}C_{i,k}^{(N)}+K_j^{'}C_{j,k}^{(N)}}$$

Using Finite Difference Approximation, we obtain

$$\frac{dC_{i,k}^{(N)}}{dt}=-v\frac{dC_{i,k}^{(N)}}{dz}+D_L\frac{d^2C_{i,k}^{(N)}}{dz^2}-\frac{1-\varepsilon}{\varepsilon}\frac{dq_{i,k}^{(N)}}{dt} \qquad \text{…….(D.2)}$$

$$\frac{dC_{i,k}^{(N)}}{dt}=-\frac{Q_k}{\varepsilon A}\frac{\left[C_{i,k}^{(N)}-C_{i,k-1}^{(N)}\right]}{\Delta z}+D_L\frac{\left[C_{i,k+1}^{(N)}-C_{i,k}^{(N)}+C_{i,k-1}^{(N)}\right]}{\Delta z^2}-\frac{1-\varepsilon}{\varepsilon}\frac{dq_{i,k}^{(N)}}{dt} \qquad \text{…(D.3)}$$

$$\text{since } \Delta z=\frac{L}{N_{plate}} \text{ and } V_{col}=A\times L_c \text{ so } \Delta z=\frac{V_{col}}{A\times N_{plate}}$$

We obtain,

$$\frac{dC_{i,k}^{(N)}}{dt}=-\frac{Q_kN_{plate}}{\varepsilon V_{col}}\left[C_{i,k}^{(N)}-C_{i,k-1}^{(N)}\right]+\frac{A^2N_{plate}^2D_L}{V_{col}^2}\left[C_{i,k+1}^{(N)}-C_{i,k}^{(N)}+C_{i,k-1}^{(N)}\right]-\frac{1-\varepsilon}{\varepsilon}\frac{dq_{i,k}^{(N)}}{dt}$$

…….(D.4)

with $$\frac{dq_{i,k}^{(N)}}{dt}=k_i\left[\frac{NK_iC_{i,k}^{(N)}}{1+K_iC_{i,k}^{(N)}+K_jC_{j,k}^{(N)}}+\frac{NK_i^{'}C_{i,k}^{(N)}}{1+K_i^{'}C_{i,k}^{(N)}+K_j^{'}C_{j,k}^{(N)}}-q_{i,k}^{(N)}\right]$$

APPENDIX E.

Elitist Non-dominated Sorting Genetic Algorithm with Jumping Genes

GA is a search technique developed by Holland (1975) that mimics the process of natural selection and natural genetics. In this algorithm, a set of decision variables are first coded in the form of a set of randomly generated chromosomes, thereby creating a 'population (gene pool)'. A model of the process is then used to provide values of the objective function (reflects its 'fitness' value) for each chromosome. The Darwinian principle of 'survival of the fittest' is used to generate a new and improved gene pool (new generation). This is done by preparing a 'mating pool', comprising of copies of chromosomes, the number of copies of any chromosome being proportional to its fitness (Darwin's principle). Pairs of chromosomes are then selected randomly, and pairs of daughter chromosomes generated using three operations (reproduction, crossover and mutation) similar to those in genetic reproduction. The gene pool evolves, with the fitness improving over the generations.

In order to handle multiple objective functions and to find Pareto-optimal solutions, the simple genetic algorithm (SGA) has been modified to Non-dominated Sorting Genetic Algorithm I (NSGA-I), which differs from SGA only in the way the selection operator works (Deb, 2001). NSGA-I uses a ranking selection method to emphasize the good points and a niche method to create diversity in the population without losing a stable sub-population of good points. In the new procedure, several groups of non-dominated chromosomes from among all the members of the population at any generation are

identified. To distribute (spread out) the points evenly, the fitness value is assigned according to a sharing procedure. The population is found to converge rapidly to the Pareto set.

However, experience with NSGA-I indicates that this algorithm has some disadvantages. The sharing function used to evaluate niche count of any chromosome requires the values of two parameters, which are difficult to assign a-priori. In addition, NSGA-I does not use any elite-preserving operator and so, good parents may get lost. Deb et al. (2002) have recently developed an elitist non-dominated sorting genetic algorithm (NSGA-II) to overcome these limitations. In NSGA-II, a different sorting and sharing method is used, which reduces the numerical complexity to MN_p^2 operations in contrast to MN_p^3 operations required for NSGA-I, where M is the number of objective functions, and N_p is the number of chromosomes in the population.

Kasat et al. (2002) recently introduced a modified mutation operator, borrowing from the concept of jumping genes (JG) in natural genetics. This algorithm is being called as NSGA-II-JG. This is a macro-macro mutation, and counteracts the decrease in the diversity created by elitism. The jumping genes operation is carried out after crossover and normal mutation in NSGA-II. A part of the binary strings in the selected chromosomes is replaced with a newly (randomly) generated string of the same length. Only a single jumping gene was assumed to replace part of any selected chromosome. This helps save considerable amounts of the computation time (at times, gives correct solutions, which are missed by other algorithms) and is important for compute-intense

multiobjective problems like that of the SMB and Varicol process. Nandasana et al. (2003) has reviewed recently the applications of different adaptations of NSGA in chemical engineering.